MULTIDISCIPLINARY CENTER FOR EARTHQUAKE ENGINEERING RESEARCH
A National Center of Excellence in Advanced Technology Applications

ISSN 1520-295X

Effect of Vertical Ground Motions on the Structural Response of Highway Bridges

by

Martin R. Button, Colman J. Cronin and Ronald L. Mayes
Dynamic Isolation Systems, Inc.
3470 Mt. Diablo Boulevard, Suite A200
Lafayette, California 94549

Technical Report MCEER-99-0007

April 10, 1999

This research was conducted at Dynamic Isolation Systems, Inc. and was supported by the Federal Highway Administration under contract number DTFH61-92-C-00112.

NOTICE

This report was prepared by Dynamic Isolation Systems, Inc., as a result of research sponsored by the Multidisciplinary Center for Earthquake Engineering Research (MCEER) through a contract from the Federal Highway Administration. Neither MCEER, associates of MCEER, its sponsors, Dynamic Isolation Systems, Inc., nor any person acting on their behalf:

a. makes any warranty, express or implied, with respect to the use of any information, apparatus, method, or process disclosed in this report or that such use may not infringe upon privately owned rights; or

b. assumes any liabilities of whatsoever kind with respect to the use of, or the damage resulting from the use of, any information, apparatus, method, or process disclosed in this report.

Any opinions, findings, and conclusions or recommendations expressed in this publication are those of the author(s) and do not necessarily reflect the views of MCEER or the Federal Highway Administration.

Effect of Vertical Ground Motions on the Structural Response of Highway Bridges

by

Martin R. Button[1], Colman J. Cronin[2] and Ronald L. Mayes[3]

Publication Date: April 10, 1999
Submittal Date: July 28, 1998

Technical Report MCEER-99-0007

Task Number 112-D-7

FHWA Contract Number DTFH61-92-C-00112

1 Director of Engineering, Dynamic Isolation Systems, Inc.
2 Engineer, Dynamic Isolation Systems, Inc.
3 President, Dynamic Isolation Systems, Inc.

MULTIDISCIPLINARY CENTER FOR EARTHQUAKE ENGINEERING RESEARCH
University at Buffalo, State University of New York
Red Jacket Quadrangle, Buffalo, NY 14261

Preface

The Multidisciplinary Center for Earthquake Engineering Research (MCEER) is a national center of excellence in advanced technology applications that is dedicated to the reduction of earthquake losses nationwide. Headquartered at the University at Buffalo, State University of New York, the Center was originally established by the National Science Foundation in 1986, as the National Center for Earthquake Engineering Research (NCEER).

Comprising a consortium of researchers from numerous disciplines and institutions throughout the United States, the Center's mission is to reduce earthquake losses through research and the application of advanced technologies that improve engineering, pre-earthquake planning and post-earthquake recovery strategies. Toward this end, the Center coordinates a nationwide program of multidisciplinary team research, education and outreach activities.

MCEER's research is conducted under the sponsorship of two major federal agencies, the National Science Foundation (NSF) and the Federal Highway Administration (FHWA), and the State of New York. Significant support is also derived from the Federal Emergency Management Agency (FEMA), other state governments, academic institutions, foreign governments and private industry.

The Center's FHWA-sponsored Highway Project develops retrofit and evaluation methodologies for existing bridges and other highway structures (including tunnels, retaining structures, slopes, culverts, and pavements), and improved seismic design criteria and procedures for bridges and other highway structures. Specifically, tasks are being conducted to:

- assess the vulnerability of highway systems, structures and components;
- develop concepts for retrofitting vulnerable highway structures and components;
- develop improved design and analysis methodologies for bridges, tunnels, and retaining structures, which include consideration of soil-structure interaction mechanisms and their influence on structural response;
- review and recommend improved seismic design and performance criteria for new highway structures.

Highway Project research focuses on two distinct areas: the development of improved design criteria and philosophies for new or future highway construction, and the development of improved analysis and retrofitting methodologies for existing highway systems and structures. The research discussed in this report is a result of work conducted under the new highway structures project, and was performed within Task 112-D-7, "Effect of Vertical Acceleration on Structural Response" of that project as shown in the flowchart on the following page.

The overall objective of this task was to investigate the conditions where vertical acceleration is critical in determining the demands placed on key elements of typical highway bridges. In this report, a representative group of six bridges, with a range of input ground motions that include and exclude the vertical component of motion, were analyzed to determine when the vertical component can be safely ignored and when it should be included in the design or analysis of highway bridges. On the

basis of results from linear and nonlinear analyses, recommendations are made regarding when to explicitly include vertical motions in design, when the effects of vertical motion can be adequately addressed by simple load combination rules, and when the impact of vertical motions is less than 10% and thus can safely be ignored. It is important to note, however, that this study was limited only to the six bridge types analyzed, and generic or widely applicable recommendations should not be drawn or interpreted from these results.

A large body of additional information, including response ratios computed from response spectrum analyses of all six bridges and for varying deck stiffnesses and foundation fixity in bridges 4 and 6, mode shapes with modal mass participation ratios greater that 10% for all six bridges, SAP2000 input files, and the ANSR-II input file for bridge 6, are not included in this report but are available from the publications section of MCEER's web site (http://mceer.buffalo.edu/pubs.html) where they can be freely downloaded.

SEISMIC VULNERABILITY OF NEW HIGHWAY CONSTRUCTION
FHWA Contract DTFH61-92-C-00112

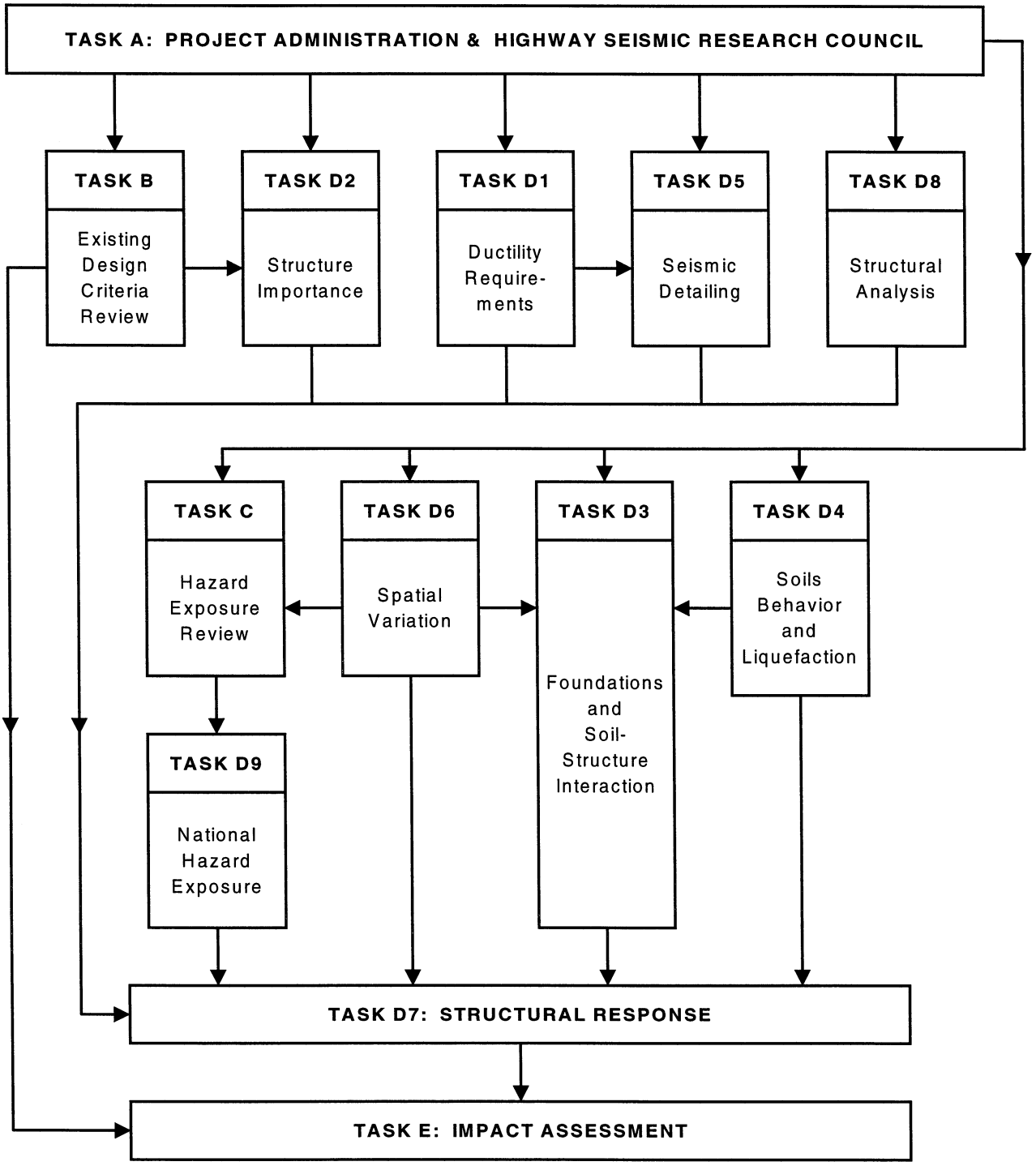

ABSTRACT

Results of a parametric study into the effects of the vertical component of seismic ground motion on the structural response of typical highway bridges are presented. The parameters include six different finite element bridge models and input ground motions representing events with magnitudes of 6.5 and 7.5 for both rock and soil site conditions at fault distances of 1, 5, 10, 20 and 40 km. Both linear and nonlinear dynamic analyses are performed.

Response spectrum analyses are performed on all six bridges using all of the above ground motion parameters for the cases of (a) two-component horizontal only input and (b) three-component input. Results for the two cases are compared. The accuracy of these results is validated by linear time history analyses of three bridges using spectrum compatible records. The additional effect of including the vertical component of motion is presented as a ratio of the dead-load only response.

Records with early-arriving short period motion in the vertical component are shown to produce a similar structural response to records that do not have these characteristics. Results from response spectrum analyses using vertical spectrum with a spectral amplitude 2/3 of the horizontal spectrum showed that the response can be up to 40% greater or less than those from empirical vertical spectra.

The effects of varying the vertical deck stiffnesses and foundation stiffnesses are studied. Results from response spectrum analyses performed on two bridges using three different directional combination rules are compared.

The response of one bridge incorporating nonlinear behavior in the piers is analyzed using spectrum compatible records representing a magnitude 6.5 event, soil site conditions and a fault distance of 5 km. This analysis is used to check the conclusions drawn from the linear analyses, but cannot be considered comprehensive.

ACKNOWLEDGEMENTS

We wish to express our sincere thanks to the following persons and organizations for the help they provided to this project:

- The Federal Highway Administration (FHWA) for funding this project through the Multidisciplinary Center for Earthquake Engineering Research (MCEER) in Buffalo.

- Ian Friedland for managing the project at MCEER.

- Dr. Ian Buckle and Steward Gloyd for reviewing drafts of this report and providing valuable feedback.

- Maury Power, Dario Rosidi and Shyh-Jeng Chiou of Geomatrix, Inc. for ensuring that the ground motion parameters used in this study were consistent with the most up-to-date information available. In particular, they provided valuable input on the vertical and horizontal spectra used, and made recommendations for recorded time history motions used. Finally, they reviewed and re-wrote the ground motions section of the report.

- Walter Silva of Pacific Engineering and Analysis for providing the V/H spectral ratios which were applied to the horizontal spectra to create the vertical spectra used.

- Lee Marsh of Berger/ABAM Engineers, Inc. for providing the input files of the bridge finite element models and all the figures shown in the bridge descriptions section. It should also be noted here that the majority of the descriptive text given in that section is directly copied from the Federal Highway Administration publication manuals FHWA-SA-97-06 through 011, which were produced by Berger/ABAM Engineers, Inc.

- Everyone at Dynamic Isolation Systems, Inc.; especially David Jones, Mark Sinclair and Alison Shaw in the Engineering department, and Stephanie Martens in the Communications department.

TABLE OF CONTENTS

SECTION	TITLE	PAGE
1	**INTRODUCTION**	**1**
2	**LITERATURE REVIEW**	**3**
2.1	Decks	3
2.2	Columns/Abutments	5
2.3	Foundations	6
2.4	Hinges	6
2.5	Bearings	6
2.6	Summary	7
3	**BRIDGE DESCRIPTIONS**	9
3.1	Bridge No. 1	9
3.2	Bridge No. 2	16
3.3	Bridge No. 3	28
3.4	Bridge No. 4	35
3.5	Bridge No. 5	42
3.6	Bridge No. 6	55
3.7	Summary Tables of Bridges	72
4	**GROUND MOTIONS**	**75**
4.1	Time Domain Characteristics of Vertical Ground Motions	75
4.2	Response Spectral Characteristics of Vertical Ground Motions	77
4.3	Development of Response Spectra for Bridge Analysis	78
4.4	Development of Three-Components of Acceleration Time Histories	81
5	**LINEAR ANALYSIS METHODOLOGY**	**87**
5.1	Eigenvector Analysis	87
5.2	Orientation of Ground Motions	87
5.3	Response Spectrum Analysis	87
5.4	Time-History Analysis	88
6	**LINEAR ANALYSIS RESULTS**	**89**
6.1	Response Quantities Reviewed	89
6.2	Description and Development of Presentation Format	89
6.3	Comparison of Time-History and Response Spectrum Results	94
6.3.1	Effect of "Early Arrival" Vertical Motions	94
6.4	Results of Response Spectrum Analyses	100
6.5	Vertical Shear Capacity of Decks at Mid-span	118
6.6	Effect of Varying Vertical Deck Stiffnesses	119
6.7	Effect of Varying Foundation Restraint	122
6.8	Comparison of Directional Combination Rules Used in Modal Analysis	124

TABLE OF CONTENTS (Cont'd)

SECTION	TITLE	PAGE
7	**NONLINEAR RESPONSE OF BRIDGE 6**	**127**
7.1	Description of Elements	127
7.2	Comparison of ANSR-II and SAP2000 Linear Results	128
7.3	Comparison of Nonlinear and Linear Response	129
7.4	Comparison of (3-2)/DL Ratios for Nonlinear and Linear Response	130
7.5	Effect of Reducing Overall Vertical Deck Stiffness	130
8	**SUMMARY, CONCLUSIONS AND RECOMMENDATIONS**	137
8.1	Summary	137
8.2	Conclusions	137
8.2.1	Ground Motions	137
8.2.2	Structural Response of Bridges in the Linear Range	138
8.2.3	Structural Response of Bridges in the Nonlinear Range	142
8.3	Recommendations	142
9	**REFERENCES**	**145**

Appendices

A	**Response Ratios Computed from Response Spectrum Analyses of Bridge Numbers 1, 2, 3, 4, 5 & 6**	*
B	**Response Ratios Computed from Response Spectrum Analyses for Varying Deck Stiffnesses and Foundation Fixity in Bridge Numbers 4 & 6**	*
C	**Mode Shapes with Modal Mass Participation Ratios Greater Than 10% for Bridge Numbers 1, 2, 3, 4, 5 & 6**	*
D	**SAP2000 Input Files**	*
E	**ANSR-II Input File of Bridge 6**	*

* The appendices are provided on MCEER's web site at *http://mceer.buffalo.edu.*

LIST OF ILLUSTRATIONS

FIGURE	TITLE	PAGE
3.1	Bridge #1 - Bridge Layout	10
3.2	Bridge #1 – Transverse Seismic Behavior	13
3.3	Bridge #1 – Longitudinal Seismic Behavior	13
3.4	Bridge #1 - Finite Element Model	14
3.5	Bridge #1 - Details of Column Elements	15
3.6a	Bridge #2 – Plan & Elevation	16
3.6b	Bridge #2 – Typical Cross-section	17
3.6c	Bridge #2 – Seat Type Abutment	18
3.6d	Bridge #2 – Pier Elevation	19
3.6e	Bridge #2 – Plate Girder Details	20
3.6f	Bridge #2 – Elastomeric Bearings at Piers	21
3.6g	Bridge #2 – Elastomeric Bearings at Abutments	22
3.7	Bridge #2 - Finite Element Model	23
3.8	Bridge #2 - Details of Column Elements	25
3.9	Bridge #2 - Plan of Pier Showing Rotation of Pier Elements	26
3.10	Bridge #2 – Orientation of Bearing Springs	27
3.11a	Bridge #3 – Plan & Section	29
3.11b	Bridge #3 – Typical Cross Section	30
3.11c	Bridge #3 – Framing Plan	31
3.11d	Bridge #3 – Abutment Section and Details	32
3.11e	Bridge #3 – Abutment Elevation and Detail	33
3.12	Bridge #3 - Finite Element Model	34
3.13a	Bridge #4 – Plan and Elevation	35
3.13b	Bridge #4 – Typical Cross Section	36
3.13c	Bridge #4 – Seat Type Abutment	37
3.13d	Bridge #4 – Box Girder Framing Plan	38
3.14	Bridge #4 - Finite Element Model	39
3.15	Bridge #4 – Details of Bent Elements	41
3.16	Bridge #4 - Details of Spring Supports	42
3.17a	Bridge #5 – Plan and Elevation	43
3.17b	Bridge #5 – Typical Cross Section	44
3.17c	Bridge #5 – Intermediate Pier Elevation	45
3.17d	Bridge #5 – Seat Type Abutment	46
3.18	Bridge #5 - Longitudinal Seismic Behavior	47
3.19	Bridge #5 - Transverse Seismic Behavior	47
3.20	Bridge #5 - Finite Element Model	48
3.21	Bridge #5 – Details of Pier Column Elements	50
3.22	Bridge #5 – Details of Pier #4 Expansion Joint	51
3.23	Bridge #5 – Details at Pier #5 and 8 Sliding Bearings	52
3.24	Bridge #5 – Details of Supports for Spring Foundation Model	53
3.25	Bridge #5 – Details of Abutment Supports	54
3.26a	Bridge #6 – Plan	55

LIST OF ILLUSTRATIONS (Cont'd)

FIGURE	TITLE	PAGE
3.26b	Bridge #6 – Developed Elevation	56
3.26c	Bridge #6 – Section at Pier	57
3.26d	Bridge #6 – Section at Abutment	58
3.26e	Bridge #6 – End Elevation at Abutment	59
3.26f	Bridge #6 – Section Through Integral Cap Beam	60
3.26g	Bridge #6 – Framing Plan	61
3.26h	Bridge #6 – Horizontal Section Through Column	62
3.26i	Bridge #6 – Horizontal Section Through Drilled Shaft	63
3.27	Bridge #6 - Finite Element Model	64
3.28	Bridge #6 - Pier Geometry and Element Layout	66
3.29	Bridge #6 – Orientation of Member Local Axis	67
3.30	Bridge #6 – Abutment Geometry	69
3.31	Bridge #6 - Soil Spring Configuration at Abutments	71
4.1	Acceleration Time Histories of the Northridge – Arleta Record	76
4.2	Acceleration Time Histories of the Northridge-Pacioma Dam (downstream) Record	76
4.3	Response Spectra for 1994 Northridge – Arleta Record	77
4.4	Response Spectra for 1992 Landers – Yermo Record	78
4.5	Distance (fault) Dependency of Response Spectral Ratios (V/H) for M6.5 at Rock and Soil Sites	79
4.6	Magnitude Dependency of Response Spectral Ratios (V/H) at Fault Distances 1 and 20 km	80
4.7	Horizontal & Vertical Spectra for Fault Distances 1, 5, 10, 20, 40 km; Magnitude 6.5 and Soil Site Conditions	82
4.8	Horizontal & Vertical Spectra for Fault Distances 1, 5, 10, 20, 40 km; Magnitude 6.5 and Rock Site Conditions	82
4.9	Horizontal & Vertical Spectra for Fault Distances 1, 5, 10, 20, 40 km; Magnitude 7.5 and Soil Site Conditions	83
4.10	Horizontal & Vertical Spectra for Fault Distances 1, 5, 10, 20, 40 km; Magnitude 7.5 and Rock Site Conditions	83
4.11	Response Spectra for Recorded Motions for Cape Mendocino Record	84
4.12	Spectra of the Frequency-scaled Record for Cape Mendocino & the Corresponding Target Spectra	84
4.13	Frequency-scaled Acceleration Time Histories of the Northridge – Arleta Record	85
6.1	Variation of Vertical Deck Moment Ratio of Three to Two Components Response at Pier Across the Six Bridges and Distance for Magnitude 7.5 and Rock	90
6.2	Variation of Vertical Deck Moment Ratio of Three to Two Components Response at Mid-span Across the Six Bridge and Distance for Magnitude 7.5. and Rock	91

LIST OF ILLUSTRATIONS (Cont'd)

FIGURE	TITLE	PAGE
6.3	Variation of Vertical Deck Moment to DL Ratio at Pier Across the Six Bridges and Distance for Magnitude 7.5 and Rock	91
6.4	Variation of Pier Axial Force Ratio of Three to Two Components Response Across the Six Bridges and Distance for Magnitude 7.5 and Rock	92
6.5	Variation of Pier Axial Force to DL Ratio Across the Six Bridges and Distance for Magnitude 7.5 and Rock	92
6.6	Variation of Vertical Deck Moment Ratio at Mid-span Across the Six Bridges and Distance for Magnitude 6.5 and Rock	93
6.7	Variation of Vertical Deck Moment to DL Ratio at Mid-span Across the Six Bridges and Distance for Magnitude 7.5 and Rock	93
6.8	Variation of Pier Axial Force "(3-2)/DL Ratio" Across the Six Bridges and Distance Magnitude 6.5 and Soil	101
6.9	Variation of Pier Axial Force "(3-2)/DL Ratio" Across the Six Bridges and Distance Magnitude 6.5 and Rock	102
6.10	Variation of Pier Axial Force "(3-2)/DL Ratio" Across the Six Bridges and Distance Magnitude 7.5 and Soil	102
6.11	Variation of Pier Axial Force "(3-2)/DL Ratio" Across the Six Bridges and Distance Magnitude 7.5 and Rock	103
6.12	Variation of Vertical Deck Shear Force "(3-2)/DL Ratio" at Pier Across the Six Bridges and Distance for Magnitude 6.5 and Soil	103
6.13	Variation of Vertical Deck Shear Force "(3-2)/DL Ratio" at Pier Across the Six Bridges and Distance for Magnitude 6.5 and Rock	104
6.14	Variation of Vertical Deck Shear Force "(3-2)/DL Ratio" at Pier Across the Six Bridges and Distance for Magnitude 7.5 and Soil	104
6.15	Variation of Vertical Deck Shear Force "(3-2)/DL Ratio" at Pier Across the Six Bridges and Distance for Magnitude 7.5 and Rock	105
6.16	Variation of Vertical Deck Moment "(3-2)/DL Ratio" at Pier Across the Six Bridges and Distance for Magnitude 6.5 and Soil	105
6.17	Variation of Vertical Deck Moment "(3-2)/DL Ratio" at Pier Across the Six Bridges and Distance for Magnitude 6.5 and Rock	106
6.18	Variation of Vertical Deck Moment "(3-2)/DL Ratio" at Pier Across the Six Bridges and Distance for Magnitude 7.5 and Soil	106
6.19	Variation of Vertical Deck Moment "(3-2)/DL Ratio" at Pier Across the Six Bridges and Distance for Magnitude 7.5 and Rock	107
6.20	Variation of Vertical Deck Moment "(3-2)/DL Ratio" at Mid-span Across the Six Bridges and Distance 6.5 and Soil	107
6.21	Variation of Vertical Deck Moment "(3-2)/DL Ratio" at Mid-span Across the Six Bridges and Distance for Magnitude 6.5 and Rock	108
6.22	Variation of Vertical Deck Moment "(3-2)/DL Ratio" at Mid-span Across the Six Bridges and Distance for Magnitude 7.5 and Soil	108
6.23	Variation of Vertical Deck Moment "(3-2)/DL Ratio" at Mid-span Across the Six Bridges and Distance for Magnitude 7.5 and Rock	109

LIST OF TABLES

TABLE	TITLE	PAGE
3.1	Bridge #1 - Section Properties	14
3.2	Bridge #2 - Properties of Superstructure	24
3.3	Bridge #2 - Elastomeric Bearing Spring Constants	27
3.4	Bridge #4 - Section Properties for Model	40
3.5	Bridge #6 - Lateral Spring Constants for Drilled Shaft	68
3.6	Bridge #6 - Spring Constants for Abutment Springs	71
3.7	Configurations & Dimensions of the Berger/ABAM Seven Series of Bridges	72
3.8	Values of Vertical Modal Percentage Mass Participation for Each Bridge Less Than Periods 0.1, 0.15, 0.2, & 0.3 Seconds	72
3.9	Data for Vertical Modes with Vertical Mass Participation Ratios Greater Than 2% for Bridge #1	73
3.10	Data for Vertical Modes with Vertical Mass Participation Ratios Greater Than 2% for Bridge #2	73
3.11	Data for Vertical Modes with Vertical Mass Participation Ratios Greater Than 2% for Bridge #3	73
3.12	Data for Vertical Modes with Vertical Mass Participation Ratios Greater Than 2% for Bridge #4	73
3.13	Data for Vertical Modes with Vertical Mass Participation Ratios Greater Than 2% for Bridge #5	74
3.14	Data for Vertical Modes with Vertical Mass Participation Ratios Greater Than 2% for Bridge #6	74
4.1	List of Selected Time History Records for Frequency Scaling	81
5.1	Computing Time Step for Time-history Analyses of Each Bridge	88
6.1	Locations on Each Bridge Where Response Quantities are Monitored	89
6.2	Bridge #1 – Time History Analysis Using Frequency-scaled Records	95
6.3	Bridge #4 – Time History Analysis Using Frequency-scaled Records	96
6.4	Bridge #5 – Time History Analysis Using Frequency-scaled Records	97
6.5	Bridge #5 – Time History Analysis Using Frequency-scaled Records	98
6.6	Bridge #5 – Time History Analysis Using Frequency-scaled Records	99
6.7	Peak Spectral Acceleration & Corresponding Period for the Response Spectra Used in the Study	100
6.8	Fault Distance Zones and Corresponding Dead Load Multiplier for All Bridges Observed for Soil Sites and a Magnitude 6.5 Event in Figures 6.8, 6.12, 6.16, and 6.20	110
6.9	Fault Distance Zones and Corresponding Dead Load Multipliers for All Bridges Observed for Rock Sites and a Magnitude 6.5 Event in Figures 6.9, 6.13, 6.17, and 6.21	111

LIST OF TABLES (cont'd)

TABLE	TITLE	PAGE
6.10	Fault Distance Zones and Corresponding Dead Load Multipliers for All Bridges Observed for Soil Sites and a Magnitude 7.5 Event in Figures 6.10, 6.14, 6.18, and 6.22	112
6.11	Fault Distance Zones and Corresponding Dead Load Multiplier for All Bridges Observed for Rock Sites and a Magnitude 7.5 Event in Figures 6.11, 6.15, 6.19, and 6.23	113
6.12	Fault Distance Zones and Corresponding Dead Load Multipliers for Bridges 1, 3 and 4 Observed for a Magnitude 6.5 Event in Figures 6.8 to 6.23	114
6.13	Fault Distance Zones and Corresponding Dead Load Multipliers for Bridges 1, 3 and 4 Observed for a Magnitude 7.5 Event in Figures 6.8 to 6.23	115
6.14	Fault Distance Zones and Corresponding Dead Load Multipliers for Bridges 1 and 4 Observed for a Magnitude 6.5 Event in Figures 6.8 to 6.23	116
6.15	Fault Distance Zones and Corresponding Dead Load Multipliers for Bridges 1 and 4 Observed for a Magnitude 7.5 Event in Figures 6.8 to 6.23	117
6.16	Comparison of Absolute Response Values for Shear at Mid-span with Lower Bound Shear Capacity Values for Bridges 1 to 6	118
6.17	Data for Vertical Modes with Vertical Mass Participation Ratios Greater Than 2% for Models of Bridge #4 with Vertical Deck Stiffnesses of 25%, 100%, and 400%	120
6.18	Data for Vertical Modes with Vertical Mass Participation Ratios Greater Than 2% for Models of Bridge #6 with Vertical Deck Stiffnesses of 25%, 100%, and 400%	120
6.19	Selected Results of a Response Spectrum Analysis Performed on Bridge #4 for 25%, 100%, and 400% of the Vertical Deck Stiffness	121
6.20	The Results of a Response Spectrum Analysis Performed on Bridge #6 for 25%, 100%, and 400% of the Vertical Deck Stiffness	121
6.21	Data for Vertical Modes with Vertical Mass Participation Ratios Greater Than 2% for Spring and Fixed Foundations of Bridge #4	122
6.22	Data for Vertical Modes with Vertical Mass Participation Ratios Greater Than 2% for Spring and Fixed Foundations of Bridge #6	122
6.23	Results of a Response Spectrum Analysis Performed on Bridge #4 for Fixed and Spring Foundations	123
6.24	Selected Results of a Response Spectrum Analysis Performed on Bridge #6 for Fixed and Spring Foundations	123
6.25	Comparison of Results From Analyses of Bridge #4 Using Three Different Directional Combination Rules and Frequency-scaled Time History Records	125
6.26	Comparison of Results From Analyses of Bridge #5 Using Three Different Directional Combination Rules and Frequency-scaled Time History Records	125
7.1	Properties of Nonlinear Pier Elements	128
7.2	Bridge #6 - Linear Time History Analysis Using Frequency-scaled Records in SAP2000	131

LIST OF TABLES (cont'd)

TABLE	TITLE	PAGE
7.3	Bridge #6 – Comparison of ANSR-II and SAP2000 Linear Time History Analysis Results	132
7.4	Bridge #6 – Comparison of Results From Non-linear and Linear Time History Analysis Using Frequency-scaled Records in ANSR-II	133
7.5	Bridge #6 – Comparison of (3-2)/DL Ratios for the Linear and Non-linear Response Using ANSR-II	134
7.6	Bridge #6 - Response of Non-linear ANSR-II Model With 25% of the Vertical Deck Stiffness	135
8.1	Fault Distance Zones and Corresponding Dead Load Multiplier for all Bridges Observed for Rock and Soil Site Conditions and a Magnitude 6.5 Event	140
8.2	Fault Distance Zones and Corresponding Dead Load Multiplier for All Bridges Observed for Rock and Soil Site Conditions and a Magnitude 7.5 Event	141

SECTION 1
INTRODUCTION

The objective of this study is to determine under what conditions the vertical component of seismic ground motion is critical in determining the demands placed on key elements of typical highway structures. In current design practice, the vertical component of motion is not usually included in the analysis of bridges or buildings, though the Uniform Building Code [1997] does specify increased multipliers on dead loads that are intended to approximate its effects. These multipliers are 0.9DL and 1.2DL for non-isolated buildings, and 0.8DL and 1.2DL for isolated buildings. Vertical spectral shapes are not defined in current bridge design codes, however when the vertical component is included, it is normally specified as a spectrum with an amplitude two-thirds of the horizontal spectrum. In recent years, various researchers have conducted statistical studies on large numbers of strong ground motion records that show this vertical-to-horizontal ratio grossly underestimates the strength of the vertical component in the near fault (< 5km) region and at short periods.

The research approach in the current work is to analyze a representative group of bridges with a range of input ground motions that include and exclude the vertical component of motion. The results of the dynamic analyses are compared for both cases and conclusions are drawn as to when the vertical component can be safely ignored and when its effects should be included in the design of highway bridges. The scope of the study involves linear analyses of finite element models of six typical highway bridges using a broad range of input motions. These elastic models were obtained from the Berger/ABAM series of bridges assembled as seismic design examples for the Federal Highway Administration. Both time history and response spectrum analyses are performed, and results compared. One bridge from this group that shows sensitivity to vertical excitation is selected for nonlinear dynamic analyses, again including and excluding the vertical component of motion.

On the basis of the results from these linear and nonlinear analyses, recommendations are made regarding cases where vertical motions should explicitly be included in design, where the effects of vertical motions can be adequately addressed by simple load combination rules, and finally, cases where the impact of vertical motions is less than 10% and thus can be ignored from a design perspective.

Section 2 gives a summary of previous research work done on the effects of the vertical component of motion on bridge decks, piers, foundations, bearings and hinges. Section 3 provides a description of each of the six bridges analyzed, including their physical dimensions, element properties used in the structural model, and vertical dynamic characteristics. Section 4 describes the characteristics of the vertical component of motion and gives details of response spectra and frequency scaled time history records used for input motions in the bridge analyses. Details of the parameters used in the linear dynamic analysis of each bridge are given in Section 5. Section 6 presents the results of the analyses and provides recommendations based on results from these analyses. Results from the response spectrum and time history analyses are compared. The effects of varying vertical deck stiffness and foundation fixity on the vertical structural response are reported. Response spectrum analysis results using three different directional combination rules are compared.

This report ends with five appendices, which contain response ratios computed from response spectrum analyses of the six bridges, response ratios computed from response spectrum analyses for varying deck stiffnesses and foundation fixity in bridge numbers 4 and 6, mode shapes with modal mass participation ratios greater than 10% for the six bridges, SAP2000 input files, and the ANSR-II input file for Bridge 6. These appendices are provided on MCEER's web site at *http://mceer.buffalo.edu.*

SECTION 2
LITERATURE REVIEW

Saadeghvaziri and Foutch [1988] completed the first major analytical study into the effects of vertical acceleration on bridges in 1988. A summary of previous analytical studies presented in their report showed that previous work on this topic was limited to the study of building structures between 6 and 10 stories. More recently, Broekhuizen [1996] and Yu [1996], in their Masters and Ph.D. theses respectively, conducted parametric studies into the effects of vertical acceleration on bridges. Their study centered on three overpasses of the SR14/I5 Interchange located about ten miles north of the epicenter of the 1994 Northridge earthquake. Two of these bridges partially collapsed during the earthquake. In the area of bridge design, Gloyd [1997] presented procedures implemented by the Orange County Transportation Corridor Agencies that accounted for the effects of the vertical component of motion on sixty new highway bridges. The majority of the following review presents a summary of the effects of the vertical component of motion on individual bridge elements as reported in the above studies.

2.1 Decks

Yu [1996] conducted an extensive study into the effects of vertical acceleration on prestressed concrete box-girder bridge decks. The study included a parametric study of single and multi-span 2D frames. Realistic models of straight and curved bridges were analyzed. The realistic models were built by using data from Ramp L, Ramp M and Ramp C of the SR14/I5 Interchange. The effect of varying the span inclination (grade) and differential support excitation in the vertical direction were investigated in these models. One curved bridge model was analyzed for three different orientations of horizontal input motions. The study concluded that the vertical component of motion is the most important when assessing seismic effects on the response of bridge decks in the vertical direction.

The single span models used in the parametric study consisted of 2D frames with rigid and hinged deck-column connections. The two and three span models consisted of monolithic deck-column connections with hinges placed at 1/10 span length from connection in half the models. Horizontal-only and vertical-only motions of the Northridge record at Sylmar Hospital were input for varying span and column lengths. Results showed that span lengths with fundamental vertical frequencies close to the dominant vertical excitation frequencies experienced the highest vertical acceleration. The longer spans showed an increase in vertical acceleration as frequencies of their higher modes moved into the range of the dominant excitation frequency. The highest accelerations were found at the hinges for both the horizontal and vertical input in the multi-span frames. Varying the column length showed that as the column height increased, the fundamental frequency of higher axial vibration modes moved into the range of the dominant excitation frequency leading to higher maximum accelerations in the deck. Longitudinal horizontal input motion was found to excite the vertical deck modes of vibration of a frame configuration with long spans and stubby columns. The study showed that the deck acceleration can be amplified by as much as a factor of three with respect to the vertical input motion.

Three simplified models of the internal spans of Ramp L of the SR14/I5 Interchange were analyzed for different configurations of their adjacent spans to compare the results to the complete model. The simplified models consisted of a single-span, two-spans and three-spans with hinges near the external columns. The configurations for adjacent spans varied in longitudinal restraint from none to full. Partial restraint was achieved by adding lumped masses to the external columns or adding the adjacent spans. It was found that all configurations gave a vertical response closer to the complete model than the horizontal response and the analysis of any one interior span will be improved by including several adjacent spans.

Straight and curved models of Ramp L were analyzed and the results compared. Two different straight models were created, one with fixed foundations and the other with piled foundations. Longitudinal horizontal motions only (i.e. no transverse) were used for the straight models. The vertical response of these two straight models was similar. The vertical component of motion was found to be the most important contributor to the vertical deck accelerations in both models. The curved model was analyzed using three different horizontal input orientations of the orthogonal motions and the results showed that the orientation can affect the vertical response of the end spans of the bridge. The curved models with both horizontal motions showed a larger vertical response than the straight models with a single horizontal motion.

Curved models of Ramp M and Ramp C were created and analyzed using the real orientation of the horizontal input motions for the Sylmar Hospital record. In both models, amplification factors of two were found at some hinges leading the author to speculate that separation of joints or unseating and fall-off of girders could take place when the connections are weak or previously damaged.

The Sylmar Hospital record was used to calculate the forces in the deck of the three curved models. The mean response ratio for the three-component to two-component input for the shear forces in the deck at the piers was found to be 1.17 with a 95% confidence interval between 1.14 and 1.20. For the bending moment at mid-span and supports, the mean ratio is 1.14 with a 95% confidence interval between 1.12 and 1.17.

The effect of differential support excitations in the vertical direction was investigated by allowing for the lag time of wave propagation velocities varying between 1000 m/sec and 10000 m/sec. Ramp M, Ramp C and Ramp L were used for this study. The vertical component of the Sylmar record was assumed to be the motion used at abutment-1 at an epicentral distance of 15 km. Differential support excitation was shown to have little effect except at hinges with longer links to the pier-girder joints where accelerations were up to 2.5 times the values of those obtained by having the same excitation at each support.

Ramp M, Ramp C and Ramp L were analyzed with inclined spans. The vertical component of motion was again found to have the dominant effect on the vertical response but in some cases such as spans 6, 7 and 8 of Ramp M, the vertical component contributed to only about half of the total vertical acceleration.

Broekhuizen [1996] investigated the effects of vertical acceleration on prestressed concrete bridge decks designed using the "load balancing" method. Using this design procedure, approximately two-thirds of the dead load of the deck is balanced by the bending moment due to the eccentricity of the prestressing force. The tensile stresses in the concrete of the decks of Ramp M, Ramp C and Ramp L were calculated assuming a 1g upward acceleration. These stresses were then compared to the allowable stresses specified in the AASHTO codes. It was found that allowable stresses in the deck can be exceeded but the author concluded that since the 1g acceleration was instantaneous, the cracking mechanism would not have time to start and any tensile cracks which did form would be controlled by the continuous reinforcement in the deck.

Gloyd [1997] presented design criteria used in the design of 60 prestressed concrete box-girder bridges for the Orange County California Transportation Corridor Agencies that allowed for the effects of vertical ground motion on the superstructure. The procedure involved the use of vertical spectral accelerations having amplitude equal to two-thirds of site specific horizontal spectra or Caltrans standard spectra. Design values for vertical deck shear and bending moment for two continuous span bridges show that the

dynamic response from vertical acceleration can be much larger than the structure dead load effects, and that a reversal of flexure can occur at both the positive and negative moment areas.

Saadeghvaziri and Foutch [1988] developed finite element models to study the inelastic behavior of two-span reinforced concrete bridges under combined earthquake horizontal and vertical motions. However, the study centered on the response of the substructure and the effects of the vertical component of motion on decks were not reported.

2.2 Columns/Abutments

Saadeghvaziri and Foutch [1988] conducted an analytical study into the effects of vertical accelerations on bridge columns and abutments using three-dimensional finite element models of eight bridges similar to the California RC box girder spans cast monolithically with the pier and abutments. The nonlinear finite element program they developed was capable of modeling the inelastic behavior of reinforced concrete columns under combined horizontal and vertical earthquake motions. The ground motion used for the study was an artificial accelerogram that generates almost the same acceleration in structures with frequencies in the range of 2 to 10Hz. The study concluded that for earthquake motions with effective peak accelerations (EPA) of 0.4g or less, the additional damage caused by the vertical component is minimal. On the other hand, for earthquake motions with EPA of 0.7g, the addition of the vertical component resulted in considerably more damage. The study showed that varying axial force in the columns results in pinched hysteresis that causes larger horizontal displacements and fluctuation in the shear capacity of the column. Results also showed that tensile forces can develop in the abutments due to vertical acceleration.

Yu [1996] analyzed the forces in all the piers of Ramp M, Ramp L and Ramp C using 3D linear models and the Sylmar Hospital record as an input motion. The study found a 21% increase in the axial force and a 7% change in the longitudinal moment due the addition of the vertical component. The change in the transverse moment was found to be negligible. Nonlinear fiber models of Ramp M and Ramp L were also built with constant reinforcement used in all the spans. The analysis results showed that the effect of the vertical component on the member force is insignificant if there is no plastic hinge formed under the action of the horizontal motions.

Broekhuizen [1996] compared forces developed in the piers of linear models of Ramp M, Ramp L and Ramp C due to the horizontal only motions of the Sylmar Hospital record, the artificial earthquake for the bridge site from Lamont-NCEER, and an artificial earthquake developed from the UBC/AASHTO spectrum. Using a Caltrans classification that assumes a plastic hinge to have formed when the ratio of the moment in the column due to earthquake plus dead load to its nominal capacity is greater than 1.5, the study found that the above motions caused four, one and nine piers to form hinges in the above bridges, respectively. The three bridges included 26 piers in total.

The bending moments in the piers due to the three-component input and two-component input only were compared using the UBC/AASHTO spectrum compatible motions. The amplitude of the vertical component was two-thirds that of the horizontal motions. It was found that the moments were increased by an overall average of 5 to 10% by the addition of the vertical component.

Soon after the Northridge earthquake, Priestley et al [1994] presented a damage analysis of seven bridges that had sections collapse during that event. Four of the seven bridges were found to have failed as a result of inadequate shear strength in columns that were stiffer and/or flexurally stronger than in other bents. Two more bridges failed by the formation of plastic hinges at locations where the effective column

height was shortened by either architectural flares or a channel wall built integral with the columns. The remaining bridge failed by unseating at highly skewed internal superstructure movement joints as a result of large rotations in the adjoining frames. The analyses conducted on the bridges were limited to lateral "push" analyses for equivalent elastic strength. On the basis of these analyses and a review of the accelerograms of the Northridge earthquake, it was concluded by the authors that the vertical component of motion did not cause or contribute to the collapse of the above bridge sections.

2.3 Foundations

Yu [1996] compared the effect of the vertical component of motion on shallow and deep foundations. The shallow foundations modeled were spread footings resting directly on soil and footings resting on pile groups. The deep foundations modeled were friction-bearing piles and end-bearing piles. The effect of the surrounding soil was modeled using distributed springs and dashpots along the soil interfaces. The single and multi-span frames with varying span lengths and column height were again used for this part of the study. These configurations were also modeled with rigid bases. The pile group and end-bearing pile foundations gave responses close to the fixed base models, whereas the spread footings and friction-bearing piles tended to give lower deck accelerations.

The response of the models was also obtained for varying pile lengths in the end-bearing and friction-bearing pile foundations. It was found that changing the length of end-bearing piles has no effect on the deck accelerations. The deck acceleration increased with increasing length of friction piles but it was concluded that this increase is insignificant over a practical range of lengths.

Soil stiffnesses were varied for spread footings and friction-pile foundations by using a range of soil shear wave velocities between 160 ft/sec and 1000 ft/sec. The maximum response was found to increase as the shear wave velocity increased (i.e. as the soil stiffness increased, the vertical stiffness of the foundations increased) and theoretically approach the values obtained with a rigid base.

2.4 Hinges

Broekhuizen [1996] analyzed the displacement at the hinges of Ramp M, Ramp L and Ramp C of the SR14/I5 Interchange using the Sylmar Hospital record with the vertical component included. The hinges were modeled by calculating the linear stiffness of the restrainers used in the retrofit of the bridges. The hinge seating width for these bridges is between 14" and 16", but some older bridges of this type have seating widths of 8". The displacement for all the hinges was found to be less than 4" except for displacements of 6" and 6.9" at two hinges in Ramp C.

Yu [1996] showed in a parametric study of multi-span 2D frames and 3D models of curved bridges that hinges located at one-tenth the length of the span from the piers can experience high vertical accelerations. In a separate part of the study, behavior of restrainers at expansion joints were studied using idealized elastic perfectly-plastic springs at hinge locations in a simple three-span bridge. This part of the study concluded that flexible restrainers (cable type) are a better choice over stiffer restrainers (bar type) provided that the joint seats are wide enough.

2.5 Bearings

Yu [1996] conducted a parametric study on the sliding behavior of concrete girders over elastomeric bearing pads by using a linear elastic spring in the vertical direction and an elastic perfectly-plastic spring in the horizontal direction with its elastic limit a function of the vertical reaction and the friction

coefficient. The bridge model consisted of two simply-supported spans resting on a single column at the center and pinned at the abutments. The parameters that varied were the column height, bearing pad stiffness, coefficient of friction and vertical component of motion. The friction coefficient varied between 0.1 and 0.5. The bearing horizontal stiffness varied between 275 kips/ft and 1710 kips/ft. The study found that the sliding amplitude is greater for shorter columns, and increasing the friction coefficient reduces the sliding amplitude while increasing the horizontal bearing stiffness reduces the vibration amplitude. The study concluded that " The effect of the vertical earthquake on the horizontal sliding over the bearing seats is not important as long as the vertical acceleration is less than 1g".

2.6 Summary

The review of previous studies on the effects of the vertical component of earthquakes on highway bridges showed that:

- Bridge decks with vertical frequencies close to the dominant excitation frequencies of the vertical input motion show the highest response.
- Prestressed concrete decks designed using the "load balancing" method will not experience significant damage from upward accelerations of up to 1g applied to the superstructure.
- Piers and abutments may experience tensile forces due to the vertical component of motion.
- Varying axial force in columns due to vertical motions can result in pinched hysteresis, which in turn can lead to larger horizontal displacements and a fluctuation in the shear capacity.

The above points show that the vertical component of motion does have an impact on bridges but to fully quantify its effects, a broader range of bridge types and ground motion parameters need to be included.

SECTION 3
BRIDGE DESCRIPTIONS

In 1996, the Federal Highway Administration funded the development of a series of seven detailed bridge design examples to illustrate the AASHTO seismic design requirements. The seven different bridges were chosen to be a representative sample of bridges in different states. The work was performed by BERGER/ABAM Engineers, Inc. of Seattle, WA and is detailed in Federal Highway Administration publication manuals FHWA-SA-97-006 through 012. Six of the seven bridges were utilized in this study.

Descriptions of bridge numbers 1 through 6 of the seven bridge design examples are given in this section. The description of each bridge includes the overall physical dimensions, structural materials and details of the finite element model. Properties of the elements used to model the deck, piers, abutments and foundations are given. Tables giving a summary of the vertical modal mass participation are shown for each bridge in Section 3.7.

3.1 Bridge No. 1

The configuration and geometry of the bridge are shown in Figure 3.1 (a to d). The superstructure is a two-span continuous prestressed concrete box-girder. The substructure elements are seat-type abutments and a single three-column bent. The intended seismic resisting mechanisms are as follows. In the transverse direction, both the superstructure and the relatively flexible bent act to resist transverse forces but the superstructure essentially acts as a simply supported horizontal beam that spans between pinned supports at the abutments. This behavior is illustrated in Figure 3.2. In the longitudinal direction, the intermediate bent columns are assumed to resist the entire longitudinal seismic force. This behavior is illustrated in Figure 3.3. The fundamental mode in the vertical direction is shown in Appendix C and has a period of 0.45 seconds as given in Table 3.9 in Section 3.7.

The abutments are seat-type abutments with space behind the end diaphragm that allows free longitudinal movement of the superstructure. The abutments are also assumed to allow free rotation about a vertical axis.

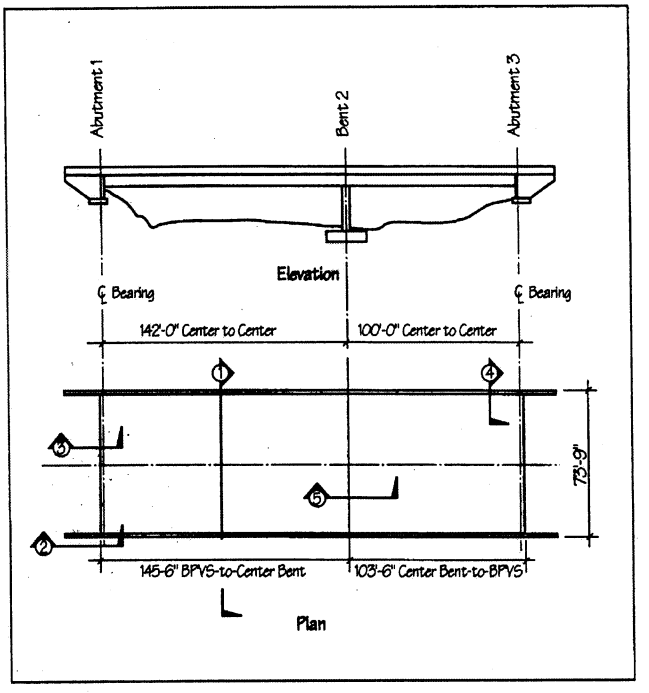

FIGURE 3.1a Bridge #1 - Bridge Layout

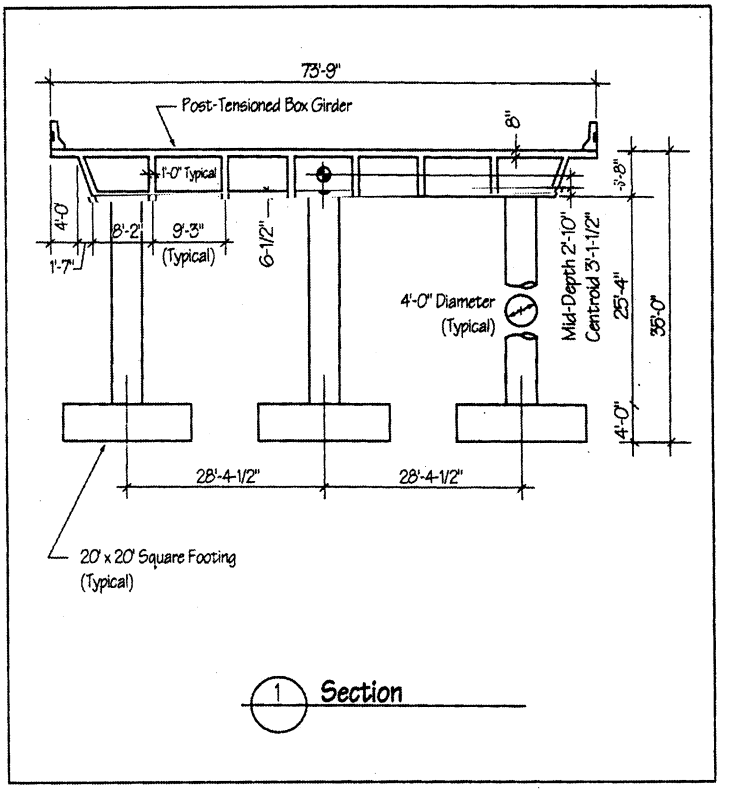

FIGURE 3.1b Bridge #1 - Bridge Layout

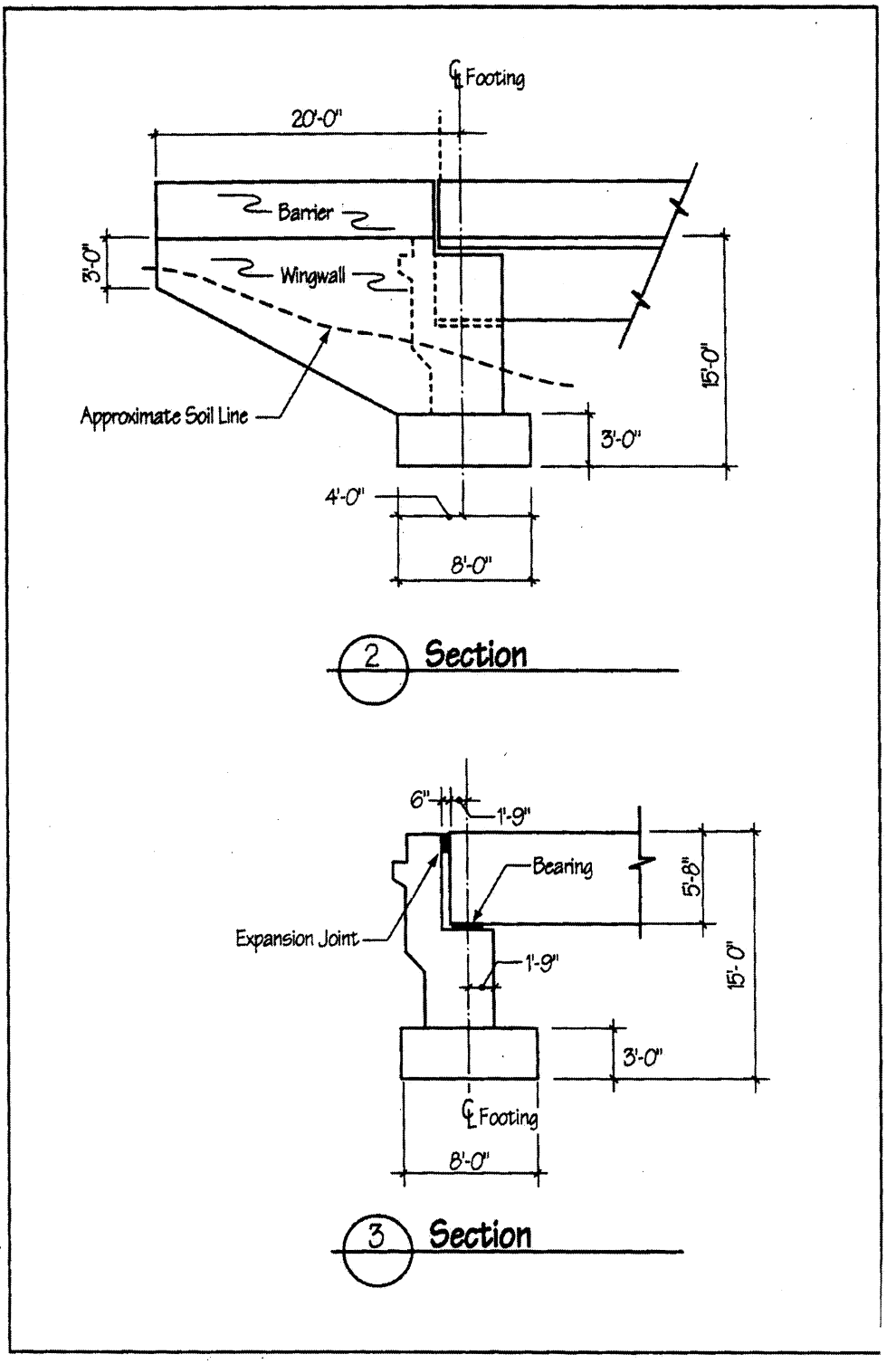

FIGURE 3.1c Bridge #1 - Bridge Layout

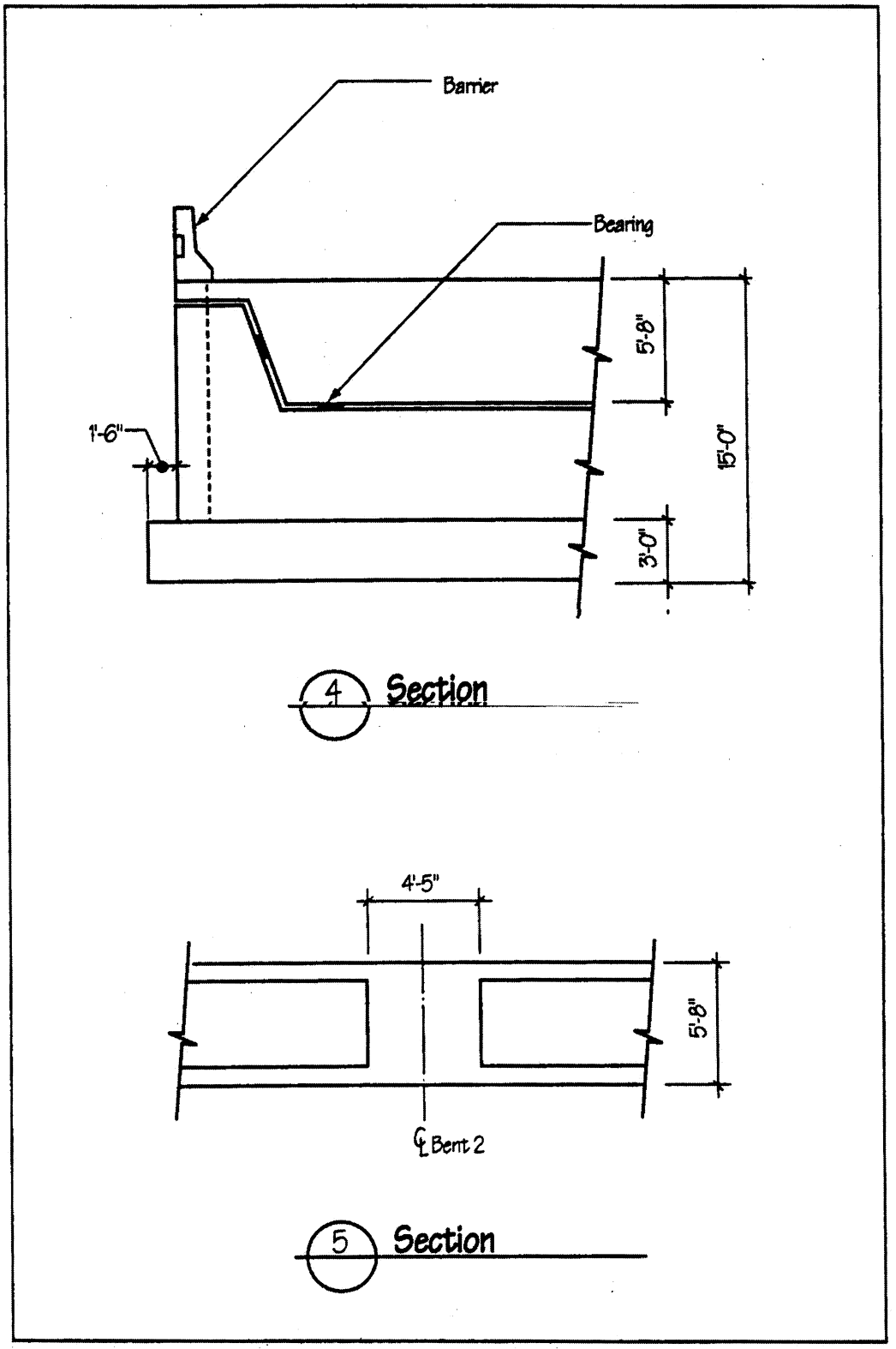

FIGURE 3.1d Bridge #1 - Bridge Layout

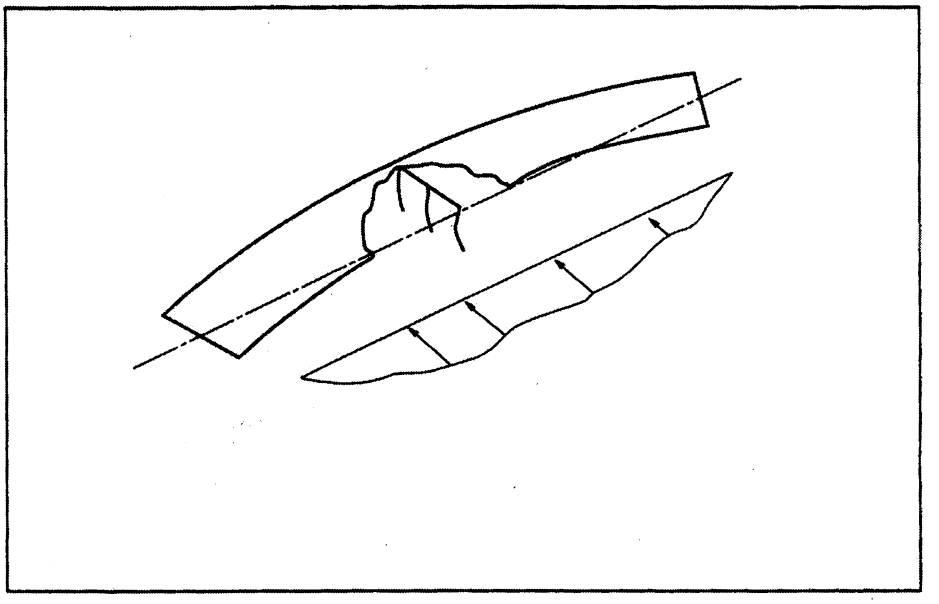

FIGURE 3.2 Bridge #1 - Transverse Seismic Behavior

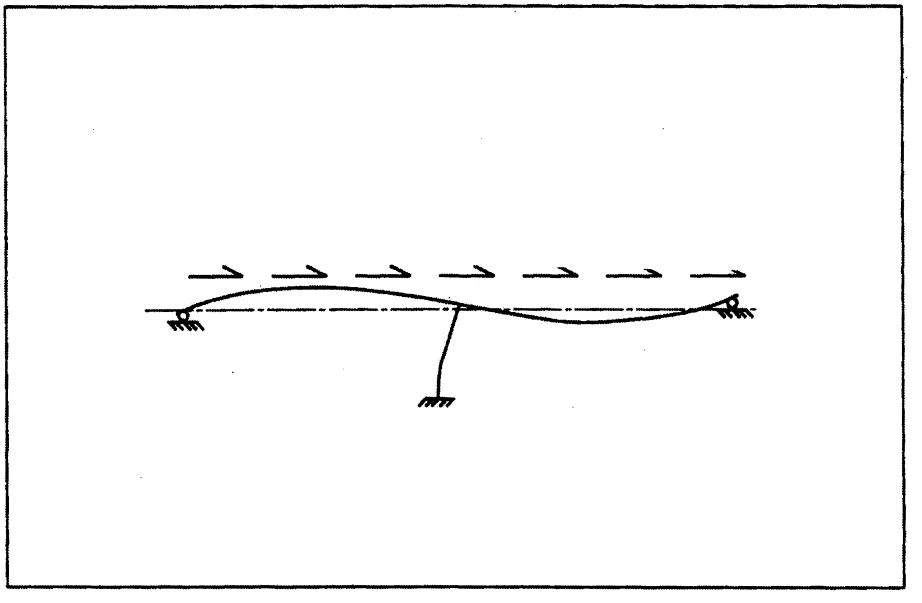

FIGURE 3.3 Bridge #1 - Longitudinal Seismic Behavior

Description of Model

The model used is shown in Figure 3.4 and includes a single line of frame elements for the superstructure and individual elements for the columns and cap beam. Cross-sectional details of each bridge element are

shown in Table 3.1. The SAP2000 text input file for the model shown in Figure 3.4 is given in Appendix D.

TABLE 3.1 Bridge #1 - Section Properties

	CIP Box Superstructure	Bent Cap Beam	Bent Columns (Each)
Area (ft^2)	120	25	12.57
Ix – Torsion (ft^4)	60000	10000	25.00
Iy – (ft^4)	575	1E+08	12.57
Iz – (ft^4)	51000	1E+08	12.57
Density (lb/ft^3)	157.5	150	150

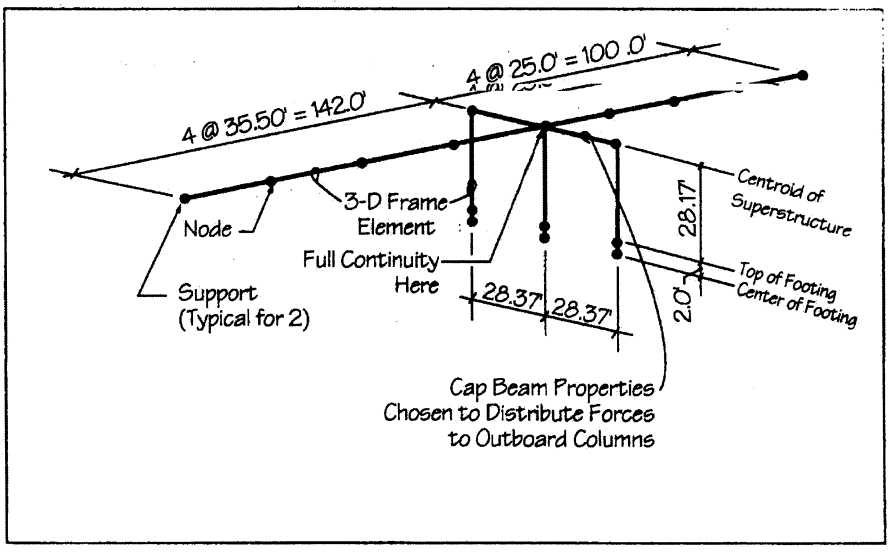

FIGURE 3.4 Bridge #1 - Finite Element Model

Superstructure

As shown in Figure 3.4, the superstructure has been collapsed into a single line of 3-D frame elements. Because the superstructure is integral with the bent, full continuity is used at the seismic model's superstructure-bent intersection. Moments of inertia and torsional stiffness of the superstructure shown in the SAP2000 input files in Appendix D are based on uncracked cross-sectional properties.

Bent

The bent is modeled with 3-D frame elements that represent the cap beam and individual columns. In the actual structure, internal forces are transferred between the superstructure and the bent in a nearly continuous fashion along the length of the cap beam. In the seismic model, the superstructure forces are transferred at the single point where the superstructure and bent intersect. Due to this difference, the forces in the cap beam from the seismic model do not represent "actual" forces very accurately, and the

stiffnesses of the cap beam must be adjusted to better represent "actual" distribution of forces to the columns. Figure 3.5 shows the relation between the actual column and the "stick" model of 3-D frame elements.

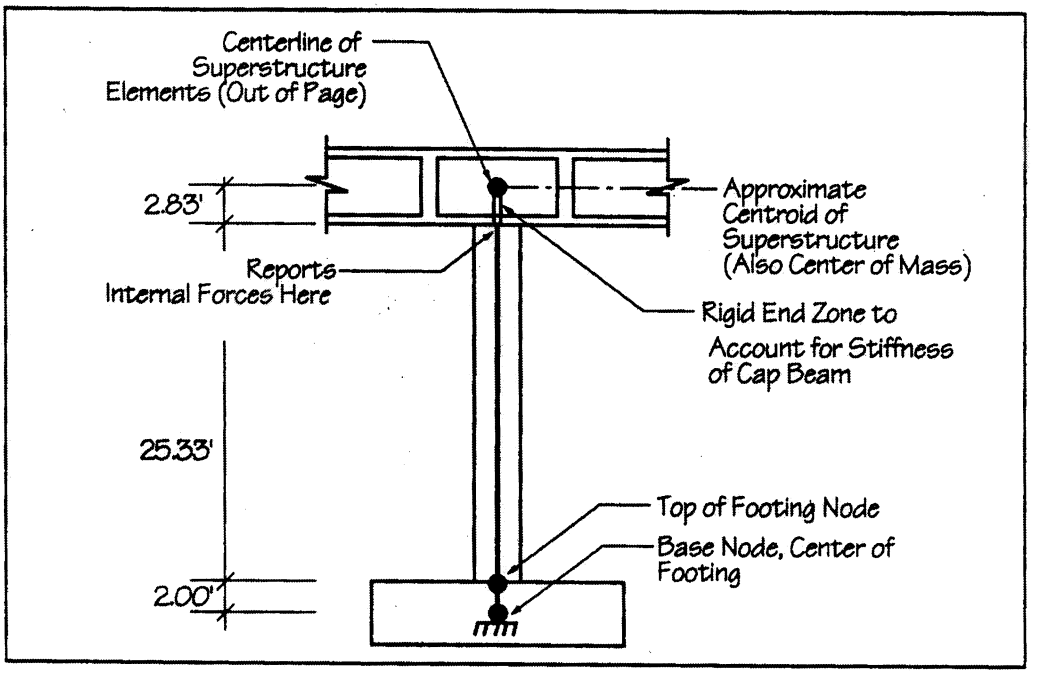

FIGURE 3.5 Bridge #1 - Details of Column Elements

The upper ends of the column elements have a rigid end zone to account for the stiffness of the cap beam. The centroidal axis (work line) of the superstructure was taken at the geometric center of the box girder. Only one element was used for the column between the top of footing and the superstructure. The moments of inertia and torsional properties of the columns are based on an uncracked section.

Bent and Abutment Foundation Stiffness

Bent Foundations

The footings were considered fixed against both translation and rotation.

As an approximation to the stiffness of the footing and soil for this model, the elastic properties of the column were used for an element that extended from the top of the footing to the mid-depth of the footing as shown in Figure 3.5.

Abutments

The model allows longitudinal response that is unrestrained at the abutment. The abutments are considered fixed against translation in the transverse direction. Abutment shear keys provide this restraint in the actual bridge. The restraints act either normal to or co-linearly with the superstructure centroidal axis (work line). They are also located at the centerline of the bearings in the longitudinal direction. Torsional response of the superstructure is restrained in the model by the abutments. Such fixity is

assumed to occur as the result of the gravity contact forces existing between the superstructure and the bearings.

3.2 Bridge No. 2

The configuration of the bridge is a three-span steel plate girder superstructure with a composite deck. The substructure elements are seat-type abutments and wall piers. The bridge is located on a rock site and all footings are founded on rock. The rock is a hard, fresh, and sound quartz biotite schist at all locations over the site. Figure 3.6 (a to g) provides details of the bridge configuration.

The alignment of the roadway over the bridge is straight and there is no vertical curve. The bridge has a 25-degree skew at all four substructure elements.

The bridge spans a river, and the two intermediate piers are located within the normal flow of the river. Due to the presence of the piers in the river, flow issues and ice loading have required that the intermediate piers be wall piers with a thick cross-section. Elastomeric bearings are placed at the juncture of the superstructure and the substructure elements to accommodate thermal movements. The fundamental mode in the vertical direction is shown in Appendix C and has a period of 0.26 seconds as given in Table 3.10 in Section 3.7.

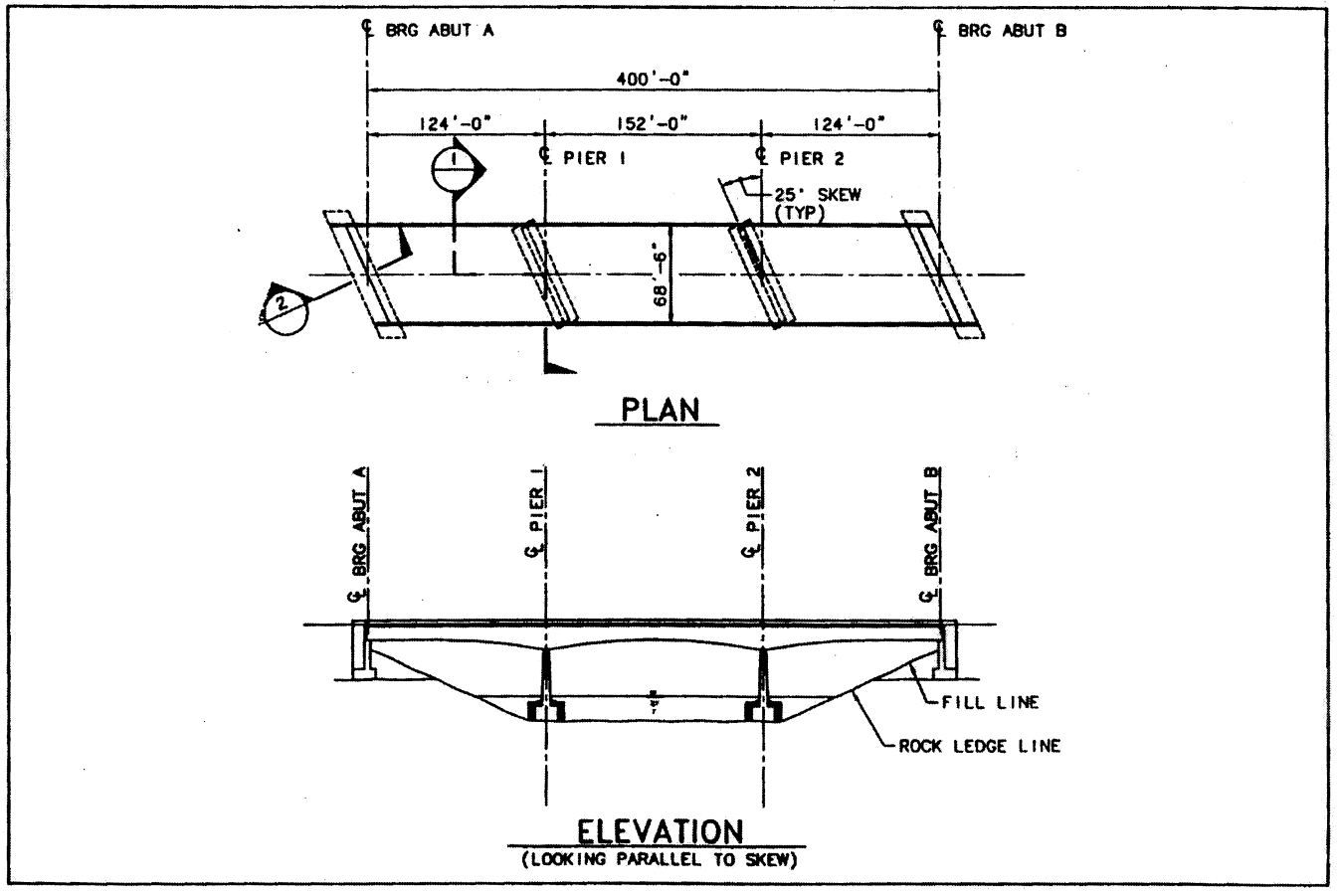

FIGURE 3.6a Bridge No. 2 – Plan and Elevation

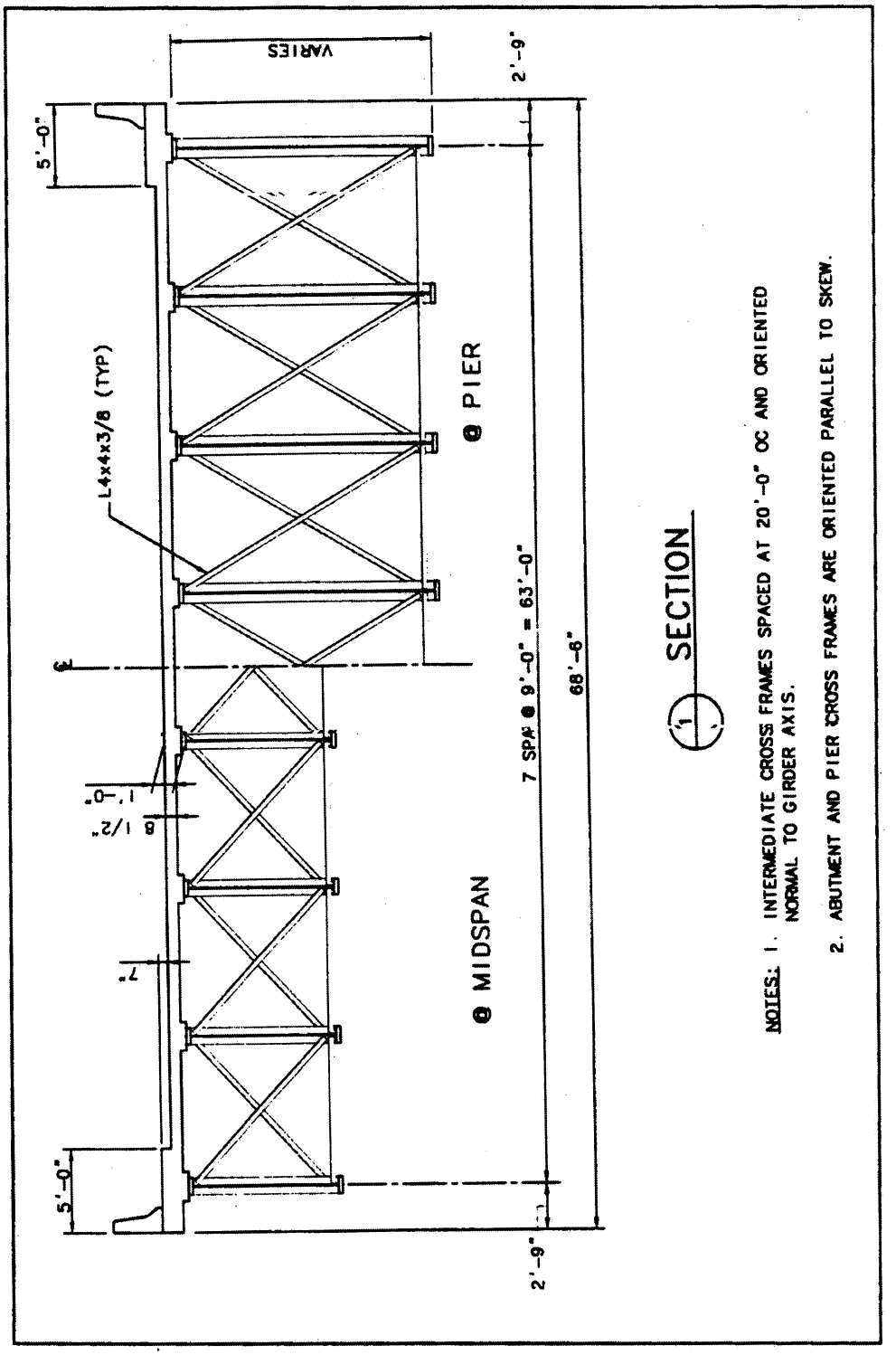

FIGURE 3.6b Bridge No. 2 – Typical Cross-section

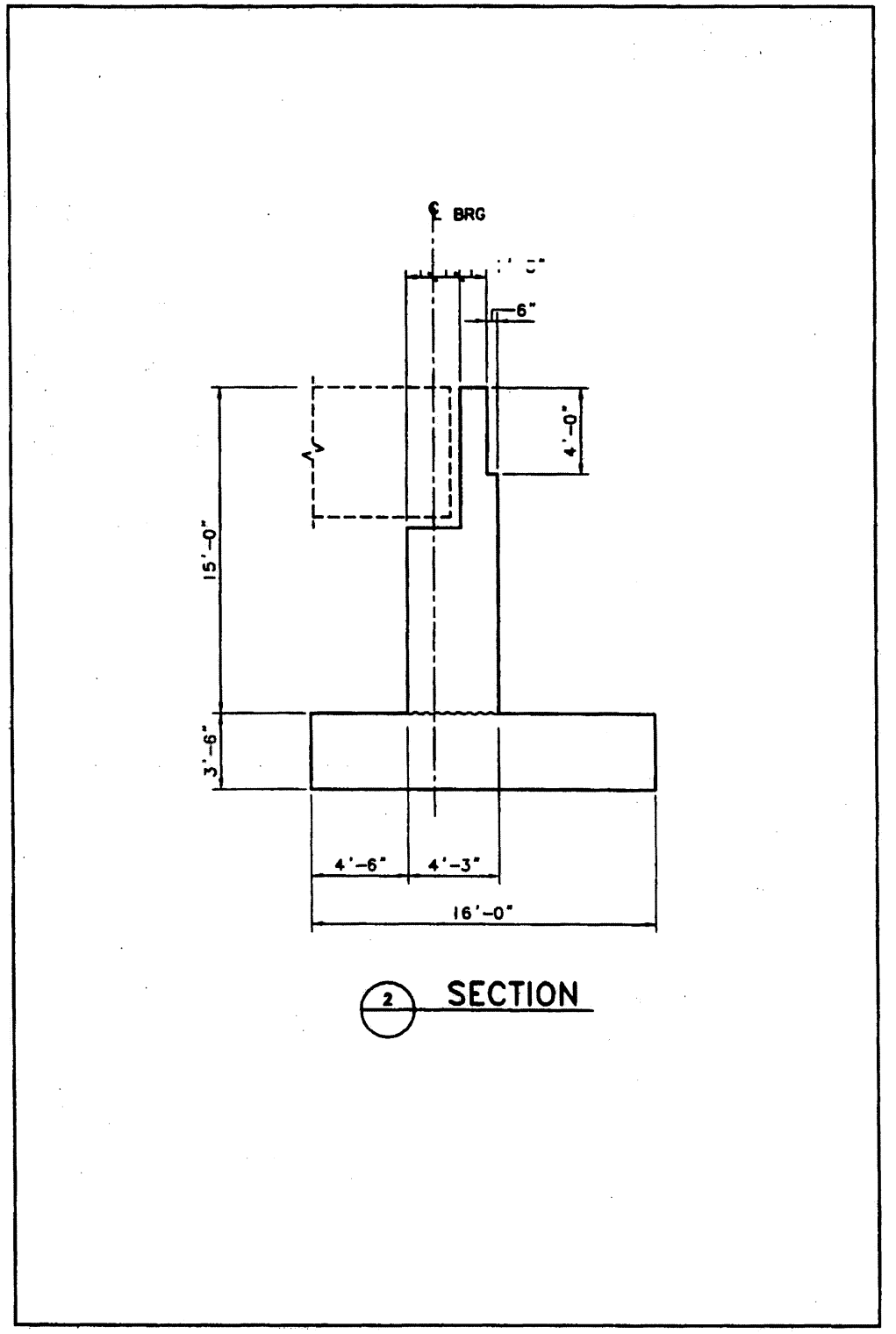

FIGURE 3.6c Bridge No. 2 – Seat Type Abutment

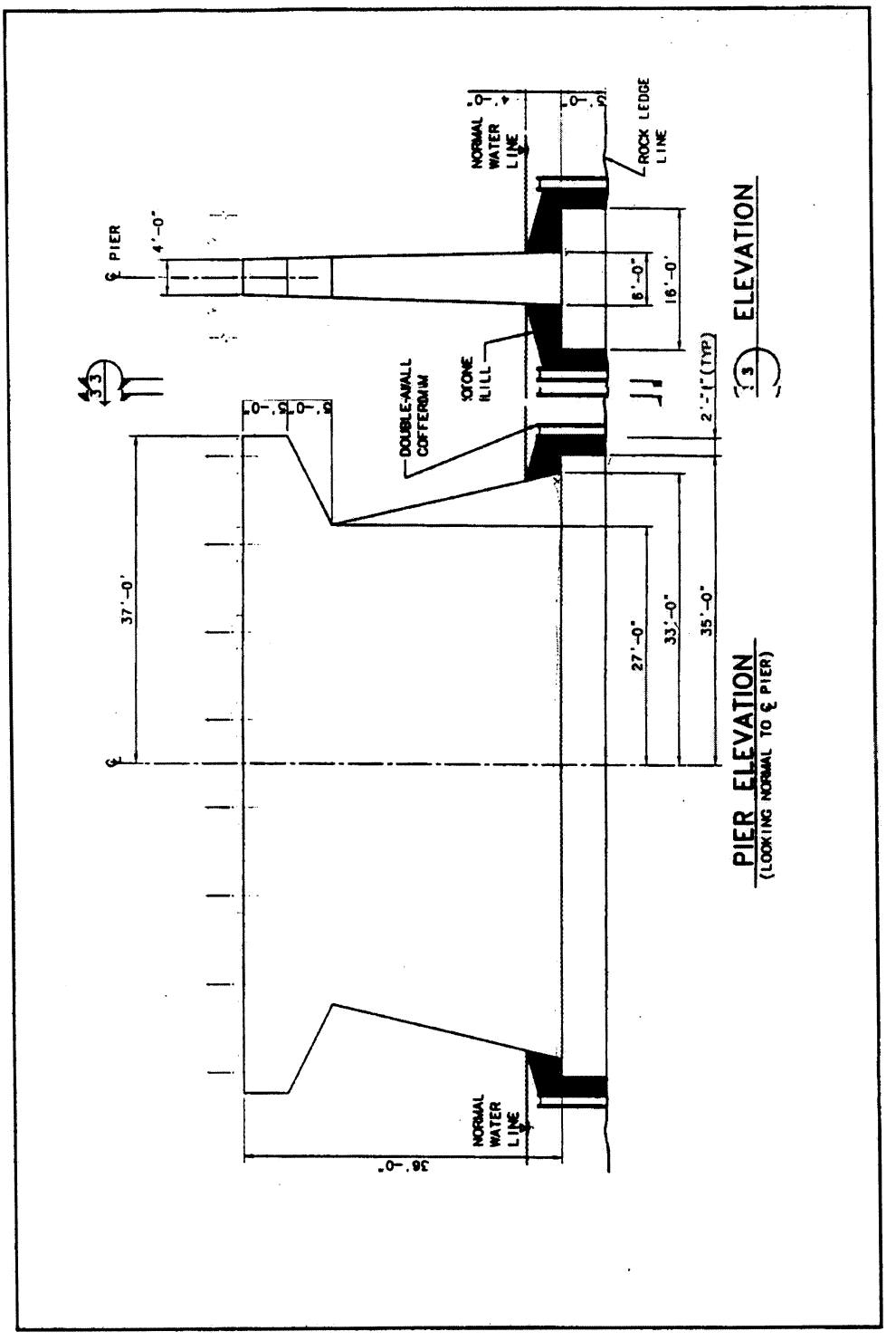

FIGURE 3.6d Bridge No. 2 – Pier Elevation

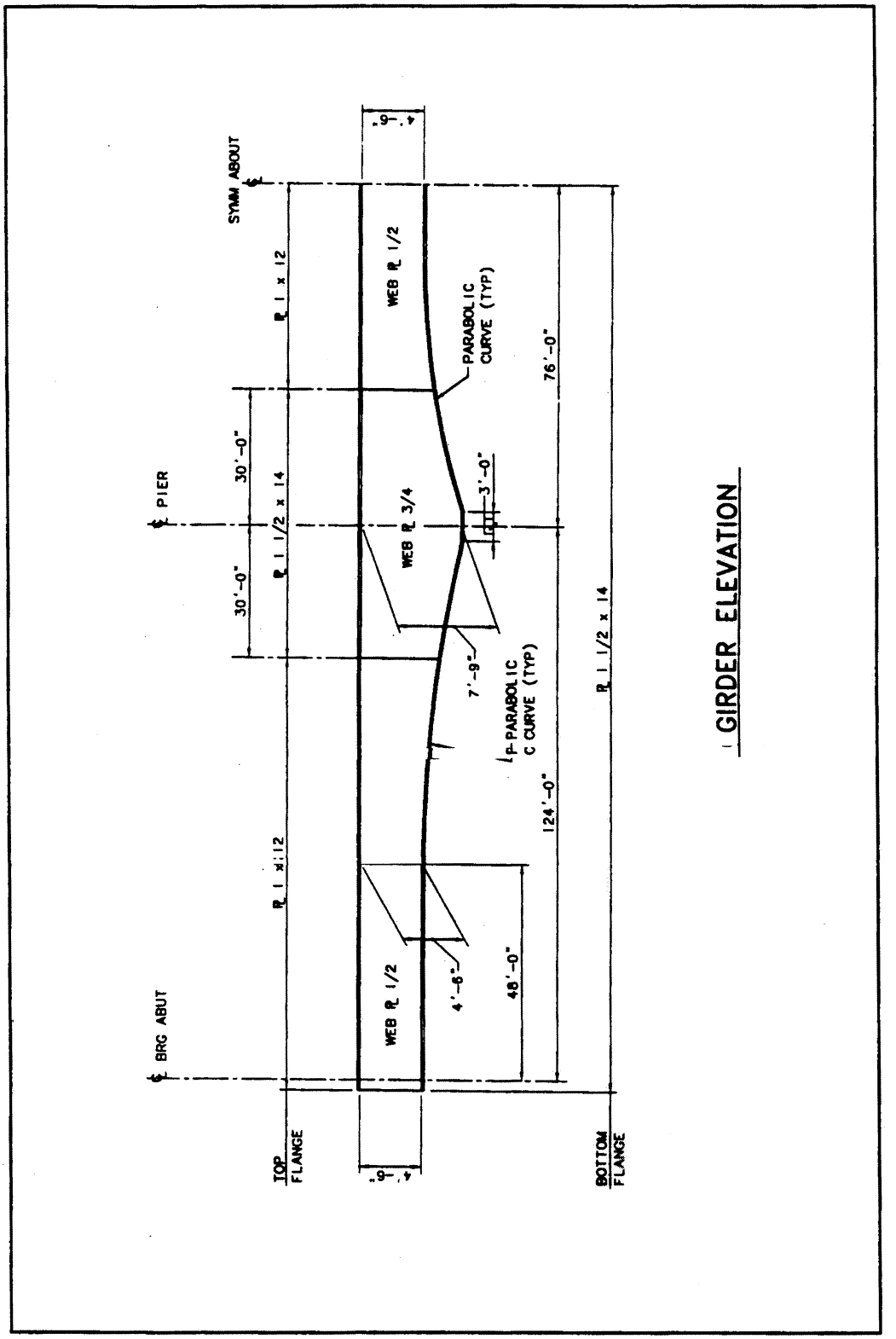

FIGURE 3.6e Bridge No. 2 – Plate Girder Details

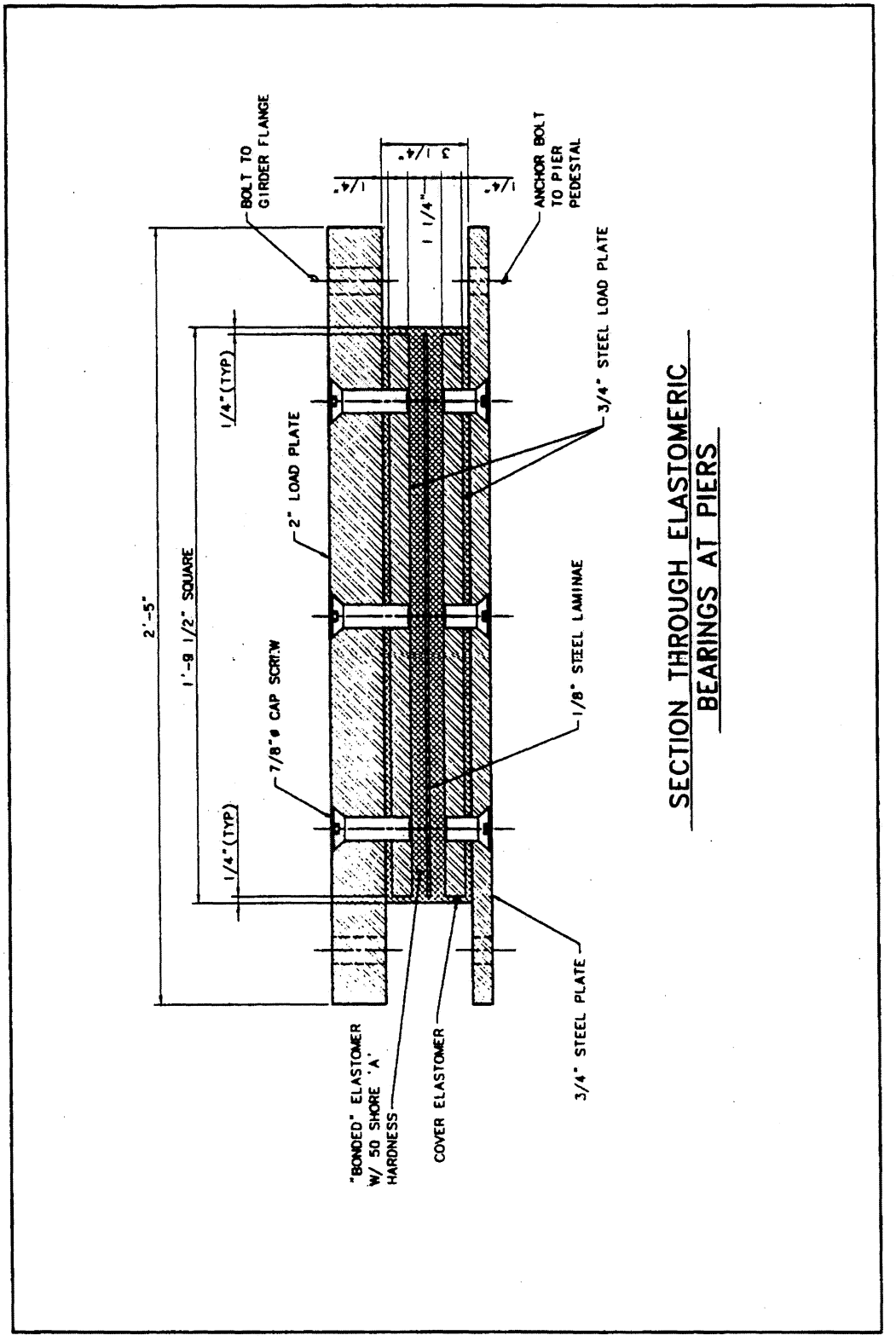

FIGURE 3.6f Bridge No. 2 – Elastomeric Bearings at Piers

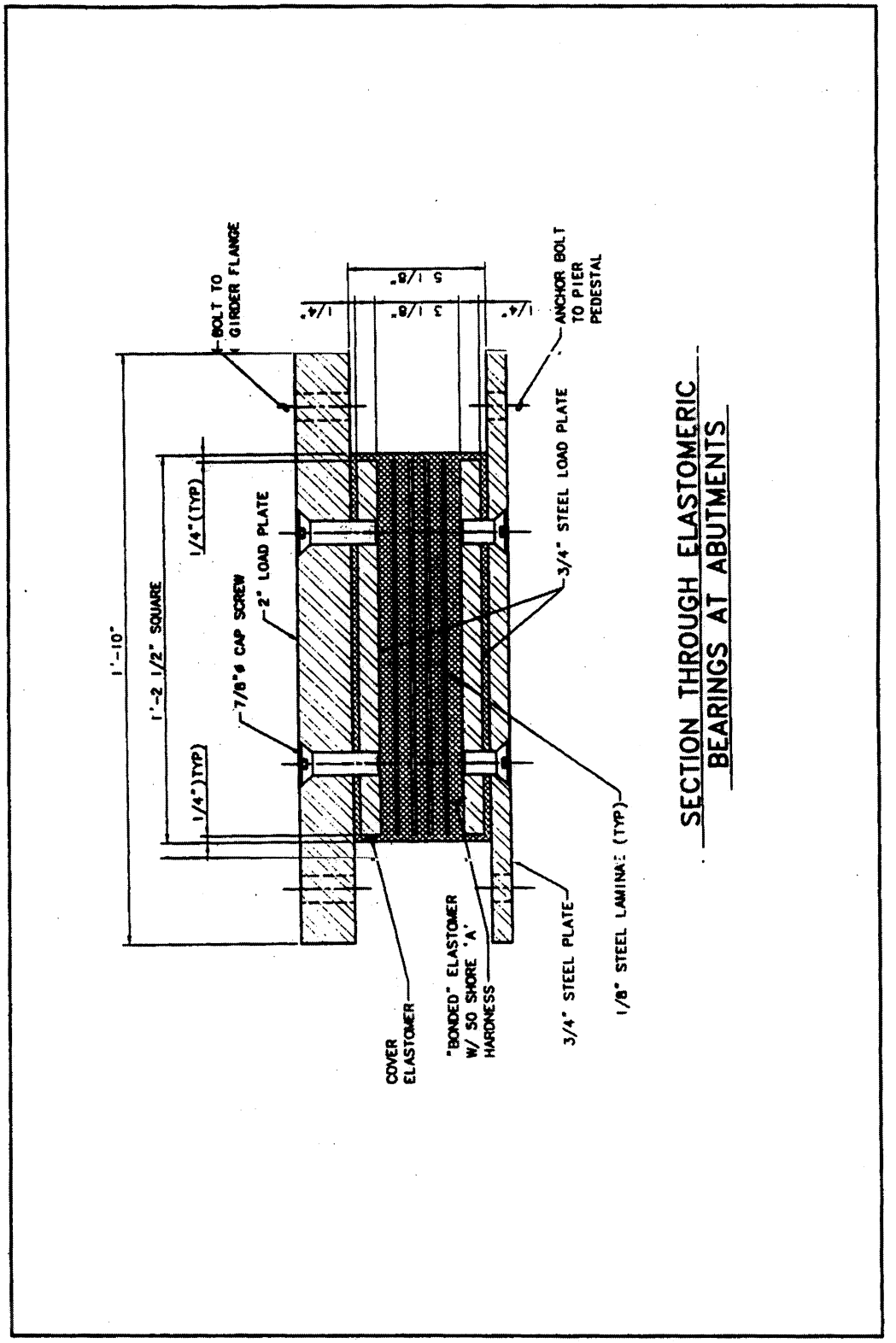

FIGURE 3.6g Bridge No. 2 – Elastomeric Bearings at Abutments

Description of Mathematical Model

The model used is shown in Figure 3.7 and includes a single line of frame elements for the superstructure and a single vertical line of elements for the piers (columns). The elastomeric bearing pads have been included as elastic springs located between the superstructure and the substructure elements. The SAP2000 text input file for the model shown in Figure 3.7 is given in Appendix D.

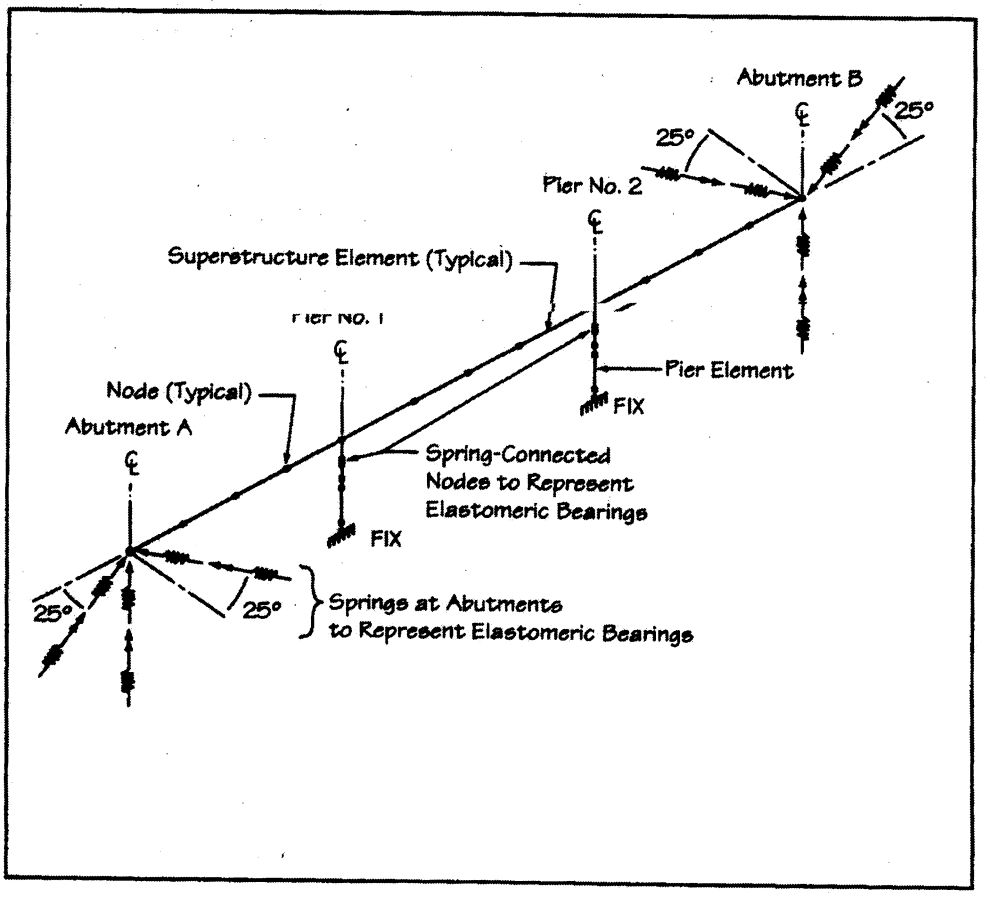

FIGURE 3.7 Bridge No. 2 - Finite Element Model

Superstructure

Geometry

As shown in Figure 3.7, the superstructure has been collapsed into a single line of 3-D frame elements. The superstructure has been modeled using four elements per span, and the longitudinal axes of the elements are located along the centroid of the superstructure. Since the girders are haunched, the centrodial depth varies along the length of the structure. This variation of depth is reflected in the model.

The centroid of the superstructure at the piers is located approximately 6.4 feet above the bottom flange of the plate girder. The connection of the superstructure to the bearings and substructure is made in the

SAP2000 model with a rigid link element that extends from the centroid to the bearings. This element is the uppermost pier element shown in Figure 3.8.

Properties

The properties of the elements have been calculated at the quarter points of each span. These properties are listed in Table 3.2.

The properties reported are equivalent concrete properties, since the superstructure is a composite of steel and concrete. 4000 psi concrete has been assumed. The areas are based on the gross area of the concrete and steel. The moment of inertia about the horizontal axis I_{horiz} is based on full composite gross sections in both positive and negative gravity moment regions. The moment of inertia about the vertical axis I_{vert} also assumes gross sections comprised of the deck, sidewalks, and all the girders.

TABLE 3.2 Bridge No. 2 - Properties of Superstructure

Location	**Area**	**Effective Density**	**Moment of Inertia**		
			About Vert. Axis	About Horiz. Axis	
	A (ft^2)	g[1] (k/ft^3)	I vert[2] (ft^4)	y bar[3] (ft)	I horiz (ft^4)
Abutment	81.0	0.166	36207	1.377	296
End Span 1/4 Pt.	81.0	0.166	36207	1.377	296
1/2 Pt.	81.3	0.166	36353	1.407	311
3/4 Pt.	84.3	0.162	37607	1.698	473
Pier	104.0	0.143	45988	2.477	996
Center Span 1/4 Pt.	83.4	0.163	37206	1.603	417
½ Pt.	81.0	0.166	36207	1.377	296

Notes:
1. Includes weight of barriers, overlay, forms, stiffeners, and cross frames.
2. I vert based on full composite action of deck and girders.
3. 'y bar' is measured from the top of the 9-inch deck.

As shown in Table 3.2, the density of concrete has been increased to include the following additional dead loads: traffic barriers, wearing surface overlays, cross frames and stiffeners, and stay-in-place steel forms with concrete. These items are considered uniformly distributed along the length of the bridge. The weight of these additional items totals 3.69 kips per lineal foot.

SAP2000 can model members that have smoothly varying cross-sections along their lengths. A linear variation of properties (not dimensions) has been used to approximate the effect of the haunched girders. For this example with the superstructure supported on elastomeric bearings, it is appropriate to use full composite action between the deck and the girders, and to assume that the concrete deck is not cracked. The presence of the skew is accounted for in the orientation of the substructure and bearing elements.

Torsional Properties: The torsional constant of the superstructure was calculated using only the deck. The contribution to torsional resistance offered by warping of the sections has been neglected.

Substructure

The single line of elements representing each pier has been divided into elements with nodes at each change in cross-section, as shown in Figure 3.8. The piers and abutments are skewed 25 degrees; thus the properties of these substructure elements are rotated in the model to properly account for the skew, as shown in Figure 3.9. The rotation of the elements is handled with the member local axis control in SAP2000. As with the superstructure, SAP2000's non-prismatic feature is used to model the continual varying cross-section of the piers. The full uncracked moments of inertia are used for the pier.

Because the main part of the pier is relatively long (26 feet), a short column element, which is only 0.2 foot long, has been included near the base of the pier. The short element is needed because the inertial effects in the pier are modeled with masses lumped at the nodes and it also allows a more refined estimate of the pier shear to be outputted.

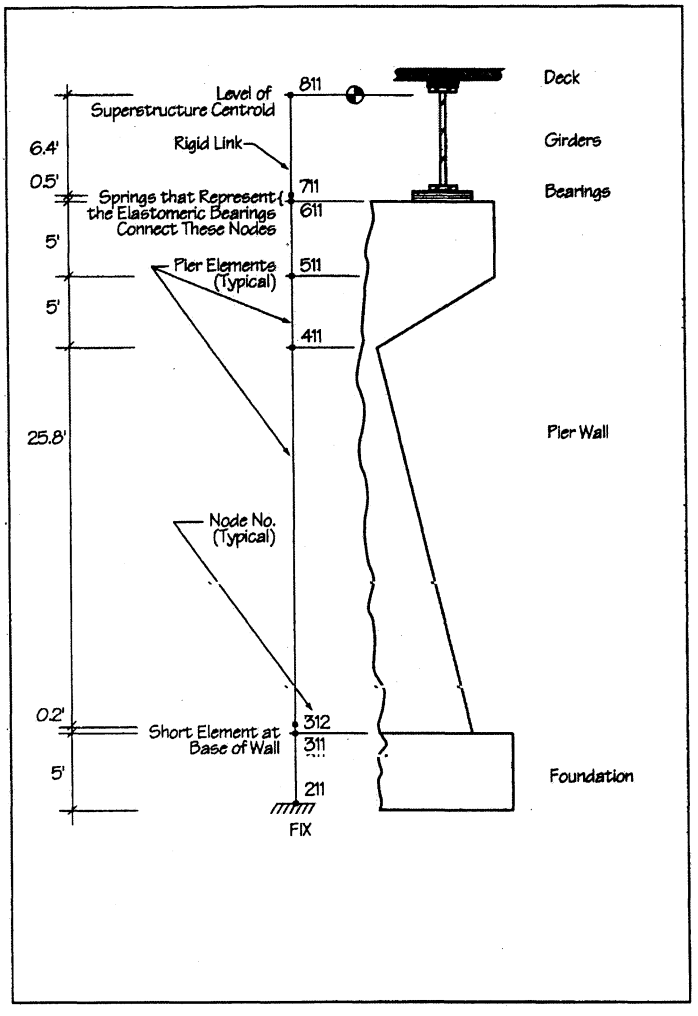

FIGURE 3.8 Bridge No. 2 - Details of Column Elements

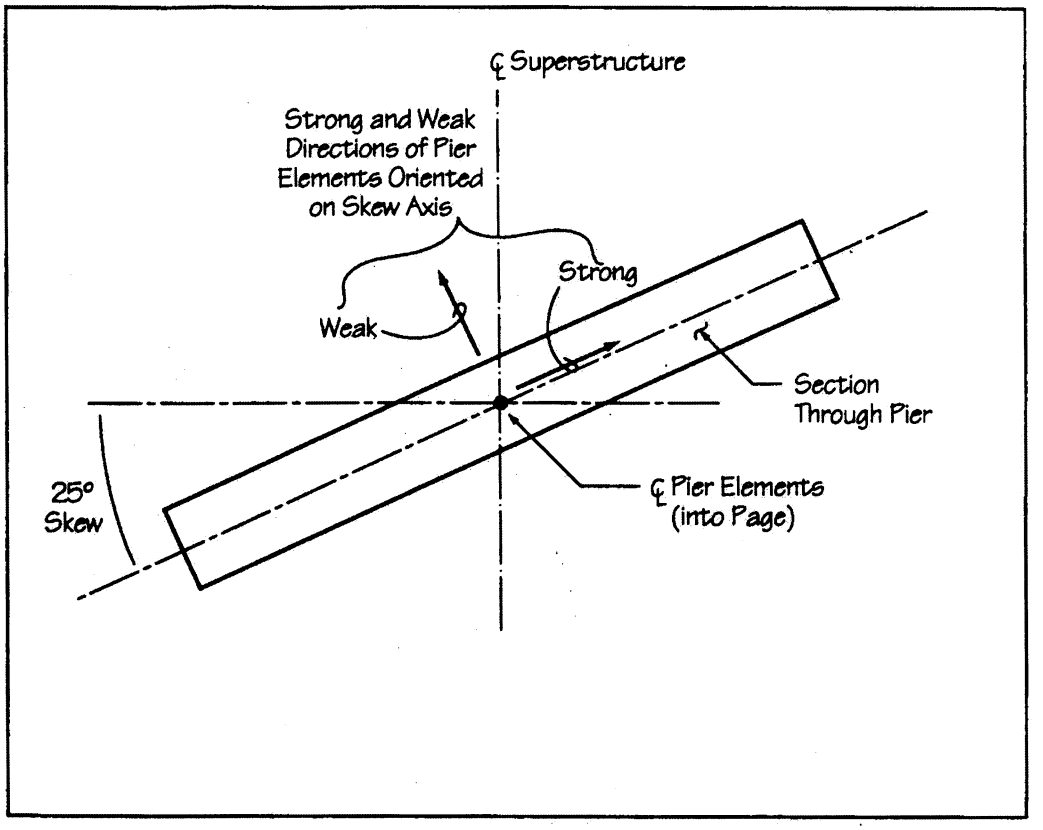

FIGURE 3.9 Bridge No. 2 - Plan of Pier Showing Rotation of Pier Elements

Connection Elements - Elastomeric Bearings

The elastomeric bearing pads at the piers and at the abutments have been included in the model as linear springs. The superstructure is not restrained in either the longitudinal or transverse directions; thus springs are provided in all three translational directions. The orientation of the springs is shown in Figure 3.10, and the corresponding spring stiffnesses are summarized in Table 3.3. Rotational springs have been provided around the vertical axis and about an axis normal to the strong directions of the piers and abutments. Rotational releases have been provided around the axes parallel to the pier and abutment strong directions. Note that the spring stiffnesses are given in a local coordinate system that coincides with the strong and weak directions of the piers and abutments.

TABLE 3.3 Bridge #2 - Elastomeric Bearing Spring Constants

	Piers	Abutments
Plan Dimensions (Based on Bonded Area)	21 Inches Square	14 Inches Square
Elastomer Height	1.125 in. Total (2 layers)	2.625 in. Total (5 layers)
k ht (kip/ft) Horizontal Translation	4328	824
k vt (kip/ft) Vertical Translation	813,000	148,000
k vr (kip-ft/rad) Rotation About Vertical	1,840,000	350,000
k sr (kip-ft/rad) Rotation About Strong Axis	346,000,000	62,900,000
k wr (kip-ft/rad) Rotation About Weak Axis	0	0

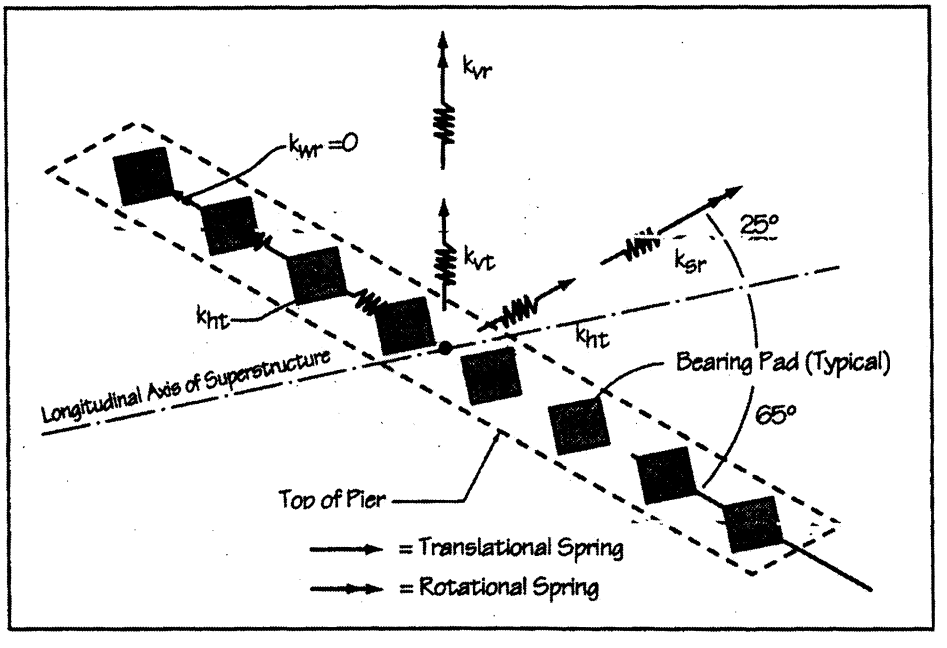

FIGURE 3.10 Bridge No. 2 - Orientation of Bearing Springs

Horizontal Translational Stiffness of Pier Bearings

The stiffness of an individual bearing pad can be calculated by determining the shear force required to produce a unit deflection on the pad. The shear modulus of the pads is 115 psi. The stiffness of the bearings is the same in both principal directions. Thus, the stiffness is the same in all directions in a horizontal plane. This extends to the total translational stiffness at each pier as well.

Rotational Stiffness of Pier Bearings

The rotational stiffness of the bearings about the vertical axis (or torsion on the pier) was found by adding the individual bearing contributions when a unit rotation is applied to the entire group. The bearings are assumed to be connected with a rigid link that transmits forces from the individual bearings to the point where the moment, which produces the unit rotation, is applied. The vertical stiffness of the bearings and the rotational stiffness about an axis perpendicular to the pier strong axis can be found using the method outlined in Section 14 of AASHTO, Division 1. The vertical stiffness is the standard axial stiffness 'AE/L,' but Young's modulus E is an equivalent linear stiffness based on Figure 14.4.1.2A of AASHTO Division 1.

Rotation has been released about an axis parallel to the strong direction of the pier ($k_{wr} = 0$). Stiffness (or restraint) in this direction is considered negligible.

Pier and Abutment Foundation Stiffnesses

Because the bridge is founded on rock, no attempt was made to include foundation stiffness. The pier foundations have been considered fixed in all directions at the base of the footing. The abutments have also been considered fixed in all directions since the stiffnesses of the elastomeric bearings are much less than that of the abutment structure.

3.3 Bridge No. 3

The configuration of the bridge consists of a single-span superstructure with precast AASHTO girders and a cast-in-place concrete deck. The substructure consists of tall closed seat type abutments with retaining walls parallel to the abutment and expansion joints provided at both ends of the bridge superstructure. Figure 3.11 (a to e) provide details of the bridge configuration. The alignment of the roadway on the bridge is straight and there is no vertical curve. The bridge has a 28 degree skew to the roadway below, thus the ends of the bridge, including the abutments, are also skewed. The fundamental mode in the vertical direction is shown in Appendix C and has a period of 0.20 seconds as given in Table 3.11 in Section 3.7.

Force Path

Connection forces will be transferred from the superstructure to the abutment through bearings and the shear key. In the global transverse direction, the abutments are assumed to provide restraint to the superstructure through the shear keys. In the global longitudinal direction, the abutments are assumed to be free to deflect at the top under earth pressures, and are considered to be free standing abutments per the code.

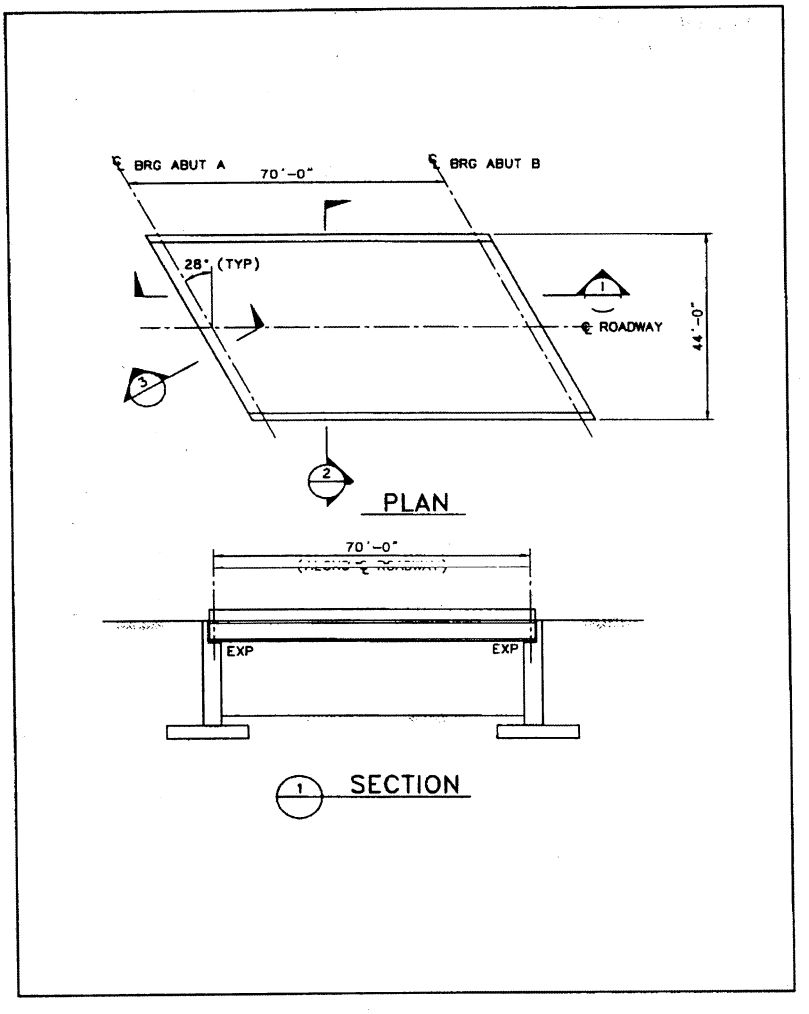

FIGURE 3.11a Bridge No. 3 - Plan and Section

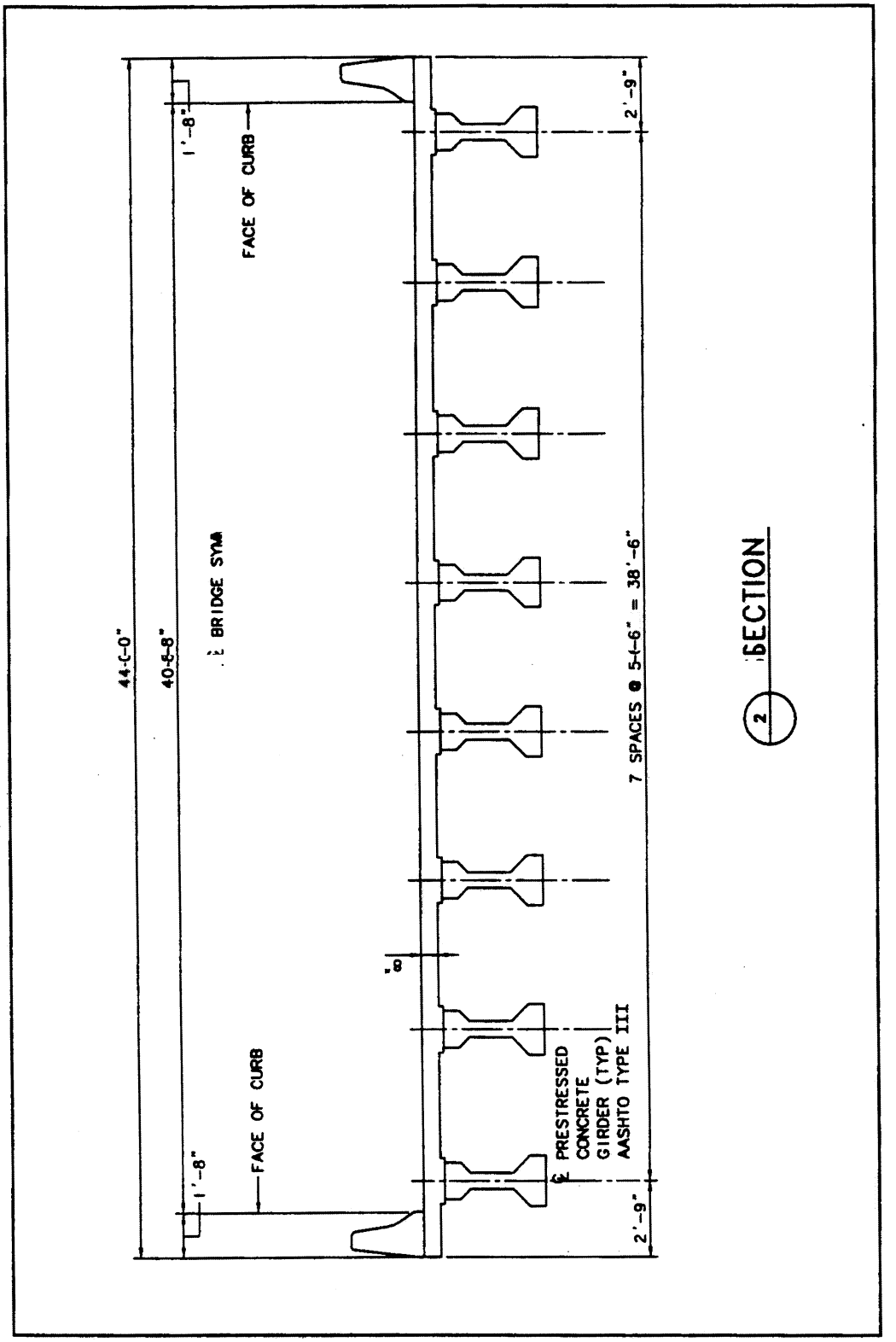

FIGURE 3.11b Bridge No. 3 - Typical Cross-section

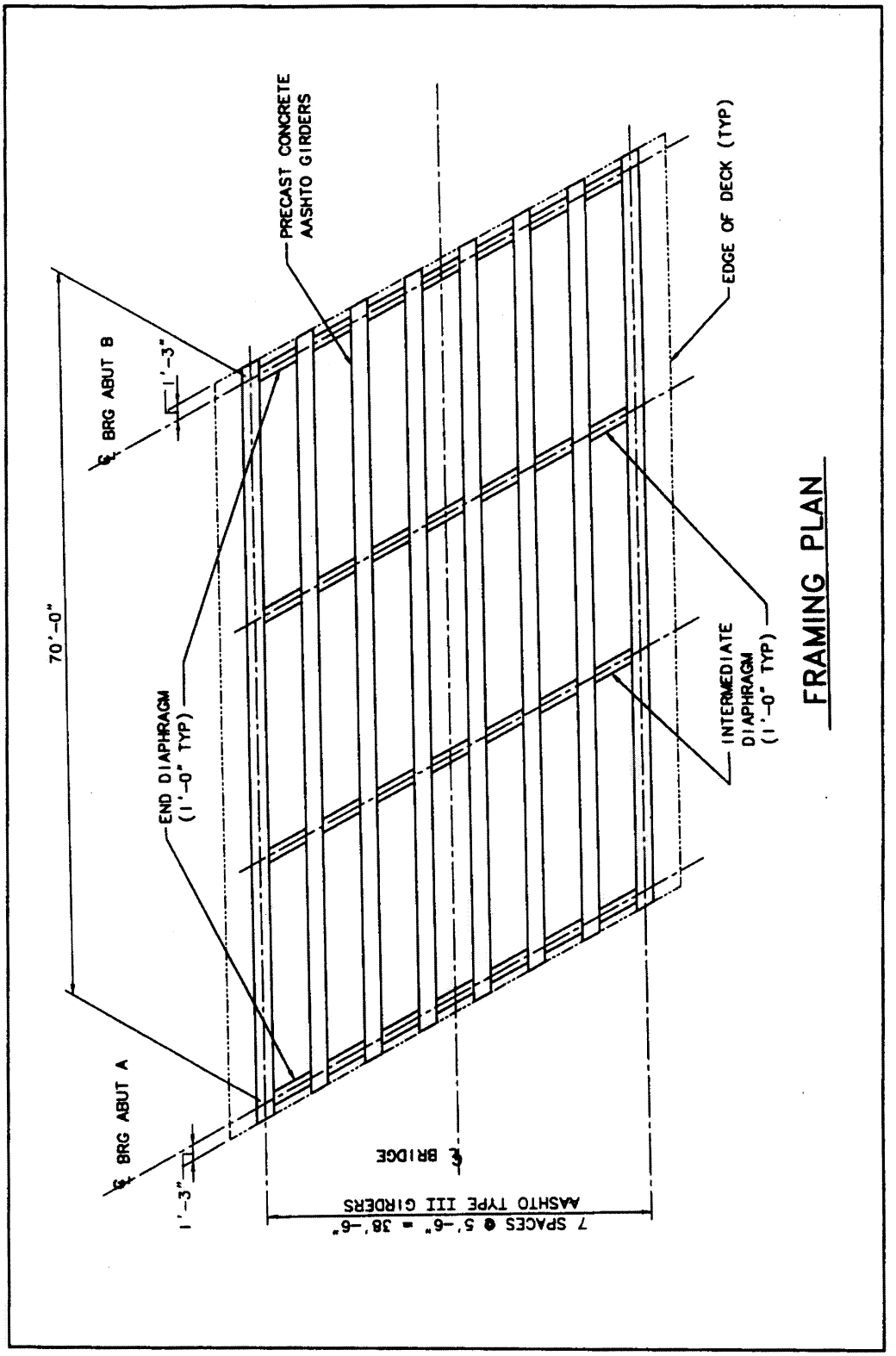

FIGURE 3.11c Bridge No. 3 - Framing Plan

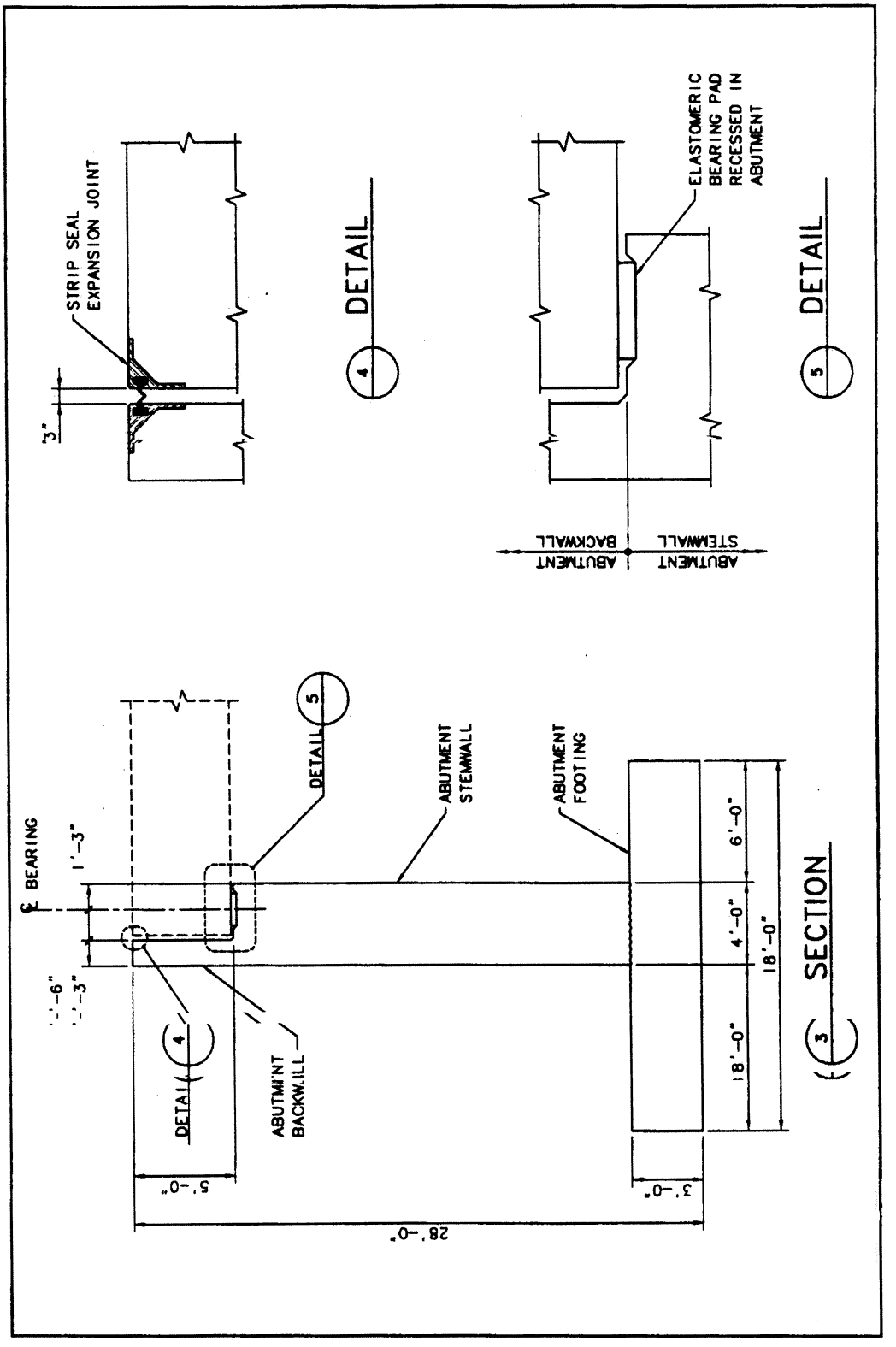

FIGURE 3.11d Bridge No. 3 - Abutment Section and Details

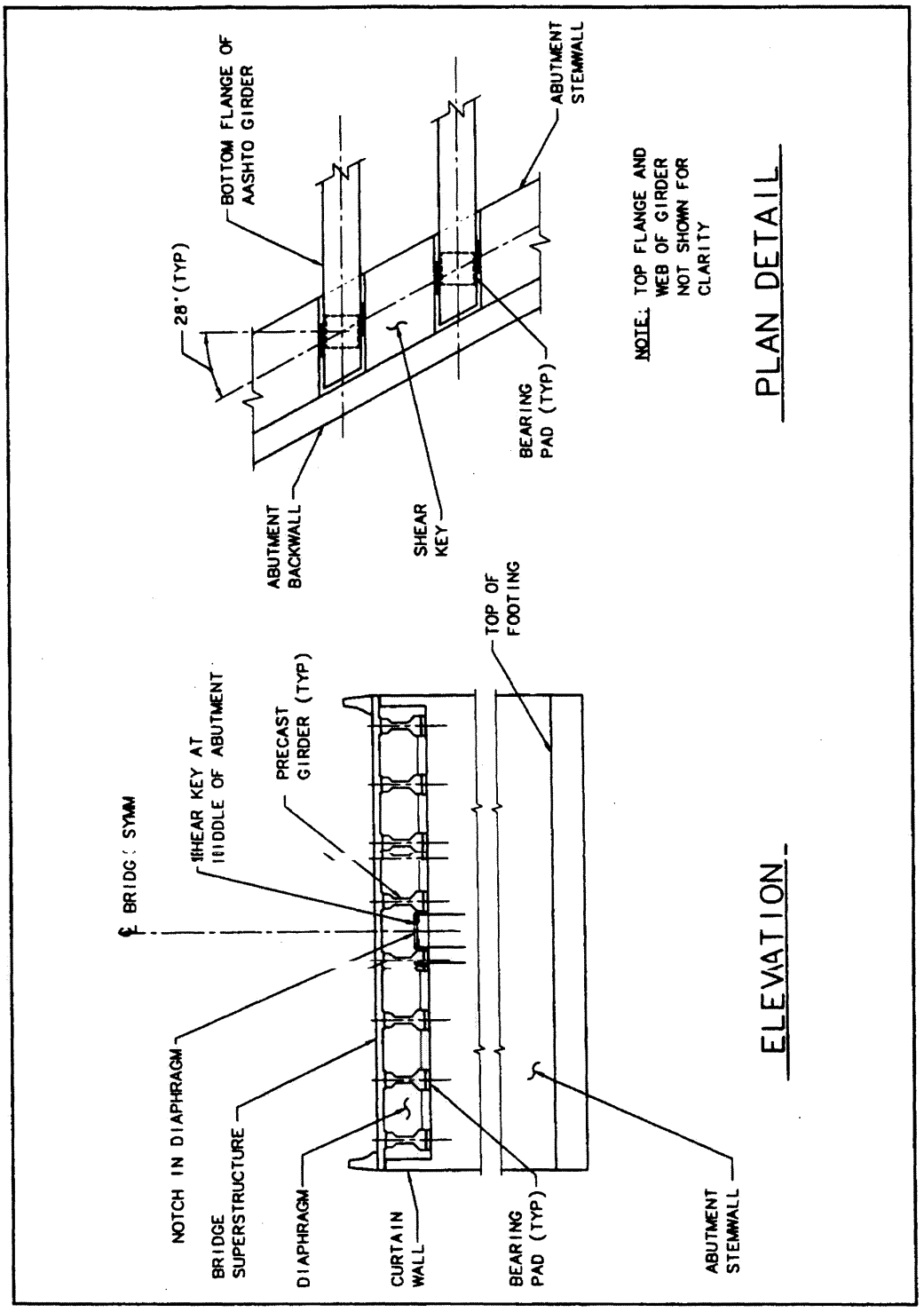

FIGURE 3.11e Bridge No. 3 - Abutment Elevation and Detail

Description of Model

The model used is shown in Figure 3.12. It includes a single line of 3D frame elements for the superstrucure and translational springs for the abutments. The SAP2000 text input file for the model shown in Figure 3.12 is given in Appendix D.

Superstructure

The superstructure has been modeled with four elements and the work line of the elements is located along the centroid of the superstructure. The moment of inertia in the vertical plane (I_y) was calculated using the composite action of the girder and the slab. The moment of inertia (I_z) in the horizontal plane and the deck torsion constant calculated using the slab only.

$I_y = 141\ ft^4$
$I_z = 4732\ ft^4$
$J = 9.77\ ft^4$

Abutments/Support Conditions

The abutments are represented in the model by three orthogonal translational springs. Their purpose is to approximately model the behavior of the abutments. The skew of the abutments is not included in the model. The longitudinal spring stiffness was calculated using a stiffness coefficient of 200 kips/in per lineal foot of the abutment wall height. The transverse flexural and shear stiffness of the abutment wall were added to obtain the spring stiffness for the direction perpendicular to the longitudinal axis of the deck. The vertical spring stiffness was calculated using the elastic half-space approach given in FHWA, *Seismic Design and Retrofit Manual for Highway Bridges* [1987] for the wall pad footing.

Longitudinal stiffness = 52,800 kips/ft
Transverse stiffness = 34,769 kips/ft
Vertical stiffness = 190,776 kips/ft

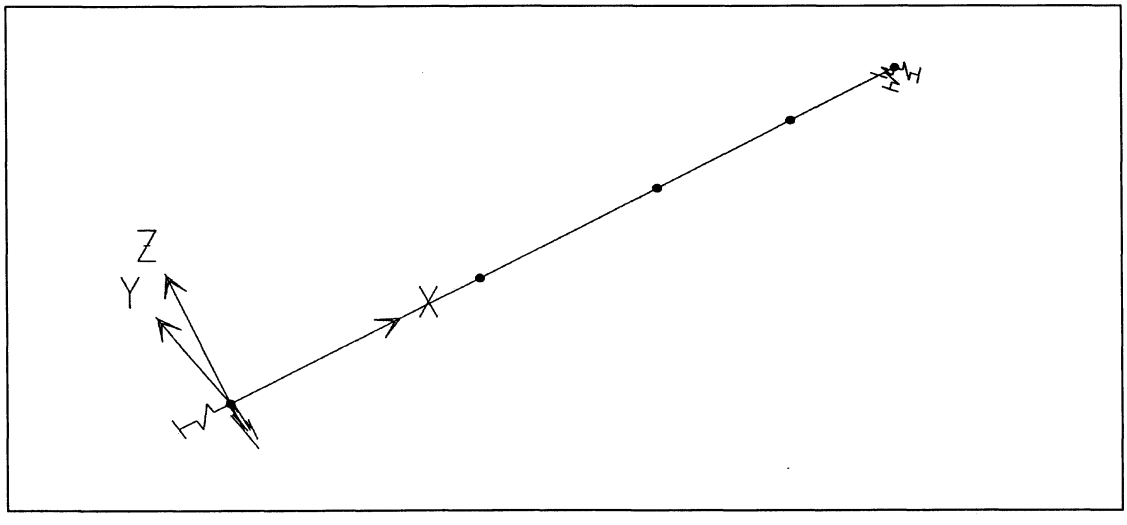

FIGURE 3.12 Bridge #3 - Finite Element Model

3.4 Bridge No. 4

The three-span bridge is 320 feet long with spans of 100, 120, 100 feet. All substructure elements are oriented at a 30-degree skew from a line perpendicular to a straight bridge centerline alignment. Figure 3.13a shows a plan and elevation of the bridge. The superstructure is a cast-in-place concrete box girder with two interior webs. The intermediate bents have a cross beam integral with the box girder and two round columns that are pinned at the top of spread footing foundations. Figure 3.13b shows a cross-section through the bridge with an elevation of an intermediate bent. The seat-type abutments are on spread footings, as shown in Figure 3.13c, and the intermediate bents are all cast-in-place concrete.
the box girder superstructure is shown in Figure 3.13d.

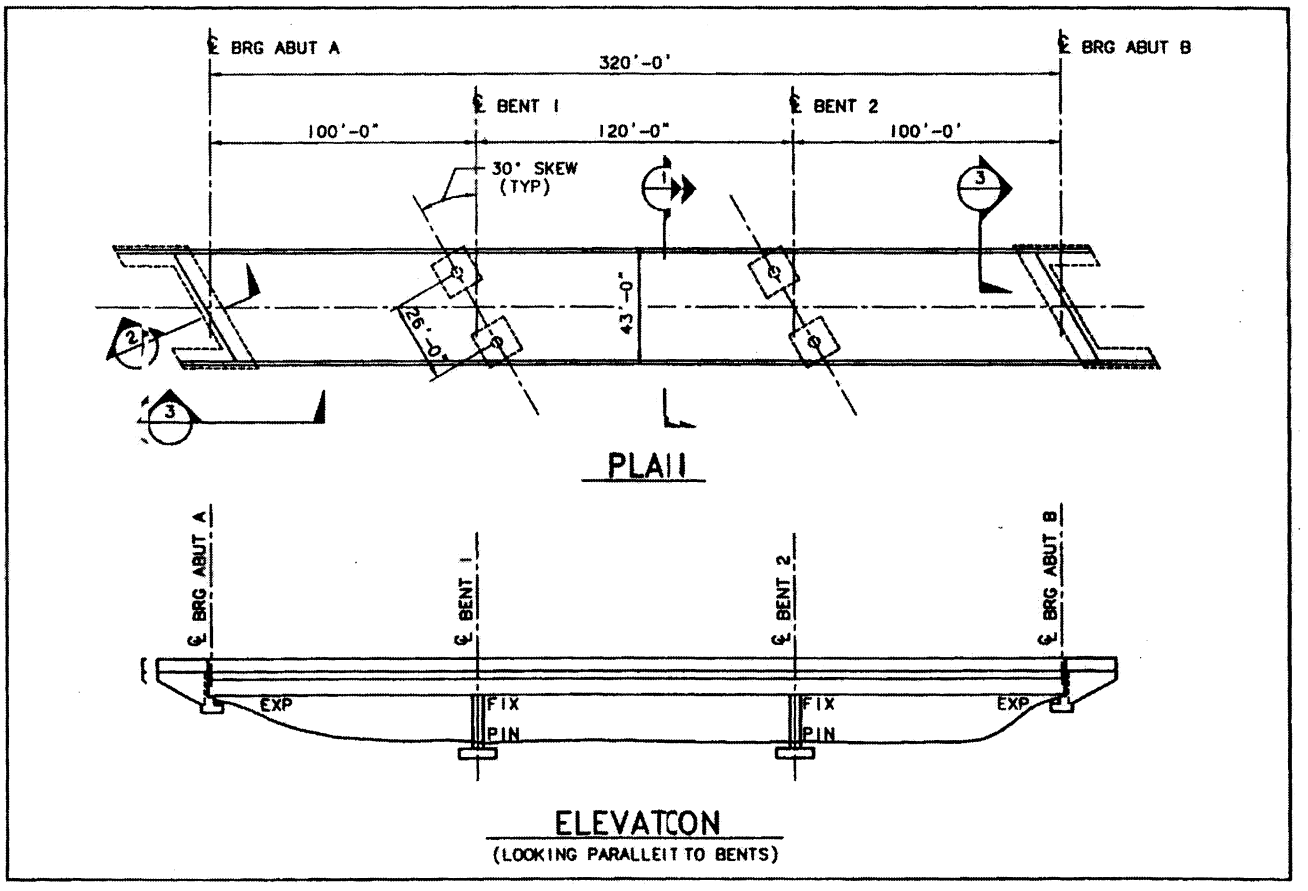

FIGURE 3.13a Bridge No. 4 – Plan and Elevation

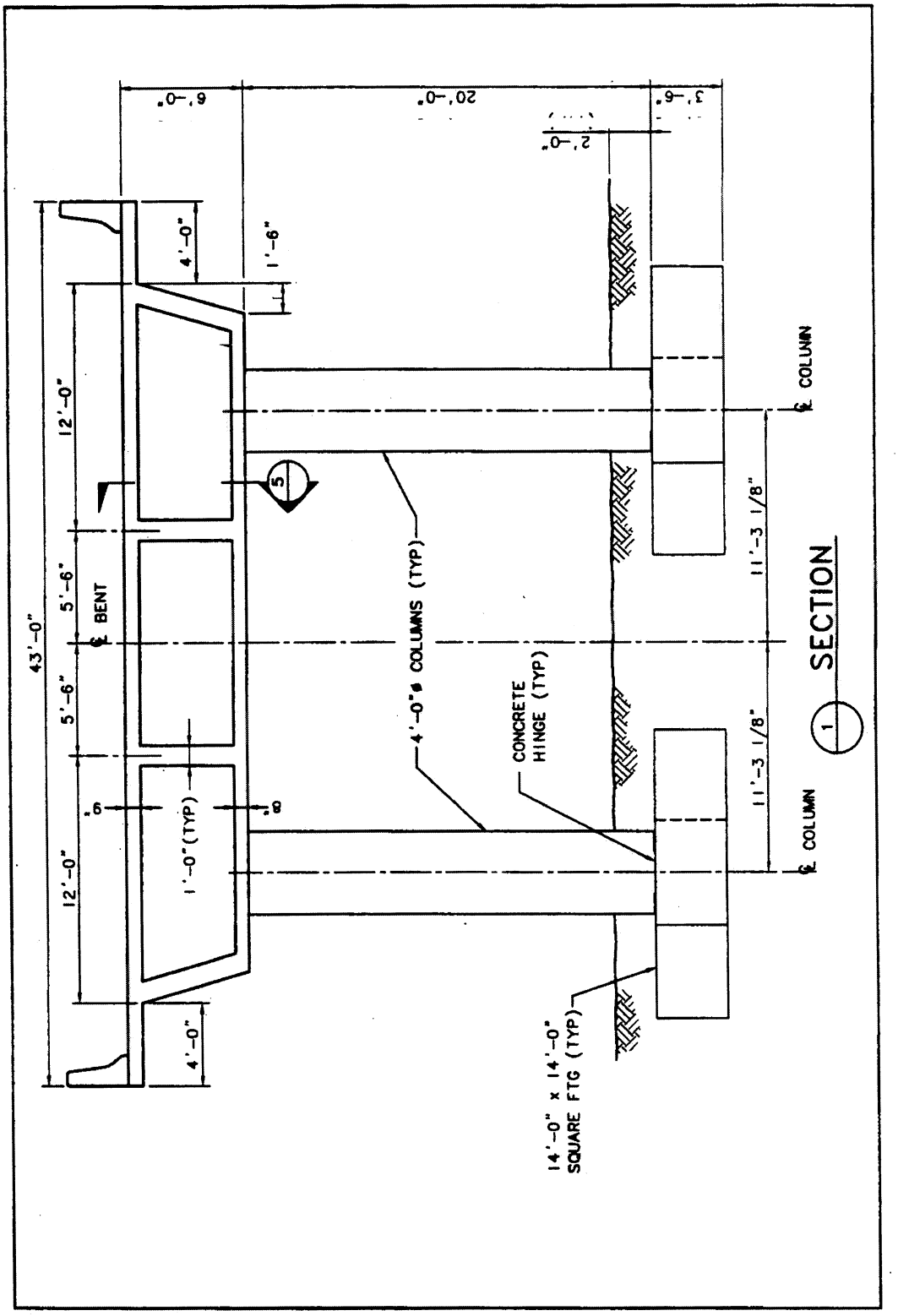

FIGURE 3.13b Bridge No. 4 – Typical Cross-section

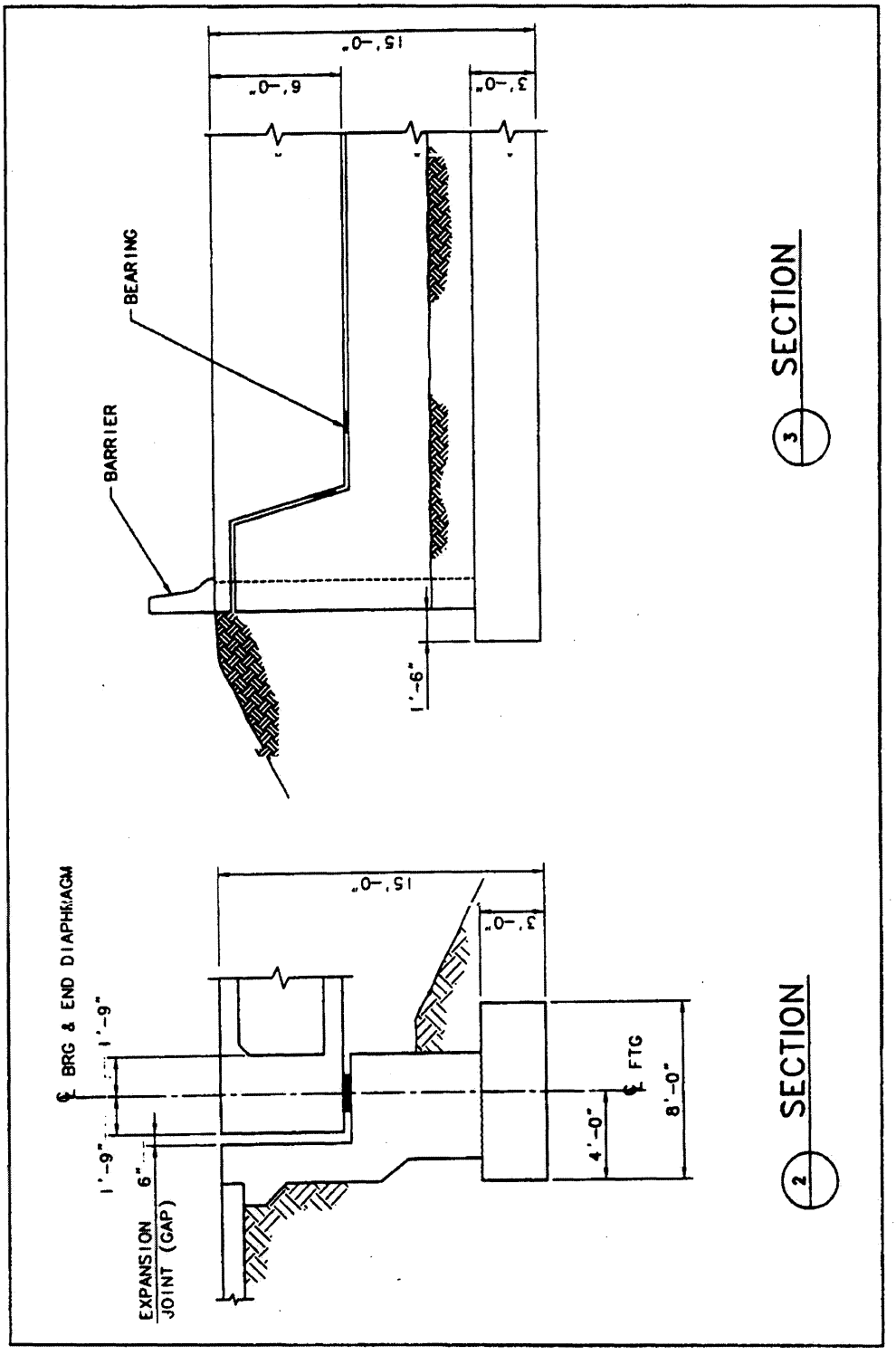

FIGURE 3.13c Bridge No. 4 – Seat Type Abutment

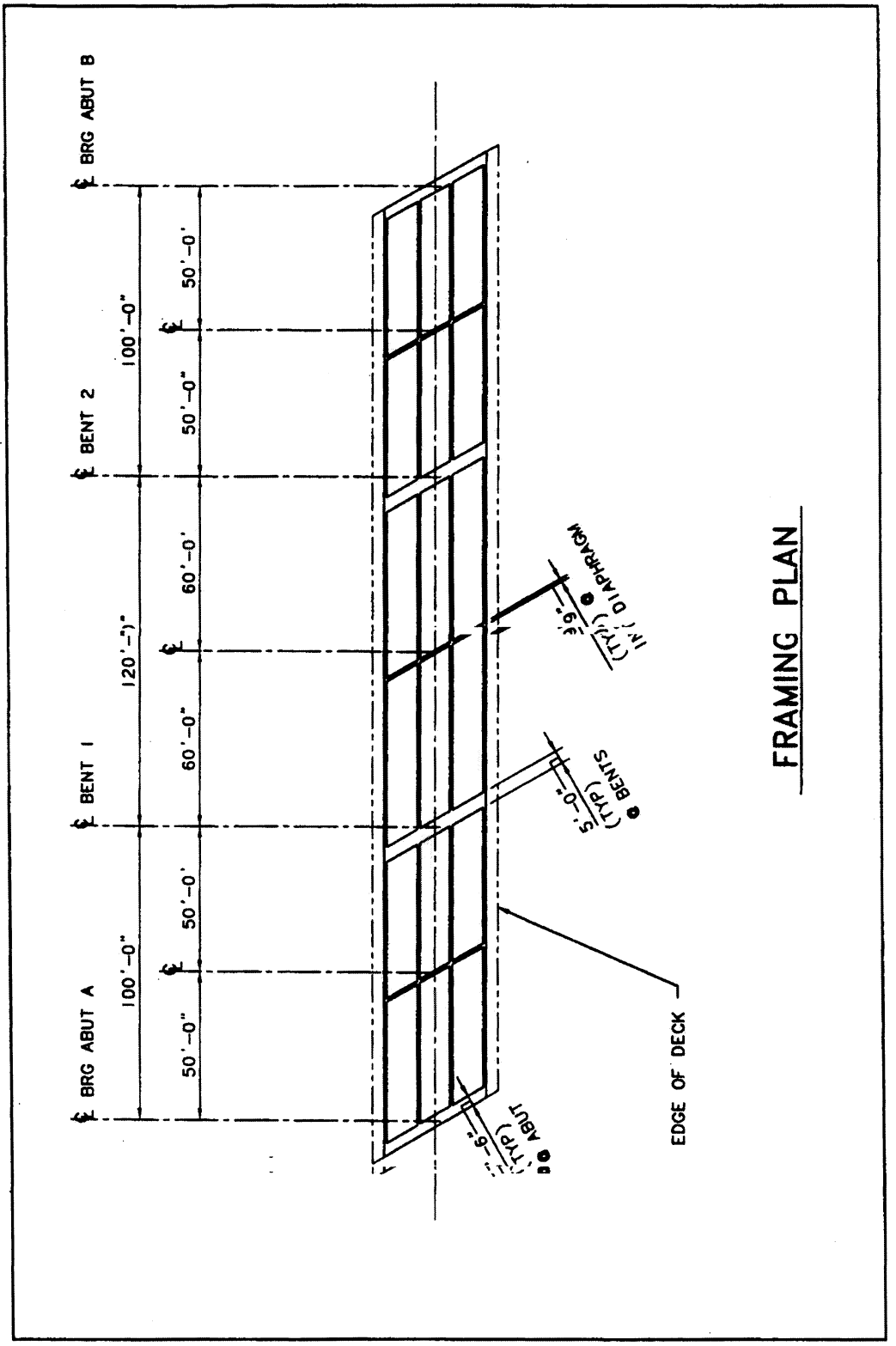

FIGURE 3.13d Bridge No. 4 – Box Girder Framing Plan

The moments of inertia of the structural elements shown in the SAP2000 input files in Appendix D are assumed to be identical to that of the full uncracked cross-section but the effect of varying the vertical deck stiffness on the structural response is presented in Section 6.

In the longitudinal direction, the intermediate bent columns are assumed to resist the entire longitudinal seismic force. The seat-type abutments will allow free longitudinal movement of the superstructure and will not provide longitudinal restraint.

In the transverse direction, the superstructure is assumed to act as a simply supported beam spanning laterally between the abutments with the maximum transverse displacement at the center of the middle span. The intermediate bents are assumed to participate in resisting the transverse seismic force along with the superstructure. Transverse restraint is provided by a shear key to enable transfer of transverse seismic forces to the abutment.

The fundamental mode in the vertical direction is shown in Appendix C and has a period of 0.20 seconds as given in Table 3.12 in Section 3.7.

Description of Finite Element Model

Figure 3.14 shows the structural model of the bridge. The SAP2000 text input file for this model shown is given in Appendix D.

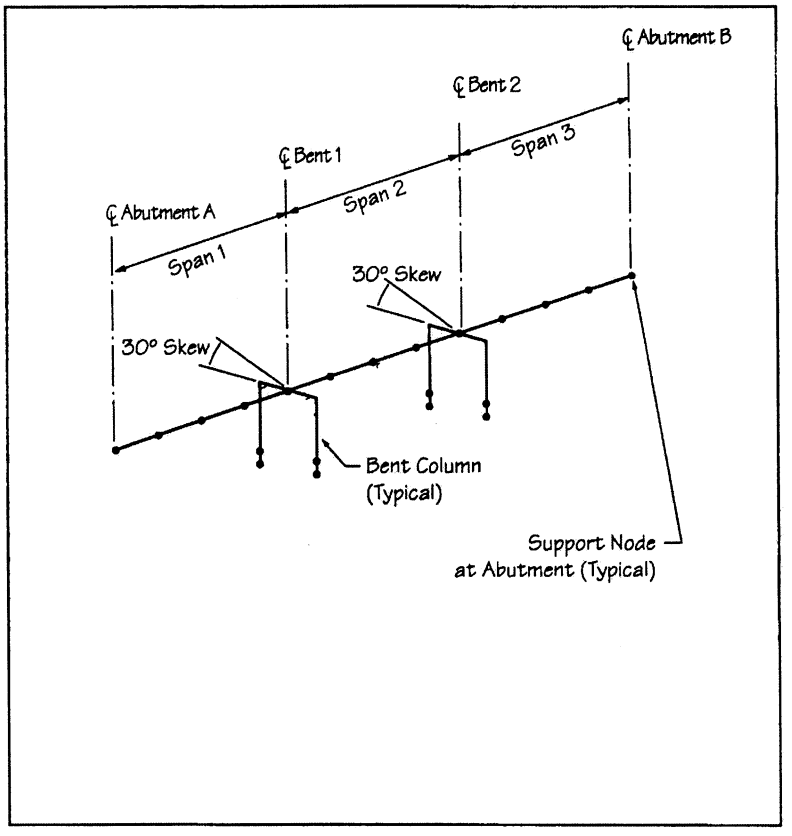

FIGURE 3.14 Bridge #4 - Finite Element Model

Superstructure

The superstructure has been modeled with four elements per span and the work lines of the elements are located along the centroid of the superstructure. The superstructure density used for the analysis has been adjusted to include additional dead loads from traffic barriers and wearing surface overlay. The total weight of these additional dead loads is 2.35 kips per lineal foot of superstructure. The properties of the structure used in the seismic model (both superstructure and substructure) are shown in Table 3.4.

Determination of moments of inertia and torsional stiffness of the superstructure are based on uncracked cross-sectional properties.

The presence of the skew is accounted for only in the orientation of the substructure elements, and is not considered in determination of the superstructure properties.

TABLE 3.4 Bridge #4 - Section Properties for Model

	CIP Box Superstructure	Bent Cap Beam	Bent Columns (Each)
Area (ft^2)	72.74	27.00	12.57
Ix – Torsion (ft^4)	1,177	100,000 (1)	25.13
Ly (ft^4)	9,697	100,000 (2)	12.57
Lz (ft^4)	401	100,000 (3)	12.57
Density (lb/ft^3	182	150	150

Notes:
1. This value has been increased for force distribution to bent columns. Actual value is Ix = 139 ft^4.
2. This value has been increased for force distribution to bent columns. Actual value is Iy = 90 ft^4.
3. This value has been increased for force distribution to bent columns. Actual value is Iz = 63 ft^4.

Substructure

The bents and abutments are skewed 30 degrees; therefore, the properties of the bent elements are rotated in the model to properly account for the skew. (There are no elements to model the abutments, only support nodes as shown in Figure 3.14). The bents are modeled with 3-D frame elements that represent the cap beam and individual columns. Figure 3.15 shows the relationship between the actual bent and the "stick" model of 3-D frame elements. A single element was used for each column between the top of footing and the soffit of the box girder superstructure. The connection of the column top at the soffit of the box girder to the center of gravity of the cap (at the superstructure centroid) beam is made with rigid link elements. The node at the top of the footing (4xx) is released for rotation in both plan directions to model the pinned column base. Foundation springs are connected to the node (3xx) at the base of the footing. For this model, the moments of inertia and torsional properties of the columns are based on uncracked sections.

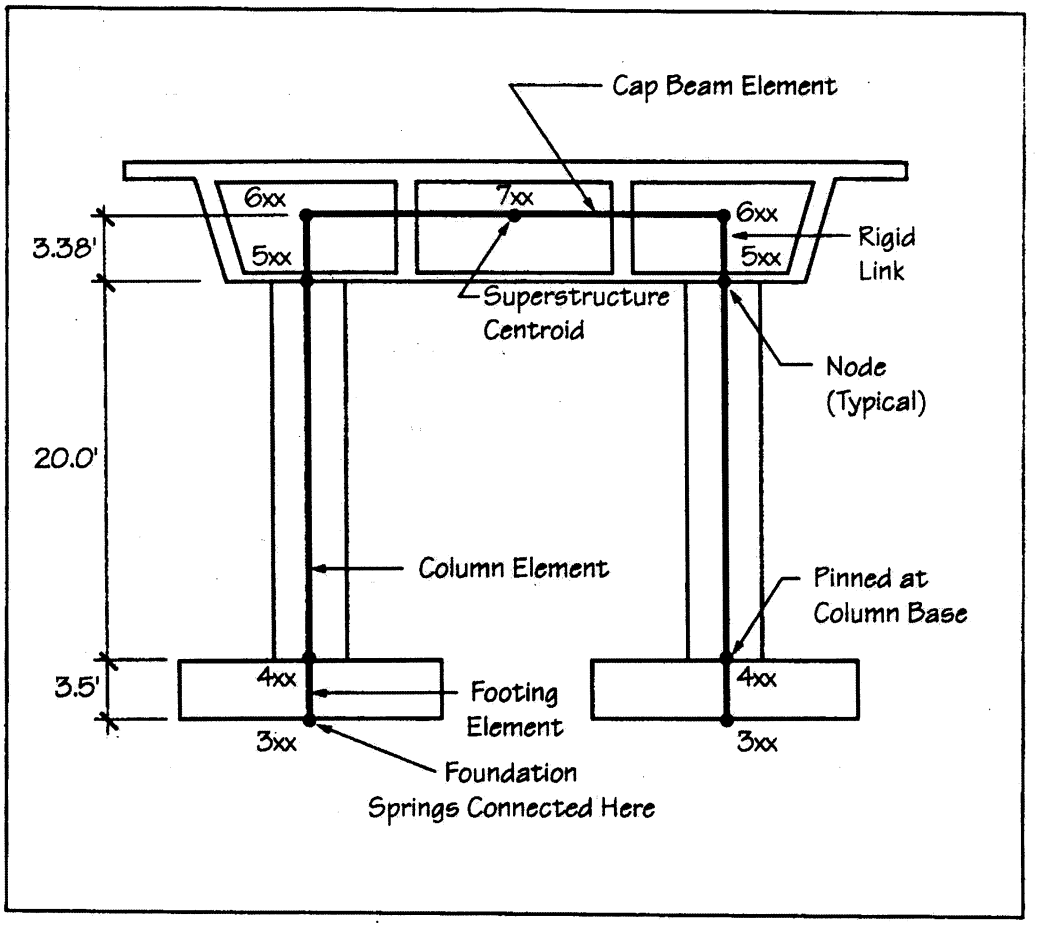

FIGURE 3.15 Bridge No. 4 – Details of Bent Elements

The torsional stiffness and moments of inertia of the model's cap beams have been increased in order to provide a more representative distribution of forces to the columns. These adjusted properties are shown in Table 3.4, along with the actual calculated properties.

Foundation Stiffnesses

Bent Foundations

The intermediate bent foundations has been modeled with equivalent spring stiffnesses for the spread footing. Figure 3.16 shows details of the spring supports. For this example, all of the intermediate bent footings use the same foundation springs. The spring stiffnesses are developed for the local bent support coordinate geometry, and are input into the SAP2000 model with the same orientation as the local bent columns.

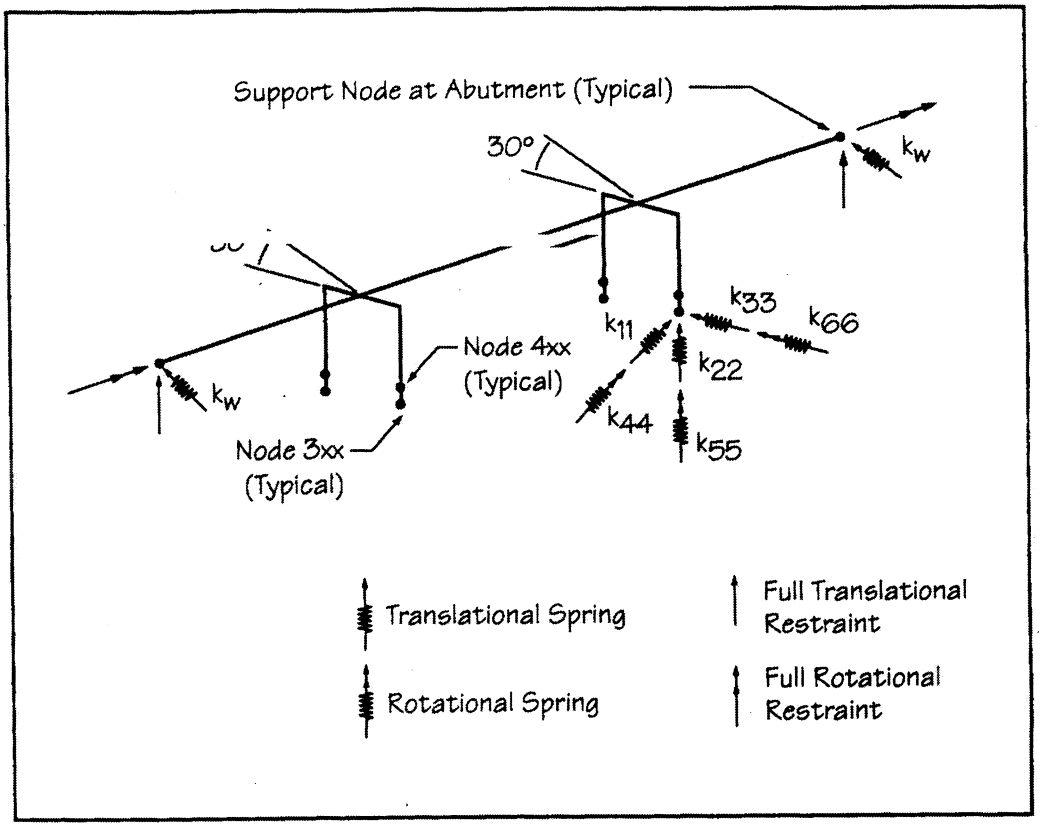

FIGURE 3.16 Bridge #4 - Details of Spring Supports

The spring stiffnesses of the spread footings at Bents 1 and 2 were calculated using an elastic half-space approach. The method used here is from FHWA, *Seismic Design and Retrofit Manual for Highway Bridges* [1987].

Abutments

The abutments have been modeled with a combination of full restraints (vertical translation and superstructure torsional rotation) and an equivalent spring stiffness (transverse translation), as shown in Figure 3.16. Other degrees of freedom are released.

3.5 Bridge No. 5

The configuration of the bridge has nine spans totaling 1488 feet and consisting of two units: a four-span tangent (Unit 1) and a five-span with a 1300-foot radius curve (Unit 2). The superstructure is composed of four steel plate girders with a composite cast-in-place concrete deck. The substructure elements, seat-type abutments, and single-column intermediate piers are all cast-in-place concrete supported on steel H-piles. All substructure elements are oriented normal to the centerline of the bridge. Figure 3.17 (a to d) provides details of the configuration.

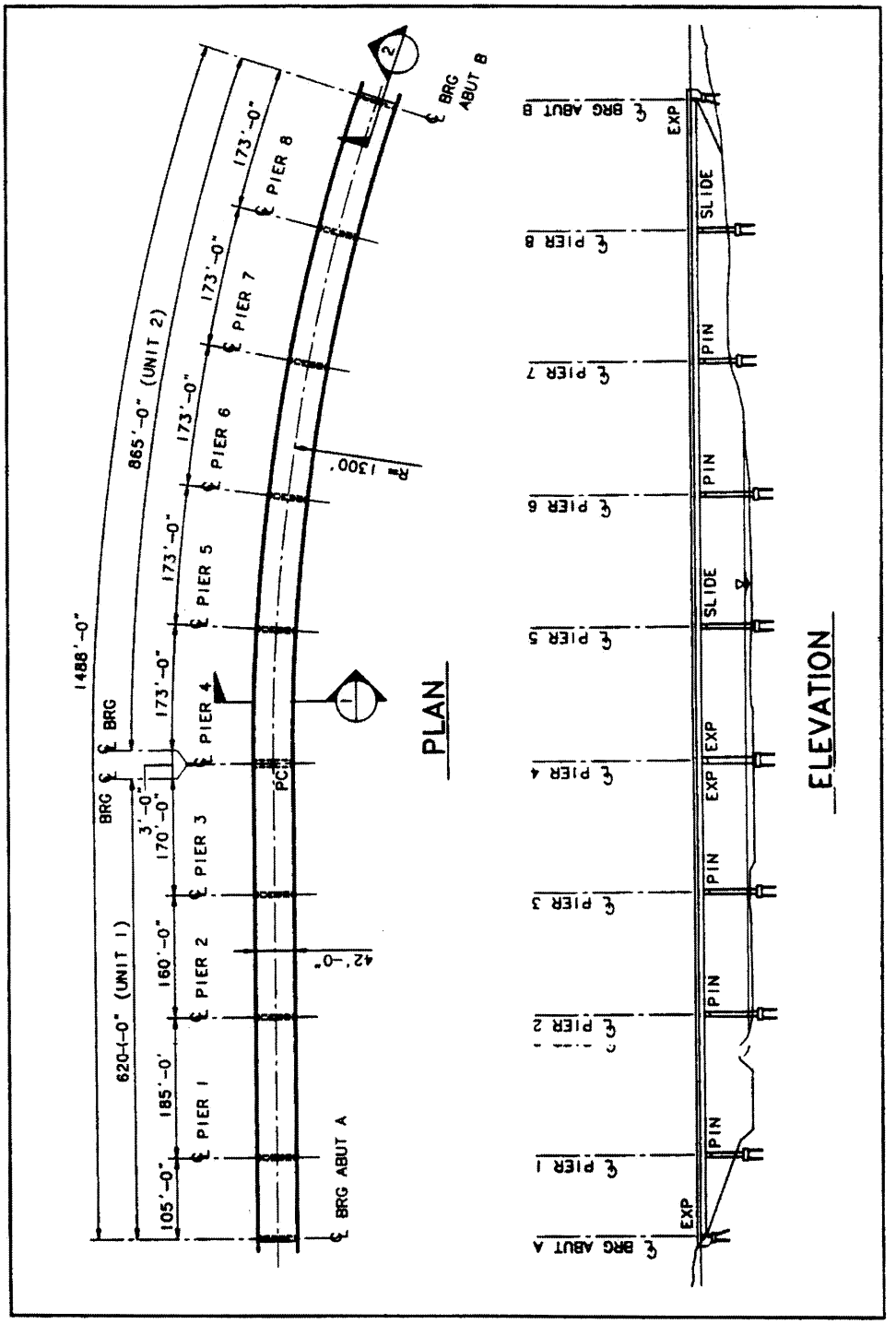

Figure 3.17a Bridge No. 5 – Plan and Elevation

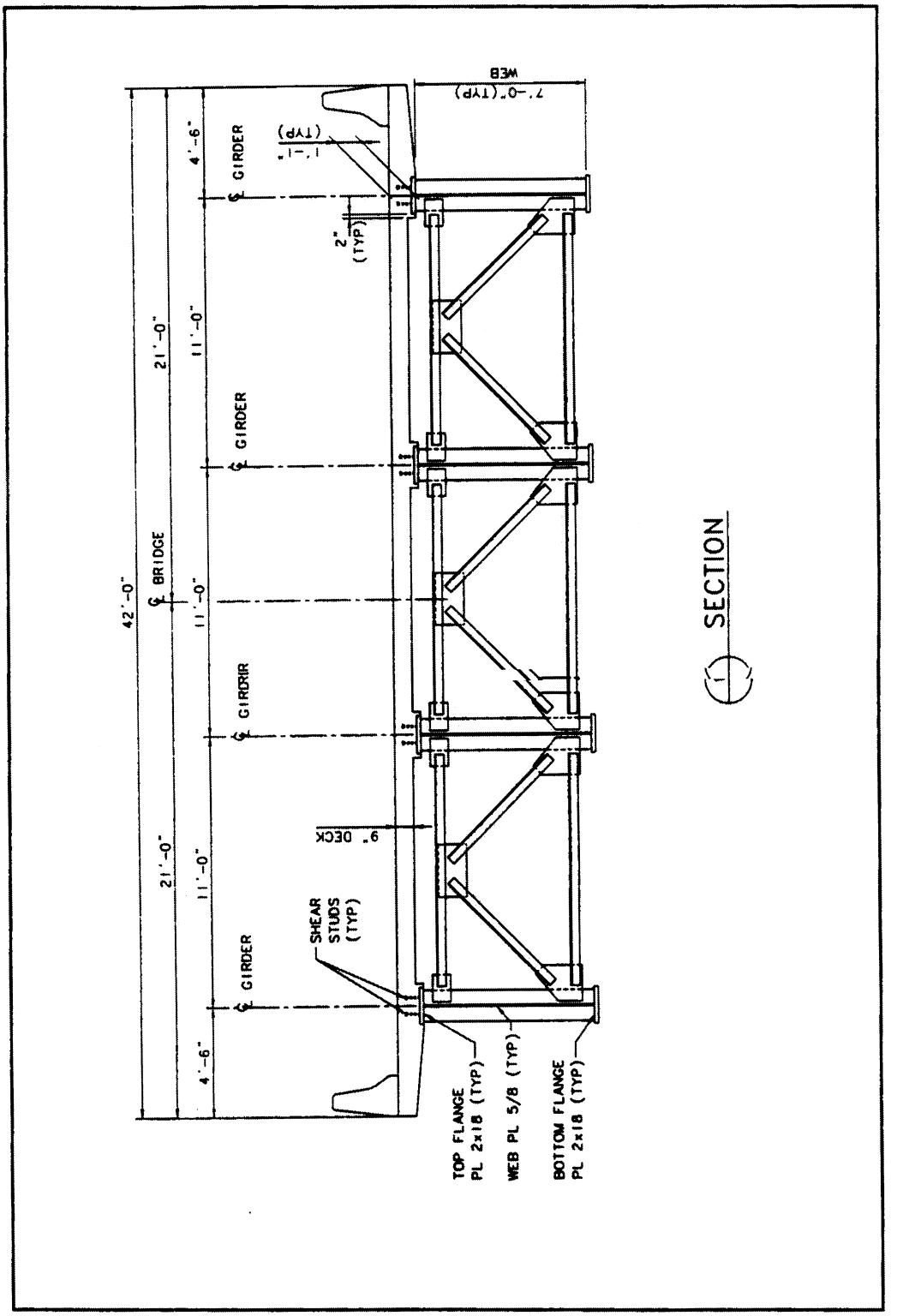

FIGURE 3.17b Bridge No. 5 – Typical Cross-section

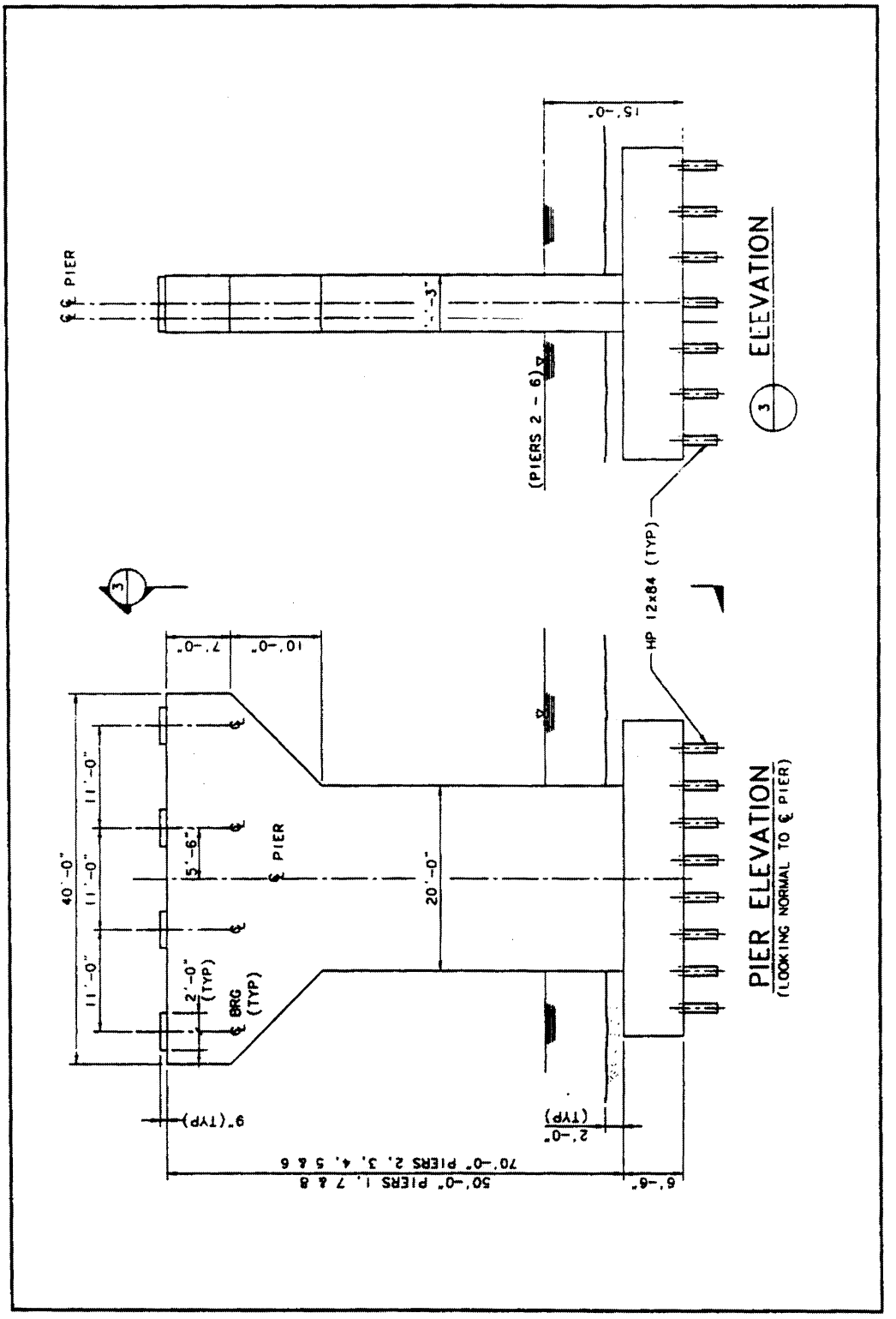

FIGURE 3.17c Bridge No. 5 – Intermediate Pier Elevation

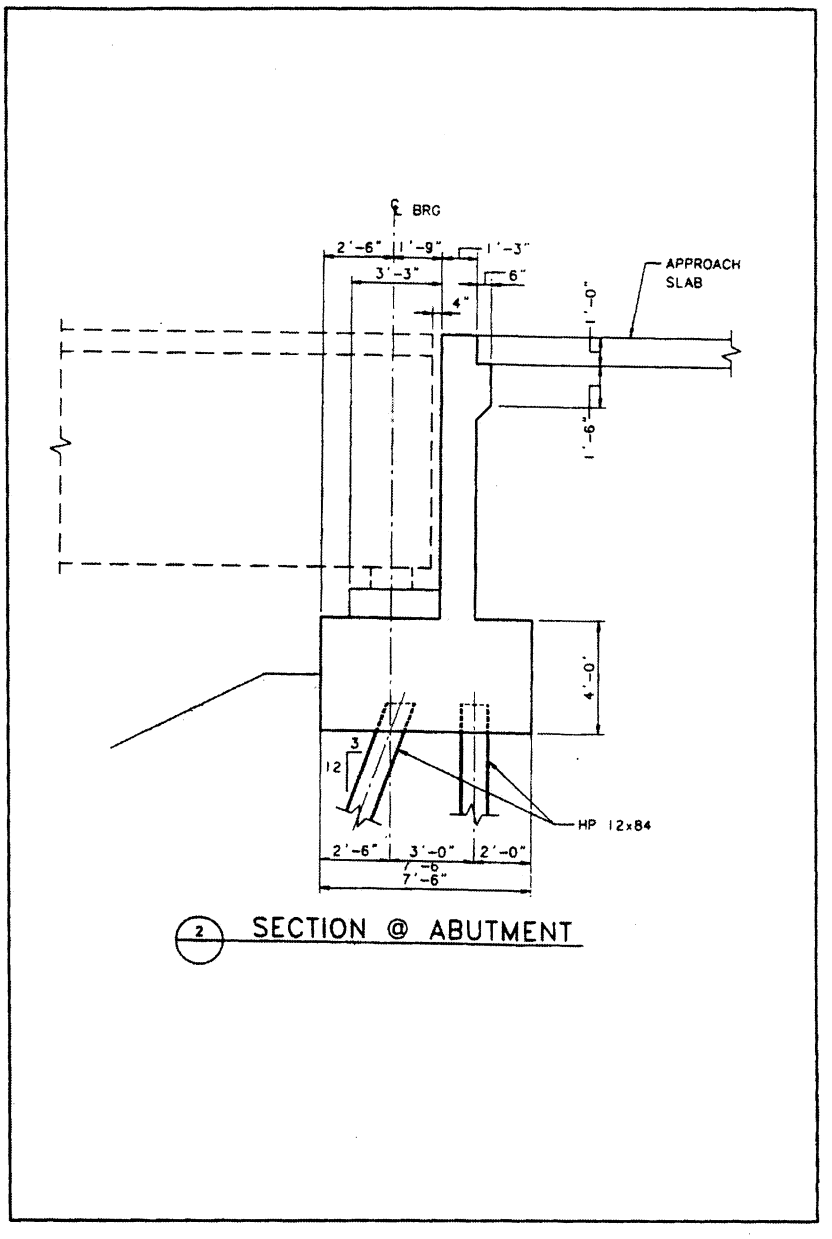

FIGURE 3.17d Bridge No. 5 – Seat Type Abutment

In the longitudinal direction, the pinned intermediate pier columns (Pier Nos. 1, 2, and 3 in Unit 1, and Pier Nos. 6 and 7 in Unit 2) are assumed to resist the entire longitudinal seismic force. The seat-type abutments and the expansion joint at Pier No. 4 will accommodate significant motion in the longitudinal direction and will provide restraint in the transverse direction. The two units of the bridge are assumed to act independently for longitudinal motion. This behavior is illustrated in Figure 3.18.

In the transverse direction, the structure is assumed to act as a two-rigid link system pivoting at the abutments with maximum transverse displacement at Pier No. 4. All of the intermediate piers and

abutments are assumed to participate in resisting the transverse seismic force. This behavior is illustrated in Figure 3.19.

In both transverse and longitudinal directions, the column bases are considered fixed against rotation at the bottom of the pile cap to account for expected lack of foundation flexibility.

The fundamental mode in the vertical direction is shown in Appendix C and has a period of 0.50 seconds as given in Table 3.13 in Section 3.7.

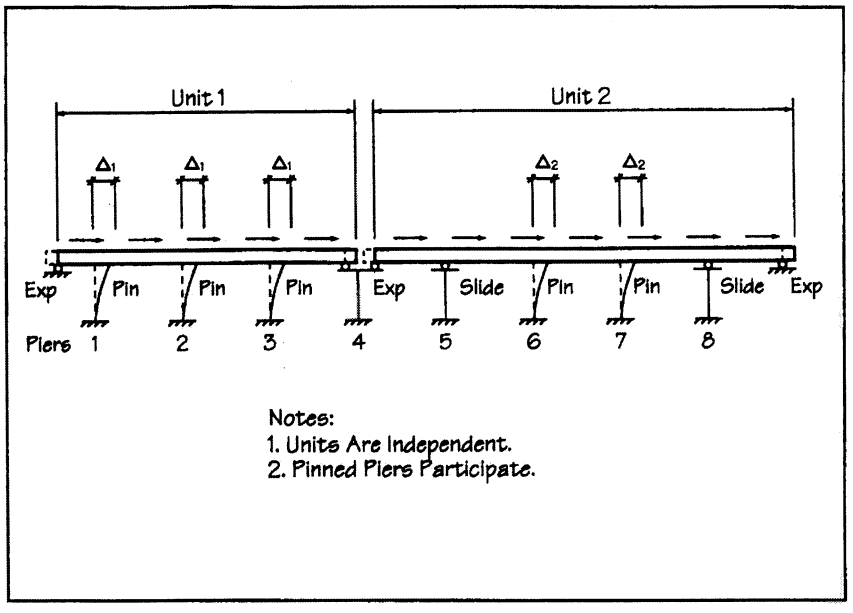

FIGURE 3.18 Bridge No. 5 - Longitudinal Seismic Behavior

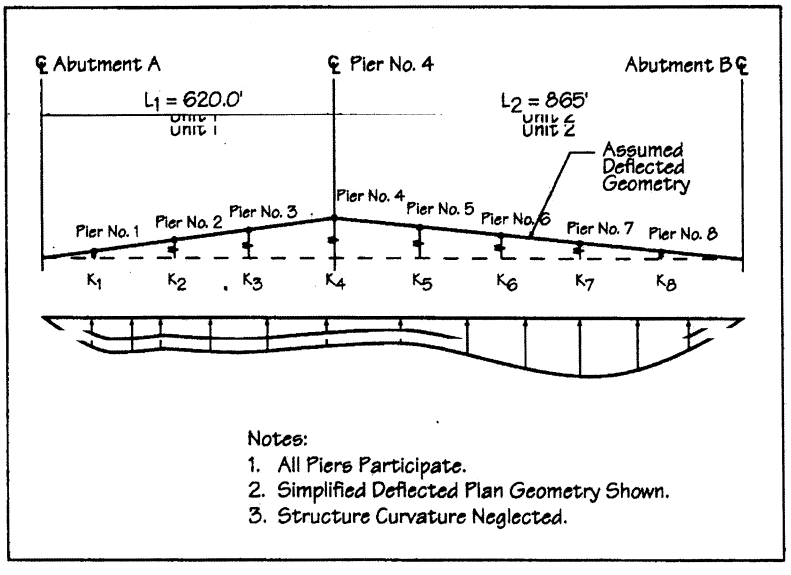

FIGURE 3.19 Bridge No. 5 - Transverse Seismic Behavior

Description of Finite Element Model

The model used is shown in Figure 3.20 and includes a single line of elements for the superstructure and a single line of vertical elements for each of the intermediate piers. The SAP2000 text input file for the model shown in Figure 3.20 is given in Appendix D.

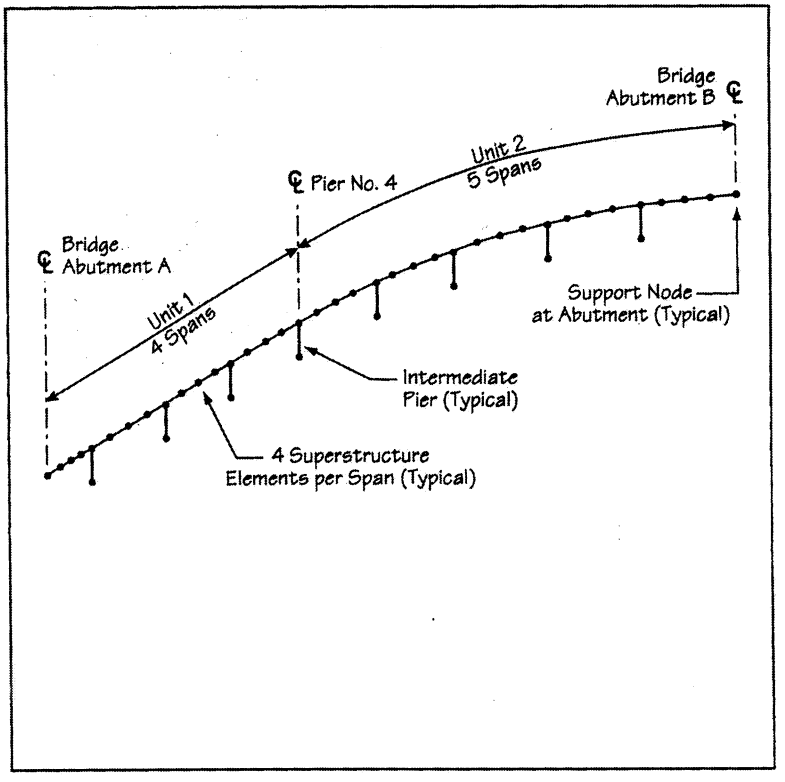

FIGURE 3.20 Bridge No. 5 - Finite Element Model

Superstructure

Geometry

The superstructure has been modeled with four elements per span. The nodes and work lines of the elements are located along the center of gravity of the superstructure.

Properties

The density has been adjusted to include additional dead loads from traffic barriers, wearing surface overlay, and stay-in-place metal forms. The total weight of these additional dead loads is 2.4 kips per lineal foot of superstructure.

The centroid of the superstructure has been located eight feet above the top of the pier to account for the height of the bearings and leveling pedestal. The connection of the superstructure to the pier is made in the SAP2000 model with rigid link elements shown in Figure 3.21 as the top elements of the piers.

Properties of the superstructure and its elements are shown below. The superstructure area and moments of inertia include the concrete deck, the girder webs, and both flanges with steel transformed to concrete using a modular ratio, n=8.

$L := 1488$ ft	Overall length of bridge
$L_1 := 620$ ft	Length of Unit 1
$L_2 := 865$ ft	Length of Unit 2
$A_d := 60$ ft^2	Cross-section area of superstructure and deck (steel transformed to concrete with modular ratio, $n=E_s/E_c = 8$)
$I_{zd} := 518$ ft^4	Moment of inertia of superstructure about a horizontal axis (steel transformed to concrete with modular ratio, n=8)
$I_{yd} := 9003$ ft^4	Moment of inertia of superstructure about a vertical axis (steel transformed to concrete with modular ratio, n=8)
$f_c := 4000$ psi	Compressive strength of concrete
$Y_{conc} := 0.15$ kip/ ft^3	Unit weight of concrete

The torsional constant of the superstructure is calculated using only the deck. The contribution to torsional resistance offered by warping of the steel sections has been neglected.

$J = 5.906$ ft^4	Torsional constant of superstructure
$E_c := 3600$ ksi	Young's Modulus of concrete

Substructure

The intermediate piers are modeled with 3-D frame elements that represent the individual columns. Figure 3.21 shows the relationship between the actual pier and the "stick" model of 3-D frame elements. Three elements have been used for the column between the top of footing and the bearings. This is to account for the varying cross-section near the top of the column since SAP2000 handles members with varying cross-sections by interpolating between the member end nodes. For this model, the moments of inertia and torsional properties of the columns are based on an uncracked section. Foundation springs are connected to the node (2xx) at the base of the pile cap. There are no elements to model the abutments, only support nodes as shown in Figure 3.20.

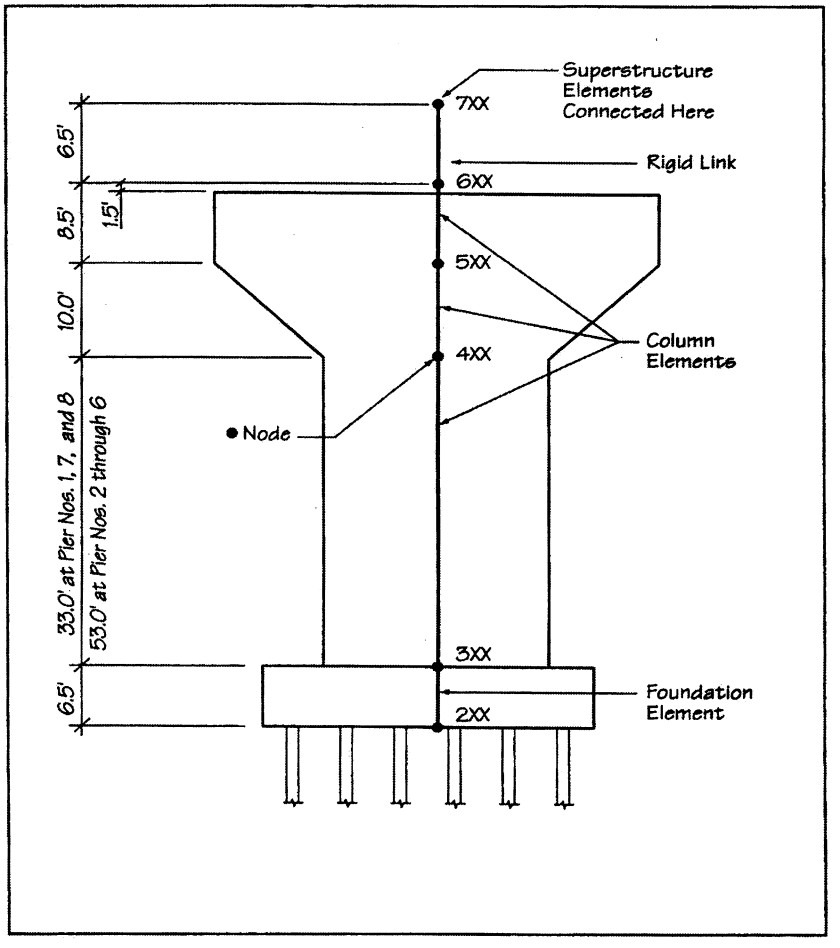

FIGURE 3.21 Bridge No. 5 – Details of Pier Column Elements

Connection of Superstructure to Piers

In the actual structure, internal forces are transferred between the superstructure and the pier through the bearings. In the seismic model, the superstructure forces are transferred at the single point where the superstructure and pier intersect. At pinned piers, node 6xx (in Figure 3.21) transfers shears from the superstructure in all directions, and is released for moment in the longitudinal direction. At Pier Nos. 4, 5, and 8, which are free to move longitudinally, only transverse shears are transferred.

Figure 3.22 shows modeling details for the connection at the top of Pier No. 4, which is the location of the expansion joint between Unit 1 and Unit 2. If the ends of the adjacent superstructure elements are connected directly to Node 741 and these element ends are released for longitudinal translation and rotation, the node (741) is still attached to the top of the rigid link and will receive the tributary mass from each end of the attached superstructure. This will result in longitudinal shears being transmitted to Pier No. 4 though the superstructure is free to move longitudinally there and should transfer no shear.

To model the behavior at the expansion joint correctly, three coincident nodes are defined at the top of the rigid link. The two additional nodes (741A and 741B) are used to define connectivity, which will result in correct forces for Pier No. 4. The end of the superstructure element from Unit 1 is connected to one of

the nodes (741A), the end of the superstructure from Unit 2 is connected to another of the nodes (741B), and the third node (741) is connected to the top of the rigid link of the pier column elements. Local coordinate systems and release constraints of each of the three nodes are defined. This prevents the column top node (741) from picking up lumped mass from the adjacent superstructure elements in the longitudinal direction, for which the structure is free to move.

Modeling details for connections at the tops of Pier Nos. 5 and 8 are shown in Figure 3.23. These piers have sliding bearings to allow unrestrained longitudinal motion. Since the superstructure is continuous, it is not necessary to provide coincident nodes as with Pier No. 4 in order to provide correct modeling for longitudinal forces. Translational and rotational releases are provided at the top end of the rigid link element. The direction for the releases is in the local column coordinate system, and so is oriented tangential to the point of curvature at the center of the pier as shown in Figure 3.23.

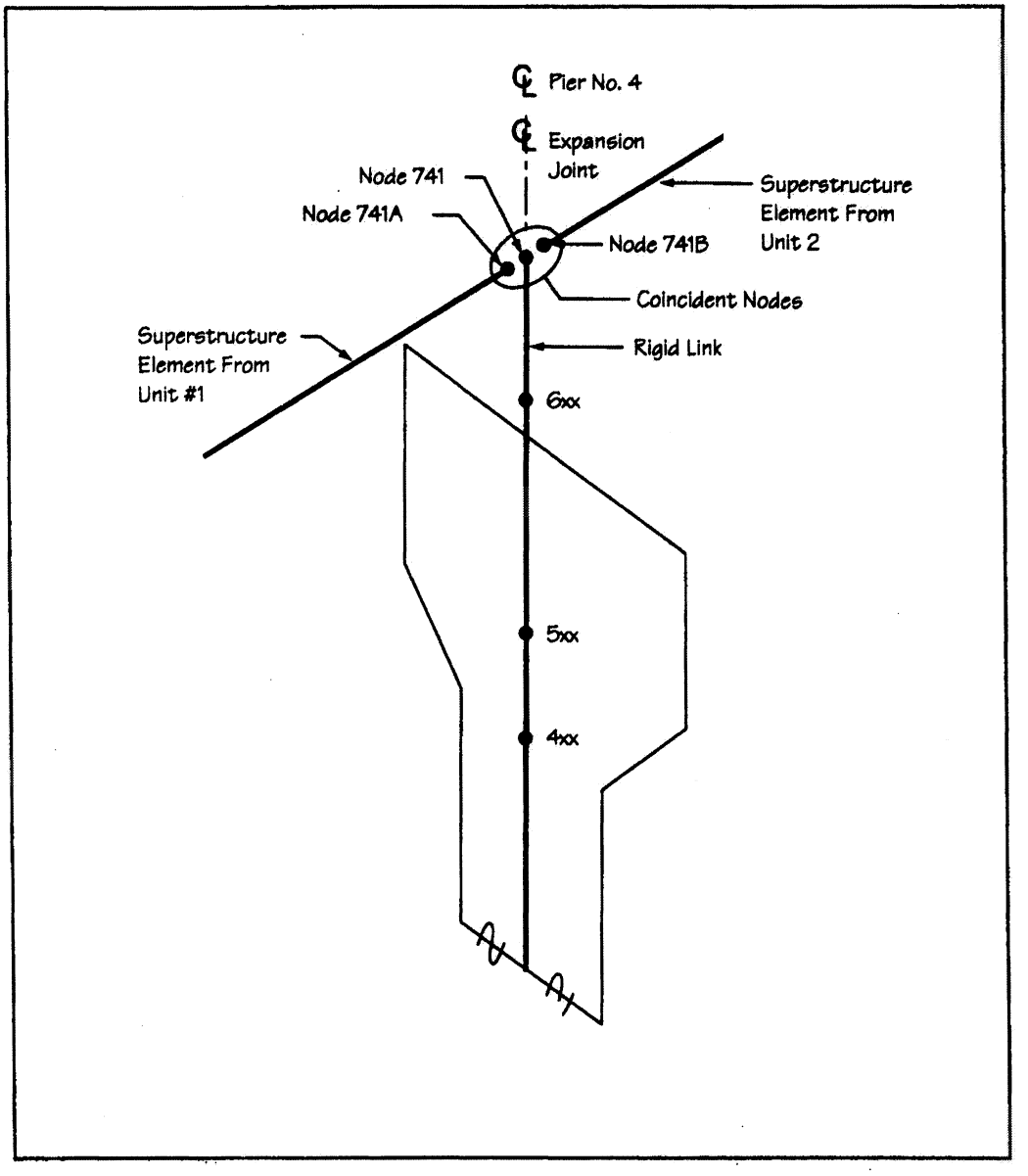

FIGURE 3.22 Bridge No. 5 – Details of Pier No. 4 Expansion Joint

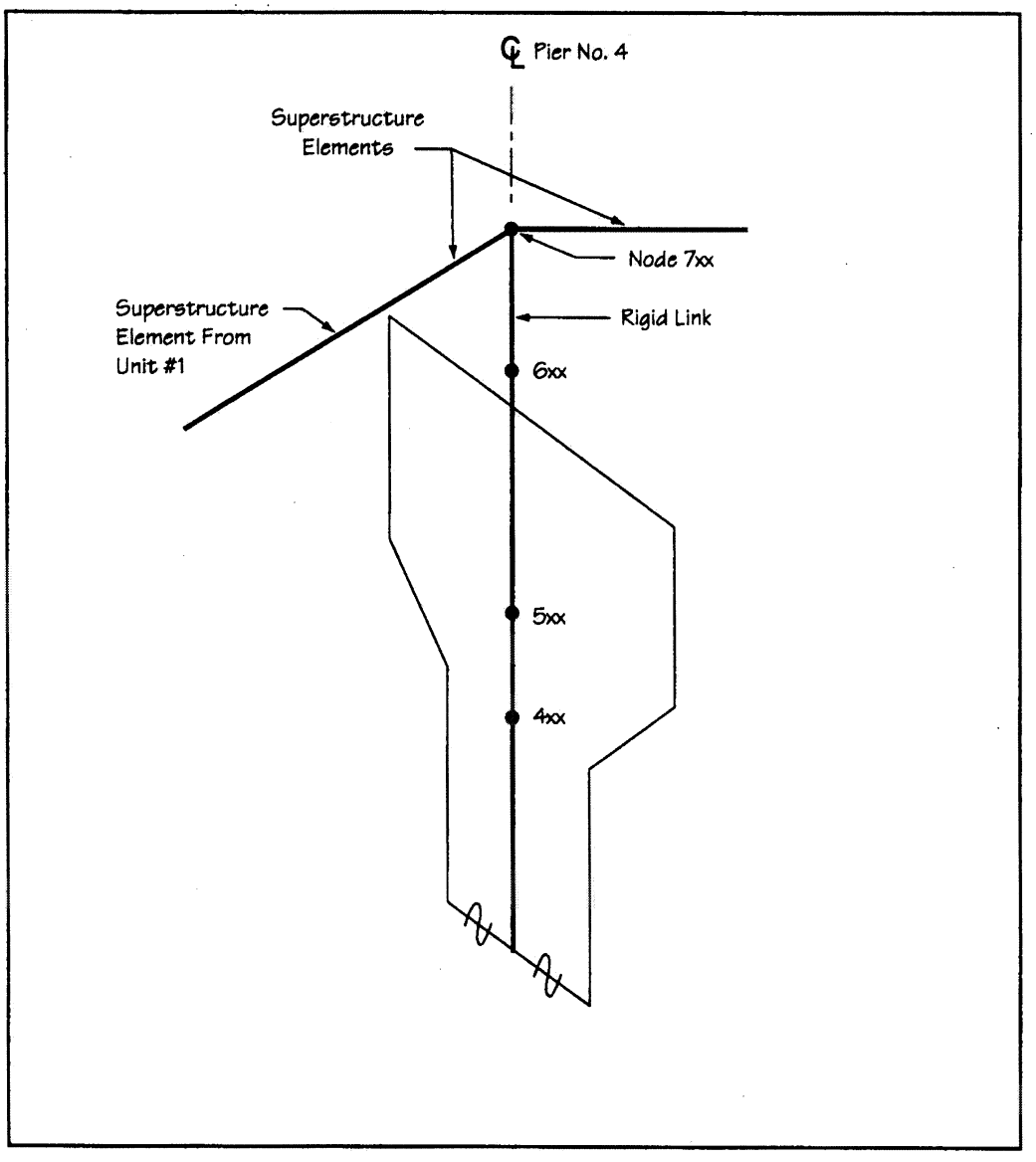

FIGURE 3.23 Bridge No. 5 – Details at Pier Nos. 5 and 8 Sliding Bearings

Foundation Stiffnesses

Pier Foundations

The intermediate pier foundations have been modeled with equivalent spring stiffnesses for the pile group. Figure 3.25 shows details of the spring supports. For this example, all of the intermediate piers use the same foundation springs. The spring stiffnesses are developed for the local pier support coordinate geometry and are input into the SAP2000 model with the same orientation as the local pier columns. Note that the local axes for the spring support nodes are identified differently in Figure 3.24 than the local axes of the column elements. The pier foundation stiffnesses used in the model for

producing final design forces are the stiffnesses of the pile group only without any stiffness contribution from the soil below the pile cap or contribution of flexibility of the cap itself. A rigid cap was assumed.

Determine Single Pile Axial Stiffness: The piles used for the foundation are all 40 feet long, HP 12x84. It is assumed that the piles are end bearing and skin friction is neglected in calculation of the axial stiffness.

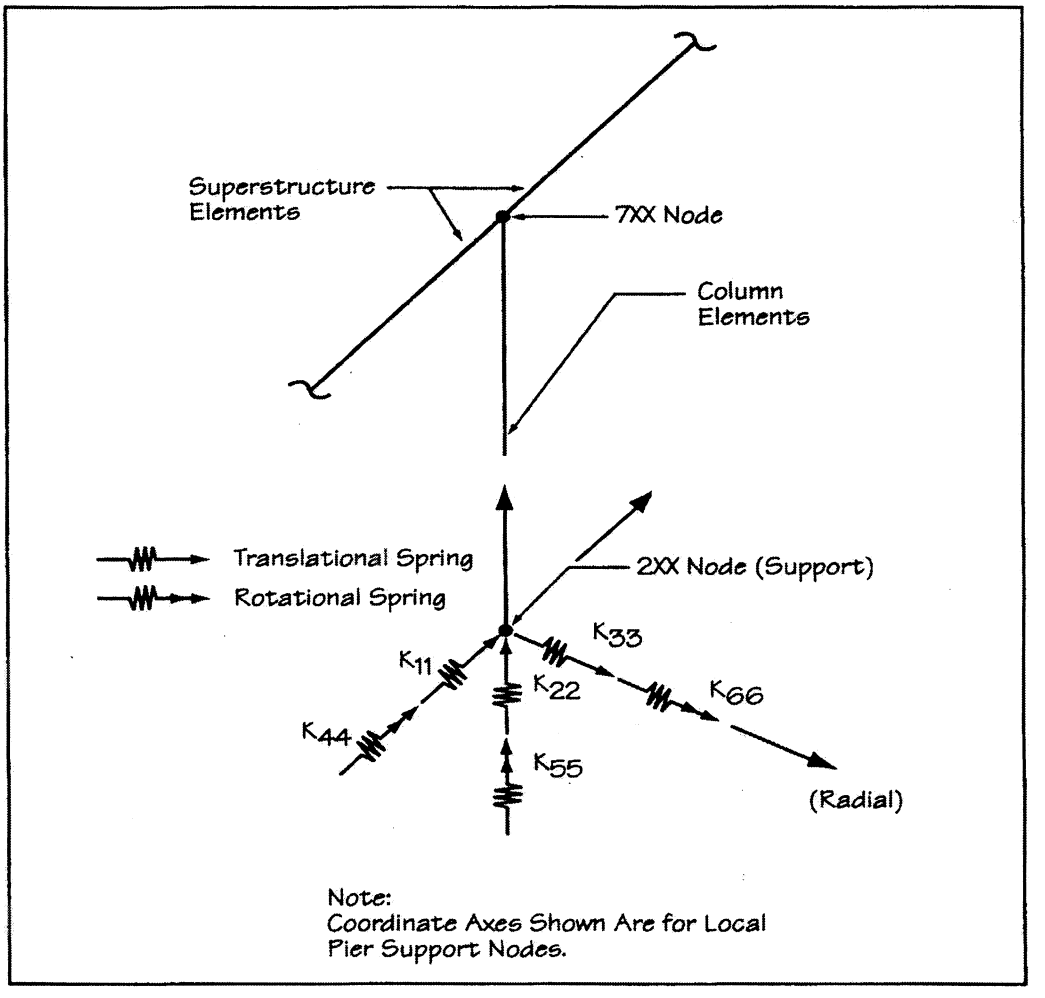

FIGURE 3.24 Bridge No. 5 – Details of Supports for Spring Foundation Model

Abutments

The abutments were modeled with a combination of full restraints (vertical translation and superstructure torsional rotation) and an equivalent spring stiffness (transverse translation) as shown in Figure 3.25. The transverse translational spring stiffness is based upon the stiffnesses of the individual pile stiffnesses used for the intermediate piers. The spring value for the abutments is a ratio of the number of abutment piles (assumed to be 12) to the number of intermediate pier piles times the value of the transverse translational spring (K_{33}) used at the intermediate piers. Other degrees of freedom at the abutment support nodes are released.

spring (K_{33}) used at the intermediate piers. Other degrees of freedom at the abutment support nodes are released.

Since SAP2000 allows for springs and releases relative to the local coordinate geometry, the longitudinal direction at the abutment nodes is oriented along the axis of the superstructure element connected at that node. The transverse direction is perpendicular to the longitudinal direction in the global x-y plane.

The support node locations at the abutments are at the intersection of the superstructure work line (at the centroid of the superstructure) and the centerline of the bearings. The abutment restraints and transverse spring act at these nodes that are oriented in the local superstructure element coordinate geometry.

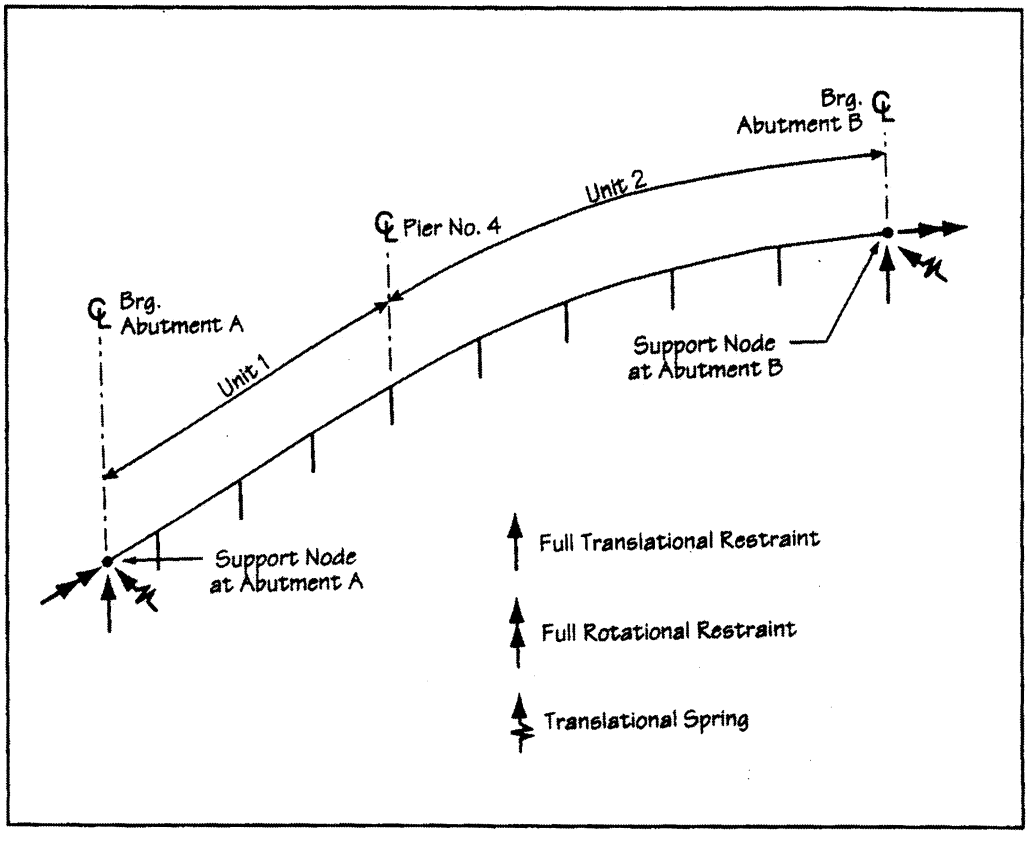

FIGURE 3.25 Bridge No. 5 – Details of Abutment Supports

3.6 Bridge No. 6

The configuration of the bridge is a three-span, concrete box girder superstructure supported on reinforced concrete columns founded on drilled shafts and on integral abutments founded on steel pipe piles. The bridge is located on a site underlain by a deep deposit of cohesionless material. Figure 3.26 (a to i) provides details of the configuration.

The alignment of the roadway over the bridge is sharply curved, horizontally (104 degrees), but there is no vertical curve or grade. The substructure elements are oriented at right angles to the bridge centerline at each substructure station.

The fundamental mode in the vertical direction is shown in Appendix C and has a period of 0.17 seconds as given in Table 3.14 in Section 3.7.

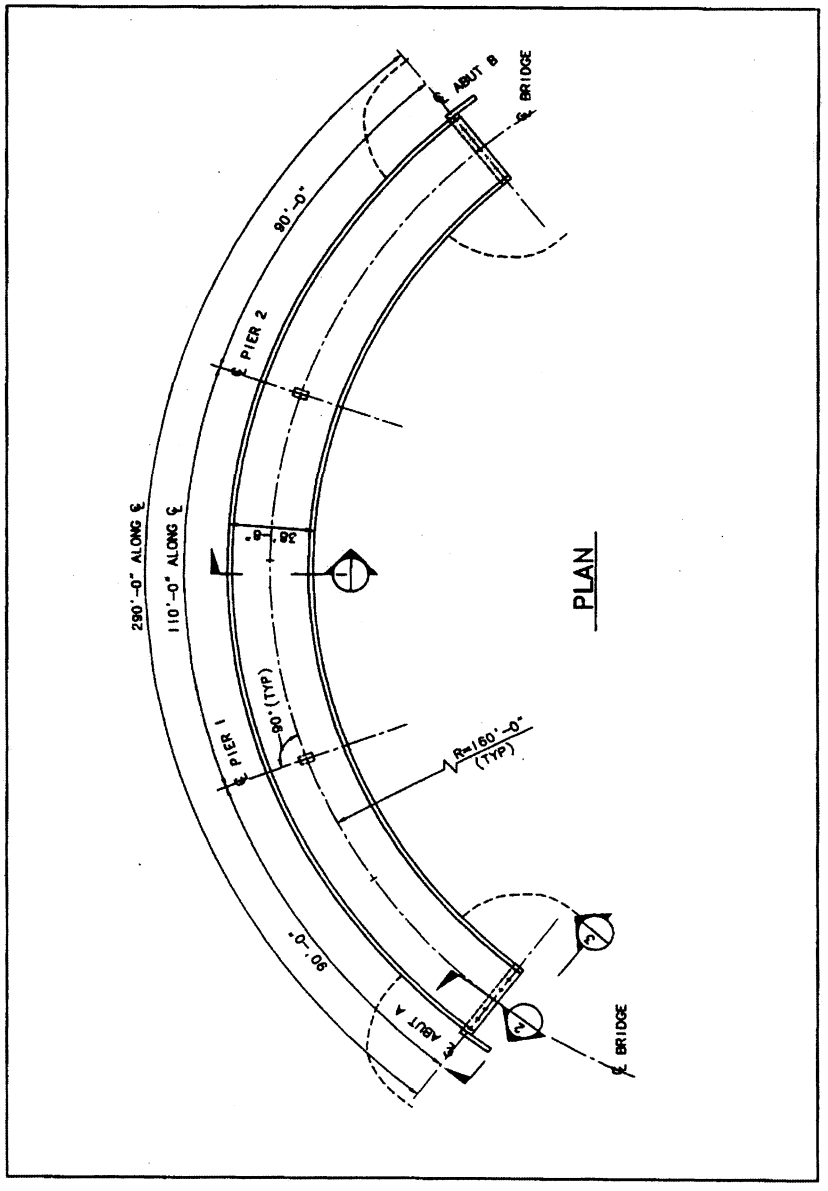

FIGURE 3.26a Bridge No. 6 – Plan

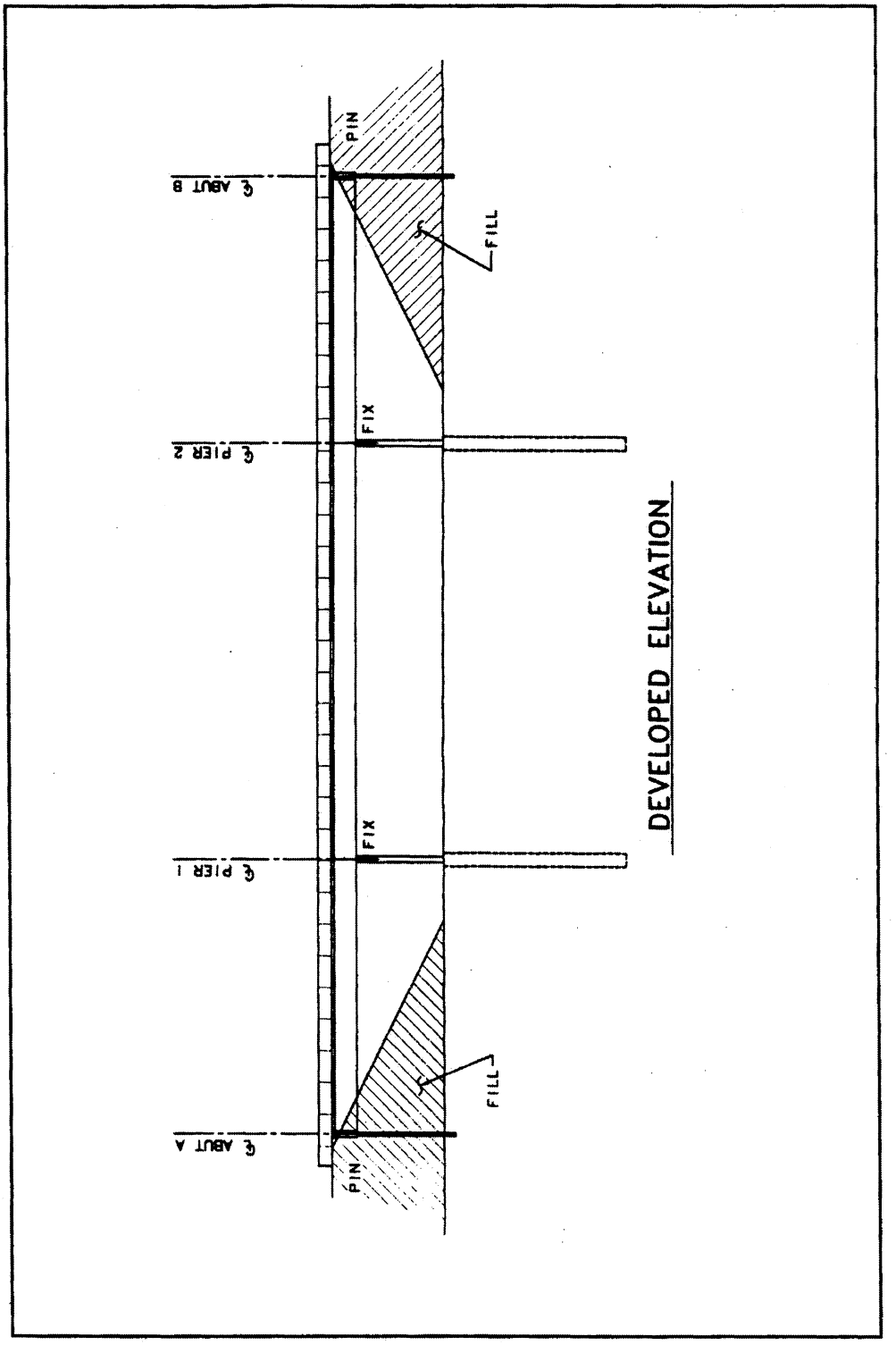

FIGURE 3.26b Bridge No. 6 – Developed Elevation

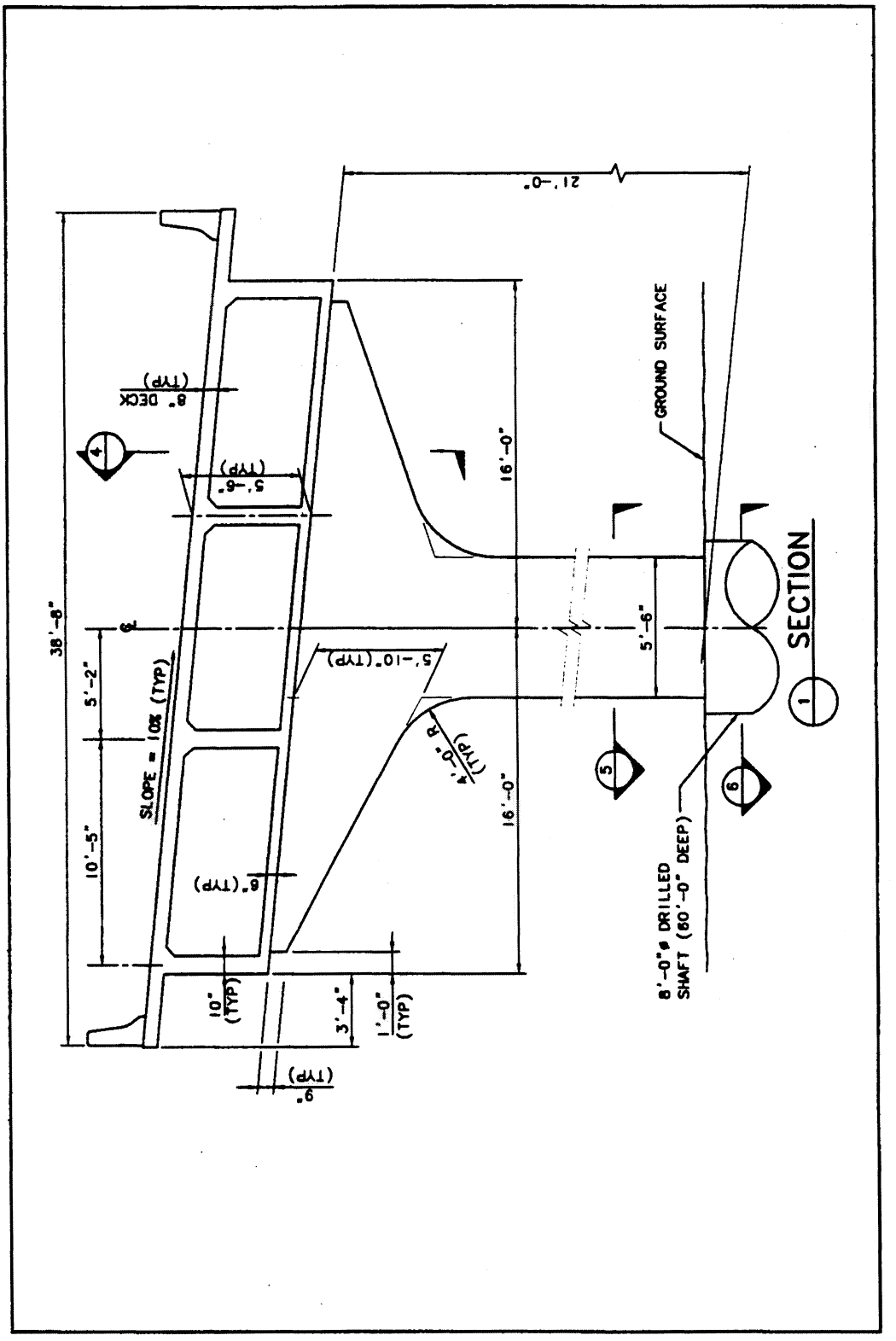

FIGURE 3.26c Bridge No. 6 – Section at Pier

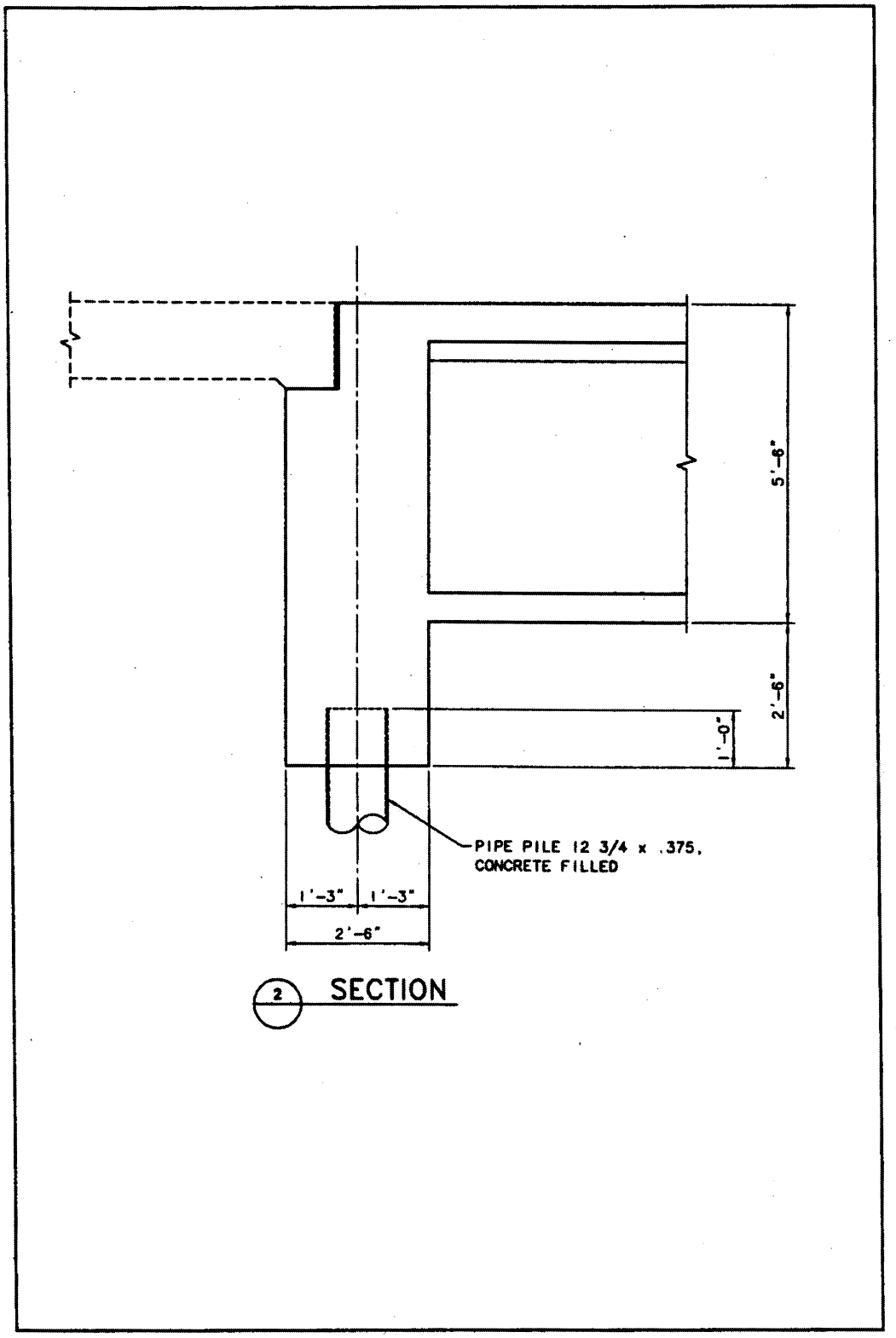

FIGURE 3.26d Bridge No. 6 – Section at Abutment

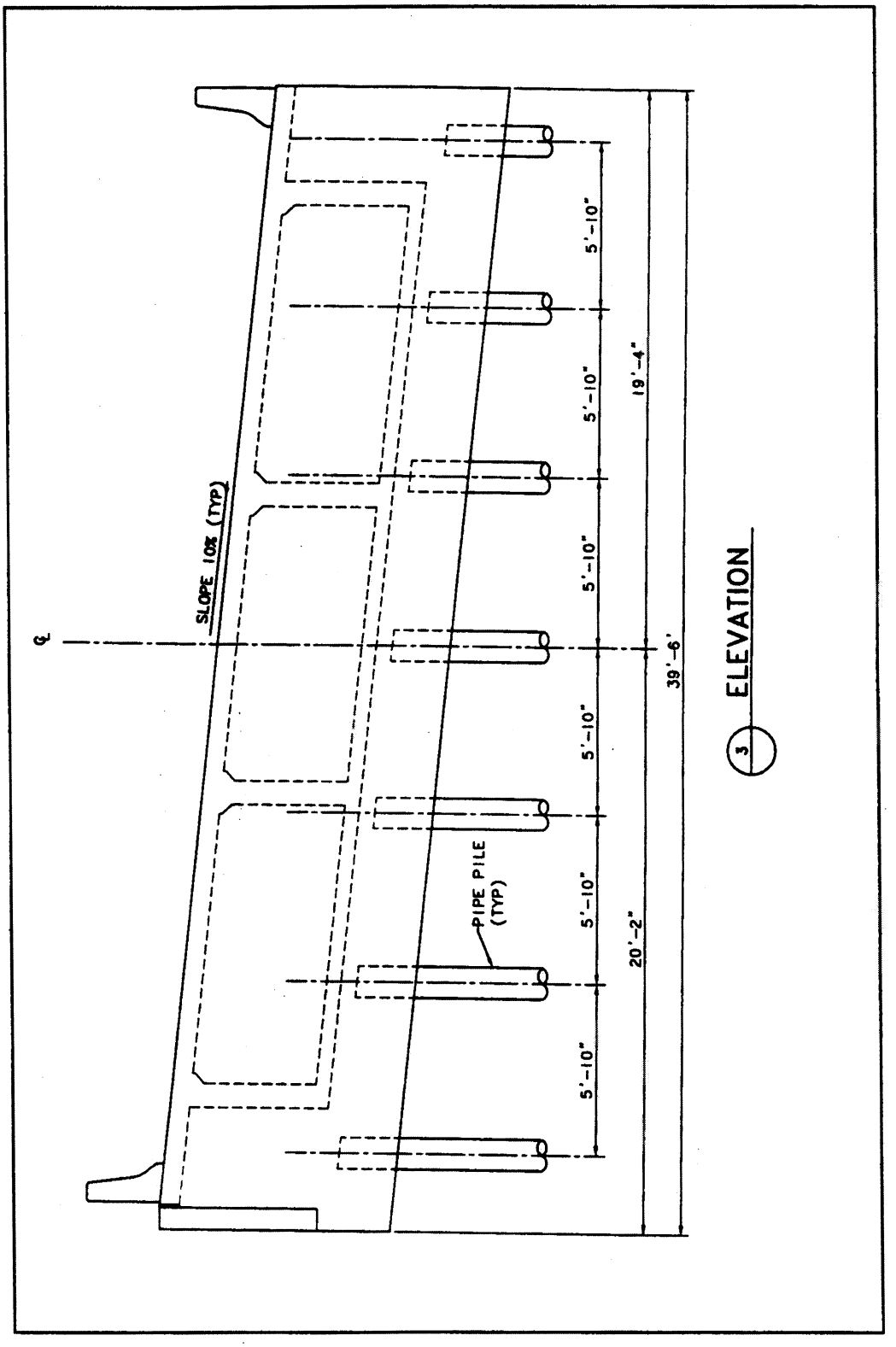

FIGURE 3.26e Bridge No. 6 – End Elevation at Abutment

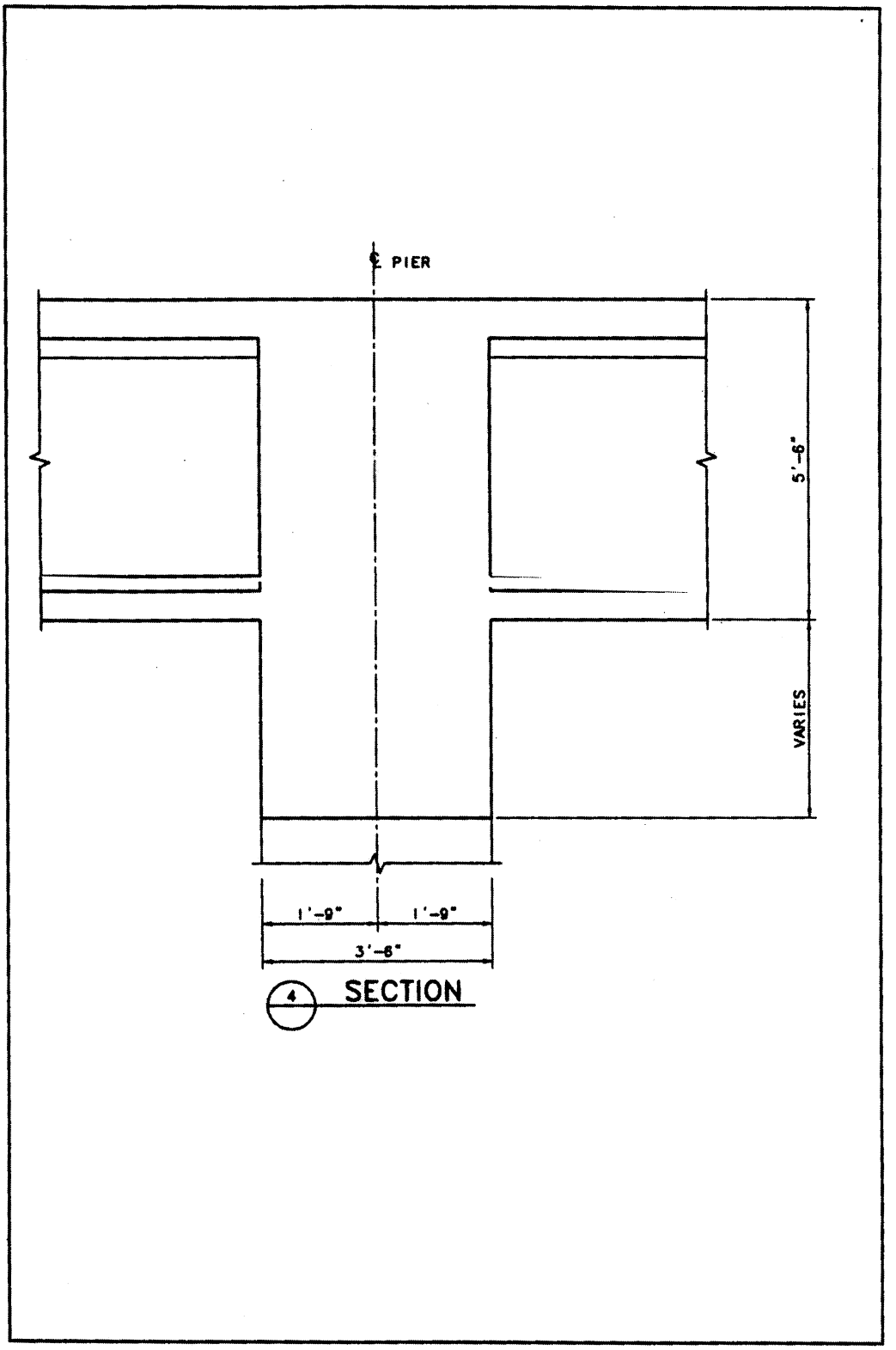

FIGURE 3.26f Bridge No. 6 – Section Through Integral Cap Beam

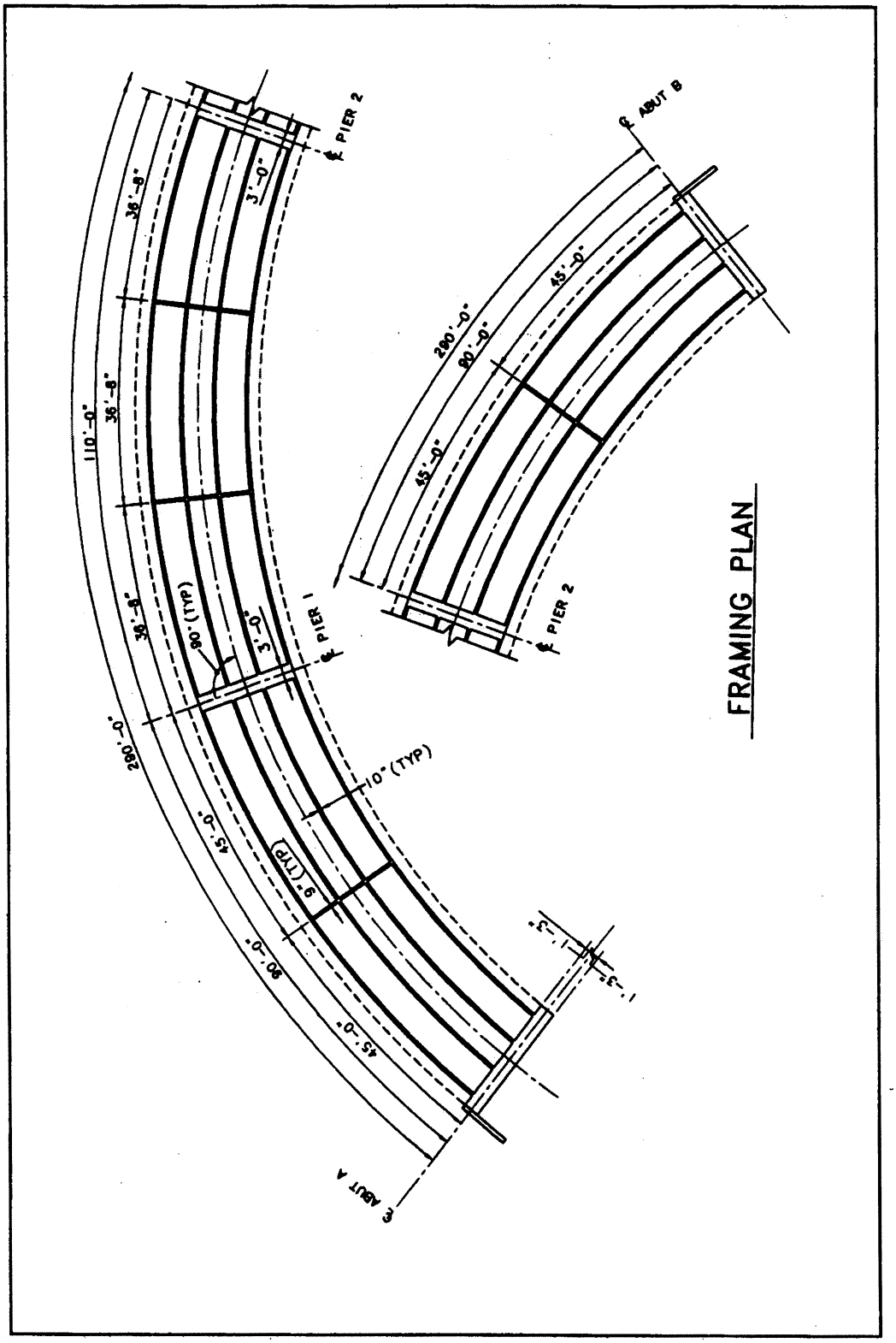

FIGURE 3.26g Bridge No. 6 – Framing Plan

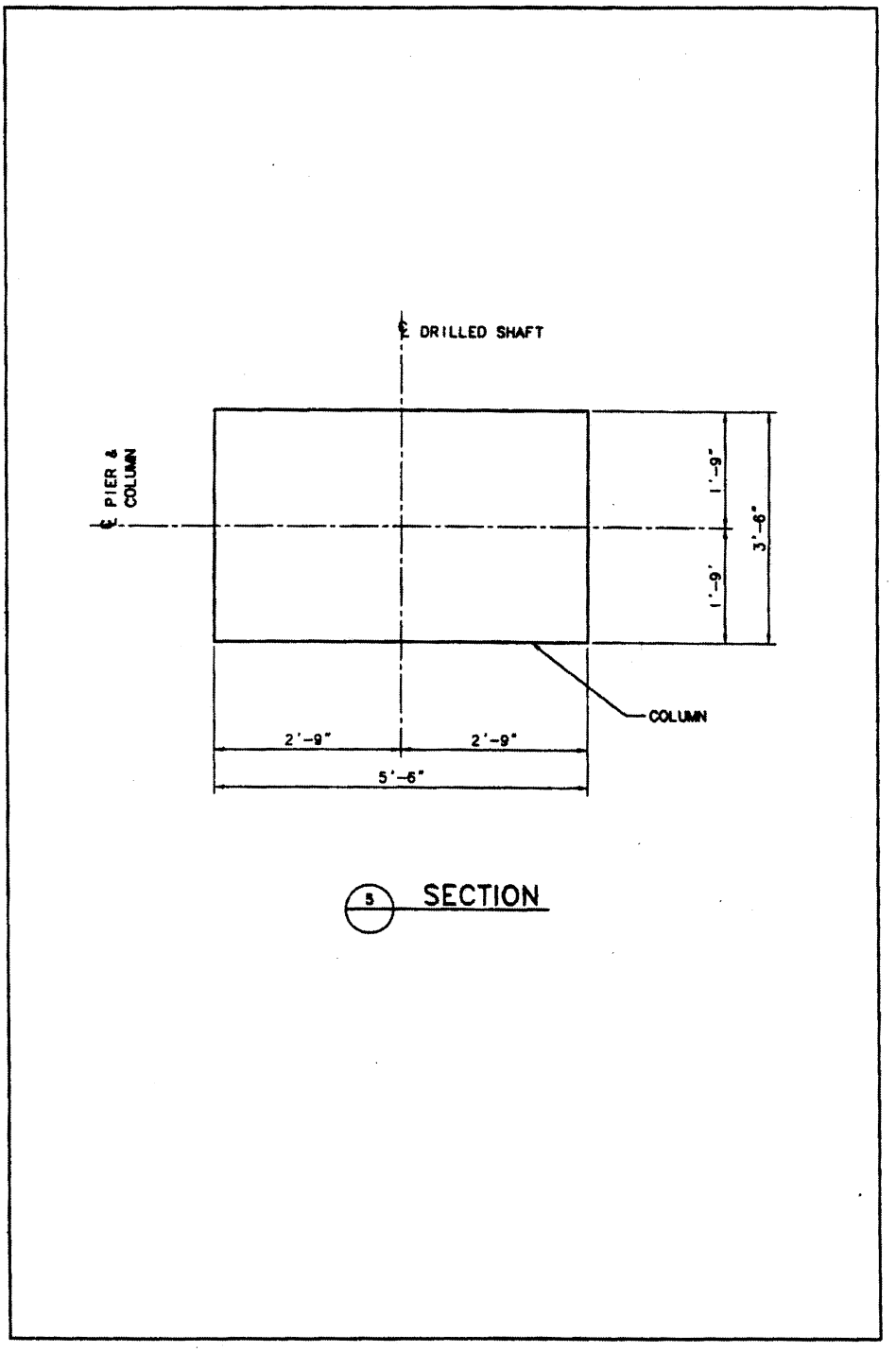

FIGURE 3.26h Bridge No. 6 – Horizontal Section Through Column

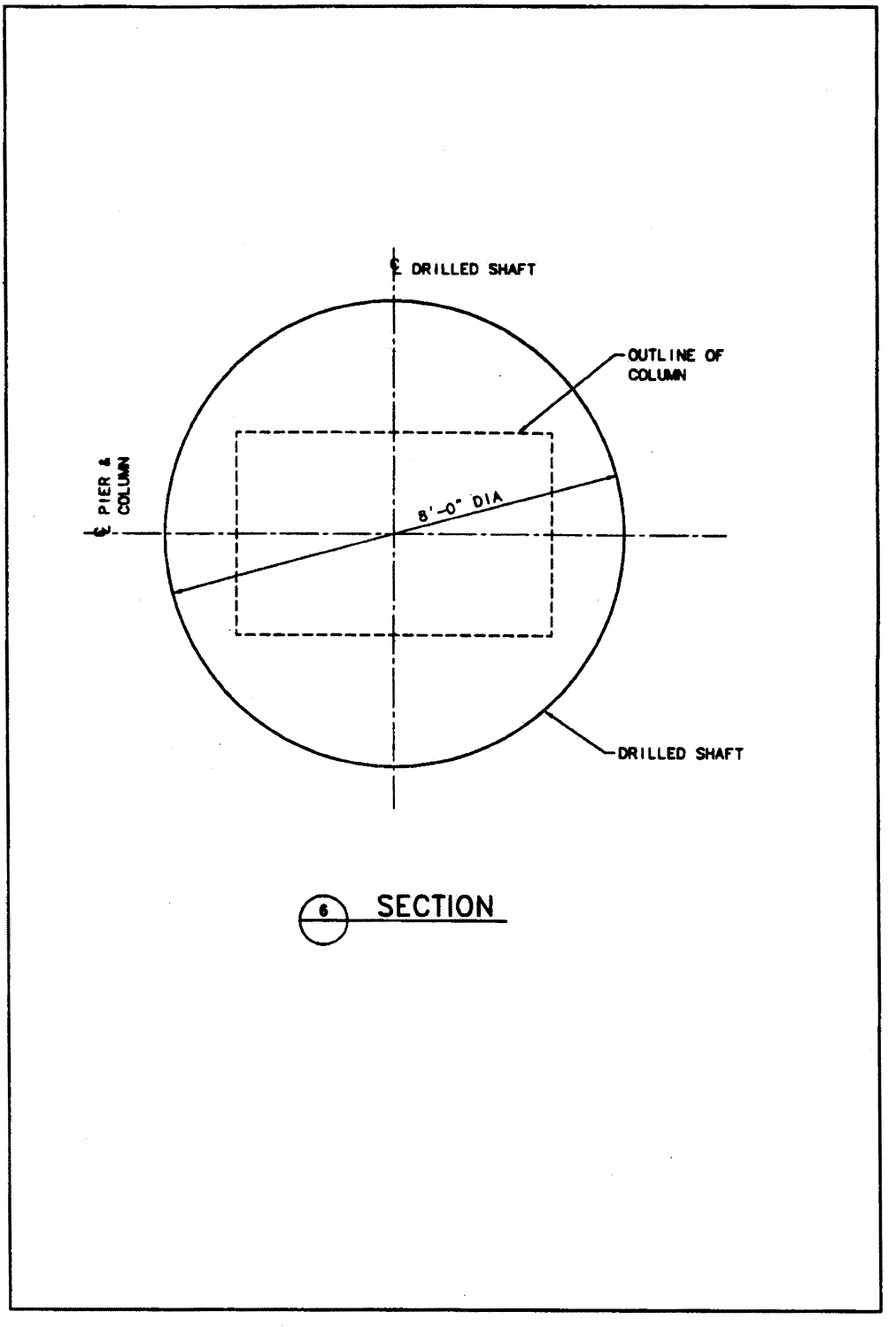

FIGURE 3.26i Bridge No. 6 – Horizontal Section Through Drilled Shaft

Description of Model

The mathematical model used is shown in Figure 3.27 and includes a single line of frame elements for the superstructure and a single line of elements for the piers, which include the full length of the drilled shafts. The drilled shafts are restrained by sets of uniformly spaced elastic springs oriented in two orthogonal directions. In the model, the abutments, which are supported on pipe piles, are supported by elastic springs. The SAP2000 text input file for the model shown in Figure 3.27 is given in Appendix D.

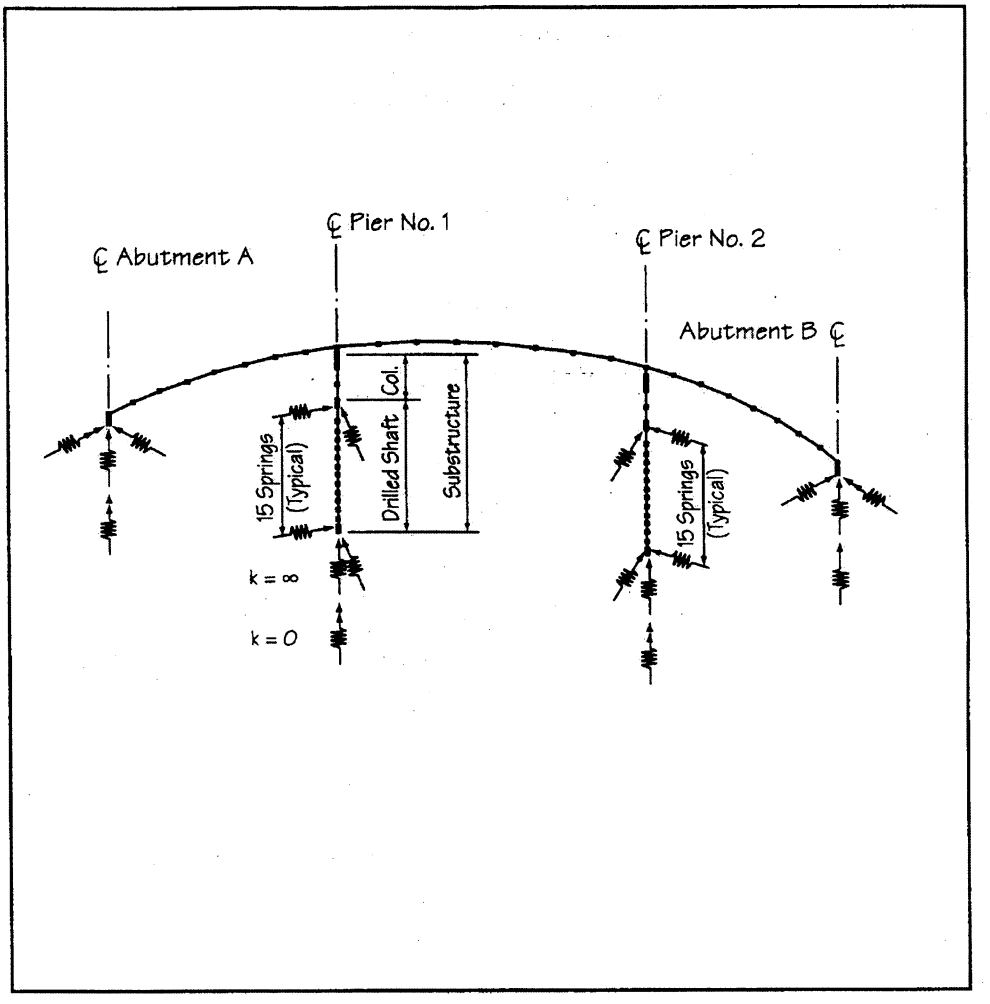

Figure 3.27 Bridge No. 6 - Finite Element Model

Superstructure

Geometry

The superstructure has been modeled using eight 3-D frame elements per span to provide a reasonable representation of the curve. The centroidal axes (work lines) of the elements are located along the centroid of the superstructure box girder.

Properties

The properties of the superstructure elements have been calculated neglecting the effect of the 10 percent superelevation. The properties are listed below. The weights listed are those that were added to the SAP2000 model.

$A_s := 56.2\ ft^2$	Cross-sectional area of superstructure
$I_{sh} := 250\ ft^4$	Moment of inertia about horizontal axis
$I_{sv} := 6526\ ft^4$	Moment of inertia about vertical axis
$J_s := 777\ ft^4$	Torsional constant of superstructure
$W_{ed} := 119\ kip$	Weight of end diaphragms at abutment
$W_{pd} := 79\ kip$	Weight of pier diaphragms or cap beams
$W_{id} := 15\ kip$	Weight of intermediate diaphragms
$W_b := 0.9\ kip/ft$	Weight of barriers per unit length
$J = 777\ ft^4$	Torsional constant. It considers the actual multicell box as a single-cell box comprised only of the perimeter elements.

Substructure

The single line of elements representing each pier has been divided into elements with nodes at each change in cross-section, as shown in Figure 3.28. A rigid link is used to model the stiff part of the column that is located in the cap beam of the superstructure. The flare at the top of the column is modeled using three elements, which are each two feet high and 3.5 feet thick. The width of the elements varies from 10 feet to 28 feet. The lower portion of the column is modeled with two elements, and the drilled shaft is modeled with 16 elements, each 4 feet long, except for the top and bottom elements, which are made 2 feet long in order to keep the tributary length of the foundation springs the same.

The piers and abutments are oriented radially; thus, these substructure elements are rotated in the model to properly account for the position of the pier on the curve. Figure 3.29 shows the direction of the first two local axes of each structure element with arrows. In SAP2000, the first local axis is always directed along the length of the member. The second axis is oriented orthogonally to the first axis. As is seen in the Figure 3.29, the pier elements are oriented in the radial direction.

The properties for the substructure elements were not input directly, instead they were calculated by SAP2000, based on the input cross-sectional dimensions. The calculated properties include both the stiffness and the mass of the piers. The mass of the elements was calculated based on the specified cross-sectional area and the densities of the elements. The program calculates the mass tributary to each node, and then lumps that mass at the node. The mass of the drilled shaft was not included, since it is located entirely below grade. The difference between the concrete density and the density of the displaced soil is not great enough to warrant assigning mass to the foundation. This mass was excluded by assigning zero density to the elements representing the drilled shaft.

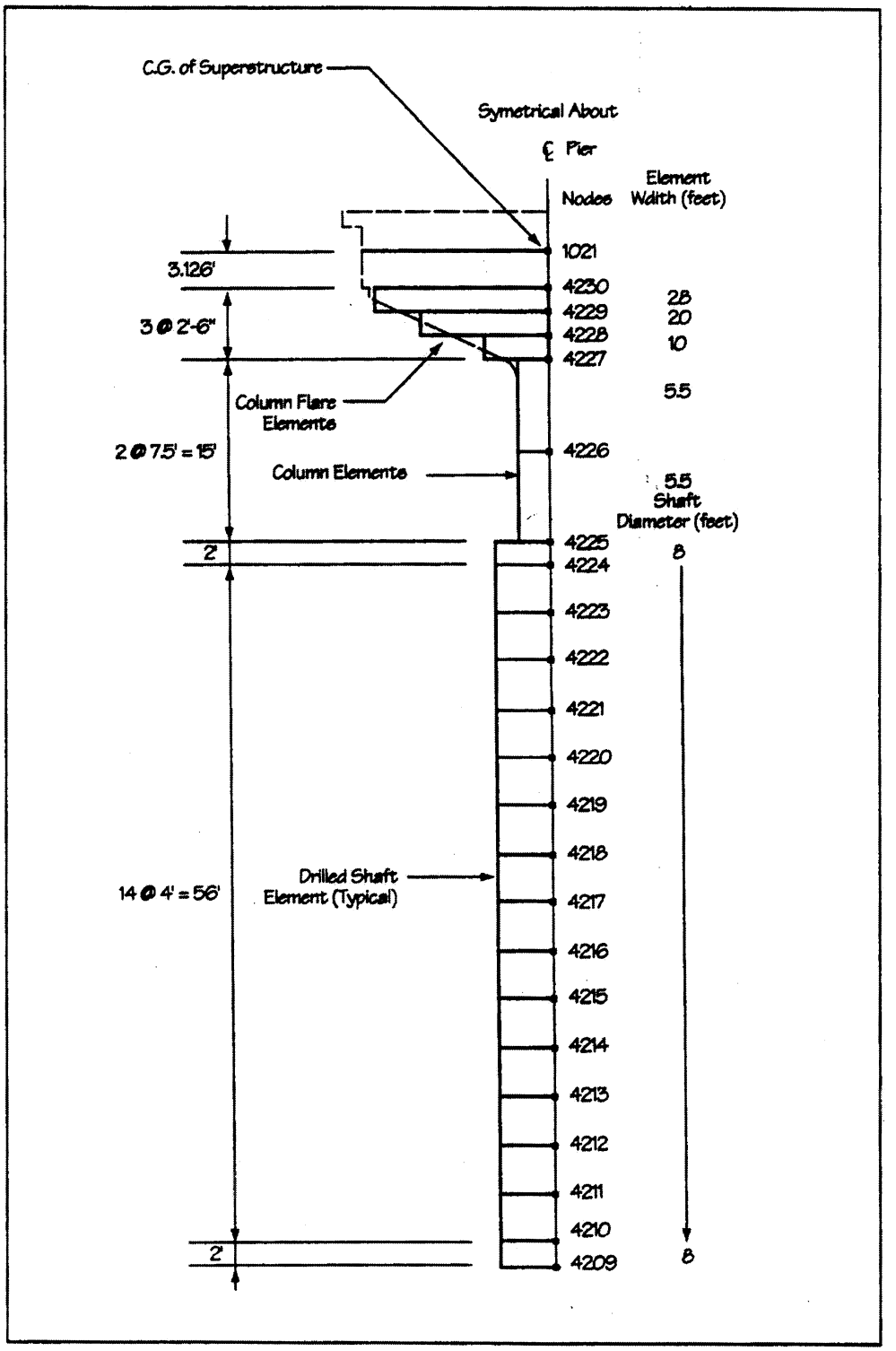

FIGURE 3.28 Bridge No. 6 – Pier Geometry and Element Layout

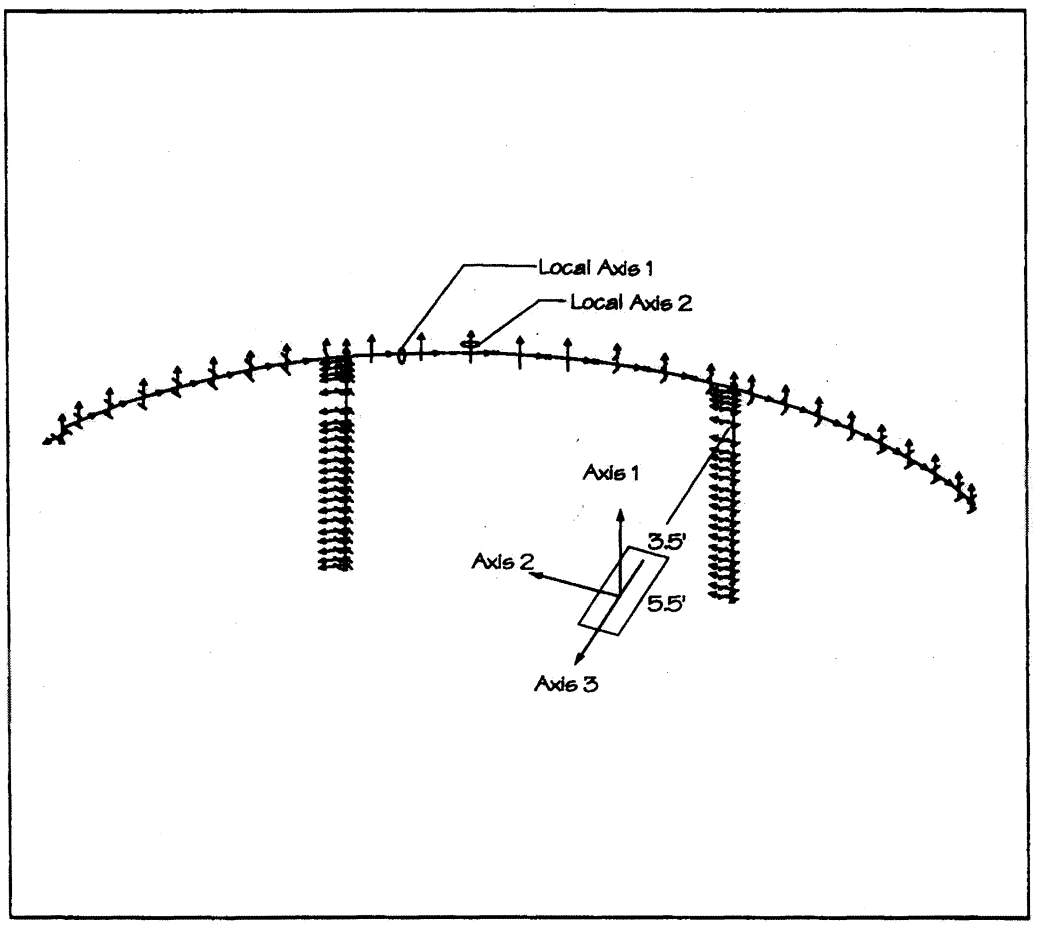

Figure 3.29 Bridge No. 6 – Orientation of Member Local Axis

Drilled Shafts

For this example, the equivalent soil springs method was selected to model the drilled shaft. The soil springs at each depth are calculated using a coefficient of horizontal subgrade reaction that increases linearly with depth and is inversely proportional to the cross-sectional dimension of the shaft. The stiffness of the soil is based on the water table extending all the way to the ground surface. A full listing of the spring constants used along the length of the shaft is given in Table 3.5.

TABLE 3.5 Bridge #6 - Lateral Spring Constants for Drilled Shaft

Depth Z (ft)	**Coefficient of Horizontal Subgrade Reaction k_h** (kcf)	**Spring Constant k_I** (k/ft)
2	6.5	207
6	19.4	622
10	32.4	1,037
14	45.4	1,452
18	58.3	1,866
22	71.3	2,281
26	84.2	2,696
30	97.2	3,110
34	110.2	3,525
38	123.1	3,940
42	136.1	4,355
46	149.0	4,769
50	162.0	5,184
54	175.0	5,599
58	187.9	6,013

Discussion of Nonlinear Effects: The spring constants developed above are only valid provided that the lateral soil pressures do not exceed thresholds beyond which the soil behavior is nonlinear. The spring stiffnesses used to represent the soil pressures on the drilled shaft were checked to be less than forces needed to cause soil failure due to the loading applied (Response Coefficient = 0.5).

Vertical Supports at Base of Shaft: As shown in Figure 3.27, vertical movement of the drilled shaft is restrained by an infinitely stiff spring at the base of the shaft. Actual vertical resistance occurs via skin friction and end bearing. However, for this example, the simplification of restraining only the base of the shaft is felt to be reasonable. Likewise, torsional movement of the shaft would be resisted by skin friction. However, no torsional restraint was used in this model, as shown in Figure 3.27. The response is not sensitive to lack of torsional restraint in the shaft, and this can be demonstrated by simple bounding analyses.

Abutments

The abutments are modeled with rigid links that extend downward from the superstructure centroid to the approximate force transfer point located between the piles and the end diaphragm. This arrangement is shown in Figure 3.30. The springs that represent the piles are connected to the lowermost nodes (e.g. node 4101), and the springs that represent the abutment backfill, which is considered in the bounding of response, are connected to the middle nodes (e.g. node 4102).

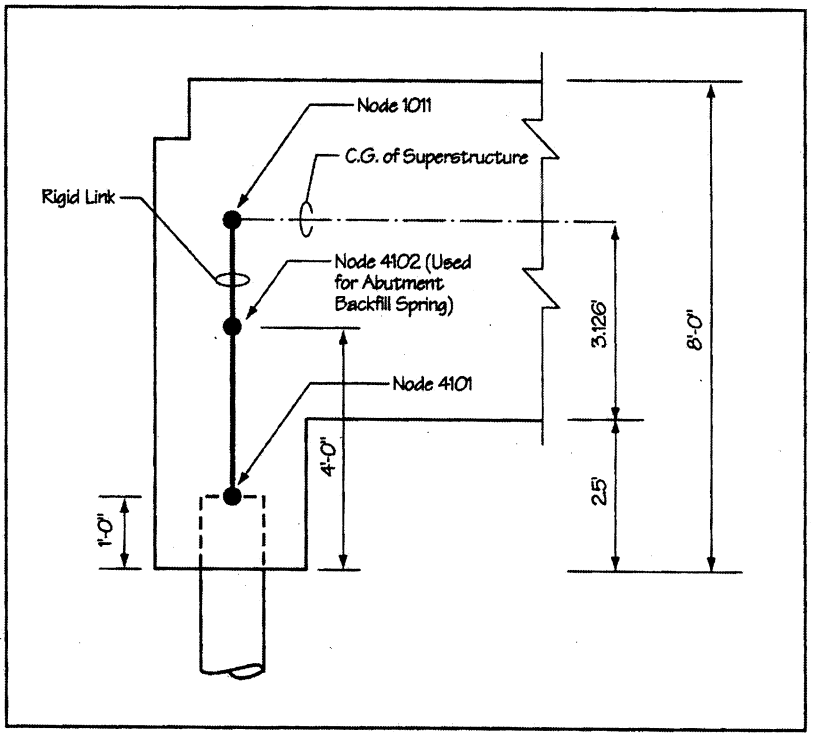

FIGURE 3.30 Bridge No. 6 – Abutment Geometry

Pipe Piles: The DM7 Method is used in this example to calculate the abutment pipe pile spring constants. DM7 considers two forms of pile rotational restraint: pinned at the top of the pile and fixed at the top of the pile. The top may be either at the ground surface or above it. The connection between the end diaphragm and the steel pipe pile for this example is considered more nearly pinned than fixed.

Horizontal Longitudinal Stiffness: The stiffness of the pile in the longitudinal direction is determined by multiplying the stiffness of a single pile by the total number of piles at the abutment. There is no accounting for group effects, since the loading is perpendicular to the line of piles.

$$K_{long} = 2569 * kip/ft$$

Horizontal Transverse Stiffness: The stiffness of the piles in the transverse direction is reduced for group effects, because the piles are close enough to one another to reduce their stiffnesses.

$$K_{trans} = 2074 * kip/ft$$

Vertical Stiffness: The piles are friction piles and the skin friction in this case may be assumed to be uniformly distributed along the pile. Also, the bottoms of the piles are assumed not to deflect downwards.

$$K_{vert} = 2.917 * 10^5 * kip/ft$$

Rotation About Vertical Axis:

$$K_I = 367 * kip/ft$$

Rotation About Longitudinal Axis: The rotation about the longitudinal axis of the superstructure is resisted by axial forces developed in the piles. Thus, the axial stiffness of the piles is used to develop the rotational stiffness.

$$K_{rl} = 3.97 * 10^7 * kip*ft/ rad$$

Rotation About Transverse Axis: Because the tops of the piles are assumed to be pins, no rotational stiffness will be used about this axis.

Summary of the Abutment Spring Values

The values are summarized in Table 3.6, and the locations and orientations of the springs are explained in Figure 3.31.

TABLE 3.6 Bridge #6 - Spring Constants for Abutment Springs

K_{long} (kip/ft) Longitudinal Translation	2,569
K_{trans} (kip/ft) Transverse Translation	2,074
K_{vert} (kip/ft) Vertical Translation	291,700
k_{rv} (kip-ft/rad) Rotation About Vertical Axis	349,600
K_{rl} (kip-ft/rad) Rotation About Longitudinal Axis	39,700,000
K_{rt} (kip/ft) Rotation About Transverse Axis	0
K_{back} (kip/ft) Translation Into Backfill Translation Away From Backfill	94,800 0

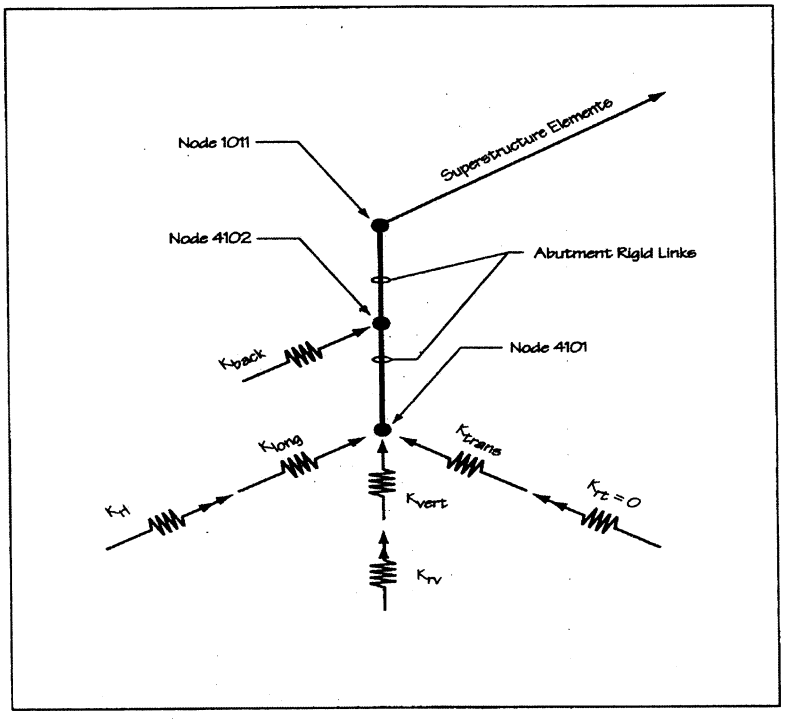

FIGURE 3.31 Bridge #6 - Soil Spring Configuration at Abutments

3.7 Summary Tables of Bridges

Table 3.7 Configurations and Dimensions of the Berger/ABAM Seven Series of Bridges

Bridge #	Description	Super-Structure Type	Span(s) Length (ft)	Deck Depth (ft)	Deck Width (ft)	Pier Type	Column Size (ft)	Column Height (ft)
1	Two-span Continuous	CIP Concrete Box	145.5 103.5	5.7	73.8	Three Column Integral Bent	Dia. = 4	25.5
2	Three-span Continuous	Steel Girder	152 124	4.5 - 7.8	68.5	Wall Type Pier	60 x 5	36
3	Single-span	AASHTO Precast Concrete Girder	70	4.5	44	(N/A)	Abutments Only	Abutments Only
4	Three-span Continuous	CIP Concrete	120 100	6.0	43	Two Column Integral Bent	Dia. = 4	20
5	Nine-Span Viaduct	Steel Girder	173 185	7.75	42	Single Column (Variable Heights)	20 x 6.3	50 70
6	Three-span Continuous	CIP Concrete Box	110 90	5.5	39	Single Column	5.5 x 3.5	21

Table 3.8 Values of Vertical Modal Percentage Mass Participation for Each Bridge Less Than Periods 0.1, 0.15, 0.2 and 0.3 Seconds

	< 0.1 seconds	< 0.15 seconds	< 0.2 seconds	< 0.3 seconds
Bridge #1	23	27	27	73
Bridge #2	61	62	62	99
Bridge #3	25	25	25	100
Bridge #4	20	20	20	100
Bridge #5	64	64	70	70
Bridge #6	33	33	99	99

Table 3.9 Data for Vertical Modes With Vertical Mass Participation Ratios Greater Than 2% for Bridge #1

Mode #	Period	Percentage Mass Participation	Cumulative Percentage Mass Participation
2	0.4454	26.8	26.8
3	0.2196	45.5	72.3
5	0.1271	4.4	76.8
7	0.0642	8.0	84.8
10	0.0383	12.4	97.2

Table 3.10 Data for Vertical Modes With Vertical Mass Participation Ratios Greater Than 2% for Bridge #2

Mode #	Period	Percentage Mass Participation	Cumulative Percentage Mass Participation
7	0.2645	37.8	38.1
16	0.0724	2.8	41.8
18	0.0530	7.0	48.7
21	0.0400	2.5	51.3
26	0.0276	11.5	62.8
36	0.0133	16.1	79.9
56	0.0034	18.3	98.2

Table 3.11 Data for Vertical Modes With Vertical Mass Participation Ratios Greater Than 2% for Bridge #3

Mode #	Period	Percentage Mass Participation	Cumulative Percentage Mass Participation
Translation springs at abutments.			
1	0.2013	74.9	74.9
6	0.0266	16.4	91.4
8	0.0199	8.7	100

Table 3.12 Data for Vertical Modes With Vertical Mass Participation Ratios Greater Than 2% for Bridge #4

Mode #	Period	Percentage Mass Participation	Cumulative Percentage Mass Participation
6	0.2050	79.3	79.3
9	0.0822	12.3	92.1
13	0.0579	6.0	98.2

Table 3.13 Data for Vertical Modes With Vertical Mass Participation Ratios Greater Than 2% for Bridge #5

Mode #	Period	Percentage Mass Participation	Cumulative Percentage Mass Participation
12	0.5042	2.3	4.9
20	0.3228	16.6	21.5
21	0.3061	8.0	29.4
36	0.1919	4.0	34.2
58	0.0809	3.4	39.7
59	0.0795	2.0	41.7
62	0.0783	9.5	51.8
65	0.0750	8.6	60.7
66	0.0743	10.3	71.0
68	0.0691	5.4	77.0
69	0.0662	2.6	79.6
76	0.0629	4.4	86.4
79	0.0587	9.4	95.6

Table 3.14 Data for Vertical Modes With Vertical Mass Participation Ratios Greater Than 2% for Bridge #6

Mode #	Period	Percentage Mass Participation	Cumulative Percentage Mass Participation
7	0.1730	66.8	66.9
10	0.0620	2.9	69.9
14	0.0475	4.7	74.7
15	0.0466	10.8	85.5
18	0.0346	9.3	94.8

SECTION 4
GROUND MOTIONS

The study of vertical ground motions for seismic design has not traditionally received the same level of attention as horizontal ground motions. In the past, the general design rule has been to use two-thirds of the horizontal response spectra. In this study, we have used attenuation relationships by Sadigh and others [1993; 1997] and Abrahamson and Silva [1997] to define both the horizontal and vertical response spectra suitable for the Western United States (WUS) or active tectonic environment.

This section begins with a brief description of the time-domain characteristics of vertical ground motion as described by Silva [1997], followed by the development of response spectra and frequency-scaled time histories used in the bridge analyses. Response spectra suitable for WUS rock and soil site conditions were computed from the above mentioned empirical attenuation relationships at five distances (1, 5, 10, 20, and 40 km) and two magnitudes (6.5 and 7.5). Twenty sets of 3-component acceleration time histories, representing rock and soil motions at distances of 5 and 20 km from a M6.5 event, are selected and matched to the design spectra. These time histories will be used in the time history analyses of bridge numbers 1, 4, and 5.

4.1 Time Domain Characteristics of Vertical Ground Motions

Silva [1997] presented a series of recorded time histories that show typical characteristics of vertical motions in relation to the horizontal motions at both close-in and distant recording stations. The time history plots typically show the pattern of short period motion on the verticals being out-of-phase (arriving early) with the main horizontal motions, while the longer period motion becomes more in-phase between the three components of motions. As an example, Figure 4.1 shows the recorded 3-component of accelerations at Arleta (a soil site about 9 km from the fault) during the 1994 Northridge earthquake and the early arriving short period motion is revealed in the vertical component of motions. The exception to the usual pattern of early arriving short-period vertical motions is the close-in rock site, where the vertical component is in-phase (similar arrival time) and shows similar motions to the horizontal components. Acceleration time histories for a close-in rock site (fault distance = 10km) that exhibit these characteristics are given in Figure 4.2. They were recorded at Pacioma Dam (downstream) station during the 1994 Northridge earthquake. These observed trends in time-domain characteristics might be of significance to structural analyses.

Silva [1997] attributes the early arriving short period vertical motions to the dominance of compressional-wave on the vertical component. At the soil site, the dominance of compressional-wave is explained by the fact that shear-wave energy does not project significantly onto the vertical component due to the severe refraction at the soil/rock interface (leading to near vertical incidence at the free surface) and to the large amplification of compressional-wave near the surface. At close-in rock sites, the inclined SV-wave is expected to dominate vertical motions and is responsible for the above-mentioned exception to the usual pattern. However, at larger distances (larger than 10 to 20 km), compressional-wave again tends to be dominant on the vertical component because the SV-wave is beyond its critical angle and does not propagate to the surface effectively.

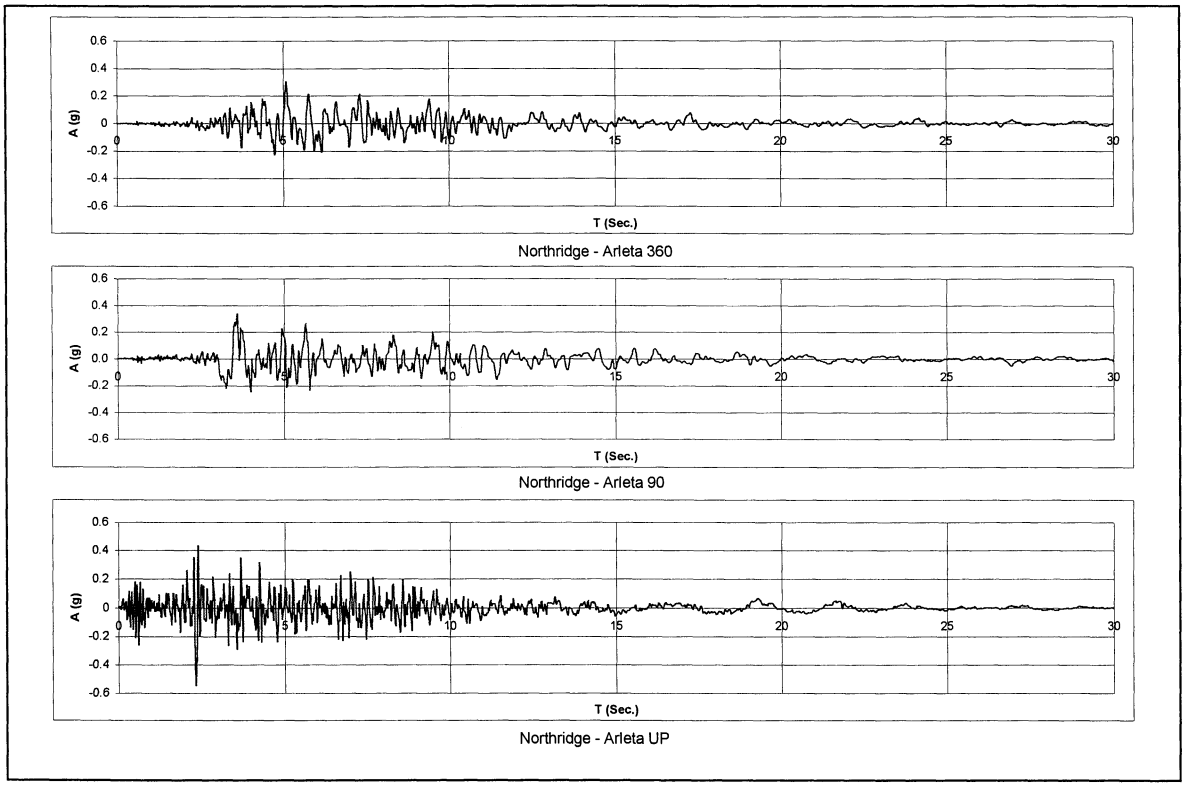

Figure 4.1 Acceleration Time Histories of the Northridge – Arleta Record

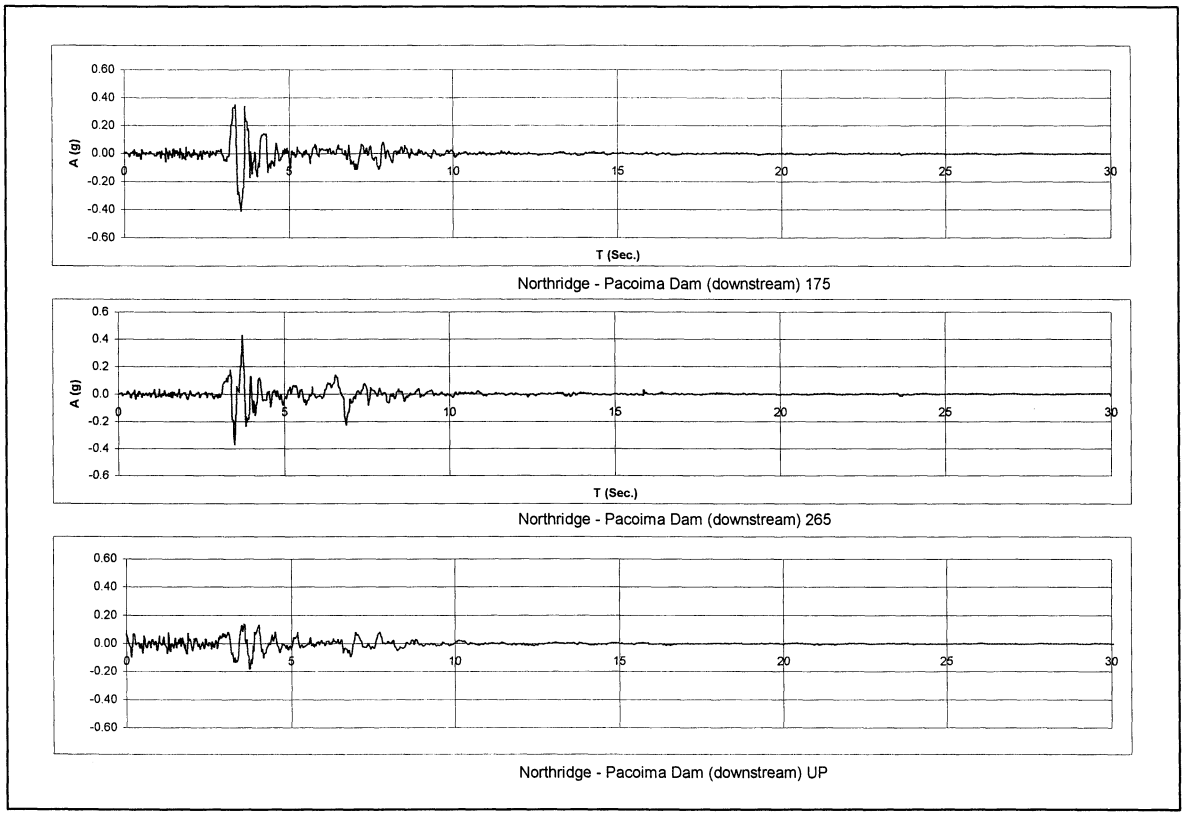

Figure 4.2 Acceleration Time Histories of the Northridge – Pacoima Dam (downstream) Record

4.2 Response Spectral Characteristics of Vertical Ground Motions

At close-in distances, the vertical spectra can exceed the horizontal spectra at periods shorter than 0.1 seconds. As an example, response spectra from the Arleta record of the Northridge earthquake are shown in Figure 4.3. At periods longer than 2 seconds, the vertical spectrum of this record has a spectral acceleration similar to those of the two horizontal motions. At a distant site *(Figure 4.4 – 1992 Landers earthquake, Yermo – soil site, 25km),* the vertical spectra tend to be less than the horizontal spectra at short periods but again approach the smaller of the horizontal spectra at periods beyond 2 to 4 seconds.

To further explore the relationship between vertical and horizontal spectra, Silva [1997] computed the vertical-to-horizontal ratio (V/H) using two empirical attenuation relationships (Sadigh and others [1993; 1997]; Abrahamson and Silva [1997]) and these ratios are reproduced on Figures 4.5 and 4.6. It should be noted that the average value of the two horizontal components was used to derive the attenuation relationship for horizontal motions. Because Sadigh and others [1993] did not present a vertical relationship for soil site, soil V/H ratio is computed solely from Abrahamson and Silva [1997]. The empirical V/H ratio for magnitude 6.5 has a peak value of about 1.1 and 1.9 for rock and soil, respectively, and the peak ratio increases to about 1.3 (rock) and 2.6 (soil) for magnitude 7.5. Thus vertical effects are likely to become more important during larger magnitude events. For periods longer than 0.2 to 0.3 seconds, the V/H ratio reduces to less than the commonly used ratio of 2/3. Figures 4.5 and 4.6 also reveal that the distance and magnitude effects on V/H ratio are stronger for soil site than for rock site.

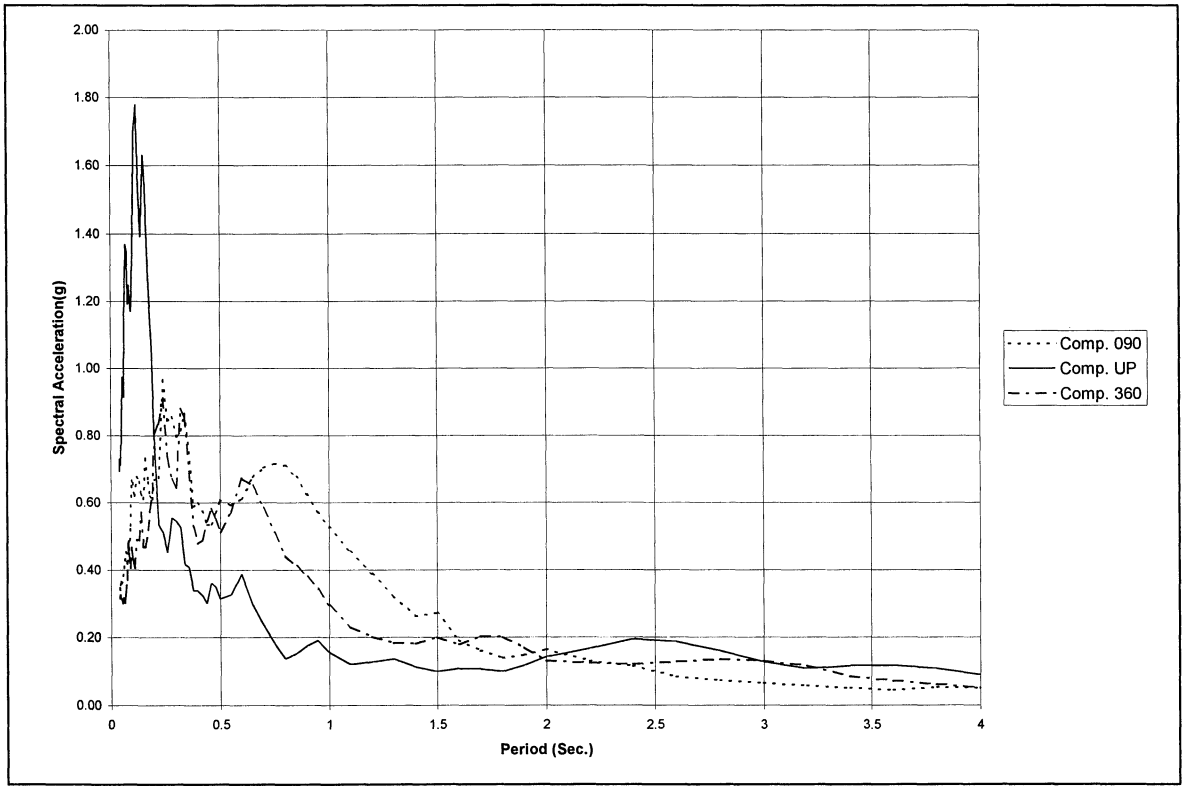

Figure 4.3 Response Spectra for 1994 Northridge – Arleta Record

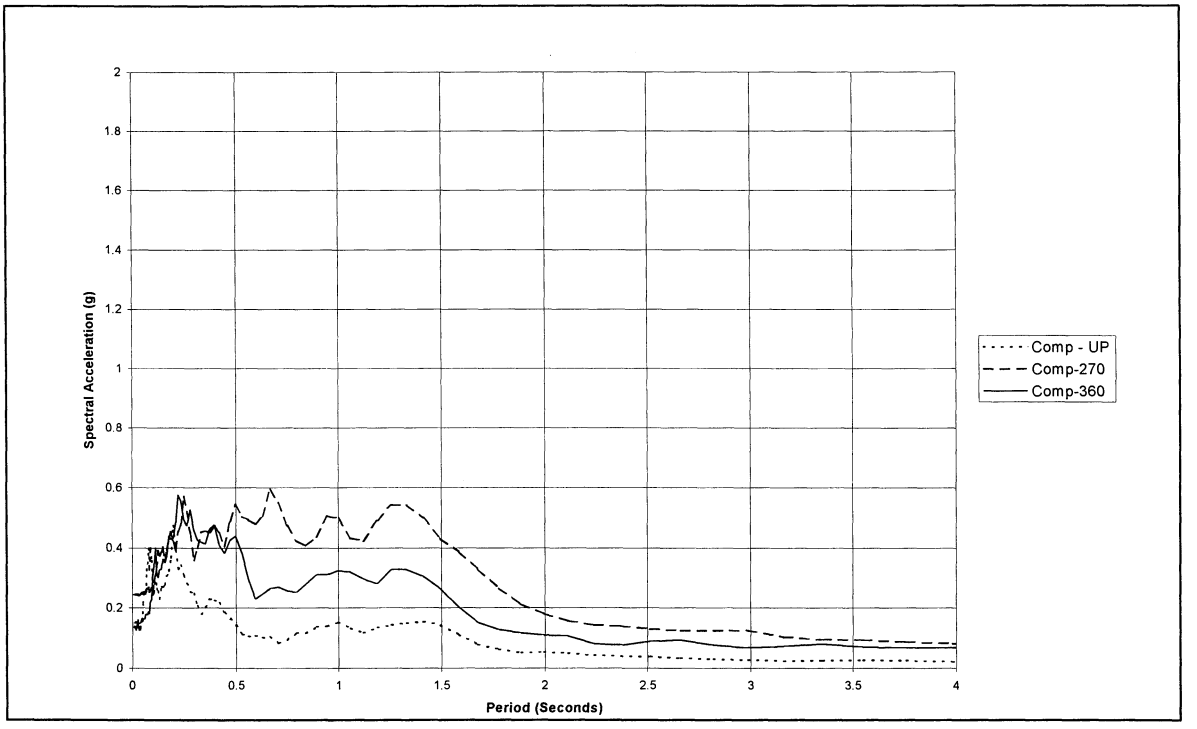

Figure 4.4 Response Spectra for 1992 Landers – Yermo Record

4.3 Development of Response Spectra for Bridge Analyses

In this study, empirical attenuation relationships by Sadigh and others [1993; 1997] and Abrahamson and Silva [1997] are used to define the horizontal and vertical response spectra to be used in the bridge analyses. These two attenuation relationships are based on data recorded in WUS or active tectonic regions and give 5% damped spectral accelerations. Horizontal and vertical spectra for magnitudes 6.5 and 7.5 at distances of 1, 5, 10, 20, and 40 km are developed and shown on Figures 4.7 to 4.10. The horizontal design spectra and vertical rock spectra are defined as the average spectra of Sadigh and others [1993; 1997] and Abrahamson and Silva [1997]. Because Sadigh and others [1993] did not present a vertical relationship for soil site, soil V/H ratio from Abrahamson and Silva [1997] is used to derive the soil vertical spectrum from the corresponding horizontal spectrum.

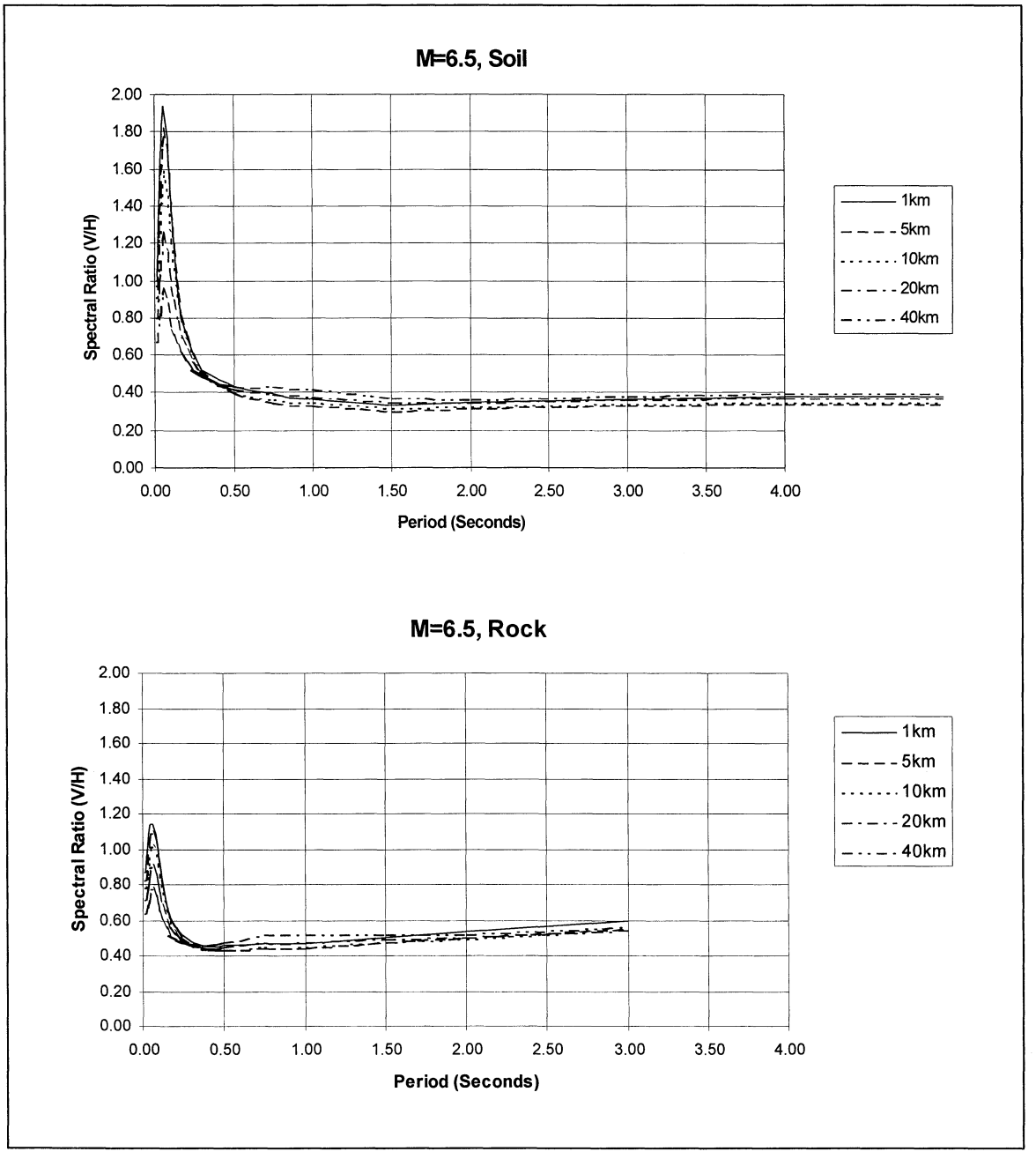

Figure 4.5 Distance (fault) Dependency of Response Spectral Ratios (V/H)

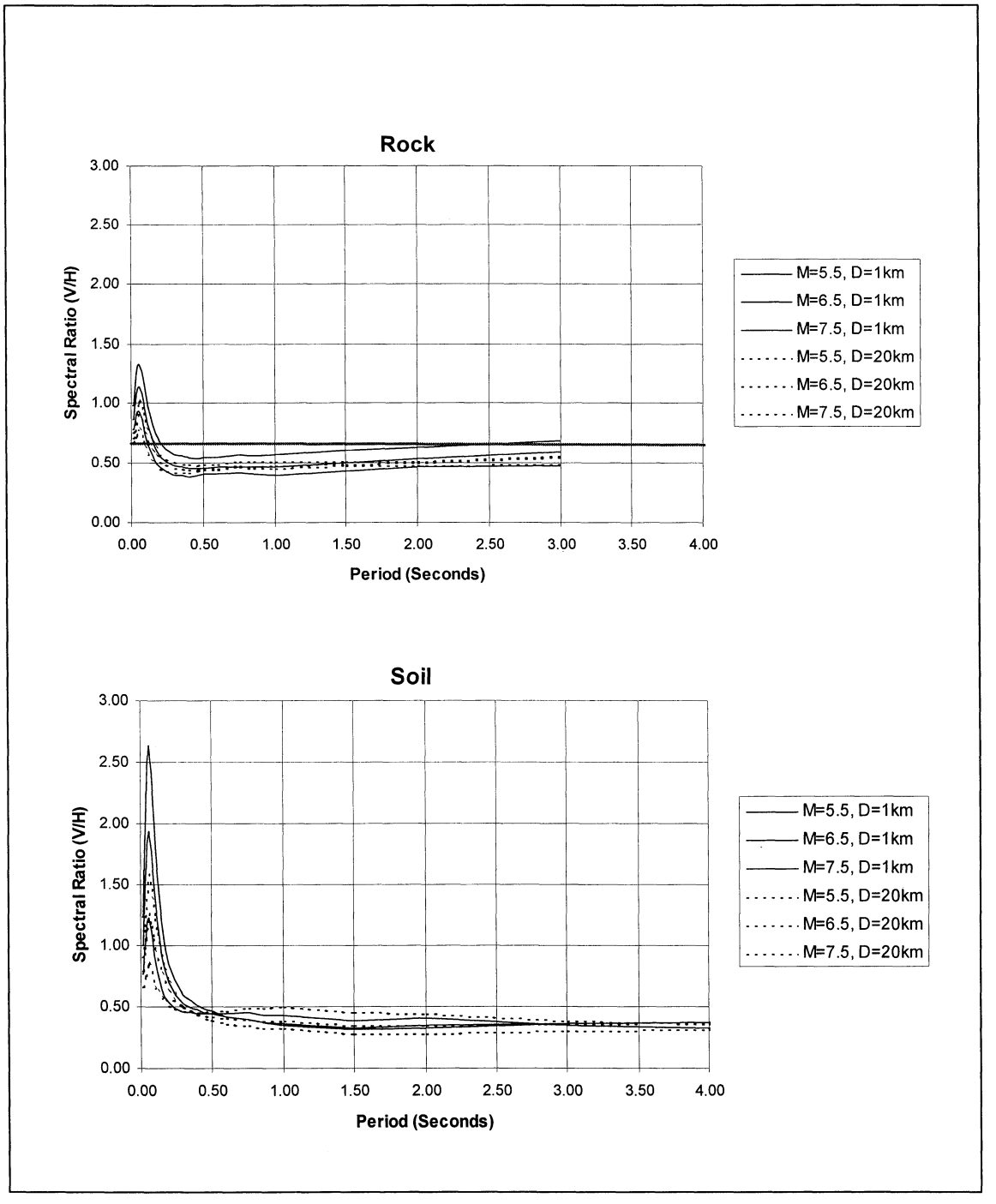

Figure 4.6 Magnitude Dependency of Response Spectral Ratios (V/H) at Fault Distances 1 and 20 km

4.4 Development of Three-Components of Acceleration Time Histories

Time history analyses are performed on bridge numbers 1, 4 and 5 using frequency scaled records. The 'seeds' for these records are given in Table 4.1. Both recorded horizontal components are frequency scaled to the same horizontal target spectrum, and the recorded vertical component is frequency scaled to the vertical target spectrum. This process is achieved by decomposing the recorded motion as a sum of harmonic components and associated phase angles (Fourier decomposition). The amplitudes of the Fourier components are iteratively adjusted until the response spectrum of the motion matches the target spectrum. The phase angles for the component harmonics are left unchanged from those in the recorded motion. The "before" (recorded) and "after" (frequency scaled) acceleration traces for the Arleta record are shown in Figures 4.1 and 4.13, respectively. It can be seen that the time-domain characteristics (e.g. early arriving short period waves on the vertical component) of the record are preserved after scaling.

The shape of response spectra for unscaled and scaled records of Cape Mendocino are shown in Figures 4.11 and 4.12, respectively. After scaling, all three components of motions closely match the target spectra, also shown in Figure 4.12.

The M6.5 spectra (shown on Figures 4.7 and 4.8) for rock and soil sites at distances of 5 and 20 km are used as target spectra for each of the four groups of time history listed in Table 4.1.

TABLE 4.1 List of Selected Time History Records for Frequency Scaling

Site Conditions	Earthquake	Year	Station	Magnitude (Mw)	Fault Distance (km)
Rock					
(1–7km)	Gazli, USSR	1976	Karakyr Point	6.8	3.0
representative	Nahani	1985	Site 1	6.8	6.0
distance = 5km	Loma Prieta	1989	Gilroy #1	6.9	11.2
	Cape Mendocino	1992	Cape Mendocino	7.1	8.5
	Northridge	1994	Pocioma Dam, downstream	6.7	9.8
Rock	Tabas	1978	Dayhook	7.4	17.0
(15 – 30 km)	Nahani	1985	Site 3	6.8	16.0
representative	Loma Prieta	1989	Gilroy #6	6.9	19.9
distance = 20km	Northridge	1994	Vasquez Rocks Park	6.7	20.1
	Northridge	1994	Lake Hughes 9	6.7	28.3
Soil	Imperial Valley	1979	El Centro #8	6.5	3.8
(1 – 7 km)	Imperial Valley	1979	El Centro D.A.	6.5	5.3
representative	Loma Prieta	1989	Corrilitas	6.9	5.1
distance = 5km	Northridge	1994	Arleta	6.7	9.2
	Northridge	1994	New Hall – LA Fire St.	6.7	7.6
Soil	Imperial Valley	1979	El Centro #12	6.5	18.2
(15 – 30 km)	Loma Prieta	1989	Hollister South & Pine	6.9	28.8
Representative	Landers	1992	Yermo	7.3	24.9
distance = 20km	Northridge	1994	Lake Hughes 12 A	6.7	24.6
	Northridge	1994	Sylmar	6.7	16.0

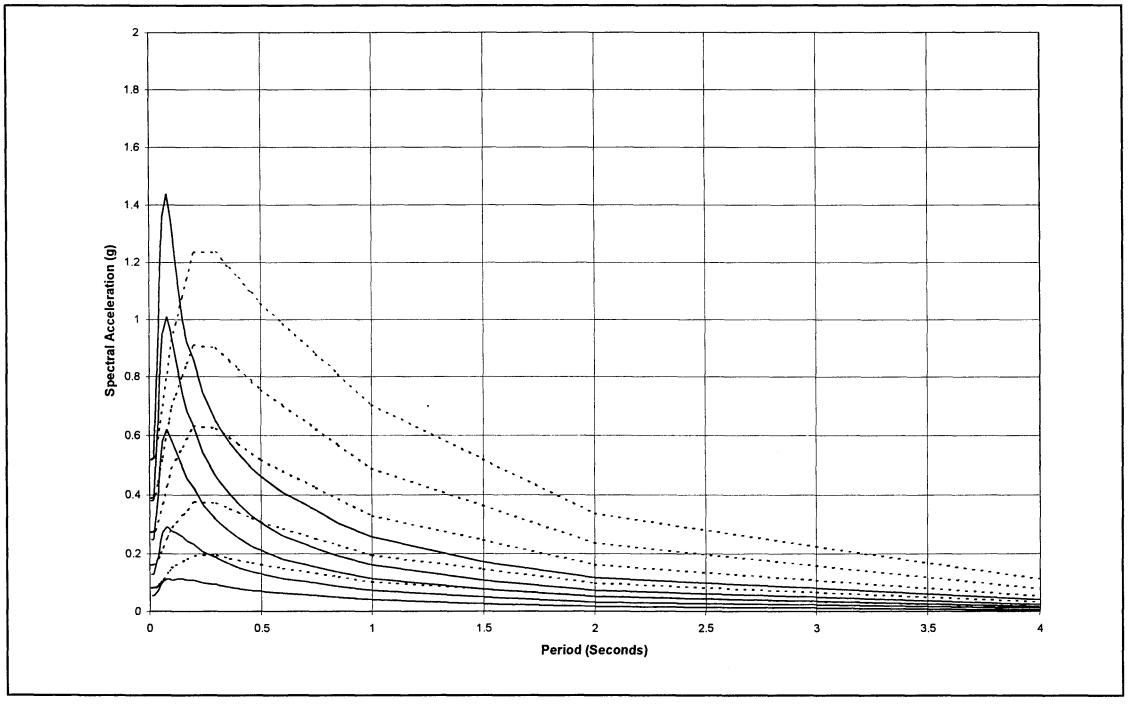

Figure 4.7 Horizontal (dotted lines) and Vertical Spectra for Fault Distances 1, 5, 10, 20, 40 km; Magnitude 6.5 and Soil Site Conditions

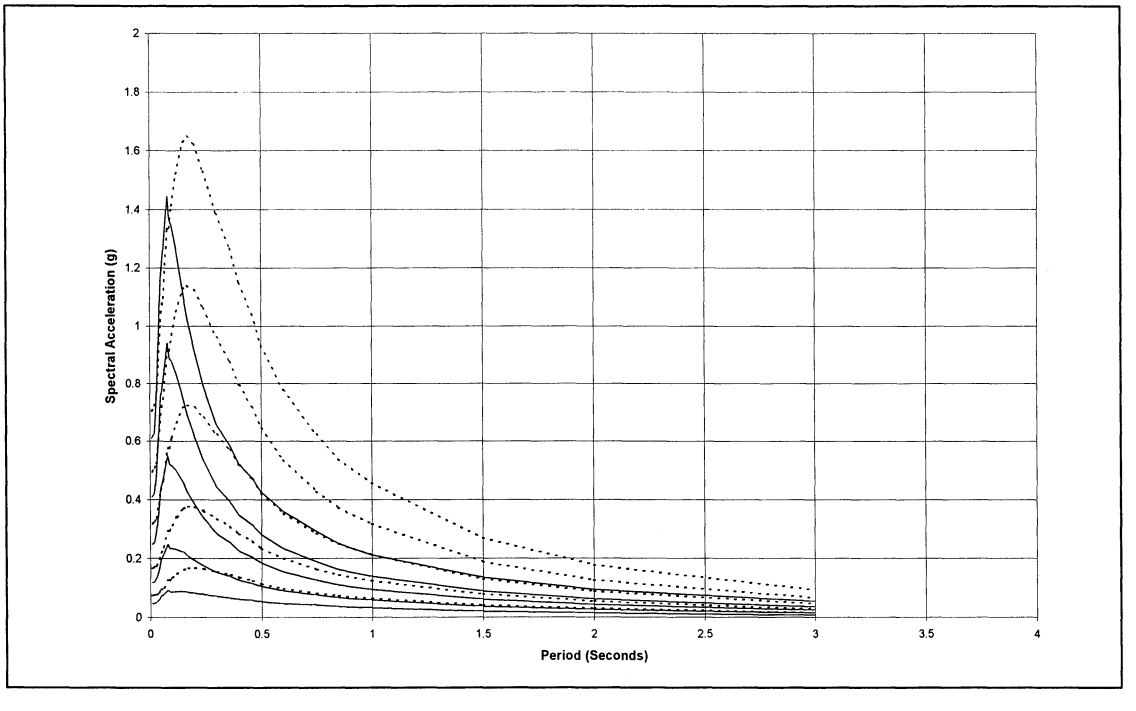

Figure 4.8 Horizontal (dotted lines) and Vertical Spectra for Fault Distances 1, 5, 10, 20 40 km; Magnitude 6.5 and Rock Site Conditions

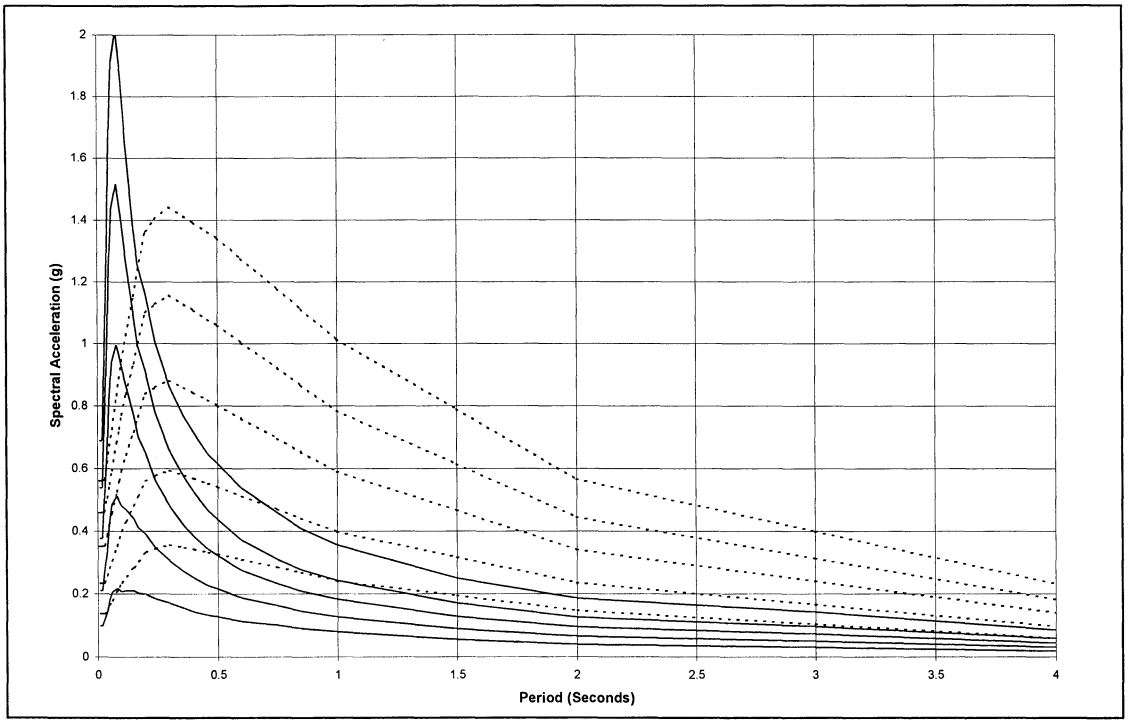

FIGURE 4.9 Horizontal (dotted lines) and Vertical Spectra for Fault Distances 1, 5, 10, 20, 40 km; Magnitude 7.5 and Soil Site Conditions

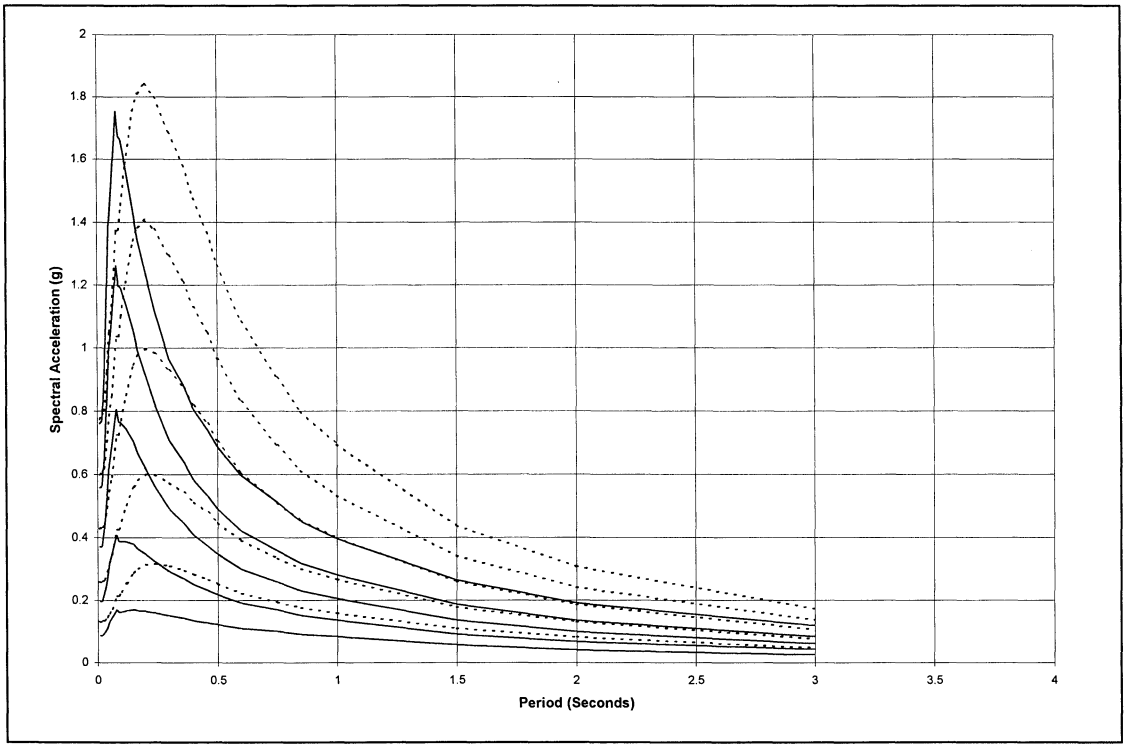

FIGURE 4.10 Horizontal (dotted lines) and Vertical Spectra for Fault Distances 1, 5, 10, 20, 40 km; Magnitude 7.5 and Rock Site Conditions

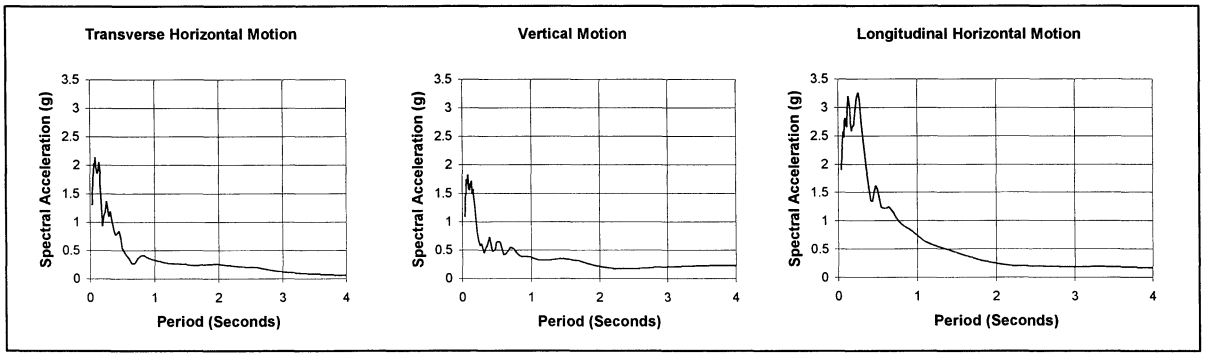

FIGURE 4.11 Response Spectra for Recorded Motions for Cape Mendocino Record

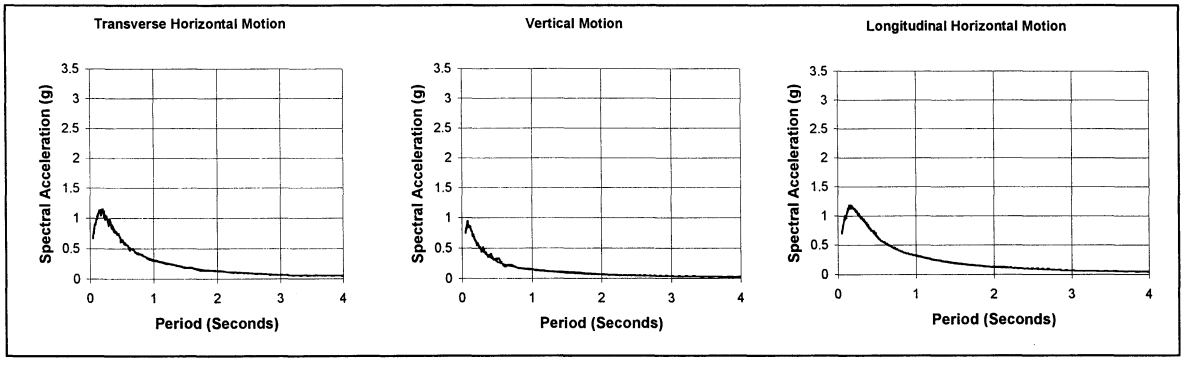

FIGURE 4.12 Spectra of the Frequency-scaled Record for Cape Mendocino (dotted lines) and Corresponding Target Spectra (M6.5, Rock, 5 km)

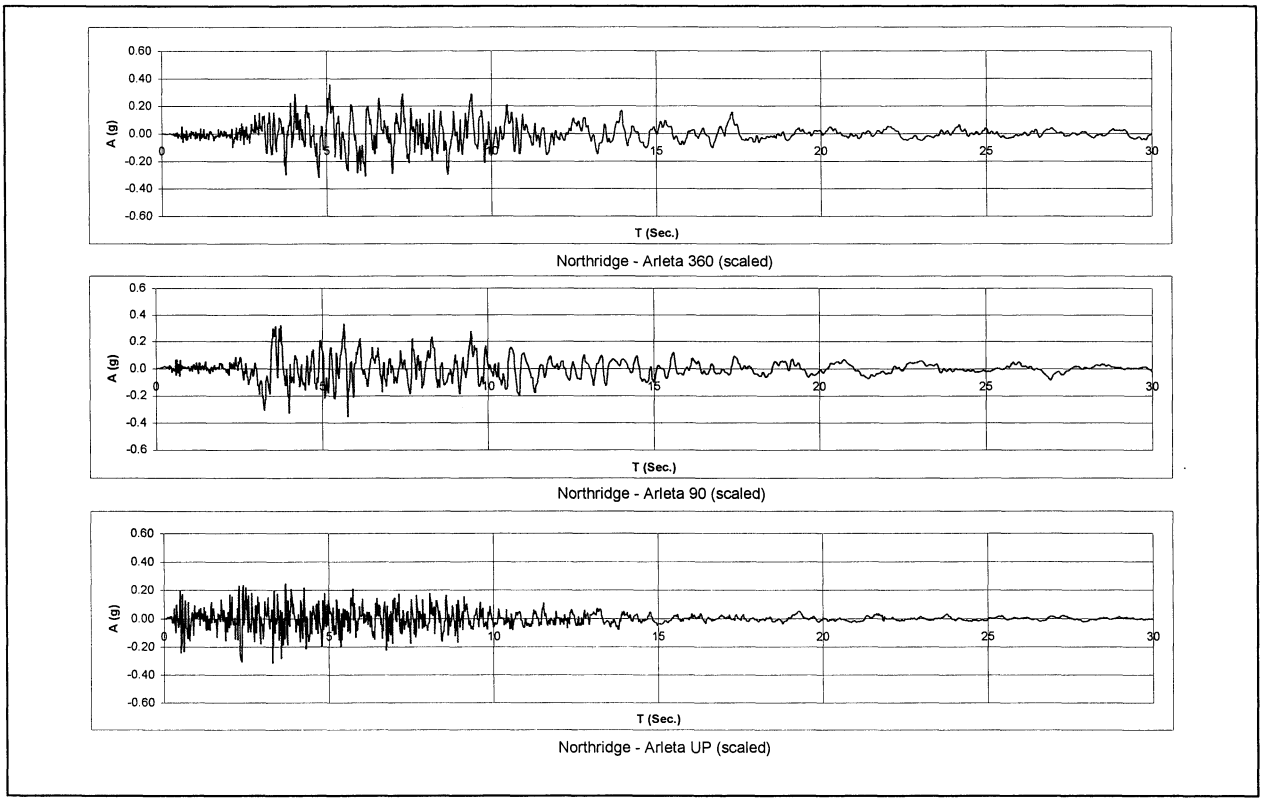

Figure 4.13 Frequency-scaled Acceleration Time Histories of the Northridge – Arleta Record

SECTION 5
LINEAR ANALYSIS METHODOLOGY

Response spectrum analyses are performed on each of the six bridges using a wide range of input spectra with varying soil type, distance and magnitude. Time history analyses are conducted on bridge numbers 1, 4 and 5 using frequency-scaled time history records at a limited number of distances and one magnitude. The results of the time history analyses are used to demonstrate the applicability of the response spectrum results.

The computation parameters that define the accuracy of the results from these analyses are given in this section. These include the number of modes specified, damping ratio, ground motion input orientation, modal combination and direction combination methods and time-steps in the time history analyses. All linear dynamic analyses were performed using the commercial analysis program SAP2000 [1997].

5.1 Eigenvector Analysis

The undamped free vibration mode shapes and periods of each bridge were computed by an Eigenvector analysis. The number of modes used in the analysis of each bridge were determined so that the total cumulative mass participation was at least 95% of the total mass in each direction. Table 5.1 shows the number of modes used for each bridge.

5.2 Orientation of Ground Motions

The global coordinate system was used to define the orientation of horizontal ground motion for bridge numbers 1, 2, 3, and 4. The local coordinate systems for bridge numbers 5 and 6 are different from the global system because these bridges have curved superstructures. The horizontal axes of the local coordinate system for these two bridges are aligned parallel and perpendicular to a straight line passing through the bridge abutments, and these axis are used to define the horizontal ground motion orientation. Since both horizontal spectra are identical, no permutations of horizontal motions are necessary.

5.3 Response Spectrum Analysis

The response spectra described in Section 4.3 were used as the input motions for response spectrum analyses on each bridge. Twenty spectra were used to cover the range of fault distances 1, 5, 10, 20, and 40km; magnitude 6.5 and 7.5 events, rock and soil site conditions. For a particular magnitude, site condition and fault distance, each bridge was analyzed for two separate seismic load cases. Key response quantities were obtained for the two-component input case (horizontal only) and the three-component input case.

The Complete Quadratic Combination (CQC) technique was specified for each analysis to combine the forces and displacements for all modes of vibration.

The CQC method takes into account the statistical coupling between closely spaced modes. The modal-damping ratio specified for all modes was five percent. The SRSS method was used for the directional combination. This method combines the quantities resulting from modal combination due to each uni-directional input in turn, by adding the square root of the sum of their squares for the three directions. The result is not dependent on the model coordinate system if the input horizontal response spectrum curves are the same.

5.4 Time-History Analysis

The frequency scaled time history records described in Section 4.4 were used to conduct linear time history analyses on bridge numbers 1, 4 and 5. As with the response spectrum analysis, two analysis cases consisting of a two-component (both horizontal) input case and a three-component (2 horizontal, 1 vertical) input case were conducted. For each case, the larger of the horizontal motions shown in the response spectra of the unscaled records was specified in the transverse direction (it should be noted that both time-histories were scaled to the same horizontal spectra). This is the direction perpendicular to the longitudinal axis of the superstructure elements in bridge numbers 1, 2, 3, and 4. For bridges 5 and 6, it is the direction perpendicular to the chord joining the bridge abutments.

Table 5.1 shows the time steps used in the time history analysis of each bridge. The time steps were specified at increments small enough so that the response of the higher modes would be accurately captured in the analysis. In two bridges (numbers 1 and 4), the shortest periods corresponded to transverse modes and these controlled the selected analysis time step. A modal damping ratio of five percent was specified for all modes.

TABLE 5.1 Computing Time Step for Time-history Analysis of Each Bridge

Bridge No.	Period of Highest Mode (Sec.)	No. of Modes for 95% Mass Participation	Direction	% Mass Contribution	Total Cumulative % Mass Contribution	Computing Time Step (Sec.)
1	0.020573	13	Transverse	7.1	97.2	0.005
1	0.038302	10	Vertical	12.4	98.3	
2	0.003401	57	Vertical	17.7	98.2	0.001
3	0.019922	8	Vertical	8.0	100	0.005
4	0.038581	25	Transverse	8.4	100	
4	0.057935	13	Vertical	6.0	98.2	0.005
5	0.057684	79	Vertical	9.4	95.6	0.005
6	0.029440	18	Vertical	2.8	96.1	0.005

SECTION 6
LINEAR ANALYSIS RESULTS

The section begins with a list of the response quantities reviewed, and their location on each bridge. The various stages in the development of the final presentation format of the analysis results are described. Results for response spectrum and time history analyses using frequency-scaled records are compared. The results of response spectrum analyses on six different bridges are presented. Bridge numbers 4 and 6 are analyzed with varying vertical deck stiffnesses and foundation fixity, and the different responses are compared. Finally, a comparison of results obtained using three different directional combination methods for modal analyses of bridge numbers 4 and 5 is given.

6.1 Response Quantities Reviewed

Forces and displacements were compared at the following locations and directions in each bridge. In multi-span bridges, responses were monitored at selective piers and spans.

1. Vertical displacement at mid-span.
2. Longitudinal displacement at mid-span.
3. Transverse displacement at mid-span.
4. Vertical displacement at the top of the piers.
5. Longitudinal displacement at the top of the piers.
6. Transverse displacement at the top of the piers.
7. Vertical shear force in the deck at mid-span.
8. Vertical bending moment in the deck at mid-span.
9. Vertical shear force in the deck at the piers.
10. Vertical bending moment in the deck at the piers.
11. Axial force at the base of the pier.
12. Transverse shear force at the base of the pier.
13. Longitudinal shear force at the base of the pier.

TABLE 6.1 Locations on Each Bridge Where Response Quantities are Monitored

	Span Number	Pier Number
Bridge 1	Span 1 (long span)	Middle Column of Bent
Bridge 2	Center Span	Pier 1
Bridge 3	Single-Span Bridge	Abutments only
Bridge 4	Center Span	Bent 1, One Col. in Portal
Bridge 5	Span 7	Pier 6
Bridge 6	Center Span	Pier 2

6.2 Description and Development of Presentation Format

The format for the final presentation of results evolved over several trial formats. Initially, the effect of the vertical component on the bridge response was measured by the ratio of the response of the three-component input to horizontal only input. A typical plot showing this response ratio for vertical bending-moment in the deck over a pier is shown in Figure 6.1 for all six bridges. This response ratio was rejected

because it gave a distorted view of the impact of the vertical component for some quantities. An example of this is shown for moment at mid-span in Figure 6.2, where the ratio is very large because the moment due to the two-component input is very small.

To overcome this problem, it was decided to relate the response of the seismic input to the dead load response. Figure 6.3 shows curves for the ratio of the response of the three-component input over the dead load only response. This ratio was also found to distort the full impact of the vertical component on some bridge configurations. For example, if Figures 6.4 and 6.5 are compared, it can be seen that the "Ratio" (3-component over 2-component) for the pier axial force in bridge 4 is small while its "DL Ratio" is the largest amongst the bridges. This discrepancy in the ratios can be explained by the large axial force generated by the transverse horizontal motion due to portal frame action at the bents.

Figures 6.6 and 6.7 show another example where these two ratios are very different. The "Ratio" (3/2) show that adding the vertical component has little effect on the moment at mid-span yet the "DL Ratio" is very high. Bridge 1 is unrestrained in the longitudinal direction and the deck is effectively integral with the columns. The longitudinal motions induce large moments at mid-span due to this configuration and therefore the "Ratio" (3/2) is small. The large value for the "DL Ratio" at this location can be explained by the low dead load moment caused by the uneven span lengths of 103.5 ft. and 145.5 ft.

A further response ratio was created to eliminate or reduce the distortions due to structural configurations similar to those above. This ratio is defined as the absolute difference between the three-component response and two-component response over the dead load only response. This ratio is also beneficial in evaluating the response to the various input motions because it expresses the incremental response due to vertical input relative to the dead load demand on any element, and thus is consistent in format with load factors on dead loads in the current Unified Building Code [1997]. The ratio is discussed further in Section 6.4 and is shown in Figures 6.8 through 6.23.

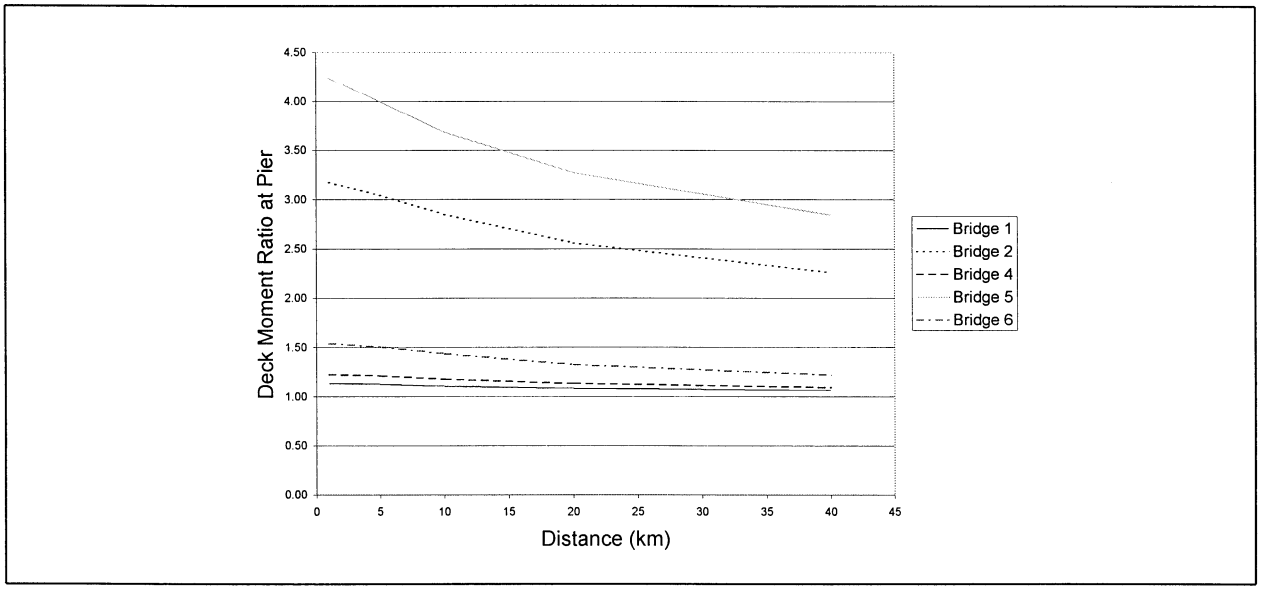

Figure 6.1 Variation of Vertical Deck Moment Ratio* of Three to Two Component Response at Pier Across the Six Bridges and Distance for Magnitude 7.5 and Rock** (*Ratio = Three-component response over two-component response; **Bridge 3 is a simply-supported single span bridge)

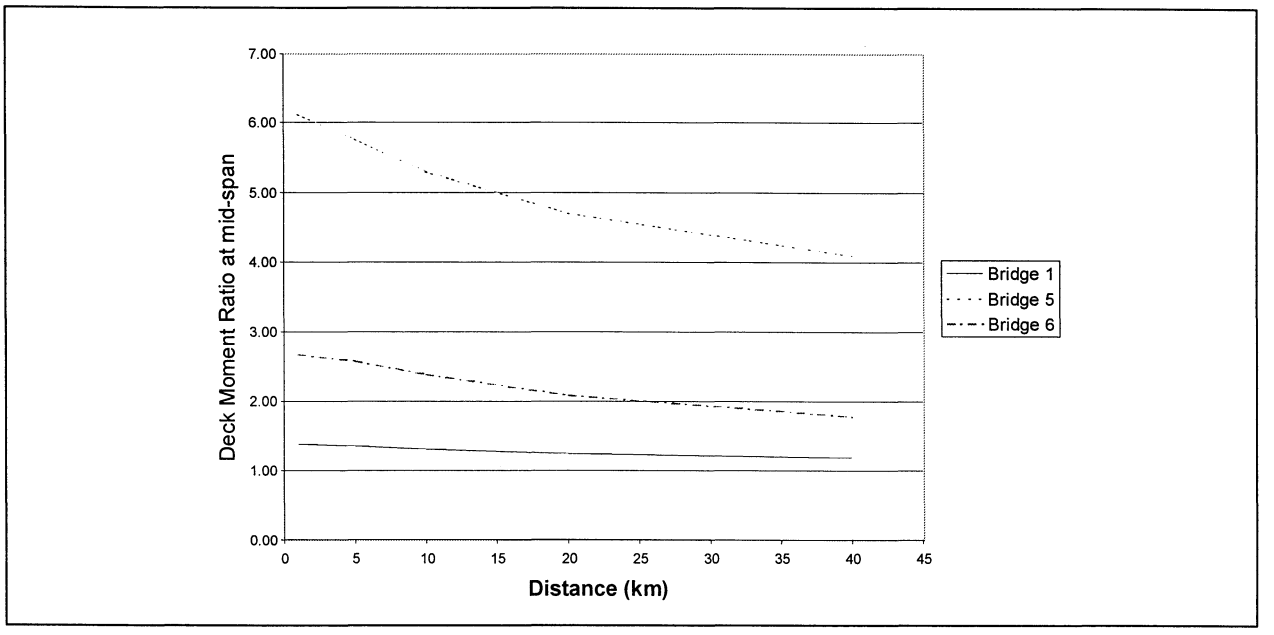

Figure 6.2 Variation of Vertical Deck Moment Ratio of Three to Two Component Response at Mid-span Across the Six* Bridges and Distance for Magnitude 7.5 and Rock (Ratio = Three-component response over two-component response; * Bridge 3 is a simply-supported single span bridge)

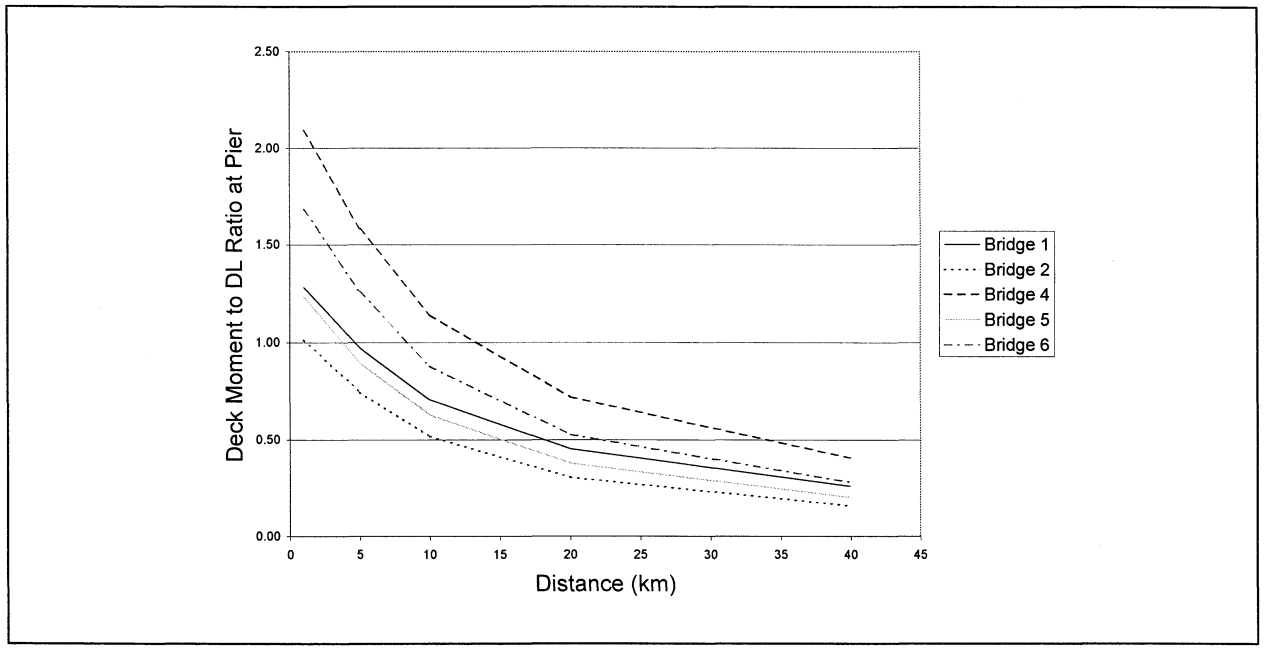

Figure 6.3 Variation of Vertical Deck Moment to DL Ratio at Pier Across the Six Bridges and Distance for Magnitude 7.5 and Rock (DL Ratio = Three-component response over Dead-load only response; * Bridge 3 is a simply-supported single span bridge)

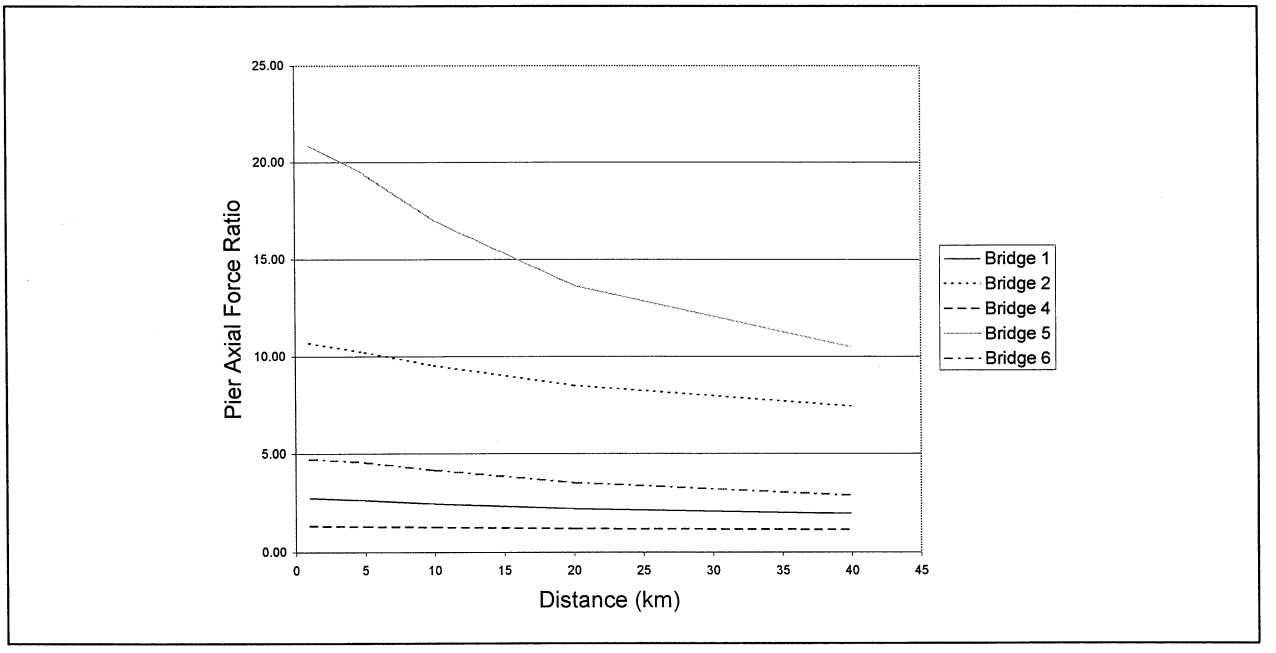

Figure 6.4 Variation of Pier Axial Force Ratio Three to Two Components Response Across the Six* Bridges and Distance for Magnitude 7.5 and Rock (Ratio = Three-component response over two-component response.; * Bridge 3 is a simply-supported single span bridge)

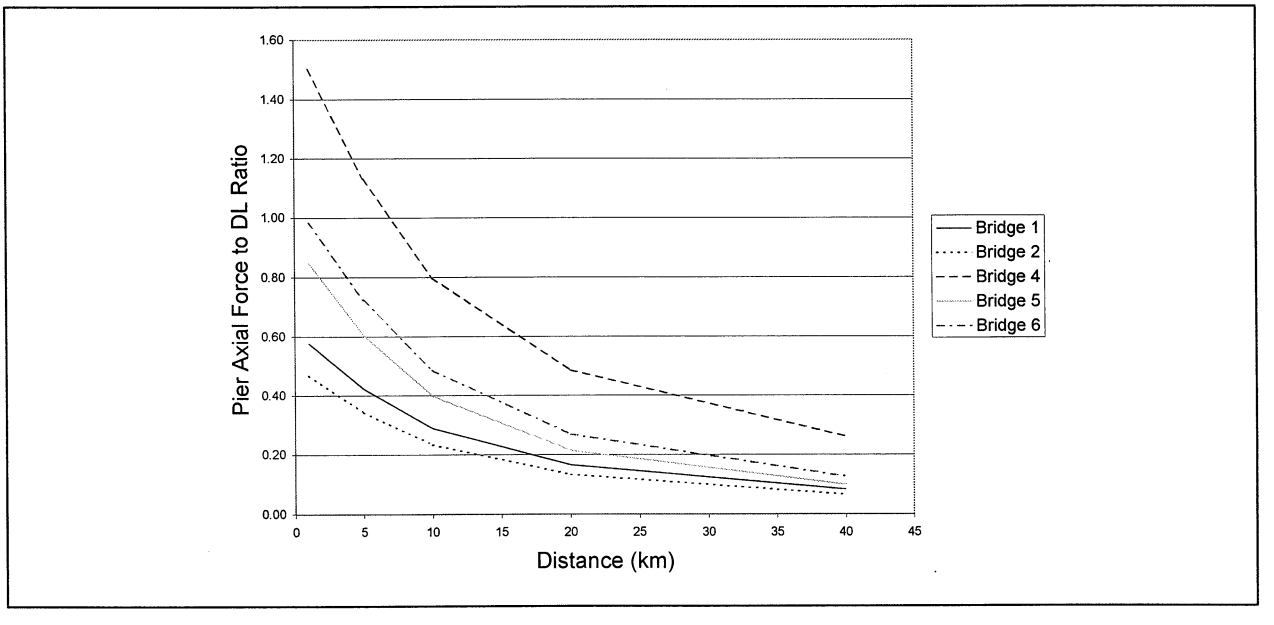

Figure 6.5 Variation of Pier Axial Force to DL Ratio Across the Six* Bridges and Distance for Magnitude 7.5 and Rock (DL Ratio = Three-component response over Dead-load only response; * Bridge 3 is a simply-supported single span bridge)

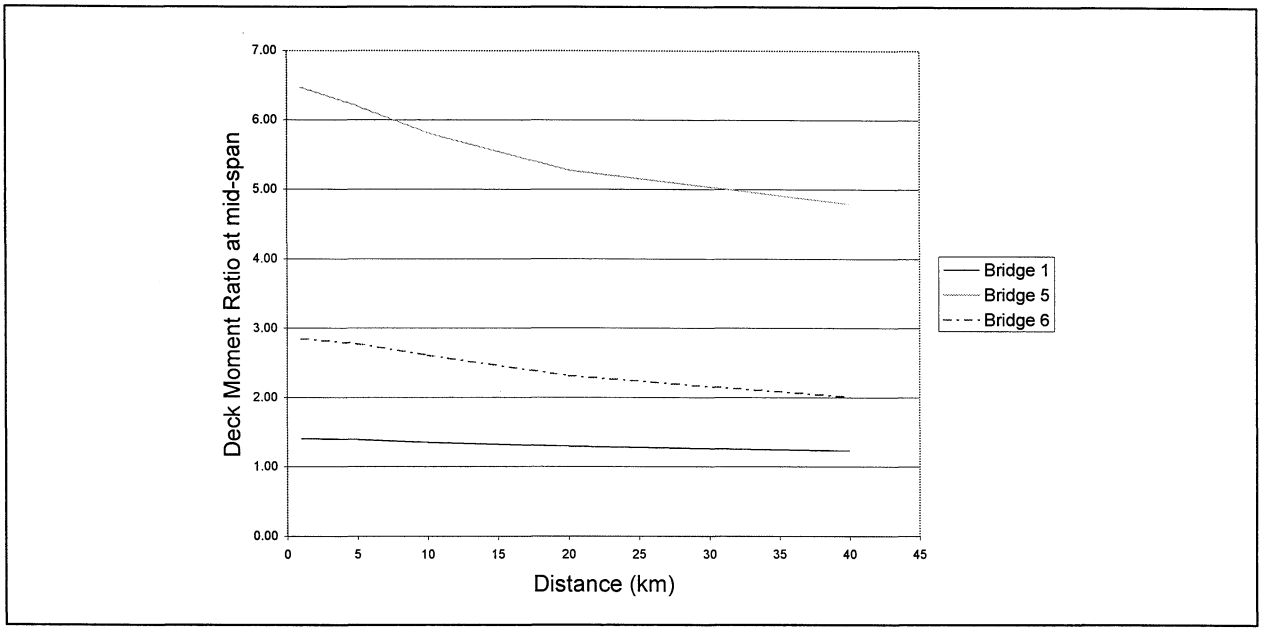

Figure 6.6 Variation of Vertical Deck Moment Ratio at Mid-span Across the Six* Bridges and Distance for Magnitude 6.5 and Rock (Ratio = Three-component response over two-component response; * All bridges may not be shown because their ratios may be very large)

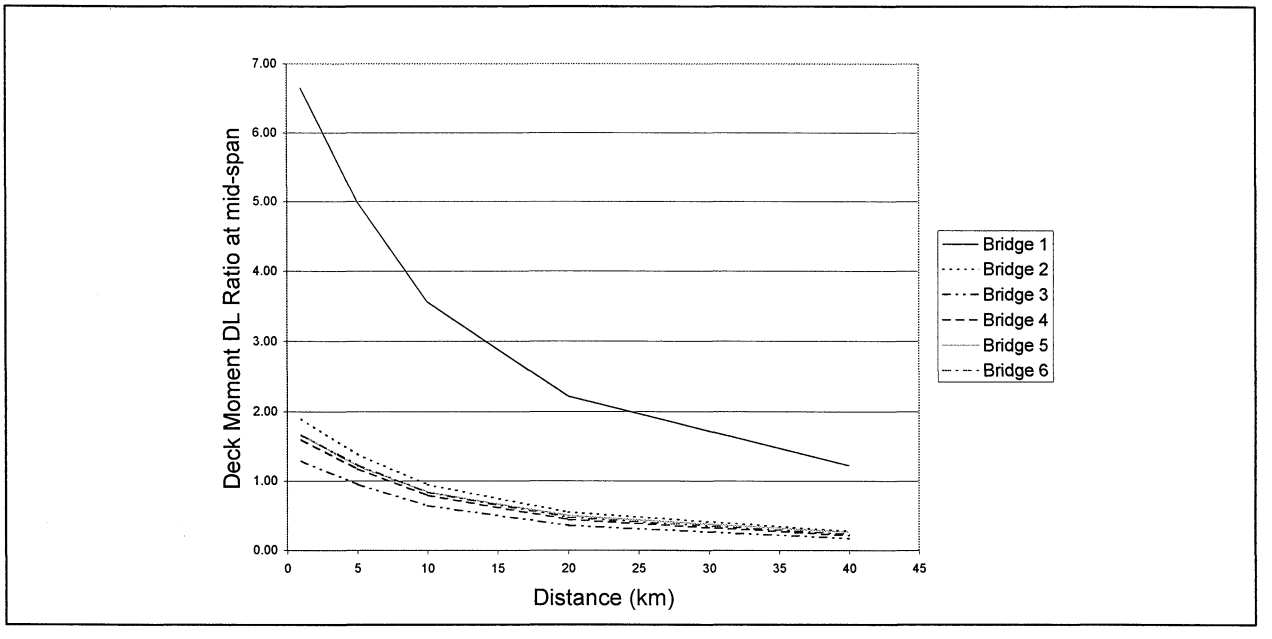

Figure 6.7 Variation of Vertical Deck Moment to DL Ratio at Mid-span Across the Six Bridges and Distance for Magnitude 7.5 and Rock (DL Ratio = Three-component response over dead-load only response)

6.3 Comparison of Time-History and Response Spectrum Results

The frequency-scaled time history records used for analyses are given in Section 4.4. These records were used to analyze three bridges. Time history analyses remove any approximation in modal and directional combination associated with response spectrum analyses. A favorable comparison of response between these two analytical methods would indicate that conclusions drawn based solely on response spectrum analysis are valid. The results from a response spectrum analysis were compared with the average response from five records frequency-scaled to the same spectrum. Results for records frequency-scaled to a target spectrum with parameters of magnitude 6.5, fault distance of 20 km and soil site conditions are shown in Tables 6.2, 6.3, 6.4 for bridges 1, 4, and 5, respectively. Table 6.5 shows the results for bridge 5 using records frequency-scaled to a target spectrum with parameters of magnitude 6.5, fault distance of 5km and rock site conditions. Table 6.6 shows the results for bridge 5 using records frequency-scaled to a target spectrum with parameters of magnitude 6.5, fault distance of 5km and rock site conditions.

In each table (6.2 to 6.6), the four shaded columns show three comparisons. The first two shaded columns (columns 12 & 14) compare the average ratio of the three-component to the two-component response for the five time history records with the corresponding response spectrum ratio. The difference between the ratios is less than ten percent for all response quantities.

The response ratios for individual time histories are given in columns 3, 5, 7, 9 and 11. The ratios for mid-span displacements and moments shown with scientific notation in Table 6.3 are very large for these mid-span quantities because the response to the horizontal motions is almost zero.

The third shaded column (column 20) compares the absolute response of a response spectrum analysis with that of a time history analysis for the three component input case. The values in this column are the average of the five individual ratios given in columns 15 to 19. The individual record response ratios in these columns were obtained by computing the ratio of the values shown in column 13 over those in columns 2, 4, 6, 8, and 10. The difference between the response spectrum and time history results does not exceed 15% and the majority are within 5%.

Based on these results, it is concluded that response spectrum analyses (using the parameters described) can accurately represent the vertical response of complex three-dimensional bridges to multi-component seismic excitation. Therefore, all subsequent linear analysis is confined to response spectrum analyses.

The last column in the tables shows ratios that compare the results obtained from a response spectrum analysis using (a) two-thirds of the horizontal spectra, and (b) vertical component spectra computed from attenuation relationships. The ratios are within 10% of unity for bridges 1 and 4 but for bridge 5, the difference is as much as 40%. This larger difference can be attributed to the higher mass participation in bridge 5 at periods in the range of the peak spectral acceleration of the vertical spectra. We recommend that the use of a vertical spectrum equal to 2/3 of the corresponding horizontal spectrum be discontinued.

6.3.1 Effect of "Early Arrival" Vertical Motions

A question has arisen in the current study as to whether records that show early-arriving strong short period motion in the vertical component (Arleta, Figure 4.1) produce a significantly different structural response from those that have all three components arriving at the same time (in-phase) (Pacoima Dam, Figure 4.2). It can be seen that the results for Arleta in Table 6.6 (columns 8 & 9) do not differ greatly from the results shown for the other four records in the table. Furthermore, if the Arleta results are compared with those for Pacoima Dam in Table 6.5 (columns 10 & 11), it can be seen that the response ratios are similar for both records. Thus, it can be concluded from Tables 6.5 and 6.6 that the early arrival of strong vertical motions does not significantly effect the structural response of typical highway bridges.

Table 6.2 Bridge #1 – Time History Analysis Using Frequency-scaled Records

	Frequency-Scaled Time History Records to Target Spectrum with parameters M=6.5, D=20km and Soil													Response Spectrum/Time History (RS/TH)						Response Spectrum
	El Cen. #12 (1)		Hollister (2)		Yermo (3)		Lake Hughes (4)		Sylmar (5)											
Response Quantity	Time History Abs.	(3/2) Ratio	Time History Abs.	(3/2) Ratio	Time History Abs.	(3/2) Ratio	Time History Abs.	(3/2) Ratio	Time History Abs.	(3/2) Ratio	Avg. Ratio	Resp. Spect. Abs.	(3/2) Ratio	1	2	3	4	5	Avg. (RS/TH)	2/3(H) V/H(H)
1	2	3	4	5	6	7	8	9	10	11	12	13	14	15	16	17	18	19	20	21
Pier Displ. (in.)																				
Longitudinal	-1.436	1.00	1.461	1.01	-1.499	1.00	1.348	1.01	-1.473	1.02	1.01	1.433	1.00	1.00	0.98	0.96	1.06	0.97	0.99	1.00
Transverse	-0.132	1.00	-0.132	1.00	-0.138	1.00	-0.118	1.00	0.131	1.00	1.00	0.127	1.00	0.97	0.96	0.92	1.07	0.97	0.98	1.00
Vertical	-0.007	1.83	0.007	1.97	0.007	1.71	0.008	2.54	0.008	2.00	1.99	0.007	2.14	0.98	0.95	1.00	0.84	0.90	0.93	1.07
Mid-Span Displ. (in.)																				
Longitudinal	-1.442	1.00	1.467	1.01	-1.506	1.00	1.354	1.01	-1.480	1.02	1.01	1.440	1.00	1.00	0.98	0.96	1.06	0.97	0.99	1.00
Transverse	-0.109	1.00	-0.109	1.00	-0.114	1.00	-0.098	1.00	0.108	1.00	1.00	0.105	1.00	0.96	0.96	0.92	1.07	0.97	0.98	1.00
Vertical	-0.752	1.02	-0.833	1.22	-0.796	1.21	0.565	1.04	-0.760	1.10	1.12	0.664	1.08	0.88	0.80	0.83	1.17	0.87	0.91	1.09
Forces (kips)																				
Pier (Axial)	-125	1.83	129	2.00	122	1.71	146	2.54	136	2.00	2.00	122	2.14	0.98	0.95	1.00	0.84	0.90	0.93	1.07
Pier (Long. Shear)	-360	1.00	379	1.02	-386	0.99	344	1.01	-386	1.05	1.01	371	1.00	1.03	0.98	0.96	1.08	0.96	1.00	1.00
Pier (Trans. Shear)	-42	1.00	-42	1.00	-44	1.00	-38	1.00	42	1.00	1.00	40	1.00	0.97	0.96	0.92	1.07	0.97	0.98	1.00
Deck over Pier																				
Vert. Shear (kips)	194	1.52	253	1.85	200	1.39	200	1.84	217	1.76	1.66	187	1.47	0.96	0.74	0.94	0.94	0.86	0.89	1.23
Moment (kip-ft)	-7066	1.13	-8686	1.31	9779	1.31	7402	1.50	8481	1.50	1.34	7689	1.20	1.09	0.89	0.79	1.04	0.91	0.94	1.11
Deck at Mid-Span																				
Vert. Shear (kips)	92	1.11	95	1.25	97	1.23	87	1.30	140	1.81	1.34	90	1.24	0.98	0.95	0.94	1.04	0.64	0.91	0.96
Moment (kip-ft)	9179	1.03	10906	1.31	10054	1.26	-6723	1.03	9602	1.16	1.16	8240	1.12	0.90	0.76	0.82	1.23	0.86	0.91	1.12

Abs. = Absolute value of response quantity to three-component seismic input.

(3/2) Ratio = Absolute value of three-component response over absolute value of two-component response for time history analyses and response spectrum analysis.

Avg. Ratio = Sum of three-component time history response values over sum of two-component time history response value for all five records.

Table 6.3 Bridge #4 – Time History Analysis Using Frequency-scaled Records

	Frequency-Scaled Time History Records to Target Spectrum with parameters M=6.5, D=20km and Soil													Response Spectrum/Time History (RS/TH)						Response Spectrum
	El Cen. #12 (1)		Hollister (2)		Yermo (3)		Lake Hughes (4)		Sylmar (5)											
Response Quantity	Time History Abs.	(3/2) Ratio	Time History Abs.	(3/2) Ratio	Time History Abs.	(3/2) Ratio	Time History Abs.	(3/2) Ratio	Time History Abs.	(3/2) Ratio	Avg. Ratio	Resp. Spect. Abs.	(3/2) Ratio	1	2	3	4	5	Avg. (RS/TH)	2/3(H) V/H(H)
1	2	3	4	5	6	7	8	9	10	11	12	13	14	15	16	17	18	19	20	21
Pier Displ. (in.)																				
Longitudinal	-1.609	1.00	1.519	1.00	-1.566	1.00	-1.490	1.00	-1.552	1.00	1.00	1.564	1.00	0.97	1.03	1.00	1.05	1.01	1.01	1.00
Transverse	0.786	1.00	0.925	1.00	-0.761	1.00	-0.820	1.00	-0.868	1.00	1.00	0.793	1.00	1.01	0.86	1.04	0.97	0.91	0.96	1.00
Vertical	-0.029	3.71	0.026	2.43	0.035	4.44	0.027	3.24	0.031	3.66	3.42	0.030	3.70	1.05	1.15	0.86	1.12	0.99	1.03	1.04
Mid-Span Displ. (in.)																				
Longitudinal	-1.611	1.00	1.521	1.00	-1.568	1.00	-1.492	1.00	-1.554	1.00	1.00	1.566	1.00	0.97	1.03	1.00	1.05	1.01	1.01	1.00
Transverse	0.921	1.00	1.086	1.00	-0.896	1.00	-0.959	1.00	-1.026	1.00	1.00	0.930	1.00	1.01	0.86	1.04	0.97	0.91	0.96	1.00
Vertical	-0.126	1.E+08	0.114	-7.E+07	-0.131	9.E+07	0.130	-1.E+08	0.139	9.E+07	9.E+07	0.123	9.E+07	0.98	1.08	0.94	0.94	0.89	0.97	1.09
Forces (kips)																				
Pier (Axial)	-330	1.32	-269	1.02	289	1.20	-258	1.04	-338	1.33	1.18	296	1.21	0.90	1.10	1.02	1.15	0.87	1.01	1.02
Pier (Long. Shear)	-245	1.00	291	1.00	249	1.00	232	1.00	-271	1.00	1.00	236	1.00	0.97	0.81	0.95	1.02	0.87	0.92	1.00
Pier (Trans. Shear)	209	1.00	174	1.00	192	1.00	180	1.00	-170	1.00	1.00	183	1.00	0.88	1.05	0.96	1.02	1.08	1.00	1.00
Deck over Pier																				
Vert. Shear (kips)	-174	1.37	148	1.00	-187	1.51	177	1.50	-200	1.48	1.36	184	1.49	1.06	1.24	0.98	1.04	0.92	1.05	1.05
Moment (kip-ft)	-7890	1.01	8949	0.98	-9219	1.20	7652	1.06	-9276	1.06	1.06	8396	1.11	1.06	0.94	0.91	1.10	0.91	0.98	1.02
Deck at Mid-Span																				
Vert. Shear (kips)	-132	0.99	167	1.07	-140	1.07	151	1.21	-171	1.24	1.11	145	1.12	1.10	0.87	1.04	0.96	0.85	0.96	1.01
Moment (kip-ft)	2554	-2.E+08	2220	1.E+08	2408	1.E+08	-2575	1.E+08	-2623	1.E+08	1.E+08	2388	6.E+07	0.93	1.08	0.99	0.93	0.91	0.97	1.07

Abs. = Absolute value of response quantity to three-component seismic input.

(3/2) Ratio = Absolute value of three-component response over absolute value of two-component response for time history analyses and response spectrum analysis.

Avg. Ratio = Sum of three-component time history response values over sum of two-component time history response value for all five records.

Table 6.4 Bridge #5 – Time History Analysis Using Frequency-scaled Records

	Frequency-Scaled Time History Records to Target Spectrum with parameters M=6.5, D=20km and Soil																			Response Spectrum
	El Cen. #12 (1)		Hollister (2)		Yermo (3)		Lake Hughes (4)		Sylmar (5)					Response Spectrum/Time History (RS/TH)						
Response Quantity	Time History Abs.	Ratio	Time History Abs.	(3/2) Ratio	Time History Abs.	(3/2) Ratio	Time History Abs.	(3/2) Ratio	Time History Abs.	(3/2) Ratio	Avg. Ratio	Resp. Spect. Abs.	(3/2) Ratio	1	2	3	4	5	Avg. (RS/TH)	2/3(H) V/H(H)
1	2	3	4	5	6	7	8	9	10	11	12	13	14	15	16	17	18	19	20	21
Pier Displ. (in.)																				
Longitudinal	3.472	1.00	3.348	1.00	-3.918	1.00	-2.878	1.00	-3.200	1.00	1.00	3.294	1.00	0.95	0.98	0.84	1.14	1.03	0.99	1.00
Transverse	2.010	1.00	-1.935	1.00	2.009	1.00	1.936	1.00	-2.238	1.00	1.00	1.759	1.00	0.87	0.91	0.88	0.91	0.79	0.87	1.00
Vertical	-0.017	13.70	0.015	11.76	0.019	15.91	-0.014	14.38	-0.015	10.80	13.18	0.015	14.08	0.89	0.97	0.77	1.09	1.00	0.94	0.82
Mid-Span Displ. (in.)																				
Longitudinal	-3.404	1.00	3.185	1.00	-3.836	1.00	-2.788	1.00	3.201	1.00	1.00	3.203	1.00	0.94	1.01	0.83	1.15	1.00	0.99	1.00
Transverse	1.770	1.00	-1.876	1.00	1.824	1.00	1.975	1.00	-2.086	1.00	1.00	1.654	1.00	0.93	0.88	0.91	0.84	0.79	0.87	1.00
Vertical	0.493	2.24	0.512	2.20	-0.548	2.27	0.376	1.62	-0.431	1.91	2.05	0.427	2.08	0.87	0.83	0.78	1.14	0.99	0.92	1.37
Forces (kips)																				
Pier (Axial)	-517	11.69	452	9.57	594	13.50	411	12.01	-463	9.37	11.12	462	12.14	0.89	1.02	0.78	1.13	1.00	0.96	0.89
Pier (Long. Shear)	-453	1.00	-430	1.00	494	1.00	364	1.00	-441	1.00	1.00	439	1.00	0.97	1.02	0.89	1.20	0.99	1.01	1.00
Pier (Trans. Shear)	-598	1.00	-644	1.00	661	1.00	555	1.00	636	1.00	1.00	629	1.00	1.05	0.98	0.95	1.13	0.99	1.02	1.00
Deck over Pier																				
Vert. Shear (kips)	148	3.91	-159	3.80	-152	3.80	133	4.25	127	2.94	3.70	142	3.90	0.96	0.89	0.93	1.07	1.12	0.99	1.33
Moment (kip-ft)	5626	2.36	-5660	2.43	6319	2.86	5059	2.83	5432	2.83	2.64	5553	2.62	0.99	0.98	0.88	1.10	1.02	0.99	1.32
Deck at Mid-Span																				
Vert. Shear (kips)	-104	3.03	83	2.38	-112	3.47	77	2.86	81	2.30	2.79	88	2.81	0.84	1.05	0.78	1.15	1.08	0.98	1.09
Moment (kip-ft)	4140	4.03	4397	4.13	4213	3.38	-3424	2.96	3305	2.83	3.44	3737	3.79	0.90	0.85	0.89	1.09	1.13	0.97	1.31

Abs. = Absolute value of response quantity to three-component seismic input.

(3/2) Ratio = Absolute value of three-component response over absolute value of two-component response for time history analyses and response spectrum analysis.

Avg. Ratio = Sum of three-component time history response values over sum of two-component time history response value for all five records.

Table 6.5 Bridge #5 – Time History Analysis Using Frequency-scaled Records

	Frequency-Scaled Time History Records to Target Spectrum with parameters M=6.5, D=5km and Rock																			Response Spectrum
	Karakyr Pt. (1)		Nahani Site1 (2)		Gilroy #1 (3)		Cpe Mdno. (4)		Pcma. Dam (5)					Response Spectrum/Time History (RS/TH)						
Response Quantity	Time History Abs.	(3/2) Ratio	Time History Abs.	(3/2) Ratio	Time History Abs.	(3/2) Ratio	Time History Abs.	(3/2) Ratio	Time History Abs.	(3/2) Ratio	Avg. Ratio	Resp. Spect. Abs.	(3/2) Ratio	1	2	3	4	5	Avg. (RS/TH)	2/3(H) V/H(H)
1	2	3	4	5	6	7	8	9	10	11	12	13	14	15	16	17	18	19	20	21
Pier Displ. (in.)																				
Longitudinal	-4.718	1.00	-4.297	1.00	-3.733	1.00	4.971	1.00	5.012	1.00	1.00	4.292	1.00	0.91	1.00	1.15	0.86	0.86	0.96	1.00
Transverse	-2.736	1.00	-3.035	1.00	-3.003	1.00	3.134	1.00	-3.156	1.00	1.00	2.868	1.00	1.05	0.95	0.96	0.92	0.91	0.95	1.00
Vertical	0.045	23.12	-0.050	26.84	0.042	20.24	0.046	20.20	0.042	21.44	22.23	0.044	26.40	1.00	0.89	1.06	0.97	1.05	0.99	0.80
Mid-Span Displ. (in.)																				
Longitudinal	-4.504	1.00	-4.056	1.00	-3.608	1.00	4.801	1.00	4.800	1.00	1.00	4.171	1.00	0.93	1.03	1.16	0.87	0.87	0.97	1.00
Transverse	-2.484	1.00	2.731	1.00	-3.021	1.00	2.887	1.00	-3.219	1.00	1.00	2.608	1.00	1.05	0.96	0.86	0.90	0.81	0.92	1.00
Vertical	0.799	2.30	1.035	4.23	-1.241	4.71	-1.244	5.25	1.202	4.18	4.00	0.909	3.16	1.14	0.88	0.73	0.73	0.76	0.85	1.43
Forces (kips)																				
Pier (Axial)	1393	19.94	-1482	21.98	1290	17.19	1350	16.29	1259	17.60	18.47	1369	22.45	0.98	0.92	1.06	1.01	1.09	1.01	0.86
Pier (Long. Shear)	644	1.00	-535	0.99	-515	1.00	-582	1.00	-614	1.00	1.00	570	1.00	0.88	1.06	1.11	0.98	0.93	0.99	1.00
Pier (Trans. Shear)	-1117	1.00	-1247	1.00	1079	1.00	1176	1.00	-1104	1.00	1.00	1081	1.00	0.97	0.87	1.00	0.92	0.98	0.95	1.00
Deck over Pier																				
Vert. Shear (kips)	-304	4.80	390	7.58	-436	6.43	350	5.92	-326	5.17	5.93	339	6.25	1.12	0.87	0.78	0.97	1.04	0.95	1.39
Moment (kip-ft)	-11294	2.76	14738	4.29	-14923	4.10	14615	4.01	-13818	4.01	3.80	12715	4.33	1.13	0.86	0.85	0.87	0.92	0.93	1.42
Deck at Mid-Span																				
Vert. Shear (kips)	233	4.23	-208	4.45	-273	4.77	196	3.81	230	3.86	4.22	231	4.89	0.99	1.11	0.85	1.18	1.00	1.03	1.06
Moment (kip-ft)	8099	4.27	-9550	8.36	-10933	8.02	9891	6.88	-9017	4.91	6.19	9039	6.21	1.12	0.95	0.83	0.91	1.00	0.96	1.33

Abs. = Absolute value of response quantity to three-component seismic input.

(3/2) Ratio = Absolute value of three-component response over absolute value of two-component response for time history analyses and response spectrum analysis.

Avg. Ratio = Sum of three-component time history response values over sum of two-component time history response value for all five records.

Table 6.6 Bridge #5 – Time History Analysis Using Frequency-scaled Records

	Frequency-Scaled Time History Records to Target Spectrum with parameters M=6.5, D=5km and Soil													Response Spectrum/Time History (RS/TH)						Response Spectrum
	Imp. Val. #8 (1)		Imp. Vl. D.A (2)		Corralitas (3)		Arleta (4)		New Hall (5)											
Response Quantity	Time History	(3/2)	Time History	(3/2)	Time History	(3/2)	Time History	(3/2)	Time History	(3/2)	Avg.	Resp. Spect.	(3/2)	1	2	3	4	5	Avg.	2/3(H)
	Abs.	Ratio	Abs.	Ratio	Abs.	Ratio	Abs.	Ratio	Abs.	Ratio	Ratio	Abs.	Ratio						(RS/TH)	V/H(H)
1	2	3	4	5	6	7	8	9	10	11	12	13	14	15	16	17	18	19	20	21
Pier Displ. (in.)																				
Longitudinal	-7.510	1.00	-7.419	1.00	-7.961	1.00	7.520	1.00	7.096	1.00	1.00	8.162	1.00	1.09	1.10	1.03	1.09	1.15	1.09	1.00
Transverse	-5.129	1.00	4.596	1.00	4.536	1.00	4.171	1.00	5.705	1.00	1.00	4.369	1.00	0.85	0.95	0.96	1.05	0.77	0.92	1.00
Vertical	0.053	16.54	0.051	16.96	0.058	21.05	0.047	19.89	0.052	16.66	18.06	0.048	18.62	0.91	0.94	0.83	1.02	0.92	0.93	0.60
Mid-Span Displ. (in.)																				
Longitudinal	7.198	1.00	-7.162	1.00	-7.561	1.00	7.271	1.00	6.816	1.00	1.00	7.936	1.00	1.10	1.11	1.05	1.09	1.16	1.10	1.00
Transverse	-4.666	1.00	4.451	1.00	-4.585	1.00	-3.729	1.00	-5.821	1.00	1.00	4.105	1.00	0.88	0.92	0.90	1.10	0.71	0.90	1.00
Vertical	0.858	1.78	1.082	2.31	1.101	2.02	-0.944	2.05	1.475	3.24	2.26	1.042	2.04	1.21	0.96	0.95	1.10	0.71	0.99	1.37
Forces (kips)																				
Pier (Axial)	1621	13.94	1570	14.33	1791	17.79	1431	16.56	1534	13.48	15.09	1478	15.69	0.91	0.94	0.82	1.03	0.96	0.93	0.67
Pier (Long. Shear)	-1008	1.00	-975	1.00	-1085	1.00	981	1.00	-919	1.00	1.00	1087	1.00	1.08	1.12	1.00	1.11	1.18	1.10	1.00
Pier (Trans. Shear)	1574	1.00	-1688	1.00	-1442	1.00	-1766	1.00	1911	1.00	1.00	1563	1.00	0.99	0.93	1.08	0.89	0.82	0.94	1.00
Deck over Pier																				
Vert. Shear (kips)	351	3.43	-328	3.41	322	3.34	385	4.52	443	4.67	3.85	361	4.01	1.03	1.10	1.12	0.94	0.81	1.00	1.27
Moment (kip-ft)	13305	2.33	-14133	2.70	-12359	2.34	13664	2.82	17306	2.82	2.60	13865	2.64	1.04	0.98	1.12	1.01	0.80	0.99	1.28
Deck at Mid-Span																				
Vert. Shear (kips)	-251	3.43	221	2.54	-283	3.74	267	4.02	242	3.49	3.40	255	3.30	1.02	1.15	0.90	0.95	1.05	1.01	0.91
Moment (kip-ft)	-9758	4.26	-8414	3.70	-9835	3.80	-9906	4.54	-10970	5.30	4.29	9712	3.97	1.00	1.15	0.99	0.98	0.89	1.00	1.23

Abs. = Absolute value of response quantity to three-component seismic input.

(3/2) Ratio = Absolute value of three-component response over absolute value of two-component response for time history analyses and response spectrum analysis.

Avg. Ratio = Sum of three-component time history response values over sum of two-component time history response value for all five records.

6.4 Results of Response Spectrum Analysis

As mentioned in Section 6.2, the final format for the results from the linear response spectrum analyses of the selected six bridges is a ratio that relates the additional impact due to the vertical component of ground motions to the dead load only response. The ratio is denoted "(3-2)/DL Ratio" and is computed by dividing the difference in response between the three and two component input by the dead load only response. All three response ratios (3/2, 3/DL and (3-2)/DL) discussed in Section 6.2 are shown for each bridge in Tables A-1 to A-6 in Appendix A.

Values for the (3-2)/DL Ratio are plotted in Figures 6.8 to 6.23 for the response quantities of pier axial force, deck vertical shear at the pier, deck vertical moment over the pier and at mid-span. Each plot shows the variation of the response ratio for each bridge with fault distance for either magnitude 6.5 and 7.5 and soil or rock site conditions.

These figures show the expected trends of decreasing ratios as the fault distance increases. A magnitude 7.5 event and soil site conditions produce the highest ratios for pier axial force for all distances and for deck shear at the pier and moment at mid-span at distances beyond 10 km. Rock site conditions produce the highest ratios for these two quantities for distances less than 10 km and for deck moment over the pier for all distances.

Looking next at the bridges most affected by including the vertical component in an analysis, it can be seen that bridges 2, 5, and 6 tend to have the highest ratios for all response quantities. An examination of Table 3.8 in Section 3.7 shows that these three bridges have the highest percentage of modal mass participation for periods less than 0.15 seconds. Furthermore, Table 6.7 shows that all vertical spectra shown in Figures 4.7 to 4.10 have spectral peaks at a period of 0.08 seconds. This indicates that these three bridges have a greater amount of modal mass participation in the peak range of the vertical spectra and therefore have higher response ratios than the other three bridges.

Table 6.7 Peak Spectral Acceleration (g) and Corresponding Period (sec) for the Response Spectra used in the Study

Site Condition		Distance				
		1km	5km	10km	20km	40km
		Sa - Period	Sa – Period	Sa - Period	Sa - Period	Sa – Period
M=6.5, Rock	H	1.65 – 0.17	1.13 – 0.15	0.73 – 0.17	0.38 – 0.17	0.17 – 0.2
	V	1.45 – 0.08	0.94 – 0.08	0.55 – 0.08	0.25 – 0.08	0.09 – 0.08
M=6.5, Soil	H	1.23 – 0.24	0.91 – 0.2	0.63 – 0.2	0.37 – 0.2	0.19 – 0.3
	V	1.44 – 0.08	1.01 – 0.08	0.62 – 0.08	0.29 – 0.08	0.12 – 0.08
M=7.5, Rock	H	1.84 – 0.2	1.41 – 0.2	1.0 – 0.2	0.6 – 0.2	0.32 – 0.24
	V	1.76 – 0.08	1.26 – 0.08	0.81 – 0.08	0.41 – 0.08	0.17 – 0.08
M=7.5, Soil	H	1.44 – 0.3	1.16 – 0.3	0.88 – 0.3	0.6 – 0.3	0.36 – 0.3
	V	2.02 – 0.08	1.52 – 0.08	1.00 – 0.08	0.51 – 0.08	0.22 – 0.08

One of the primary objectives of this study is to make recommendations as to when the vertical component of motion should be included in the seismic analysis of a bridge. The heavy dark lines shown in Figures 6.8 to 6.23 show boundaries for fault distance and percentage of dead load. The purpose of these cut-off boundaries is to simplify the design process by creating distance zones where the vertical component of motion may be ignored in analysis if each bridge element is effectively designed for additional dead load. For example, Figure 6.11 shows that if a bridge on a rock site is located more than 20 km from a fault capable of producing a magnitude 7.5 event, then the vertical component can be excluded from the analysis provided the piers are designed for an additional ±20% of the dead load. This is consistent with current practice in the UBC building code, which specifies 0.9 DL and 1.2 DL in load combination equations. Tables 6.8 to 6.11 show values for these dead multipliers extracted from Figures 6.8 to 6.23 for distance zone increments of 5km and 10 km. These tables offer a starting point for drafting bridge code requirements that permit the vertical component of motion to be taken into account in bridge design. Of course, the difficulty in generalizing from the results of a very limited number of bridge models is recognized, thus more conservative values may be warranted for design purposes.

Tables 6.12 to 6.15 show envelope values of DL multipliers for rock and soil sites for bridges where 70% of the vertical modal mass participation resides in vertical modes with periods greater than 0.2 seconds. These tables are intended to further help a code committee in classifying the bridge types that are most sensitive to the vertical component of motion. Tables 6.12 and 6.13 show values for bridge numbers 1, 3 and 4. Tables 6.14 and 6.15 show values for bridge numbers 1 and 4 only, leaving out single span bridge number 3. Bridge numbers 1, 3 and 4 show the least sensitivity to the addition of the vertical component and for the response quantities of pier axial force and deck bending moment at the pier, their DL multipliers are less than 50% of those for bridge numbers 2,5 and 6.

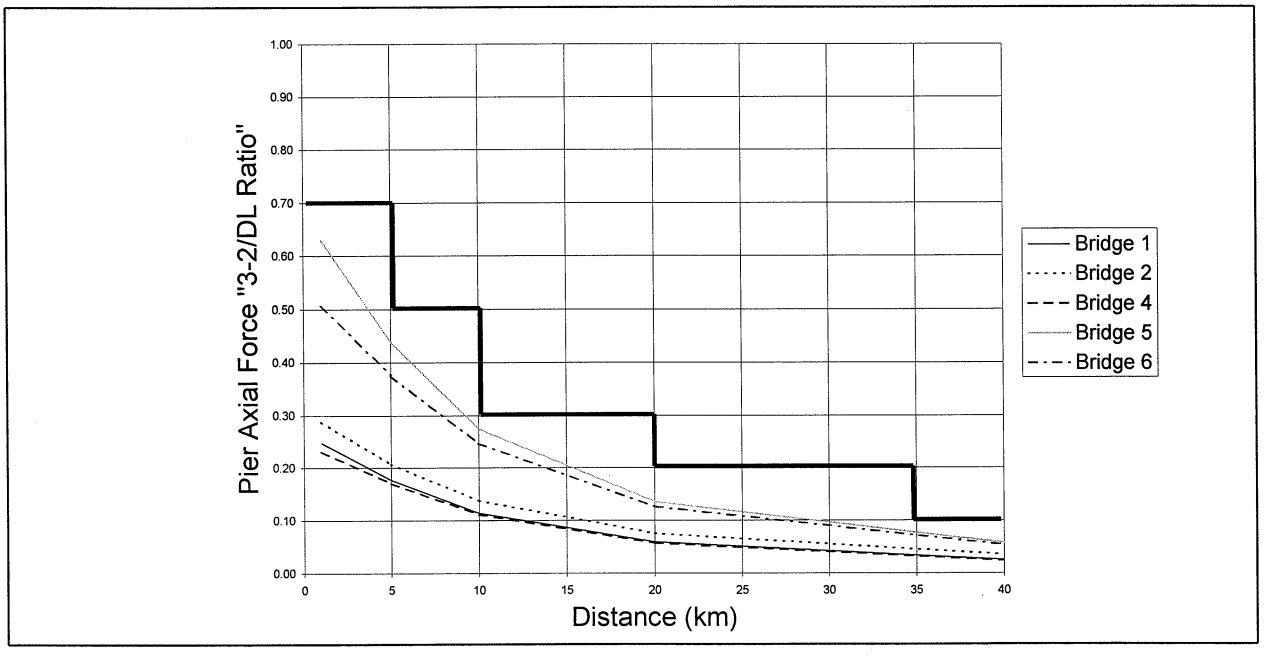

Figure 6.8 Variation of Pier Axial Force "(3-2)/DL Ratio" Across the Six* Bridges and Distance for Magnitude 6.5 and Soil ("3-2/DL Ratio" = absolute response of two-component input subtracted from absolute response of three-component input over dead-load only response; * Bridge 3 is a simply-supported single span bridge)

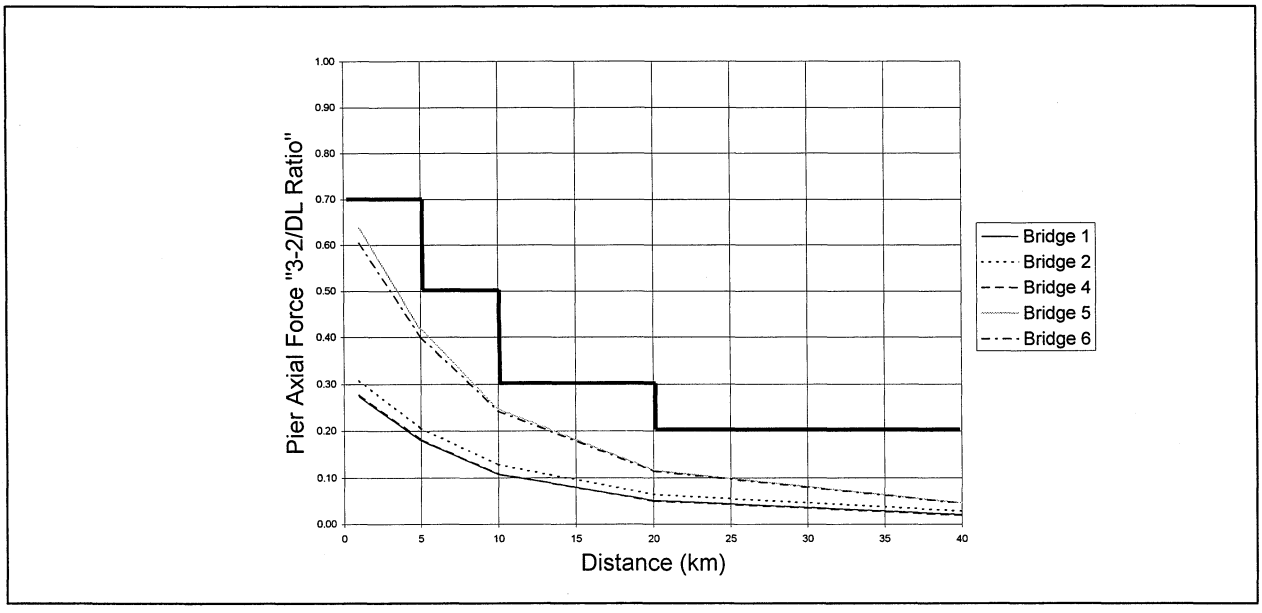

Figure 6.9 Variation of Pier Axial Force "(3-2)/DL Ratio" Across the Six* Bridges and Distance for Magnitude 6.5 and Rock ("3-2/DL Ratio" = Absolute response of two-component input subtracted from absolute response of three-component input over dead-load only response; * Bridge 3 is a simply-supported single span bridge)

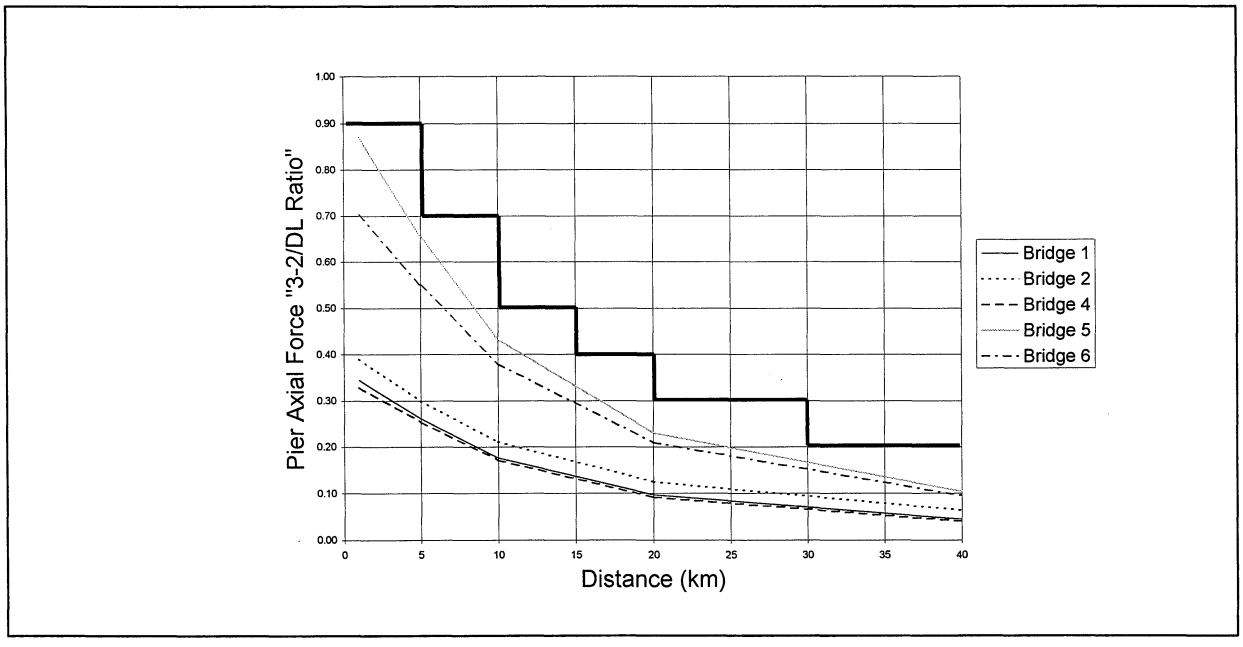

Figure 6.10 Variation of Pier Axial Force "(3-2)/DL Ratio" Across the Six* Bridges and Distance for Magnitude 7.5 and Soil ("3-2/DL Ratio" = Absolute response of two-component input subtracted from absolute response of three-component input over dead-load only response; * Bridge 3 is a simply-supported single span bridge)

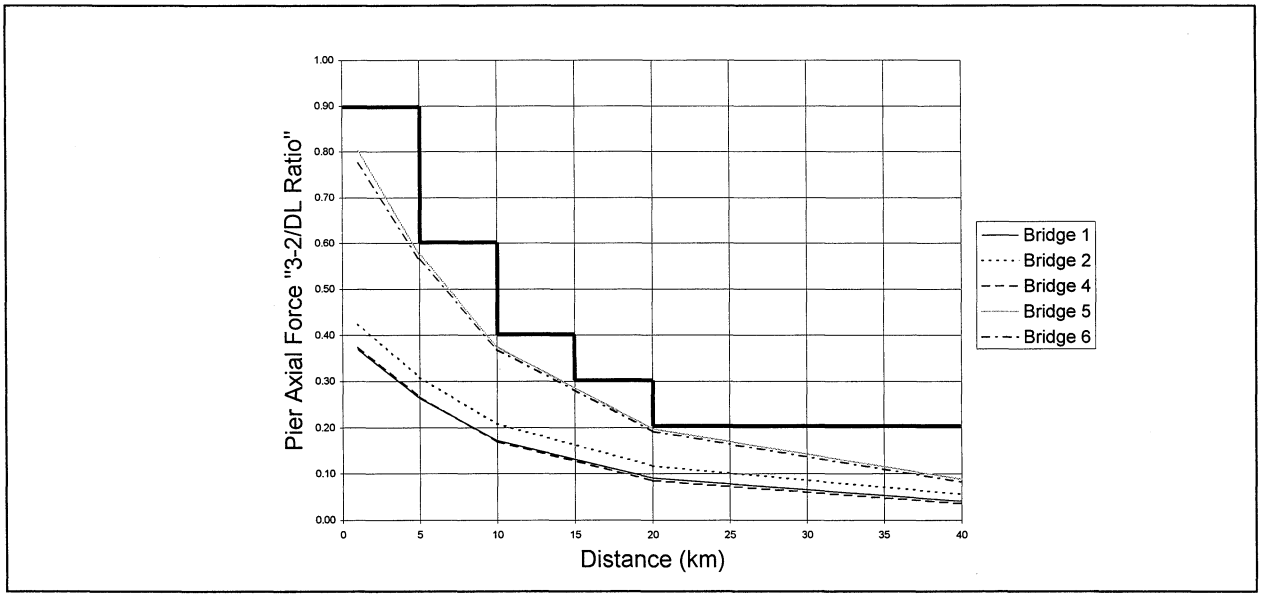

Figure 6.11 Variation of Pier Axial Force "(3-2)/DL Ratio" Across the Six* Bridges and Distance for Magnitude 7.5 and Rock ("3-2/DL Ratio" = Absolute response of two-component input subtracted from absolute response of three-component input over dead-load only response; * Bridge 3 is a simply-supported single span bridge)

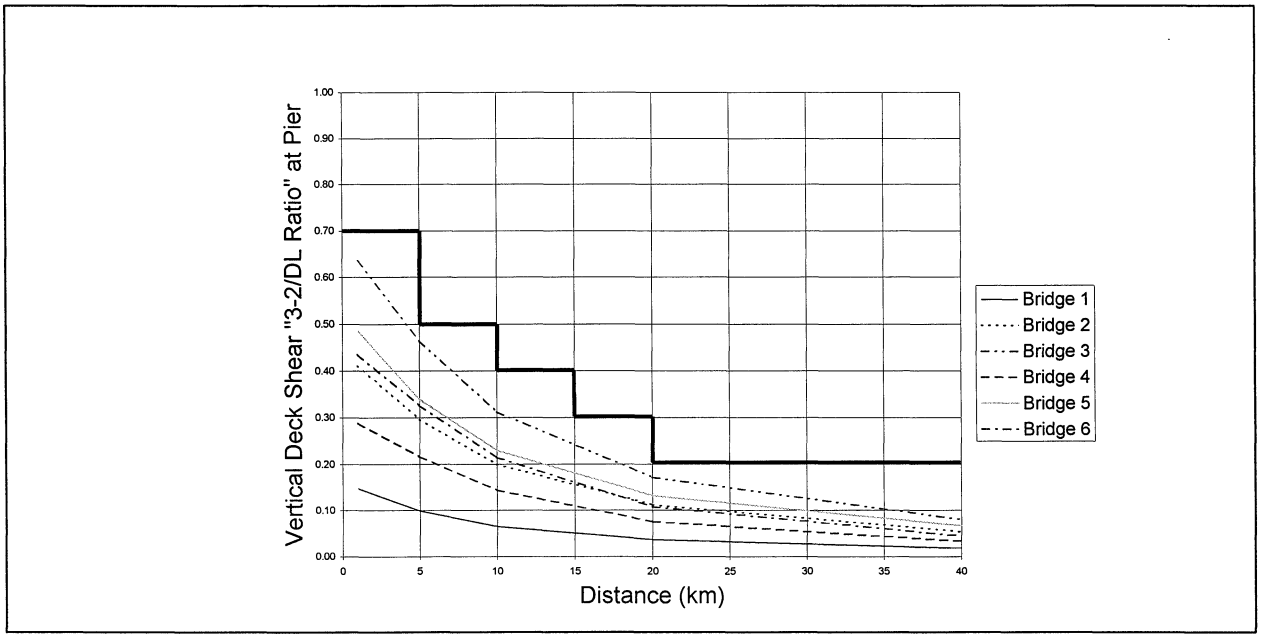

Figure 6.12 Variation of Vertical Deck Shear Force "(3-2)/DL Ratio" at Pier Across the Six Bridges and Distance for Magnitude 6.5 and Soil ("3-2/DL Ratio" = Absolute response of two-component input subtracted from absolute response of three-component input over dead-load only response)

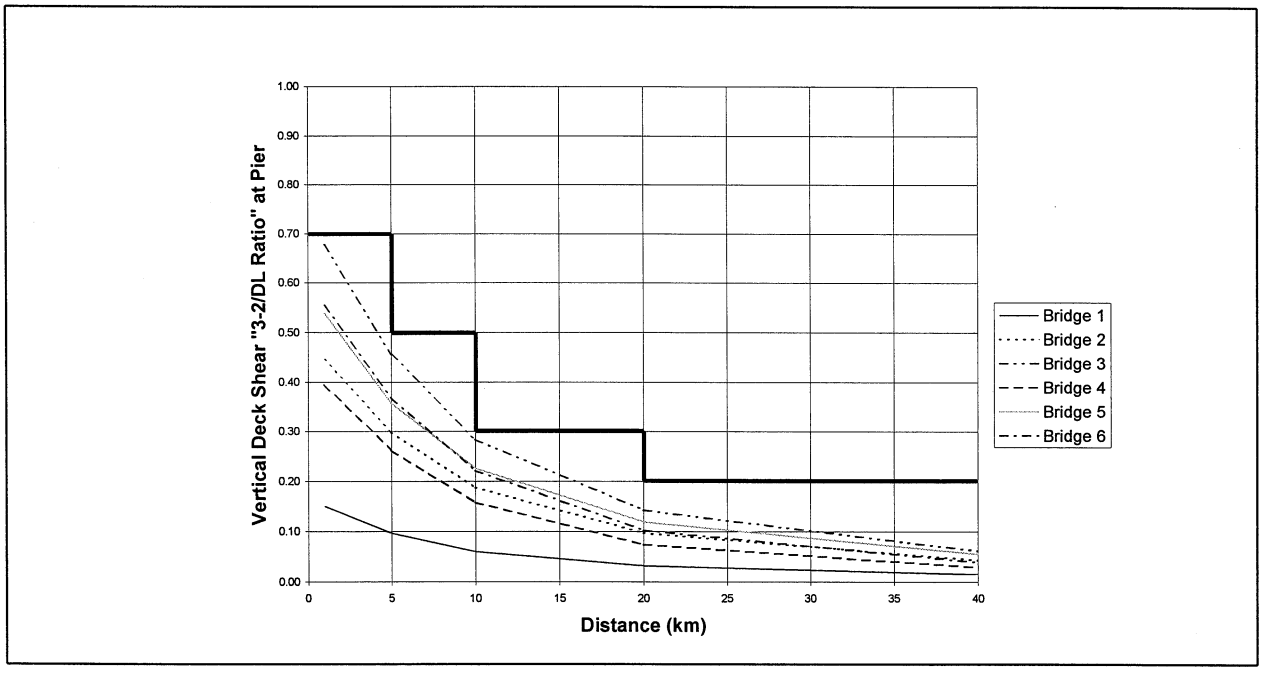

Figure 6.13 Variation of Vertical Deck Shear Force "(3-2)/DL Ratio" at Pier Across the Six Bridges and Distance for Magnitude 6.5 and Rock (3-2/DL Ratio" = Absolute response of two-component input subtracted from absolute response of three-component input over dead-load only response)

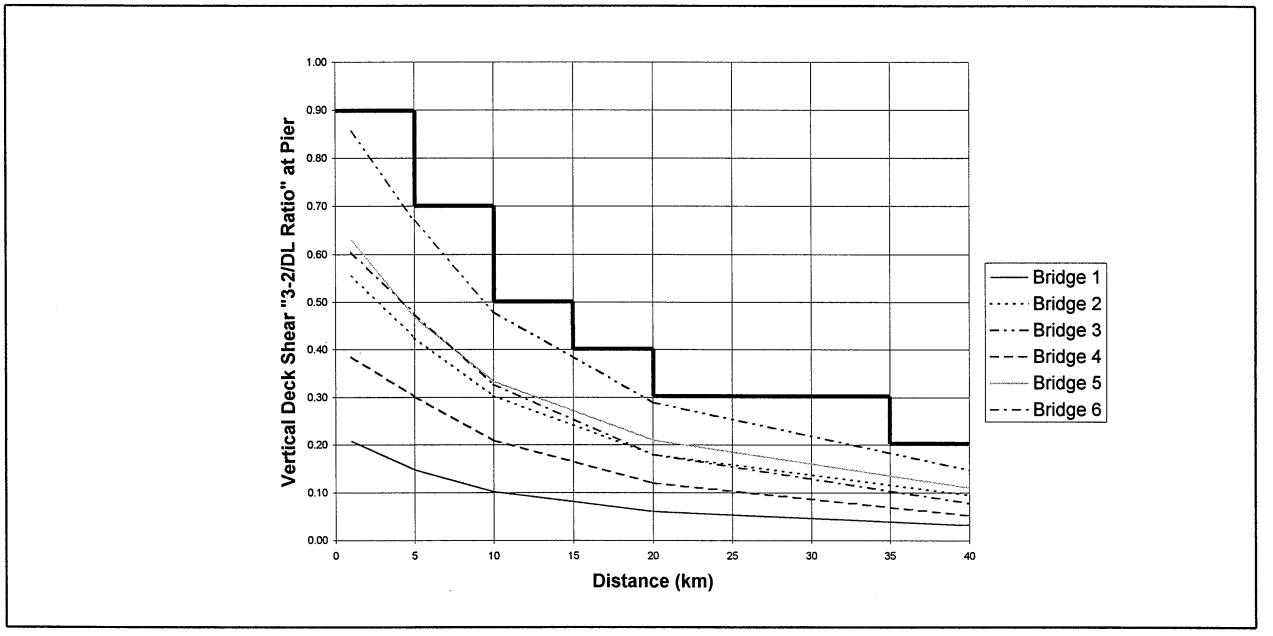

Figure 6.14 Variation of Vertical Deck Shear Force "(3-2)/DL Ratio" at Pier Across the Six Bridges and Distance for Magnitude 7.5 and Soil ("3-2/DL Ratio" = Absolute Response of two-component input subtracted from absolute response of three-component input over dead-load only response)

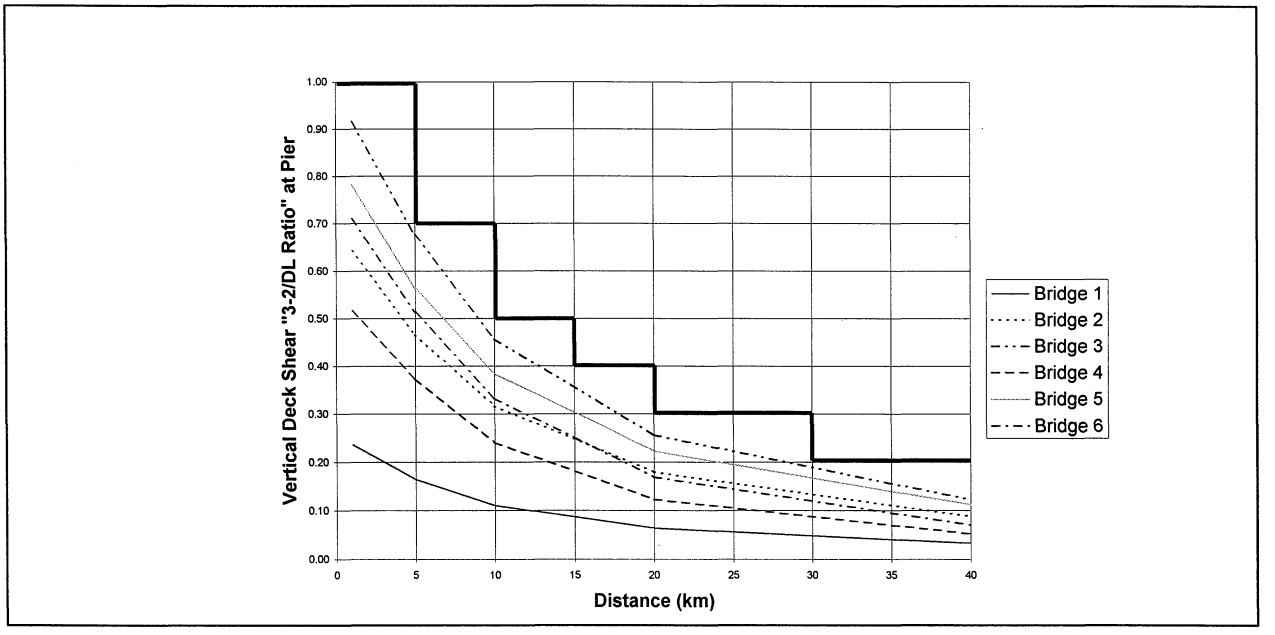

Figure 6.15 Variation of Vertical Deck Shear Force "(3-2)/DL Ratio" at Pier Across the Six Bridges and Distance for Magnitude 7.5 and Rock ("3-2/DL Ratio" = Absolute response of two-component input subtracted from absolute response of three-component input over dead-load only response)

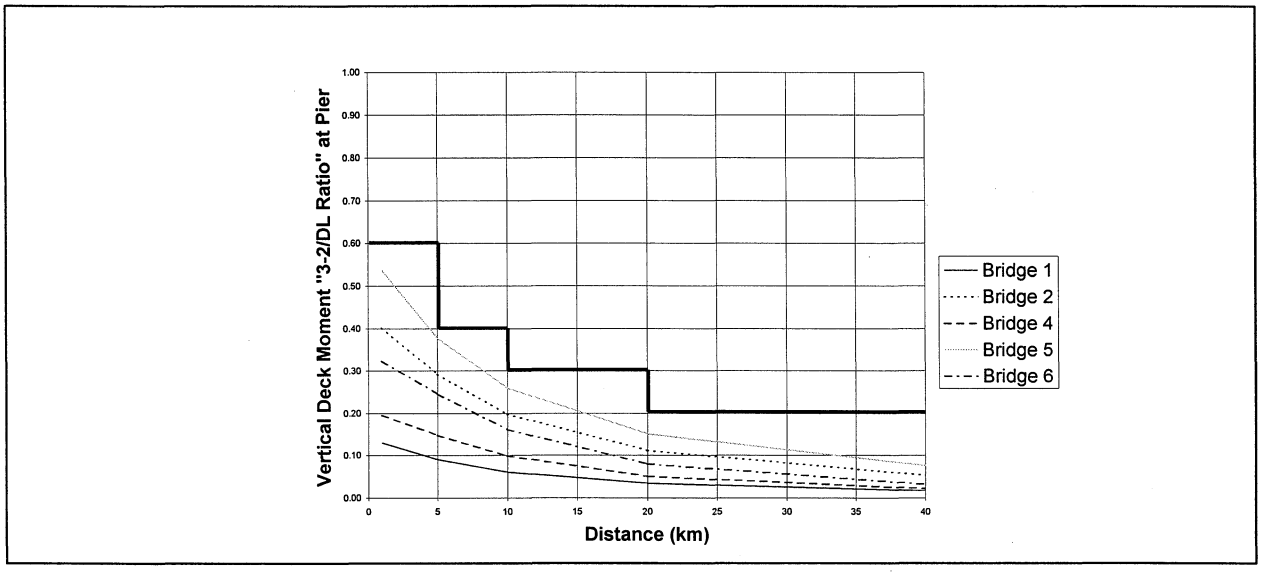

Figure 6.16 Variation of Vertical Deck Moment "(3-2)/DL Ratio" at Pier Across the Six* Bridges and Distance for Magnitude 6.5 and Soil ("3-2/DL Ratio" = Absolute response of two-component input subtracted from absolute response of three-component input over dead-load only response; * Bridge 3 is a simply-supported single span bridge)

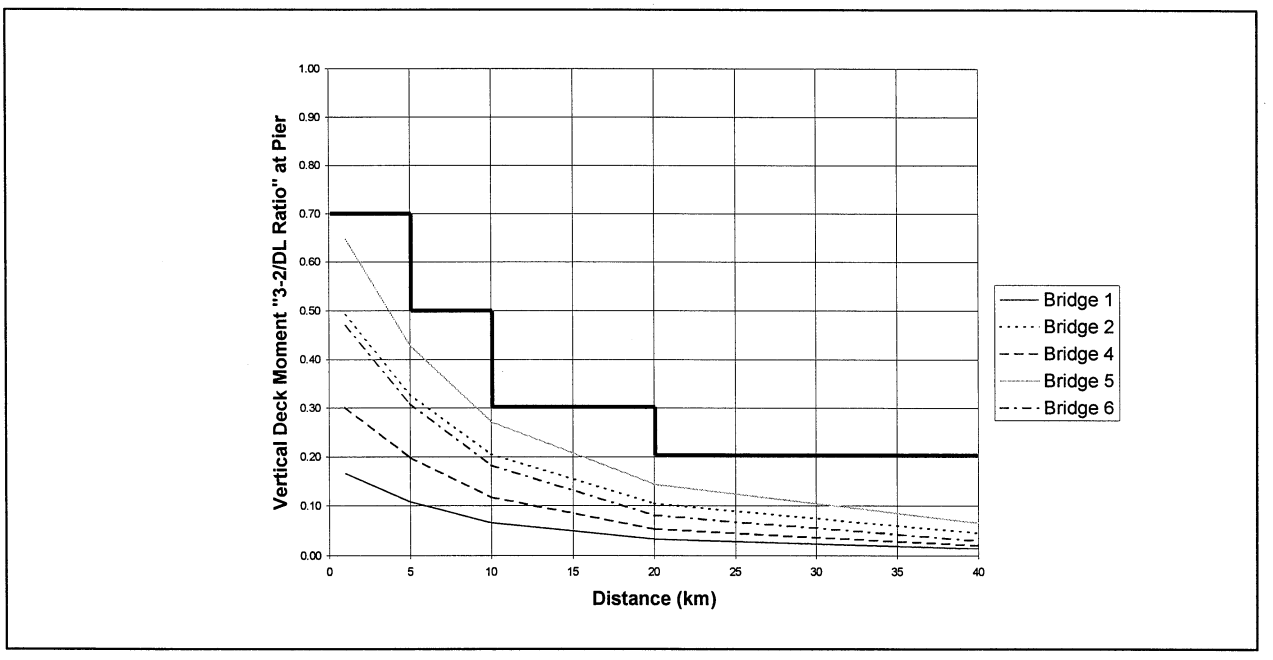

Figure 6.17 Variation of Vertical Deck Moment "(3-2)/DL Ratio" at Pier Across the Six* Bridges and Distance for Magnitude 6.5 and Rock ("3-2/DL Ratio" = Absolute response for two-component input subtracted from absolute response of three-component input over dead-load only response; * Bridge 3 is a simply-supported single span bridge)

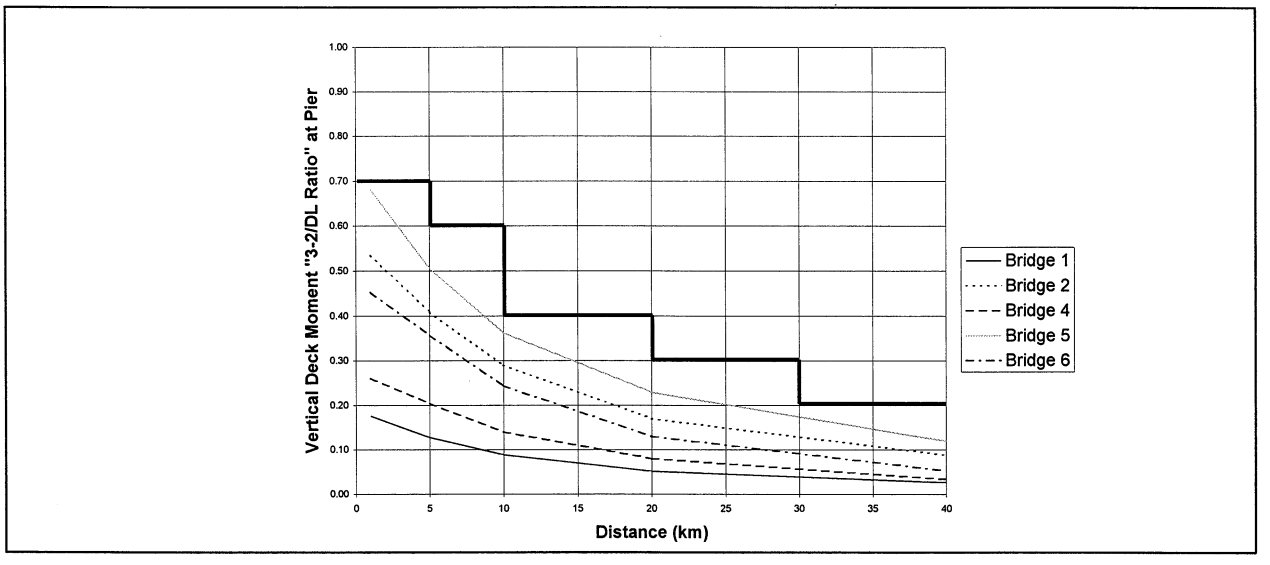

Figure 6.18 Variation of Vertical Deck Moment "(3-2)/DL Ratio" at Pier Across the Six* Bridges and Distance for Magnitude 7.5 and Soil ("3-2/DL Ratio" = Absolute response of two-component input subtracted from absolute response of three-component input over dead-load only response; * Bridge 3 is a simply-supported single span bridge)

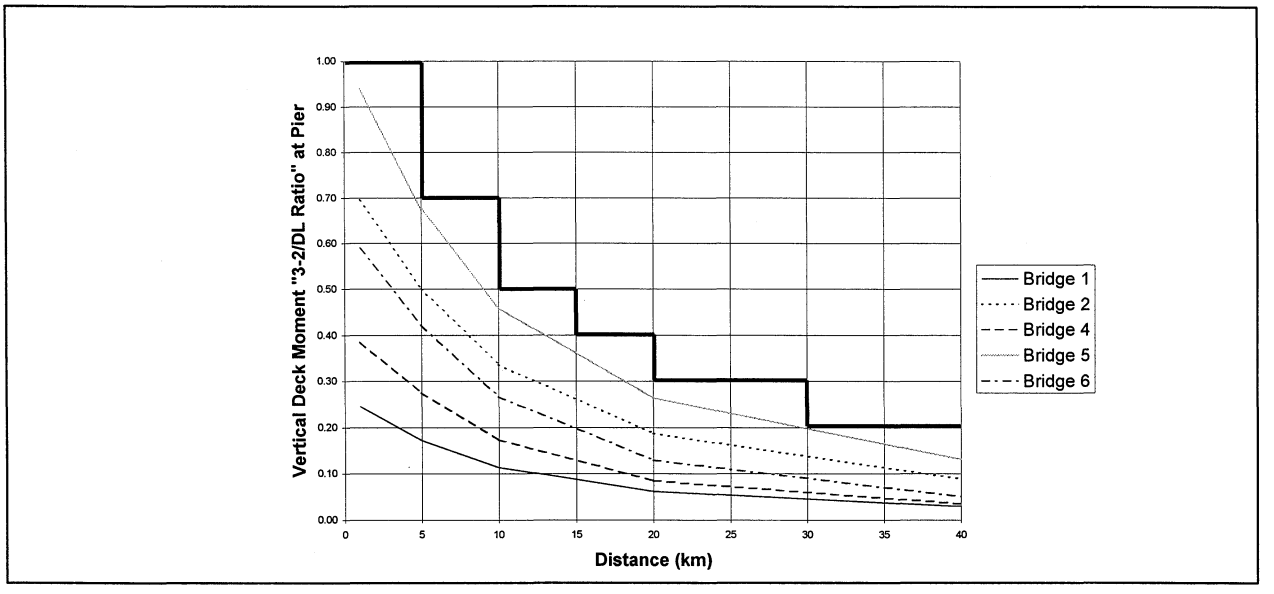

Figure 6.19 Variation of Vertical Deck Moment "(3-2)/DL Ratio" at Pier Across the Six* Bridges and Distance for Magnitude 7.5 and Rock ("3-2/DL Ratio" = Absolute response of two-component input subtracted from absolute response of three-component input over dead-load only response; * Bridge 3 is a simply-supported single span bridge)

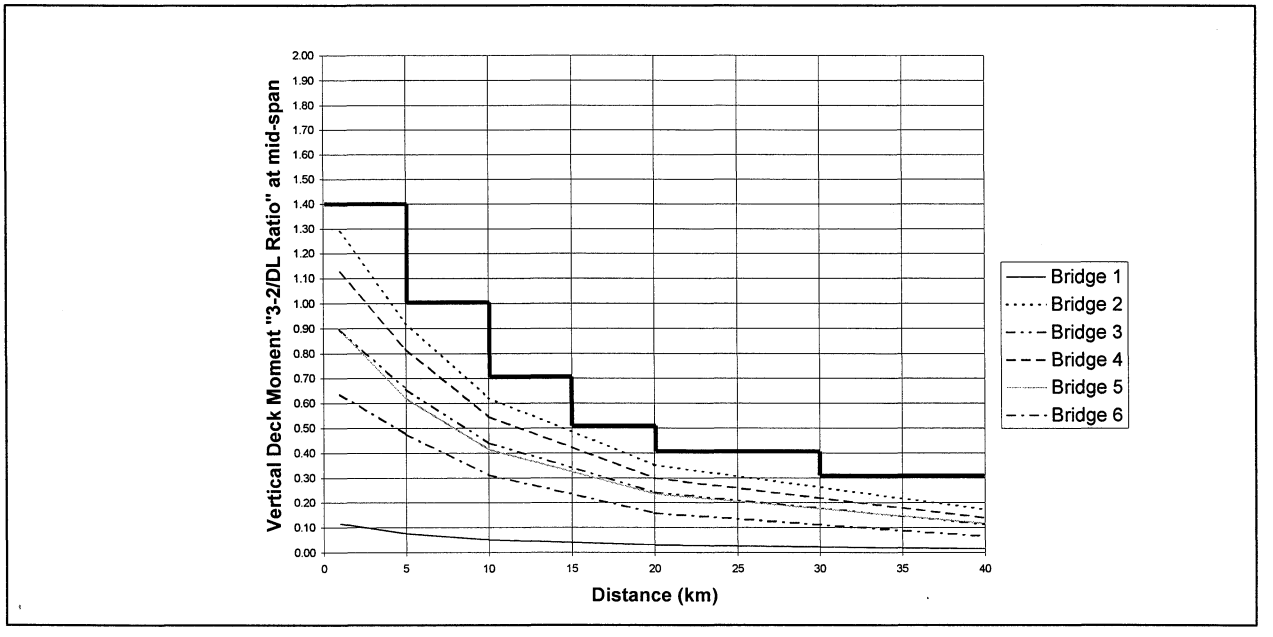

Figure 6.20 Variation of Vertical Deck Moment "(3-2)/DL Ratio" at Mid-span Across the Six Bridges and Distance for Magnitude 6.5 and Soil (3-2/DL Ratio" = Absolute response of two-component input subtracted from absolute response of three-component input over dead-load only response)

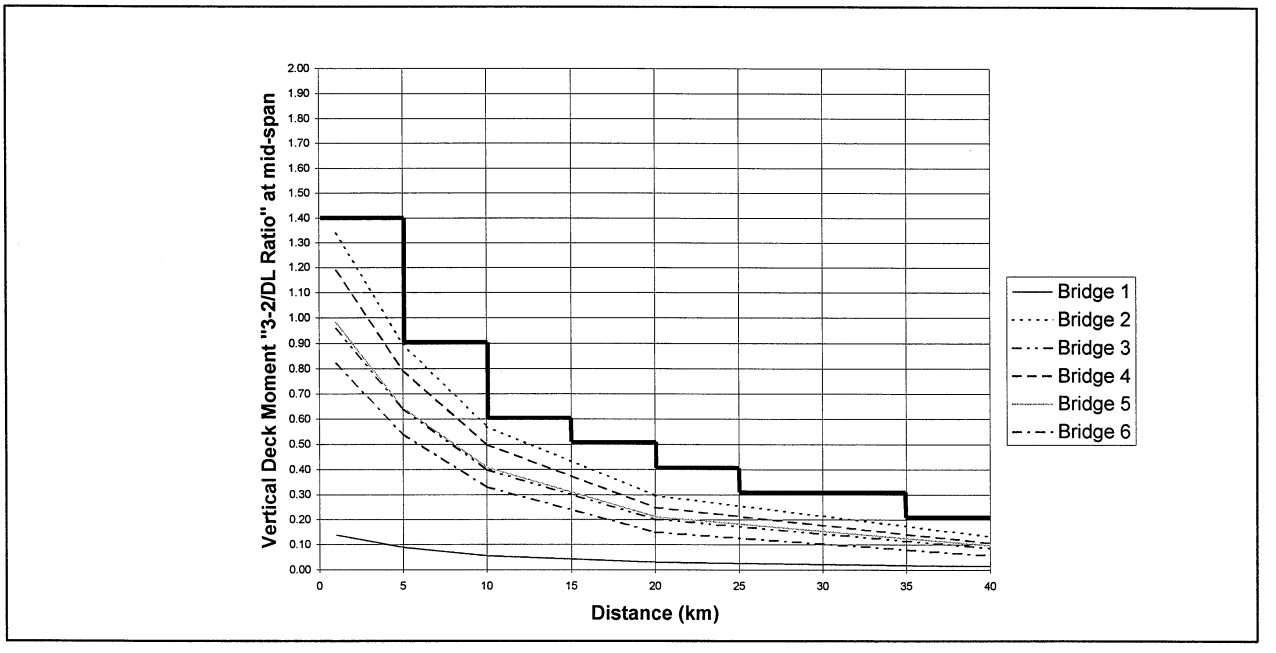

Figure 6.21 Variation of Vertical Deck Moment "(3-2)/DL Ratio" at Mid-span Across the Six Bridges and Distance for Magnitude 6.5 and Rock (3-2/DL Ratio" = Absolute response of two-component input subtracted from absolute response of three-component input over dead-load only response)

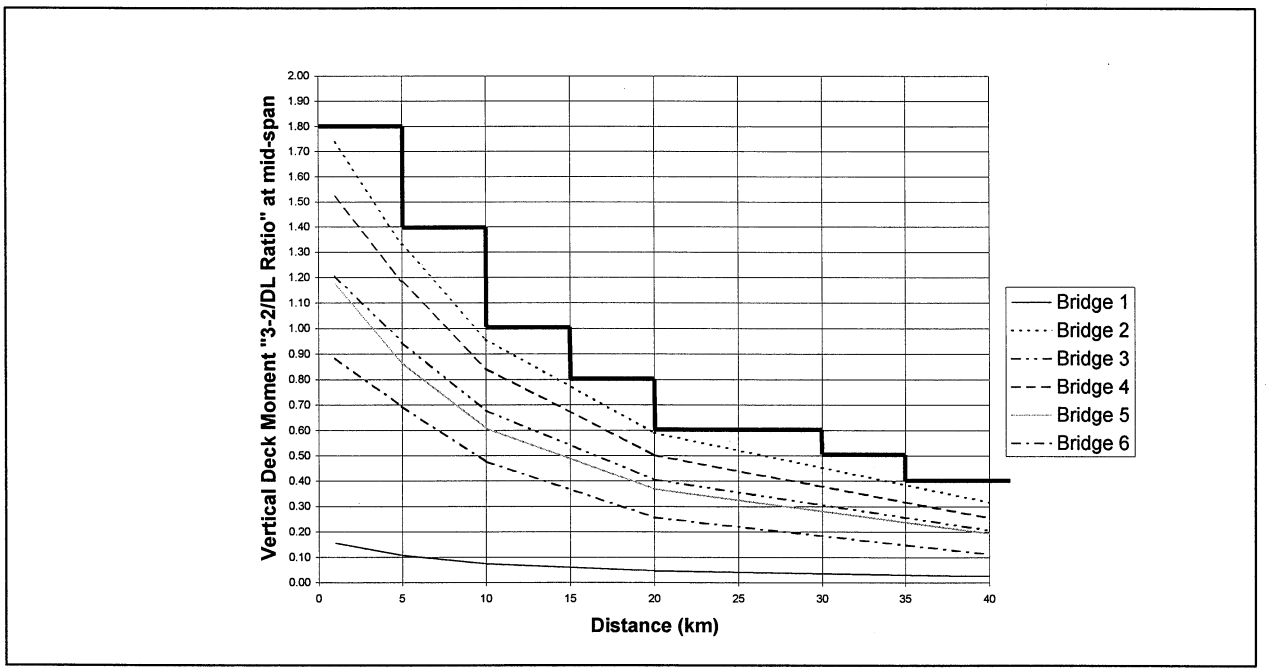

Figure 6.22 Variation of Vertical Deck Moment "(3-2)/DL Ratio" at Mid-span Across the Six Bridges and Distance for Magnitude 7.5 and Soil ("3-2/DL Ratio" = Absolute response of two-component input subtracted from absolute response of three-component input over dead-load only response)

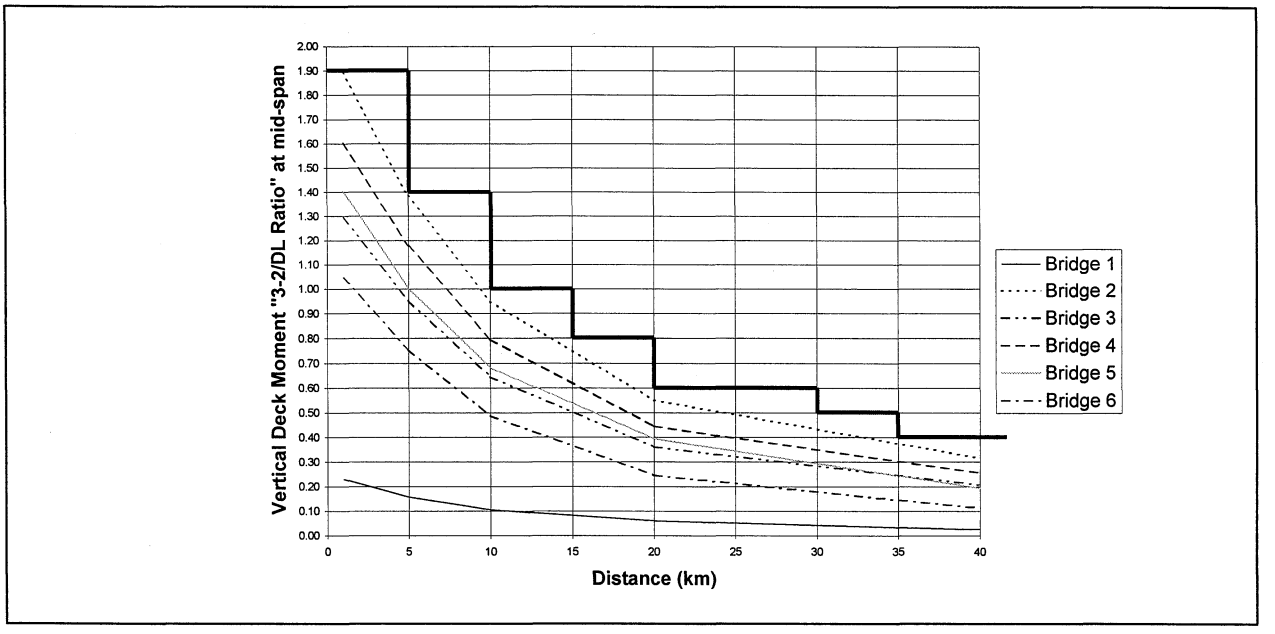

Figure 6.23 Variation of Vertical Deck Moment "(3-2)/DL Ratio" at Mid-span Across the Six Bridges and Distance for Magnitude 7.5 and Rock (3-2/DL Ratio" = Absolute response of two-component input subtracted from absolute response of three-component input over dead-load only response)

TABLE 6.8 Fault Distance Zones and Corresponding Dead Load Multipliers for ALL BRIDGES Observed for Soil Sites and a Magnitude 6.5 Event in Figures 6.8, 6.12, 6.16, and 6.20

Response Quantity	Fault Distance Zones (km)								
	0-5	5-10	10-15	15-20	20-25	25-30	30-35	35-40	>40 or given value
	0-10		10-20		20-30		30-40		
Pier Axial Force DL Multiplier	0.7	0.5	0.3	0.3	0.2		0.1		0.1
	0.7		0.3						
Deck Shear Force at Pier DL Multiplier	0.7	0.5	0.4	0.3	0.2			0.1	0.1
	0.7		0.4						
Deck Bending Moment at Pier DL Multiplier	0.6	0.4	0.3	0.3	0.2			0.1	0.1
	0.6		0.3						
Deck Shear Force at Mid-Span DL Multiplier	0.1								0.1
Deck Bending Moment at Mid-Span* DL Multiplier	1.4	1.0	0.7	0.5	0.4	0.4	0.3	0.3	0.1 (>50)
	1.4		0.7		0.4		0.3		

Footnotes

(1) The DL Multiplier values given above are in addition to the dead load; thus, an actual "load factor" would be **1.0 plus/minus** *the above numbers.*

*(2) *Broekhuizen[1997](see Section 2, 2.1 Decks) concluded that prestressed spans will not experience significant damage for upward accelerations of up to 1g applied to the superstructure.*

(3) The Live Load (LL) typically used in the design of bridge types shown in this study is in the range of 20-30% of the Dead Load (DL).

TABLE 6.9 Fault Distance Zones and Corresponding Dead Load Multipliers for ALL BRIDGES Observed for Rock Sites and a Magnitude 6.5 Event in Figures 6.9, 6.13, 6.17, and 6.21

Response Quantity	Fault Distance Zones (km)								
	0-5	5-10	10-15	15-20	20-25	25-30	30-35	35-40	>40 or given value
	0-10		10-20		20-30		30-40		
Pier Axial Force DL Multiplier	0.7	0.5	0.3	0.3	0.2	0.1			0.1
	0.7		0.3						
Deck Shear Force at Pier DL Multiplier	0.7	0.5	0.3	0.3	0.2		0.1		0.1
	0.7		0.4						
Deck Bending Moment at Pier DL Multiplier	0.7	0.5	0.3	0.3	0.2			0.1	0.1
	0.7		0.3						
Deck Shear Force at Mid-Span DL Multiplier	0.1								0.1
Deck Bending Moment at Mid-Span* DL Multiplier	1.4	0.9	0.6	0.5	0.4	0.3	0.3	0.2	0.1 (>50)
	1.4		0.6		0.4		0.3		

Footnotes

(1) The DL Multiplier values given above are in addition to the dead load; thus, an actual "load factor" would be **1.0 plus/minus** *the above numbers.*

*(2) *Broekhuizen[1997](see Section 2, 2.1 Decks) concluded that prestressed spans will not experience significant damage for upward accelerations of up to 1g applied to the superstructure.*

(3) The Live Load (LL) typically used in the design of bridge types shown in this study is in the range of 20-30% of the Dead Load (DL).

TABLE 6.10 Fault Distance Zones and Corresponding Dead Load Multipliers for ALL BRIDGES Observed for Soil Sites and a Magnitude 7.5 Event in Figures 6.10, 6.14, 6.18, and 6.22

Response Quantity	Fault Distance Zones (km)								
	0-5	5-10	10-15	15-20	20-25	25-30	30-35	35-40	>40 or given value
	0-10		10-20		20-30		30-40		
Pier Axial Force DL Multiplier									
	0.9	0.7	0.5	0.4	0.3	0.3	0.2		0.1
	0.9		0.5		0.3				
Deck Shear Force at Pier DL Multiplier									
	0.9	0.7	0.5	0.4	0.3	0.3	0.2		0.1 (>50)
	0.9		0.5		0.3				
Deck Bending Moment at Pier DL Multiplier									
	0.7	0.6	0.4	0.4	0.3	0.3	0.2		0.1 (>50)
	0.7		0.4		0.3				
Deck Shear Force at Mid-Span DL Multiplier									
			0.1						0.1
	See Section 6.5								
Deck Bending Moment at Mid-Span* DL Multiplier									
	1.8	1.4	1.0	0.8	0.6	0.6	0.5	0.4	0.1 (>60)
	1.8		1.0		0.6		0.5		

Footnotes

(1) The DL Multiplier values given above are in addition to the dead load; thus, an actual "load factor" would be **1.0 plus/minus** *the above numbers.*

*(2) *Broekhuizen[1997](see Section 2, 2.1 Decks) concluded that prestressed spans will not experience significant damage for upward accelerations of up to 1g applied to the superstructure.*

(3) The Live Load (LL) typically used in the design of bridge types shown in this study is in the range of 20-30% of the Dead Load (DL).

Table 6.11 Fault Distance Zones and Corresponding Dead Load Multiplier for ALL BRIDGES Observed for Rock Sites and a Magnitude 7.5 Event in Figures 6.11, 6.15, 6.19, and 6.23

Response Quantity	Fault Distance Zones (km)								
	0-5	5-10	10-15	15-20	20-25	25-30	30-35	35-40	>40 or given value
	0-10		10-20		20-30		30-40		
Pier Axial Force DL Multiplier	0.9	0.6	0.4	0.3	0.2				0.1
	0.9		0.4						
Deck Shear Force at Pier DL Multiplier	1.0	0.7	0.5	0.4	0.3	0.3	0.2		0.1 (>50)
	1.0		0.5		0.3				
Deck Bending Moment at Pier DL Multiplier	1.0	0.7	0.5	0.4	0.3	0.3	0.2		0.1 (>50)
	1.0		0.5		0.3				
Deck Shear Force at Mid-Span DL Multiplier			0.1						0.1
	See Section 6.5								
Deck Bending Moment at Mid-Span* DL Multiplier	1.9	1.4	1.0	0.8	0.6	0.6	0.5	0.4	0.1 (>60)
	1.9		1.0		0.6		0.5		

Footnotes

(1) The DL Multiplier values given above are in addition to the dead load; thus, an actual "load factor" would be **1.0 plus/minus** *the above numbers.*

*(2) *Broekhuizen[1997](see Section 2, 2.1 Decks) concluded that prestressed spans will not experience significant damage for upward accelerations of up to 1g applied to the superstructure.*

(3) The Live Load (LL) typically used in the design of bridge types shown in this study is in the range of 20-30% of the Dead Load (DL).

TABLE 6.12 Fault Distance Zones and Corresponding Dead Load Multipliers for BRIDGES 1, 3 and 4 Observed for a Magnitude 6.5 Event in Figures 6.8 to 6.23

Response Quantity	Fault Distance Zones (km)								
	0-5	5-10	10-15	15-20	20-25	25-30	30-35	35-40	>40 or given value
	0-10		10-20		20-30		30-40		
Pier Axial Force DL Multiplier	0.3	0.2	0.2		0.1				0.1
	0.3								
Deck Shear Force at Pier DL Multiplier	0.7	0.5	0.4	0.3	0.2			0.1	0.1
	0.7		0.4						
Deck Bending Moment at Pier DL Multiplier	0.3	0.2	0.2		0.1				0.1
	0.3								
Deck Shear Force at Mid-Span DL Multiplier	0.1								0.1
Deck Bending Moment at Mid-Span* DL Multiplier	1.2	0.8	0.5	0.4	0.3	0.3	0.2		0.1 (>50)
	1.2		0.5		0.3				

Footnotes

(1) The DL Multiplier values given above are in addition to the dead load; thus, an actual "load factor" would be **1.0 plus/minus** *the above numbers.*

*(2) *Broekhuizen[1997](see Section 2, 2.1 Decks) concluded that prestressed spans will not experience significant damage for upward accelerations of up to 1g applied to the superstructure.*

(3) The Live Load (LL) typically used in the design of bridge types shown in this study is in the range of 20-30% of the Dead Load (DL).

TABLE 6.13 Fault Distance Zones and Corresponding Dead Load Multipliers for BRIDGES 1, 3 and 4 Observed for a Magnitude 7.5 Event in Figures 6.8 to 6.23

Response Quantity	Fault Distance (km)								
	0-5	5-10	10-15	15-20	20-25	25-30	30-35	35-40	>40 or given value
	0-10		10-20		20-30		30-40		
Pier Axial Force DL Multiplier	0.4	0.3	0.2		0.1				0.1
	0.4								
Deck Shear Force at Pier DL Multiplier	1.0	0.7	0.5	0.4	0.3	0.3	0.3	0.3	0.1 (>50)
	0.9		0.5		0.3		0.2		
Deck Bending Moment at Pier DL Multiplier	0.4	0.4	0.2		0.1				0.1
	0.3								
Deck Shear Force at Mid-Span DL Multiplier			0.1						0.1
	See Section 6.5								
Deck Bending Moment at Mid-Span* DL Multiplier	1.6	1.2	0.9	0.7	0.5	0.5	0.4	0.4	0.1 (>60)
	1.6		0.9		0.5		0.4		

Footnotes

(1) The DL Multiplier values given above are in addition to the dead load; thus, an actual "load factor" would be **1.0 plus/minus** *the above numbers.*

*(2) *Broekhuizen[1997](see Section 2, 2.1 Decks) concluded that prestressed spans will not experience significant damage for upward accelerations of up to 1g applied to the superstructure.*

(3) The Live Load (LL) typically used in the design of bridge types shown in this study is in the range of 20-30% of the Dead Load (DL).

Table 6.14 Fault Distance Zones and Corresponding Dead Load Multipliers for BRIDGES 1 and 4 Observed for a Magnitude 6.5 Event in Figures 6.8 to 6.23

Response Quantity	Fault Distance Zones (km)								
	0-5	5-10	10-15	15-20	20-25	25-30	30-35	35-40	>40 or given value
	0-10		10-20		20-30		30-40		
Pier Axial Force DL Multiplier	0.3	0.2	0.2	0.1					0.1
	0.3								
Deck Shear Force at Pier DL Multiplier	0.4	0.3	0.2	0.1					0.1
	0.4								
Deck Bending Moment at Pier DL Multiplier	0.3	0.2	0.2			0.1			0.1
	0.3								
Deck Shear Force at Mid-Span DL Multiplier	0.1								0.1
Deck Bending Moment at Mid-Span* DL Multiplier	1.2	0.8	0.5	0.4	0.3	0.3	0.2		0.1
	1.2		0.5		0.3				

Footnotes

(1) The DL Multiplier values given above are in addition to the dead load; thus, an actual "load factor" would be **1.0 plus/minus** *the above numbers.*

*(2) *Broekhuizen[1997](see Section 2, 2.1 Decks) concluded that prestressed spans will not experience significant damage for upward accelerations of up to 1g applied to the superstructure.*

(3) The Live Load (LL) typically used in the design of bridge types shown in this study is in the range of 20-30% of the Dead Load (DL).

Table 6.15 Fault Distance Zones and Corresponding Dead Load Multipliers for BRIDGES 1 and 4 Observed for a Magnitude 7.5 Event in Figures 6.8 to 6.23

Response Quantity	Fault Distance Zones (km)								
	0-5	5-10	10-15	15-20	20-25	25-30	30-35	35-40	>40 or given value
	0-10		10-20		20-30		30-40		
Pier Axial Force DL Multiplier	0.4	0.3	0.2		0.1				0.1
	0.4								
Deck Shear Force at Pier DL Multiplier	0.4	0.3	0.2				0.1		0.1
	0.4								
Deck Bending Moment at Pier DL Multiplier	0.4	0.4	0.2		0.1				0.1
	0.3								
Deck Shear Force at Mid-Span DL Multiplier			0.1						0.1
	See Section 6.5								
Deck Bending Moment at Mid-Span* DL Multiplier	1.6	1.2	0.9	0.7	0.5	0.5	0.4	0.4	0.1 (>60)
	1.6		0.9		0.5		0.4		

Footnotes

(1) The DL Multiplier values given above are in addition to the dead load; thus, an actual "load factor" would be **1.0 plus/minus** *the above numbers.*

*(2) *Broekhuizen[1997](see Section 2, 2.1 Decks) concluded that prestressed spans will not experience significant damage for upward accelerations of up to 1g applied to the superstructure.*

(3) The Live Load (LL) typically used in the design of bridge types shown in this study is in the range of 20-30% of the Dead Load (DL).

6.5 Vertical Shear Capacity of Decks at Mid-span

Plots showing the "(3-2)/DL Ratio" for the vertical deck shear force at mid-span were not included with Figures 6.8 to 6.23 because the ratios are very large. They do not present a clear picture of the impact of the vertical component on this quantity because the absolute dead load and two-component response values are very small. It was decided that a clearer view of the effect of the vertical component on this response quantity would be conveyed by comparing the additional impact to a simple lower bound shear capacity value of the deck cross-sections. Table 6.16 shows this comparison for each bridge for maximum response values at a fault distance of 1 km and a magnitude 7.5 event.

Table 6.16 Comparison of Absolute Response Values for Shear at Mid-span with Lower Bound Shear Capacity Values for Bridges 1 to 6

Bridge Number	3-Component Response (kips)	Dead Load Response (kips)	Additional Impact (3 –2) (kips)	Shear Capacity (kips)
1	628	266	322	617
2	460	0	202	2444
3	130	0	133	318
4	716	0	93	363
5	466	0	290	1534
6	292	14	44	333

The vertical shear capacity at mid-span for bridge numbers 1, 3, 4 and 6 was calculated using a formula from Section 8.16.6.2 of the *Standard Specification for Highway Bridges*, 15th edition, [1992] that gives the nominal shear strength of the concrete for beams. The formula is as follows:

$$V_c = 2 f'_c b_w d$$

Where

V_c = Nominal shear strength of the concrete.
f'_c = Compressive strength of concrete (4000 psi).
b_w = Width of web.
d = Depth of beam or web.

The vertical shear capacity at mid-span of bridge numbers 2 and 5 was calculated using a formula from Section 6.10.7.2 of the *AASHTO LRFD Bridge Design Specifications*, [1994] that gives the nominal shear resistance of unstiffened webs for plate girders. The formula is as follows:

$$V_n = 4.55\sqrt{T^3 E/D}$$

Where:

V_n = Nominal shear resistance of unstiffened web.
T= Width of web.
E = Elastic modulus of steel.
D = Depth of web.

It can be seen from Table 6.16 that the additional shear force due to the vertical component does not exceed the lower bound shear resistance value given by the above formulae for all six bridges. On the other hand, this value is exceeded by the three-component response in bridge numbers 1 and 4. Both of these bridges are unrestrained in the longitudinal direction and the columns which are relatively short form effectively fixed connections to the deck. This configuration, in combination with the longitudinal motions, produces nearly all the vertical shear force in the mid-span region of bridge 4, but in bridge 1 over half the shear force can be attributed to the vertical motions. It can be concluded from these results that bridges with configurations such as bridge numbers 1 and 4 should be checked for adequate shear resistance at mid-span. It can be seen from Tables A-1 and A-4 in Appendix A that this is only required for fault distances less than 10km.

6.6 Effect of Varying Vertical Deck Stiffness

In the previous Section, the vertical deck stiffness used in the analysis of each bridge was calculated from the full uncracked cross-section. In this Section, response spectrum analyses are performed on bridge numbers 4 and 6, using moment of inertia for the vertical stiffness that are one quarter and four times the values used in the previous Section. The purpose of this exercise is to gain a broad understanding of the effect the vertical deck stiffness has on the structural response of bridges.

Tables 6.17 and 6.18 compare the changes in dynamic characteristics in the vertical direction for bridge numbers 4 and 6 for varying vertical deck stiffnesses of 25%, 100% and 400%. The tables show that, as the vertical deck stiffnesses increase, the fundamental period of the bridge model is reduced and the vertical modal mass participation is condensed into fewer modes. This implies a greater modal mass participation in the peak region of the vertical response spectra and as shown in Tables 6.19 and 6.20, higher response values will be obtained for vertically stiffer decks.

Tables 6.19 and 6.20 show selected results for the response quantities of pier axial force, vertical deck shear and moment at a pier, and vertical deck shear and moment at mid-span for varying vertical deck stiffnesses of bridge numbers 4 and 6. The results are shown for response spectra for rock and soil sites at a fault distance of 1km and a magnitude 7.5 event. The two response values given for each response quantity are the "(3-2)/DL Ratio" and the absolute response to the three-component input. The shaded cells shown in the tables contain the largest response values for a particular response quantity and site condition. It can be seen that the majority of these values are in columns representing models with the stiffest decks. Tables B-1, B-2, B-4, and B-5 in Appendix B show response results for all spectra shown in Figures 4.4 to 4.7 in Section 4.2 for 25% and 400% vertical deck stiffnesses of bridge numbers 4 and 6.

It can be concluded from the results shown in Tables 6.19 and 6.20 that the softening of the bridge deck due to cracking during an earthquake will reduce the impact of the vertical component of motion has on a bridge.

Table 6.17 Data for Vertical Modes with Vertical Mass Participation Ratios Greater Than 2% for Models of Bridge No. 4 with Vertical Deck Stiffnesses of 25%, 100% and 400%

Mode #	Period (sec.)	Percentage Mass Participation	Cumulative Percentage Mass Participation
25% Vertical Deck Stiffness			
5	0.3764	67.1	67.4
8	0.1287	3.5	70.9
11	0.0938	10.8	81.7
13	0.0722	13.6	95.3
15	0.0577	4.4	99.8
100% Vertical Deck Stiffness			
6	0.2050	79.3	79.3
9	0.0822	12.3	92.1
13	0.0579	6.0	98.2
400% Vertical Deck Stiffness			
4	0.1688	11.9	11.9
6	0.1352	84.2	96.0

Table 6.18 Data for Vertical Modes with Vertical Mass Participation Ratios Greater Than 2% for Models of Bridge No. 6 with Vertical Deck Stiffnesses of 25%, 100% and 400%

Mode #	Period (sec.)	Percentage Mass Participation	Cumulative Percentage Mass Participation
25% Vertical Deck Stiffness			
6	0.3222	60.8	61.0
12	0.0732	6.1	67.5
15	0.0543	13.3	83.0
20	0.0375	4.2	87.3
25	0.0004	6.9	95.0
100% Vertical Deck Stiffness			
7	0.1730	66.8	66.9
10	0.0620	2.9	69.9
14	0.0475	4.7	74.7
15	0.0466	10.8	85.5
18	0.0346	9.3	94.8
400% Vertical Deck Stiffness			
7	0.1034	81.5	81.8
16	0.0323	9.1	92.9
18	0.0299	5.6	98.5

Table 6.19 Selected Results of a Response Spectrum Analysis Performed on Bridge No. 4 for 25%, 100% and 400% of the Vertical Deck Stiffness

Response Quantity	Response Value	Bridge Number 4					
		Rock, 1km, M=7.5			Soil,1km, M=7.5		
		25%	100%	400%	25%	100%	400%
Pier Axial Force	Abs. (kips)	1172	1351	1508	1284	1361	1539
	(3-2)/DL Ratio	0.18	0.37	0.5	0.14	0.33	0.48
Deck Shear at Pier	Abs. (kips)	406	849	853	644	902	927
	(3-2)/DL Ratio	0.35	0.52	0.47	0.24	0.39	0.38
Deck Moment at Pier	Abs. (kip-ft)	24115	33143	34054	31176	40737	41958
	(3-2)/DL Ratio	0.23	0.39	0.35	0.13	0.26	0.27
Deck Shear at Mid-span	Abs. (kips)	497	583	556	623	716	689
	(3-2)/DL Ratio	-	-	-	-	-	-
Deck Moment at Mid-span	Abs. (kip-ft)	9694	12777	14539	9030	12131	13655
	(3-2)/DL Ratio	1.23	1.60	1.65	1.14	1.52	1.55

Table 6.20 The Results of a Response Spectrum Analysis Performed on Bridge No. 6 for 25%, 100% and 400% of the Vertical Deck Stiffness

Response Quantity	Response Value	Bridge Number 6					
		Rock, 1km, M=7.5			Soil,1km, M=7.5		
		25%	100%	400%	25%	100%	400%
Pier Axial Force	Abs. (kips)	841	1220	1783	832	1187	1993
	(3-2)/DL Ratio	0.46	0.78	1.15	0.41	0.70	1.26
Deck Shear at Pier	Abs. (kips)	393	564	736	388	554	828
	(3-2)/DL Ratio	0.44	0.71	0.95	0.36	0.61	1.02
Deck Moment at Pier	Abs. (kip-ft)	11347	16477	24251	12233	17636	28491
	(3-2)/DL Ratio	0.36	0.59	0.67	0.25	0.45	0.7
Deck Shear at Mid-span	Abs. (kips)	208	252	293	245	292	350
	(3-2)/DL Ratio	2.30	3.21	2.94	1.95	2.65	3.00
Deck Moment at Mid-span	Abs. (kip-ft)	5329	8089	14980	4922	8016	17905
	(3-2)/DL Ratio	0.78	1.04	0.52	0.67	0.88	0.53

6.7 Effect of Varying Foundation Restraint

In this section, response results for spring and fixed foundation models of bridge numbers 4 and 6 are compared. The vertical dynamic characteristics of both bridges with fixed and spring foundation models are shown in Tables 6.21 and 6.22. The tables show that the period and modal mass participation ratio of the fundamental vertical mode increase slightly with an increase in foundation flexibility.

Tables 6.23 and 6.24 show response values for the two foundation conditions in the same format as presented in Tables 6.19 and 6.20. Tables B-3 and B-6 in Appendix B show the full range of response results for fixed foundation models for bridge numbers 4 and 6 respectively. It can be seen from Tables 6.23 and 6.24 that fixed foundation models give higher values for the absolute response to the three component input. However, the majority of the "(3-2)/DL Ratio" values are higher for the spring foundation model in bridge number 6. The response values for bridge number 6 are higher for rock site conditions but results vary between the two site conditions for bridge number 4.

Table 6.21 Data for Vertical Modes with Vertical Mass Participation Ratios Greater Than 2% for Spring and Fixed Foundations of Bridge No. 4.

Mode #	Period (sec.)	Percentage Mass Participation	Cumulative Percentage Mass Participation
Spring Foundations			
5	0.2050	79.3	79.3
8	0.0822	12.3	92.1
11	0.0579	6.0	98.2
Fixed Foundations			
6	0.1877	68.9	68.9
13	0.0464	6.6	77.5
16	0.0339	10.0	87.4
18	0.0251	6.6	94.0

Table 6.22 Data for Vertical Modes with Vertical Mass Participation Ratios Greater Than 2% for Spring and Fixed Foundations of Bridge No. 6.

Mode #	Period (sec.)	Percentage Mass Participation	Cumulative Percentage Mass Participation
Drilled Shaft Foundations			
7	0.1730	66.8	66.9
10	0.0620	2.9	69.9
14	0.0475	4.7	74.7
15	0.0466	10.8	85.5
18	0.0346	9.3	94.8
Fixed Foundations			
7	0.1679	63.1	63.1
14	0.0387	9.9	73.4
16	0.0317	20.6	94.2

Table 6.23 Results of a Response Spectrum Analysis Performed on Bridge No. 4 for Fixed and Spring Foundations

Response Quantity	Response Value	Bridge Number 4			
		Rock, 1km, M=7.5		Soil,1km, M=7.5	
		Spring	Fixed	Spring	Fixed
Pier Axial Force	Abs. (kips)	1351	1434	1361	1442
	(3-2)/DL Ratio	0.37	0.26	0.33	0.23
Deck Shear at Pier	Abs. (kips)	849	862	902	916
	(3-2)/DL Ratio	0.52	0.52	0.39	0.4
Deck Moment at Pier	Abs. (kip-ft)	33143	33616	40737	41069
	(3-2)/DL Ratio	0.39	0.37	0.26	0.26
Deck Shear at Mid-span	Abs. (kips)	583	606	716	732
	(3-2)/DL Ratio	-	-	-	-
Deck Moment at Mid-span	Abs. (kip-ft)	12777	13538	12131	12776
	(3-2)/DL Ratio	1.60	1.73	1.52	1.63

Table 6.24 Selected Results of a Response Spectrum Analysis Performed on Bridge No. 6 for Fixed and Spring Foundations

Response Quantity	Response Value	Bridge Number 6			
		Rock, 1km, M=7.5		Soil,1km, M=7.5	
		Spring	Fixed	Spring	Fixed
Pier Axial Force	Abs. (kips)	1220	1276	1187	1186
	(3-2)/DL Ratio	0.78	0.52	0.70	0.51
Deck Shear at Pier	Abs. (kips)	564	669	554	614
	(3-2)/DL Ratio	0.71	0.46	0.61	0.46
Deck Moment at Pier	Abs. (kip-ft)	16477	25278	17636	22728
	(3-2)/DL Ratio	0.59	0.32	0.45	0.32
Deck Shear at Mid-span	Abs. (kips)	252	481	292	429
	(3-2)/DL Ratio	3.21	1.47	2.65	1.54
Deck Moment at Mid-span	Abs. (kip-ft)	8089	8312	8016	7850
	(3-2)/DL Ratio	1.04	0.96	0.88	0.97

6.8 Comparison of Directional Combination Rules Used in Modal Analysis

The SRSS method was used as the directional combination rule for all the modal analysis reported herein to this point; however, other directional combination rules are specified in current bridge design codes. The *AASHTO LFRD* [1994] and *AASHTO 15th Edition* [1992] codes both specify that the 100% + 30% rule should be used and in the *ATC-32 Provisional Recommendations* [1996], the 100% + 40% rule is specified for directional combination. This Section compares the results obtained using all three methods with those from time history analyses using spectrum compatible records.

Values for response quantities (e.g. pier axial force, mid-span moment) are computed for each method as follows:

SRSS Rule: $(H1^2 + H2^2 + V^2)^{1/2}$

100% + 30% Rule: Maximum of (a), (b) or (c)

(a) 1.0H1 + 0.3H2 + 0.3V
(b) 0.3H1 + 1.0H2 + 0.3V
(c) 0.3H1 + 0.3H2 + 1.0V

100% + 40% Rule: Maximum of (a), (b) or (c)

(a) 1.0H1 + 0.4H2 + 0.4V
(b) 0.4H1 + 1.0H2 + 0.4V
(c) 0.4H1 + 0.4H2 + 1.0V

Where:

H1 = Absolute response value resulting from a response spectrum analysis performed in one of the orthogonal horizontal directions.

H2 = Absolute response value resulting from a response spectrum analysis performed in a horizontal direction perpendicular to H1.

V = Absolute response value resulting from a response spectrum analysis performed in the vertical direction.

Tables 6.25 and 6.26 compare response values obtained from modal analyses of bridge numbers 4 and 5 using all three directional rules shown above and from time history analyses using frequency-scaled records. The tables show absolute response values to the three-component input and the ratio of this value to the absolute response value from the two-component horizontal input. Values shown for frequency-scaled time history analyses and the SRSS method are taken from Tables 6.3 and 6.5.

The values shown in parentheses relate the absolute values obtained from modal analyses using the three different directional combination methods with those from time history analyses. These values show that the SRSS method gives absolute response values closer to those obtained from frequency-scaled time history analyses than the other two directional combination methods. It should be noted that in a few instances, the SRSS method gives unconservative results although these unconservative results, are less than 10% below the time history result. Response values shown in the tables for the 100% + 30% rule and the 100% + 40% are all conservative.

All results and recommendations to this point are based on linear dynamic analyses. In the next section, one bridge is selected for more detailed examination by nonlinear analysis, and it is examined to determine the adequacy of the recommendations.

Table 6.25 Comparison of Results from Analyses of Bridge 4 Using Three Different Directional Combination Rules and Frequency-scaled Time History Records

Response Quantity	Bridge 4: M=6.5, Soil, Distance = 20km							
	FS Time Histories		SRSS		100% + 30%		100% + 40%	
	Abs.	Ratio	Abs.	Ratio	Abs.	Ratio	Abs.	Ratio
Pier Axial Force (kips)	297	1.33	296 (0%)	1.21	299 (+1%)	1.2	317 (+7%)	1.26
Shear Force at Pier (kips)	177	1.48	184 (+4%)	1.49	180 (+2%)	1.40	195 (+10%)	1.49
Bending Moment at Pier (kip–ft)	8597	1.06	8396 (-2%)	1.11	8977 (+4%)	1.14	9498 (+10%)	1.18
Shear Force at Mid-Span (kips)	152	1.24	145 (-5%)	1.12	155 (+2%)	1.15	164 (+8%)	1.19
Bending Moment at Mid-Span (kip-ft)	2476	1.3E+8	2388 (+4%)	1.4E+8	2388 (+4%)	5.6E+07	2387 (+4%)	4.1E+4

Abs. = Absolute response value to three-component input. For the frequency-scaled time histories, it is the average value for the five records shown in Table 6.3.
Ratio = Absolute three-component response value over the two-component response value.

Table 6.26 Comparison of Results from Analyses of Bridge 5 Using Three Different Directional Combination Rules and Frequency-scaled Time History Records

Response Quantity	Bridge 5: M=6.5, Rock, Distance = 5km							
	FS Time Histories		SRSS		100% + 30%		100% + 40%	
	Abs.	Ratio	Abs.	Ratio	Abs.	Ratio	Abs.	Ratio
Pier Axial Force (kips)	1355	18.47	1369 (+1%)	22.45	1511 (+12%)	15.38	1523 (+12%)	15.02
Shear Force at Pier (kips)	361	5.93	339 (-6%)	6.25	384 (+6%)	4.10	396 (+10%)	4.08
Bending Moment at Pier (kip–ft)	13877	3.80	12720 (-8%)	4.33	14837 (+7%)	2.71	15505 (+12%)	2.74
Shear Force at Mid-Span (kips)	192	4.22	231 (+20%)	4.89	272 (+42%)	3.38	282 (+47%)	3.39
Bending Moment at Mid-Span (kip-ft)	9492	6.19	9036 (+5%)	6.21	10409 (+10%)	4.22	10746 (+13%)	4.14

Abs. = Absolute response value to three-component input. For the frequency-scaled time histories, it is the average value for the five records shown in Table 6.5.
Ratio = Absolute three-component response value over the two-component response value.

SECTION 7
NONLINEAR RESPONSE OF BRIDGE 6

Section 6 presented the results of linear analyses on six different bridges using the commercial finite element code, SAP2000 [1997]. In this Section, the general purpose nonlinear finite element code, ANSR-II [1979], is used to analyze bridge 6 incorporating the nonlinear behavior of the piers. This bridge was chosen over the other five bridges because it is relatively sensitive to the vertical component of motion and it has single pier bents that are monolithic with the superstructure. Plastic hinges are allowed to form at two locations in the columns, at ground level and at the bottom of the column flares. All other elements in the ANSR-II model of bridge 6 are not permitted to yield or crack, and have the same properties as those given for the SAP2000 model in Section 3.6. The nonlinear behavior of the drilled shafts, foundation springs and abutment springs is beyond the scope of this study and yield values could not be calculated for the superstructure elements because reinforcement details are not provided in the design manual. The yield values for all elements except the piers were set high so that these elements would remain linear during all analyses. The input file for the ANSR-II model is given Appendix E.

7.1 Description of Elements

ANSR-II Element Type 2 is used to model the shafts, piers, superstructure, vertical and longitudinal abutment support springs. This is a three dimensional beam-column element that may be arbitrarily orientated in space. Plastic hinges can form at the element ends. Interaction among the bending moments, torsional moment and axial forces at a hinge are taken into account in determining when the hinge forms. Displacements are assumed to be small, although the P-delta effect may be considered. Tri-linear relationships can be specified for the moment-rotation relationship about all three element axes, and for axial force-extension relationship. Different yield strengths can be specified at the two ends if desired. Different strengths can also be specified for axial tension and compression. Properties of the nonlinear pier elements used in this study are shown in Table 7.1 and have the following characteristics:

1. Interaction surface type is parabolic.
2. Initial force specified for the element is equal to the dead load compression force.
3. Yielding in torsion is prevented by specifying large yield values.
4. P-Delta option is not utilized.
5. The element has the same strength type at both ends.

ANSR-II Element Type 1 (truss element) is used to model the grounded springs attached to the drilled shaft and the transverse springs at the abutments. It can transmit axial load only and may be arbitrarily orientated in space.

Table 7.1 Properties of Nonlinear Pier Elements

	K(1)	K(2)	K(3)	YS(1)	YS(2)	YS(3)
Flexural Properties about Weak Axis, EI	10.2E+6	1.22E+6	0.5E+6	766	1448	
Flexural Properties about Strong Axis, EI	25.2E+6	3.65E+6	1.26E+6	1196	2761	
Torsion Properties, GJ	15.0E+6	8.0E+6	4.0E+6	10E+10	20E+20	
Axial Properties, EA	9.99E+6	5.3E+6	3.0E+6	1676	10E+10	2600

Footnotes:
For flexural stiffness, K(i) = EI(i) in kip-ft^2
YS(i) = yield moment in kip-ft

For torsional stiffness, K(i) = GJ(i) in kip-ft^2
YS(i) = yield moment in kip-ft

For axial stiffness, K(i) = EA(i) in kip-ft^2
YS(1) = tension yield in kips
YS(3) = compression buckling in kips

7.2 Comparison of ANSR-II and SAP2000 Linear Results

To verify the accuracy of the ANSR-II model of bridge 6, linear response results are compared to SAP2000 results. Yield values in the pier elements of the ANSR-II model are set high enough such that plastic hinges do not form and thus results of the analysis can be compared with those from SAP2000. Table 7.2 presents the SAP2000 results of a time-history analysis using five records frequency-scaled to a spectrum representing a magnitude 6.5 event, soil site conditions and a fault distance of 5km. The table has the same format as Tables 6.2 to 6.6. The table is presented as a benchmark from which the accuracy of the ANSR-II model can be measured and it also lends further weight to the conclusions extracted from Tables 6.2 to 6.6.

Table 7.3 compares the absolute response values from a linear ANSR-II analysis of bridge 6 with those from time-history and response spectrum analyses in SAP2000. Columns 12 and 13 show the absolute average response from ANSR-II and SAP2000, respectively, for the five frequency-scaled records shown in Table 7.3. Column 14 shows the ratio of the ANSR-II to SAP2000 average values. The ratios in this column show that the ANSR-II model gives results that are within 10% of the SAP2000 model for all the vertical force response quantities and for the majority of the horizontal response quantities. Differences between the ANSR and SAP results can be attributed in part to the way damping is calculated in both codes. In SAP2000, a constant damping ratio of 5% is specified for all modes. In ANSR-II, Rayleigh damping is used, with the result that several key modes have lower damping relative to their SAP2000 equivalent modes.

Rayleigh damping coefficients (stiffness and mass proportional) used in the ANSR-II model were calculated with equation 7.1 using the circular frequencies of the fundamental horizontal and vertical modes and 5% damping at these frequencies. The coefficients were adjusted slightly to give response results closer to SAP2000 results: the fundamental horizontal mode has a damping ratio of 6%; the fundamental vertical mode has 5%, and for mode 21 (the highest mode retained in the SAP2000 analysis)

it is 21%. The ANSR-II model of bridge 6 can be considered accurate when these considerations are taken into account.

$$\xi = \alpha/2\omega + \beta\omega/2 \qquad (7.1)$$

Where:

ξ = damping ratio
α = mass proportional damping factor
β = initial stiffness damping factor
ω = natural circular frequency of mode

Column 21 in Table 7.3 compares the average absolute response values from ANSR-II with those obtained from a SAP2000 response spectrum analysis. All the vertical force response quantities of the response spectrum results are within 10% of the ANSR-II results, but again, there are a few instances where some of the horizontal values differ by about 20%.

These results are considered satisfactory, since the purpose of allowing nonlinear behavior is to study its effect on conclusions previously reached with respect to the vertical response for the linear analyses. Thus, linear and nonlinear results from ANSR-II are compared to make this evaluation, eliminating any discrepancies due to differing modeling.

7.3 Comparison of Nonlinear and Linear Response

Plastic hinges developed about both pier axes at both ends of the element (i.e. at ground level and at the base of the column flare) for the 2-component and 3-component loading cases of all five frequency-scaled records shown in Table 7.3. The average maximum plastic rotations for all five records about the weak and strong axes are 0.0020 radians and 0.0061 radians at ground level; 0.0045 radians and 0.0083 radians at the base of the flare. Table 7.4 compares the ANSR-II nonlinear and ANSR-II linear response of bridge 6. The following observations can be deduced.

a. Obviously, the horizontal force response quantities are affected by allowing the piers to hinge.
b. Absolute response values of the horizontal displacements and forces are not affected by the addition of the vertical component in either linear or nonlinear analyses of the bridge as shown by the (3/2) ratios in Table 7.4.
c. All three-component over two-component ratios are greater for the nonlinear response except for vertical displacement at the top of the pier.
d. The average nonlinear response is less than the linear response for all quantities except for the transverse moment at the base of the pier and the vertical displacement at the top of the pier (column 27).

As expected, the horizontal displacements were not significantly impacted by the nonlinear pier response. It can also be seen that all but one of the horizontal force quantities are reduced due to yielding in the piers. The nonlinear response values for pier axial force and vertical moment at mid-span are within 5% of the linear results but the nonlinear values for the other vertical response quantities are less than the linear values by more than 10%. It is noted that these observations are the results of nonlinear analysis for only one bridge and caution is recommended in extrapolating the results to other bridges.

7.4 Comparison of (3-2)/DL Ratios for the Nonlinear and Linear Response

As discussed in Section 6.2, a better measure of the influence of vertical motions are the (3-2)/DL ratios. Table 7.5 compares (3-2)/DL ratios from nonlinear and linear analyses. Columns 11 and 12 show the average (3-2)/DL Ratios for all five records. The (3-2)/DL ratios are generally similar for the nonlinear and linear responses. Overall response quantities are obviously affected by nonlinear behavior in the piers (see Table 7.4, column 27), especially the horizontal forces in the piers. However, it appears from this very limited analysis that the formation of plastic hinges in the bridge piers does not significantly change the additional response due to vertical motion compared to the case where nonlinear behavior is precluded. Nonlinear analyses on additional bridges are required to determine whether the observations made in this section can be generalized.

7.5 Effect of Reducing Overall Vertical Deck Stiffness

In Section 6.6, response spectrum analyses were performed on bridge numbers 4 and 6 with varying vertical deck stiffnesses of 25%, 100% and 400%. It was concluded that the softening of a bridge deck due to cracking during an earthquake would reduce the impact of the vertical component of motion on the structural response of a typical bridge. This Section investigates how this conclusion stands up when plastic hinges are allowed to form in the piers in conjunction with a reduced vertical deck stiffness.

Time history analyses are performed on bridge 6 using the frequency-scaled record of Arleta, one-quarter of the vertical deck gross stiffness and yielding pier elements. Columns 8 to 10 of Table 7.6 show the results of these analyses. This table also shows the response values for the cases of (a) ANSR-II linear analysis with 100% vertical deck stiffness (columns 2 to 4) (b) ANSR-II nonlinear analysis with 100% vertical deck stiffness (columns 5 to 7) (c) SAP2000 response spectrum analysis with 25% vertical deck stiffness (columns 11 to 13).

A comparison of response values in columns 2 to 10 shows that absolute values and ratios are generally lower in columns 8 and 9; thus the conclusion reached in Section 6.6 (i.e. softening of a bridge deck due to cracking during an earthquake will reduce the impact that the vertical motions have on the structural response of a typical bridge) remains valid when plastic hinges form in columns.

Table 7.2 Bridge #6 - Linear Time History Analysis Using Frequency-scaled Records in SAP 2000

	Frequency-Scaled Time History Records to Target Spectrum with parameters M=6.5, D=5km and Soil													Response Spectrum/Time History (RS/TH)					
	Imp. Val. #8 (1)		Imp. Vl. D.A (2)		Corralitas (3)		Arleta (4)		New Hall (5)										
Response Quantity	Time History Abs.	(3/2) Ratio	Time History Abs.	(3/2) Ratio	Time History Abs.	(3/2) Ratio	Time History Abs.	(3/2) Ratio	Time History Abs.	(3/2) Ratio	Avg. Ratio	Resp. Spect. Abs.	(3/2) Ratio	1	2	3	4	5	Avg. (RS/TH)
1	2	3	4	5	6	7	8	9	10	11	12	13	14	15	16	17	18	19	20
Pier Displ. (in.)																			
Longitudinal	2.590	1.00	3.157	1.00	2.906	1.00	2.955	1.00	3.473	1.00	1.00	2.696	1.00	1.04	0.85	0.93	0.91	0.78	0.90
Transverse	2.888	1.00	3.113	1.01	3.103	1.00	2.796	1.00	3.384	1.00	1.00	3.178	1.00	1.10	1.02	1.02	1.14	0.94	1.04
Vertical	0.030	3.56	0.038	3.42	0.036	4.45	0.030	3.53	0.035	2.71	3.45	0.031	3.73	1.01	0.81	0.85	1.03	0.88	0.92
Mid-Span Displ. (in.)																			
Longitudinal	2.622	1.00	3.196	1.00	2.939	1.00	3.001	1.00	3.518	1.00	1.00	3.008	1.00	1.15	0.94	1.02	1.00	0.86	0.99
Transverse	3.068	1.00	3.246	1.01	3.202	1.00	2.967	1.00	3.610	1.00	1.00	3.257	1.00	1.06	1.00	1.02	1.10	0.90	1.02
Vertical	0.270	1.63	0.274	1.62	0.346	2.16	0.284	1.79	0.404	2.10	1.87	0.311	1.88	1.15	1.14	0.90	1.10	0.77	1.01
Forces (kips)																			
Pier (Axial)	631	3.56	789	3.43	752	4.45	619	3.54	722	2.71	3.45	637	3.74	1.01	0.81	0.85	1.03	0.88	0.92
Pier (Long. Shear)	562	1.00	468	1.00	490	1.00	487	1.00	416	1.00	1.00	580	1.00	1.03	1.24	1.19	1.19	1.39	1.21
Pier (Trans. Shear)	541	1.00	655	1.00	509	1.00	472	1.00	742	1.00	1.00	508	1.00	0.94	0.78	1.00	1.08	0.68	0.90
Deck over Pier																			
Vert. Shear (kips)	271	2.48	331	2.16	368	2.73	266	1.90	380	2.23	2.28	299	2.28	1.11	0.91	0.81	1.13	0.79	0.95
Moment (kip-ft)	7951	1.33	10636	1.17	13012	1.70	8902	1.15	15518	1.15	1.27	9534	1.34	1.20	0.90	0.73	1.07	0.61	0.90
Deck at Mid-Span																			
Vert. Shear (kips)	154	1.27	164	1.14	179	1.33	149	1.09	177	1.12	1.18	157	1.14	1.02	0.96	0.88	1.05	0.89	0.96
Moment (kip-ft)	4152	1.97	4095	2.09	4346	2.20	3854	2.31	4745	2.16	2.14	4322	2.15	1.04	1.06	0.99	1.12	0.91	1.02

Abs. = Absolute value of response quantity to three-component seismic input.

(3/2) Ratio = Absolute value of three-component response over absolute value of two-component response for time history analyses and response spectrum analysis.

Avg. Ratio = Sum of three-component time history response values over sum of two-component time history response value for all five records.

Table 7.3 Bridge #6 - Comparison of ANSR-II and SAP2000 Linear Time History Analysis Results

	Frequency-Scaled Time History Records to Target Spectrum with parameters M=6.5, D=5km and Soil														Response spectrum over ANSR time history values					
	Imp. Val. #8 (1)		Imp. Vl. D.A (2)		Corralitas (3)		Arleta (4)		New Hall (5)		Avg.	Avg.								
Response Quantity	ANSR	SAP2K	ANSR	SAP2K	ANSR	SAP2K	ANSR	SAP2K	ANSR	SAP2K	ANSR	SAP2K	ANSR/ SAP	Resp. Spect.	1	2	3	4	5	Avg.
	Abs.	Abs.	Abs.	Abs.	Abs.	Abs.	Abs.	Abs.	Abs.	Abs.	Abs.	Abs.	Ratio	Abs.						(RS/TH)
1	2	3	4	5	6	7	8	9	10	11	12	13	14	15	16	17	18	19	20	21
Pier Displ. (in.)																				
Longitudinal	2.723	2.590	2.916	3.157	2.957	2.906	3.079	2.955	3.302	3.473	3.00	3.02	0.99	2.696	0.99	0.92	0.91	0.88	0.82	0.90
Transverse	3.623	2.888	4.052	3.113	3.911	3.103	4.084	2.796	3.120	3.384	3.76	3.06	1.23	3.178	0.88	0.78	0.81	0.78	1.02	0.85
Vertical	0.031	0.030	0.034	0.038	0.033	0.036	0.030	0.030	0.034	0.035	0.03	0.03	0.96	0.031	0.99	0.90	0.93	1.02	0.90	0.95
Mid-Span Displ.																				
Longitudinal	2.842	2.622	3.161	3.196	3.061	2.939	3.234	3.001	3.516	3.518	3.16	3.06	1.04	3.008	1.06	0.95	0.98	0.93	0.86	0.96
Transverse	4.091	3.068	4.032	3.246	3.731	3.202	4.051	2.967	4.080	3.610	4.00	3.22	1.24	3.257	0.80	0.81	0.87	0.80	0.80	0.82
Vertical	0.351	0.270	0.383	0.274	0.448	0.346	0.350	0.284	0.485	0.404	0.40	0.32	1.28	0.311	0.89	0.81	0.70	0.89	0.64	0.79
Forces (kips)																				
Pier (Axial)	637	631	703	789	564	752	617	619	703	722	645	703	0.92	637	1.00	0.91	1.13	1.03	0.91	1.00
Pier (Long. Shear)	572	562	587	468	626	490	676	487	427	416	578	485	1.19	580	1.01	0.99	0.93	0.86	1.36	1.03
Pier (Trans. Shear)	568	541	643	655	631	509	583	472	724	742	630	584	1.08	508	0.89	0.79	0.81	0.87	0.70	0.81
Deck over Pier																				
Vert. Shear (kips)	304	271	284	331	335	368	268	266	372	380	313	323	0.97	299	0.98	1.05	0.89	1.12	0.80	0.97
Moment (kip-ft)	10140	7951	10860	10636	10040	13012	10610	8902	14340	15518	11198	11204	1.00	9534	0.94	0.88	0.95	0.90	0.66	0.87
Deck at Mid-Span																				
Vert. Shear (kips)	173	154	160	164	156	179	170	149	203	177	172	165	1.05	157	0.91	0.98	1.01	0.92	0.77	0.92
Moment (kip-ft)	3762	4152	3489	4095	4371	4346	3566	3854	4763	4745	3990	4239	0.94	4322	1.15	1.24	0.99	1.21	0.91	1.10

Abs. = Absolute value of response quantity to three-component seismic input.

Table 7.4 Bridge #6 - Comparison of Results from Non-linear and Linear time History Analysis Using Frequency-scaled Records in ANSR-II

	Frequency-Scaled Time History Records to Target Spectrum with parameters M=6.5, D=5km and Soil																										
	Imperial Vallley - El Centro #8					Imperial Valley - El Centro D.A					Loma Prieta - Corralitas					Northridge - Arleta					Northridge - New Hall L.A. Fire St,					Avg.
Response Quantity	Non-Linear Abs.	(3/2) Ratio	Linear Abs.	(3/2) Ratio	N/L Ratio	Non-Linear Abs.	(3/2) Ratio	Linear Abs.	(3/2) Ratio	N/L Ratio	Non-Linear Abs.	(3/2) Ratio	Linear Abs.	(3/2) Ratio	N/L Ratio	Non-Linear Abs.	(3/2) Ratio	Linear Abs.	(3/2) Ratio	N/L Ratio	Non-Linear Abs.	(3/2) Ratio	Linear Abs.	(3/2) Ratio	N/L Ratio	N/L Ratio
1	2	3	4	5	6	7	8	9	10	11	12	13	14	15	16	17	18	19	20	21	22	23	24	25	26	27
Pier Displ. at Top																										
Longitudinal	2.558	1.00	2.723	1.00	0.94	3.013	1.00	2.916	1.00	1.03	2.850	1.00	2.957	1.00	0.96	2.634	1.00	3.079	1.00	0.86	2.661	1.00	3.302	1.00	0.81	0.91
Transverse	3.857	1.00	3.623	1.00	1.06	2.810	1.00	4.052	1.00	0.69	2.914	1.00	3.911	1.00	0.75	3.630	1.00	4.084	1.00	0.89	3.486	1.00	3.12	1.00	1.12	0.95
Vertical	0.039	2.17	0.031	3.88	1.26	0.037	1.85	0.034	4.86	1.09	0.044	1.85	0.033	5.50	1.33	0.031	1.72	0.03	4.29	1.03	0.041	2.28	0.034	2.43	1.21	1.16
Mid-Span Displ.																										
Longitudinal	2.682	1.00	2.842	1.00	0.94	3.250	1.00	3.161	1.00	1.03	3.066	1.00	3.061	1.00	1.00	2.663	1.00	3.234	1.00	0.82	2.901	1.00	3.516	1.00	0.83	0.92
Transverse	3.940	1.00	4.091	1.00	0.96	3.595	1.00	4.032	1.00	0.89	3.069	1.00	3.731	1.00	0.82	3.663	1.00	4.051	1.00	0.90	4.136	1.00	4.08	1.00	1.01	0.94
Vertical	0.254	2.19	0.351	1.19	0.72	0.257	2.07	0.383	1.40	0.67	0.332	2.24	0.448	1.52	0.74	0.259	1.66	0.35	1.18	0.74	0.326	2.61	0.485	1.60	0.67	0.76
PIER																										
Axial Force	631	8.41	637	4.49	0.99	702	7.98	703	5.33	1.00	519	6.18	564	4.34	0.92	618	7.02	617	3.98	1.00	656	4.37	703	2.41	0.93	0.97
Lg. Shear Force	287	1.00	572	1.00	0.50	350	1.00	587	1.00	0.60	343	1.00	626	1.00	0.55	286	1.00	676	1.00	0.42	267	1.00	427	1.00	0.63	0.58
Ts. Shear Force	434	1.00	568	1.00	0.76	449	1.00	643	1.00	0.70	394	1.00	631	1.00	0.62	447	1.00	583	1.00	0.77	520	1.00	724	1.00	0.72	0.76
L. Mom. at base	2248	1.00	2447	1.00	0.92	2666	1.00	2631	1.00	1.01	2572	1.00	2727	1.00	0.94	2175	1.00	2969	1.00	0.73	2103	1.00	1749	1.00	1.20	0.94
T. M. at base	3091	1.00	2480	1.00	1.25	3191	1.00	2445	1.00	1.31	2565	1.00	2277	1.00	1.13	3207	1.00	2465	1.00	1.30	3801	1.00	2495	1.00	1.52	1.23
L.M. at flare	2196	1.00	6139	1.00	0.36	2632	1.00	6187	1.00	0.43	2615	1.00	6660	1.00	0.39	2141	1.00	7188	1.00	0.30	1913	1.00	4760	1.00	0.40	0.42
T.M. at flare	3456	1.00	6203	1.00	0.56	2781	1.00	6187	1.00	0.45	2951	1.00	7268	1.00	0.41	3513	1.00	7188	1.00	0.49	4042	1.00	8480	1.00	0.48	0.52
Deck over Pier																										
Vert. Shear	277	4.11	304	2.29	0.91	281	4.28	284	2.23	0.99	256	3.41	335	2.57	0.76	268	3.32	268	2.07	1.00	268	3.73	372	2.09	0.72	0.86
Moment	7639	2.08	10140	1.44	0.75	7204	1.81	10860	1.35	0.66	7299	1.92	10040	1.47	0.73	6553	1.75	10610	1.38	0.62	9071	1.72	14340	1.32	0.63	0.72
Deck - Mid-Span																										
Vert. Shear	100	1.36	173	1.21	0.58	93	1.30	160	1.18	0.58	87	1.22	156	1.07	0.56	82	1.20	170	1.13	0.48	114	1.74	203	1.27	0.56	0.60
Moment	3842	2.60	3762	1.95	1.02	3478	2.69	3489	1.99	1.00	4279	3.43	4371	3.10	0.98	3574	2.45	3566	2.18	1.00	4650	3.08	4763	3.14	0.98	0.99

Abs. = Absolute value of response quantity to three-component seismic input.

(3/2) Ratio = Absolute value of three-component response over absolute value of two-component response for time history analyses.

L.M = Longitudinal Moment T.M. = Transverse Moment All displacement are in inches. All forces are in kips and feet.

N/L Ratio = Non-linear 3-component response over linear 3-component response.

Table 7.5 Bridge #6 - Comparison of (3-2)/DL Ratios for the Linear and Non-linear Response Using ANSR-II

	Frequency-Scaled Time History Records to Target Spectrum with parameters M=6.5, D=5km and Soil											
	Imp. Vlly. - El Centro #8		Imp. Vlly. - El Centro D.A		Loma Prieta - Corralitas		Northridge - Arleta		Northridge - New Hall		Average for five records	
Response Quantity	Non-Linear	Linear	Non-Linear	Linear	Non-Linear	Linear	Non-Linear	Linear	Non-Linear	Linear	Non-Linear	Linear
	(3-2)/DL Ratio	(3-2)/DL Ratio	(3-2)/DL Ratio	(3-2)/DL Ratio	(3-2)/DL Ratio	(3-2)/DL Ratio	(3-2)/DL Ratio	(3-2)/DL Ratio	(3-2)/DL Ratio	(3-2)/DL Ratio	(3-2)/DL Ratio	(3-2)/DL Ratio
1	2	3	4	5	6	7	8	9	10	11	11	12
Pier Displ. at Top												
Vertical	0.36	0.39	0.29	0.46	0.34	0.46	0.22	0.39	0.39	0.34	0.32	0.41
Mid-Span Displ.												
Vertical	0.34	0.14	0.32	0.27	0.45	0.37	0.25	0.13	0.49	0.44	0.37	0.27
PIER												
Axial Force	0.45	0.40	0.49	0.46	0.35	0.35	0.43	0.37	0.41	0.33	0.43	0.38
Deck over Pier												
Vert. Shear	0.41	0.33	0.42	0.31	0.35	0.40	0.36	0.27	0.38	0.38	0.38	0.34
Moment	0.40	0.32	0.33	0.29	0.36	0.33	0.29	0.30	0.39	0.36	0.35	0.32
Deck - Mid-Span												
Vert. Shear	1.94	2.17	1.57	1.75	1.14	0.70	0.98	1.40	3.51	3.13	1.83	1.83
Moment	0.49	0.38	0.45	0.36	0.63	0.61	0.44	0.40	0.65	0.67	0.53	0.48

(3/2)/DL Ratio = Absolute value of two-component response subtracted from absolute value of three-component response over dead-load only response.

L.M. = Longitudinal Moment T.M. = Transverse Moment

All displacements are in inches. All forces are in kips and feet.

Table 7.6 Bridge #6 - Response of Non-linear ANSR-II Model with 25% of the Vertical Deck Stiffness

	Frequency-scaled time history of Northridge - Arleta record to a target spectrum with parameters M=6.5, D=5km and Soil											
	ANSR Linear - 100% deck stiffness			ANSR Non-linear - 100% deck stiffness			ANSR Non-linear - 25% deck stiffness			SAP2K Linear - 25% deck stiffness		
Response Quantity	Linear Abs.	(3-2)/DL Ratio	3/2 Ratio	Non-Linear Abs.	(3-2)/DL Ratio	3/2 Ratio	Non-Linear Abs.	(3-2)/DL Ratio	3/2 Ratio	Response Spectrum Abs.	(3-2)/DL Ratio	3/2 Ratio
1	2	3	4	5	6	7	8	9	10	11	12	13
Pier Displ. at Top												
Longitudinal	3.079	0.00	1.00	2.634	0.00	1.00	2.961	0.00	1.00	3.123	0.00	1.00
Transverse	4.084	0.00	1.00	3.630	0.00	1.00	3.743	0.00	1.00	3.265	0.00	1.00
Vertical	0.03	0.39	4.29	0.031	0.22	1.72	0.030	0.21	1.58	0.021	0.19	2.51
Mid-Span Displ.												
Longitudinal	3.234	0.00	1.00	2.663	0.00	1.00	3.016	0.00	1.00	3.176	0.00	1.00
Transverse	4.051	0.00	1.00	3.663	0.00	1.00	3.727	0.00	1.00	3.34	0.00	1.00
Vertical	0.35	0.13	1.18	0.259	0.25	1.66	1.078	0.22	1.18	0.874	0.40	1.33
PIER												
Axial Force	617	0.37	3.98	618	0.43	7.02	380	0.21	3.58	437	0.22	2.51
Longitudinal Shear Force	676	0.00	1.00	286	0.00	1.00	289	0.00	1.00	508	0.00	1.00
Transverse Shear Force	583	0.00	1.00	447	0.00	1.00	455	0.00	1.00	497	0.00	1.00
Longitudinal Mom. at base	2969	0.00	1.00	2175	0.00	1.00	2155	0.00	1.00	3173	0.00	1.00
Transverse Moment at base	2465	0.00	1.00	3207	0.00	1.00	3147	0.00	1.00	2872	0.00	1.00
Longitudinal Moment at flare	7188	0.00	1.00	2141	0.00	1.00	2186	0.00	1.00	4407	0.00	1.00
Transverse Moment at flare	7188	0.00	1.00	3513	0.00	1.00	3685	0.00	1.00	4655	0.00	1.00
Deck over Pier												
Vert. Shear	268	0.27	2.07	268	0.36	3.32	184	0.19	1.81	206	0.16	1.89
Moment	10610	0.30	1.38	6553	0.29	1.75	5103	0.13	1.32	6542	0.13	1.24
Deck - Mid-Span												
Vert. Shear	170	1.40	1.13	82	0.98	1.20	83	0.97	1.19	131	0.96	1.11
Moment	3566	0.40	2.18	3574	0.44	2.45	2666	0.35	1.94	2620	0.27	2.92

Abs. = Absolute value of response quantity to three-component seismic input.

3/2 Ratio = Absolute value of three-component response over absolute value of two-component response for time history analyses.

(3/2)/DL Ratio = Absolute value of two-component response subtracted from absolute value of three-component response over dead-load only response.

All displacements are in inches. All forces are in kips and feet.

SECTION 8
SUMMARY, CONCLUSIONS AND RECOMMENDATIONS

8.1 Summary

The objective of this study was to determine under what conditions the vertical component of seismic ground motion is critical in determining the demands placed on key elements of typical highway bridges. The research approach utilized was to analyze a representative group of bridges with a range of input ground motions that include and exclude the vertical component of motion and compare the results from the dynamic analyses for both loading cases. The scope of the study involves linear response spectrum analyses of finite element models of six different bridges, linear time history analyses of three of the six bridges and nonlinear time history analysis of one of the six bridges incorporating the nonlinear behavior of the piers.

The horizontal and vertical response spectra used in the analyses were computed from attenuation relationships developed by Abrahamson and Silva [1997], and Sadigh et al [1993; 1997] and represent events with magnitudes of 6.5 and 7.5 for both rock and soil conditions at fault distances of 1, 5, 10, 20, and 40 km. The ground motion records used for the linear and nonlinear time history analyses were frequency-scaled to horizontal and vertical spectra representing a magnitude 6.5 event, with rock and soil site conditions, and fault distances of 5 and 20 km. Fifteen sets of 3-component time history records were used for the linear analysis and five sets for the nonlinear analysis.

The impact of including the vertical component of motion is assessed by expressing the increase in design forces (deck shear and moments, column axial forces) as a ratio or percentage of the dead-load only response. In addition to the main objective of this study, the following topics were also included:

- Comparison of results from response spectrum analyses performed on two bridges using three different directional combination rules.
- Comparison of results from linear response spectrum and time history analyses in order to validate the accuracy and appropriateness of response spectrum analyses for the types of loading and structures used in this study.
- An investigation of the structural significance of early arriving strong short period motion in the vertical component of ground motion.
- Comparison of response values obtained from vertical spectra that are two-thirds of the amplitude of the horizontal spectra with those from the vertical spectra developed by Abrahamson and Silva [1997], and Sadigh et al [1993; 1997] used in this study.
- An assessment of the effects of varying the vertical deck stiffnesses and foundation stiffnesses on the vertical response quantities.

8.2 Conclusions

8.2.1 Ground Motions

The traditional approach of assessing the impact of the vertical component of ground motion has been to assume the vertical response spectra is two-thirds the horizontal response spectra. In this study, state-of-the-art information on vertical ground motion and vertical spectra are based on the most recent work by Silva [1997, especially Figures 26 and 27], Abrahamson and Silva [1997], and Sadigh et al [1993; 1997]. The conclusions related to the ground motions are as follows:

1. The vertical component of seismic ground motion at close-in soil sites and distant rock and soil sites is relatively rich in short period waves that arrive earlier than the largest horizontal motions.
2. Records at some close-in rock sites (less than 10 to 15 km) exhibit longer period motions in the vertical component that have similar arrival times and more similar frequencies to the largest horizontal motions.
3. At both rock and soil sites, and for magnitudes above 5.5 and distances less than 40 km, for periods in the range of approximately 0.2 to 3.0 seconds the vertical to horizontal (V/H) spectral ratio (as computed by Silva [1997]) is less than the commonly used value of 2/3. For periods shorter than approximately 0.2 seconds, the V/H spectral ratio is greater than 2/3.
4. For soil sites with distances up to approximately 20 km, in the period range of approximately 0.02 to 0.15 seconds the V/H ratio exceeds 1.0 for all magnitudes above 5.5.
5. For rock sites with distances up to approximately 10 km, in the period range of approximately 0.03 to 0.1 seconds the V/H ratio exceeds 1.0 for magnitudes above 6.5.
6. The V/H spectral ratio for magnitude 6.5 events has a peak value of about 1.1 and 1.9 for rock and soil respectively, and the peak ratio increases to about 1.3 (rock) and 2.6 (soil) for magnitude 7.5 events. The V/H spectral ratio increases with increasing earthquake magnitude for all periods less than approximately 1.0 seconds. At longer periods, the magnitude dependence is much less apparent.

8.2.2 Structural Response of Bridges in the Linear Range

Most of the design office analyses that are performed on bridges are based on linear elastic models using the response spectrum method of analysis. Very rarely is the vertical component included in such analyses. If vertical motions are included in an analysis, they generally use two-thirds of the amplitude of the horizontal response spectra. Bridge codes to date have not provided load multipliers or specific vertical response spectra that allow for the impact of vertical motions.

All six bridges included in this study have been analyzed using linear elastic models with and without the vertical component of motion. Both response spectra and time history analyses have been performed. The conclusions are as follows:

1. Bridges with the greatest percentage of modal mass lying in the range of the peak spectral acceleration of the vertical response spectra experience the greatest impact from the vertical seismic motions. An attempt was made to assess the amount of modal mass less than 0.2 seconds that caused significant vertical response. Unfortunately, the six bridges used in this study were not sufficient to develop a specific recommendation on this issue.
2. Tables 6.8 to 6.15, Figures 6.8 to 6.23, and Tables 8.1 and 8.2 give DL multipliers that may be applied to various response quantities in order to eliminate the need to include the vertical component of motion in a dynamic analysis. Three different response ratios (3/2, 3/DL, (3-2)/DL) were examined in this study. It was found that the (3-2)/DL ratio gave the best practical measure of the impact of the vertical component of motion on bridges. The (3-2)/DL ratio is computed by dividing the difference in absolute response values from the three-component input and two-component input loading cases by the dead load only response value. Tables 8.1 and 8.2 present the ratios for magnitude 6.5 and 7.5 events, respectively, for both rock and soil conditions. These ratios increase substantially as the bridge site gets closer to the fault.
3. In order to envelop the design forces as a function of DL on all bridges for both magnitude 6.5 and 7.5 events, the multipliers get quite large, especially when the bridge site is within 10km of a fault. For magnitude 6.5 events a DL multiplier of ±0.4DL would envelop all forces in the 20-50km range. A multiplier of ±0.7DL would be required in the 0-20km range except for the mid-

span moment in which a ±1.4DL multiplier would be necessary. For magnitude 7.5 events, a DL multiplier of ±0.6DL would envelop all forces in the 20-60km range. A multiplier of ±1.0DL would be required in the 0-20km range except for the mid-span moment in which a ±1.9DL multiplier would be necessary. As a consequence, it would seem prudent to consider the use of an appropriate DL multiplier on all bridge deck design forces and column axial design forces when the bridge location is 20 to 50km from a fault. When the bridge site has a fault distance of less than 20 km, it would seem prudent to require the inclusion of a vertical ground motion analysis in the analysis of a bridge rather than specifying very large multipliers. Beyond 60 km from the fault, the value of ±10% of the dead load design value would adequately account for the impact of the vertical component of motion on all vertical design forces. As a consequence, the impact of the vertical component of motion could be ignored when a bridge site is greater than 60km from a fault.

4. Values of horizontal response quantities are not significantly affected by the vertical component of motion.
5. Results from linear response spectrum analyses using the CQC modal combination method and the SRSS directional combination method are mostly within 10% of the average linear response from time history analyses using five records frequency-scaled to the input spectra.
6. Response values from a modal analysis using vertical spectra computed from attenuation relationships by Abrahamson and Silva [1997], and Sadigh et al [1993; 1997] can be up to 40% greater or less than those obtained from vertical spectra that have a spectral amplitude equal to 2/3 of the horizontal spectra. It be should be noted that the "2/3 spectra" generally give conservative results for vertical deck response quantities; but for pier axial force, the results are mostly unconservative. For this reason, it is recommended that the use of the 2/3 multiplier to obtain the vertical spectra from the horizontal spectra should be discontinued.
7. Softening of a bridge deck due to cracking during an earthquake will generally reduce the effect the vertical component of motion has on the bridge (see Tables 6.19 and 6.20). As a consequence, the DL multipliers shown in Tables 6.8 to 6.15, Tables 8.1 and 8.2 and Figures 6.8 to 6.23 are conservative in that no deck stiffness reduction is included in their development.
8. Bridge models with fixed foundations give higher absolute response values for a three component input whereas flexible foundations tend to give higher (3-2)/DL ratios (see Tables 6.23 and 6.24).
9. Vertical shear at mid-span may need to be checked in bridges that are located within 10km of a fault and are designed for M7.5 loading, have uneven span lengths, and have columns that are effectively fixed to the deck.
10. The early arrival of the vertical component of motion does not have a significant effect on the structural response of typical highway bridges.
11. A magnitude 7.5 event and soil site conditions produces the highest (3-2)/DL ratios for pier axial force for all distances, and for deck shear at the pier and moment at mid-span at distances beyond 10 km. Rock site conditions produce the highest ratios for these two quantities for distances less than 10 km and for deck moment over the pier for all distances.
12. A comparison of results from modal analyses using the following three directional combination rules (a) SRSS rule (b) 100% + 30% rule (c) 100% + 40% rule showed that using the SRSS method produced results that were closest to the average result from time history analyses using five spectrum compatible records (see Tables 6.25 and 6.26).

Table 8.1 Fault Distance Zones and Corresponding Dead Load Multiplier for ALL BRIDGES Observed for Rock and Soil Site Conditions and a Magnitude 6.5 Event

Response Quantity	Fault Distance Zones (km)								
	0-5	5-10	10-15	15-20	20-25	25-30	30-35	35-40	>40 or given value
	0-10		10-20		20-30		30-40		
Pier Axial Force DL Multiplier	0.7	0.5	0.3	0.3	0.2		0.1		0.1
	0.7		0.3						
Deck Shear Force at Pier DL Multiplier	0.7	0.5	0.4	0.3	0.2			0.1	0.1
	0.7		0.4						
Deck Bending Moment at Pier DL Multiplier	0.6	0.4	0.3	0.3	0.2			0.1	0.1
	0.6		0.3						
Deck Shear Force at Mid-Span DL Multiplier	0.1								0.1
Deck Bending Moment at Mid-Span* DL Multiplier	1.4	1.0	0.7	0.5	0.4	0.4	0.3	0.3	0.1 (>50)
	1.4		0.7		0.4		0.3		

Footnotes

(1) The DL Multiplier values given above are in addition to the dead load; thus, an actual "load factor" would be **1.0 plus/minus** *the above numbers.*

*(2) *Broekhuizen[1997](see Section 2, 2.1 Decks) concluded that prestressed spans will not experience significant damage for upward accelerations of up to 1g applied to the superstructure.*

(3) The Live Load (LL) typically used in the design of bridge types shown in this study is in the range of 20-30% of the Dead Load (DL).

Table 8.2 Fault Distance Zones and Corresponding Dead Load Multiplier for ALL BRIDGES Observed for Rock and Soil Site Conditions and a Magnitude 7.5 Event

Response Quantity	Fault Distance Zones (km)								
	0-5	5-10	10-15	15-20	20-25	25-30	30-35	35-40	>40 or given value
	0-10		10-20		20-30		30-40		
Pier Axial Force DL Multiplier	0.9	0.6	0.4	0.3	0.2				0.1
	0.9		0.4						
Deck Shear Force at Pier DL Multiplier	1.0	0.7	0.5	0.4	0.3	0.3	0.2		0.1 (>50)
	1.0		0.5		0.3				
Deck Bending Moment at Pier DL Multiplier	1.0	0.7	0.5	0.4	0.3	0.3	0.2		0.1 (>50)
	1.0		0.5		0.3				
Deck Shear Force at Mid-Span DL Multiplier			0.1						0.1
	See Section 6.5								
Deck Bending Moment at Mid-Span* DL Multiplier	1.9	1.4	1.0	0.8	0.6	0.6	0.5	0.4	0.1 (>60)
	1.9		1.0		0.6		0.5		

Footnotes

(1) The DL Multiplier values given above are in addition to the dead load; thus, an actual "load factor" would be **1.0 plus/minus** *the above numbers.*

*(2) *Broekhuizen[1997](see Section 2, 2.1 Decks) concluded that prestressed spans will not experience significant damage for upward accelerations of up to 1g applied to the superstructure.*

(3) The Live Load (LL) typically used in the design of bridge types shown in this study is in the range of 20-30% of the Dead Load (DL).

8.2.3 Structural Response of Bridges in the Nonlinear Range

The results presented in Section 8.2.2 are in conflict with current design practice since it has been assumed to date that the vertical ground motion does not have a significant impact on the design of a bridge. One of the obvious questions resulting from the linear analyses is what impact does the nonlinear response of key components of the bridge have on the results discussed in Section 8.2.2. Deck softening was discussed in Item 6 of Section 8.2.2 although this was not part of a nonlinear study. Unfortunately, it was not possible to perform an extensive study on the nonlinear response of each bridge. Bridge 6 was re-analyzed incorporating the nonlinear response of the piers. These nonlinear results were compared with the linear response results and the following observations resulted from the limited nonlinear modeling of this one bridge.

1. Including nonlinear behavior in the piers strongly influences the horizontal response of the structure although the horizontal displacements are not significantly impacted.
2. Response values for horizontal quantities are not significantly affected by the vertical component of motion in the bridge studied. However, earlier research has indicated some sensitivity of the horizontal response to the inclusion of vertical motions in inelastic bridges
3. (3-2)/DL ratios are slightly greater but essentially the same for the nonlinear and linear response of the majority of response quantities for this one bridge.

Generalizations from the above observations are not warranted until further nonlinear analysis are performed on a wider range of bridge structures.

8.3 Recommendations

The results of this study are important and will be a surprise to many because it has been commonly assumed to date that vertical ground motions do not have a significant impact on the response of a bridge. As a consequence, current bridge design codes do not incorporate any design provisions to account for the response resulting from vertical ground motions. This clearly is not a valid assumption for bridge sites located within 20km of a fault and for some bridges, the vertical response may be important when the site is located within 40km of a fault.

There are two methods that design codes can utilize to address the vertical response issue. The first is simply to require the inclusion of a vertical component of motion in the design and analysis process when a bridge site is within some distance of a fault (e.g. 10km). The second is more complex from a code perspective but more straightforward from a design perspective. It involves the incorporation of a percentage (e.g. ±40%) of the dead load design force on the design of the deck, columns and bearings without the necessity of performing a vertical analysis. The complexity of this method arises because the design forces that need to be addressed vary significantly by the distance of the bridge site from the fault and, as the site gets within 10km of a fault, some of the percentages get into the 70 – 190% range. It would therefore seem prudent under these circumstances to require the inclusion of the vertical component of motion rather than have very high multipliers that of necessity have to envelop the results obtained in this study.

In order to aid in the development of future code provisions, the following recommendations are offered for consideration.

1. The values for DL multipliers in Tables 8.1 to 8.2 should be considered for inclusion in code provisions in lieu of conducting explicit vertical analyses. If the design process is to be simplified as

much as possible, an envelop of the multipliers could be considered and consideration should be given to having appropriate multipliers when the bridge site is located within certain distances, i.e., 0 to 20km; 20 to 40km; 40 to 60km. At a distance greater than 60km the impact of the vertical response is less than ± 10% of the dead load design value for all of the design quantities included in this study and can therefore be ignored. Decisions will need to be made on the distance from a fault and whether or not to envelop the magnitude 7.5 and 6.5 events or to have separate multipliers for different magnitude events.

2. Vertical motions should be explicitly included in the analysis and design of most bridges within 10km of a major fault. This will avoid the use of very high envelop multipliers, e.g. ± 1.9 on the DL design forces.
3. If linear analysis is appropriate for a particular bridge, response spectrum analyses can accurately represent the vertical response of complex three-dimensional bridges to multi-component seismic excitation.
4. Use of a vertical spectrum equal to 2/3 of the corresponding horizontal spectrum is not recommended.
5. Additional nonlinear work is required to validate the conclusions reached in this research, although it does appear that further nonlinear analyses will reduce the impact of the vertical ground motions.

SECTION 9
REFERENCES

AASHTO 15th Edition (1992), Standard Specifications for Highway Bridges

AASHTO LFRD (1994), Load Factor Resistance Design - Standard Specifications for Highway Bridges

Abrahamson, N.A. and Silva, W.J. (1997), "Empirical response spectral attenuation relations for shallow crustal earthquakes." Seism. Soc. AM., 68(1), 94-127.

ANSR-II (1979), Analysis of Nonlinear Structural Response User's Manual by Digambar P. Mondkar and Graham H. Powell, Earthquake Engineering Research Center, University of California, Berkeley, Report No. UCB/EERC 79/17, July 1979.

ATC-32 (1996), Improved Seismic Design Criteria for California Bridges: Provisional Recommendations by Applied Technology Council.

Bozorgnia, Y., Niazi, M. and Campbell, K.W. (1995), "Characteristics of free-field vertical ground motion during the Northridge earthquake," Earthquake Spectra, Volume II, No. 4, November 1995.

Broekhuizen, D.S. (1996), "Effects of vertical acceleration on prestressed concrete bridges," M.S. Thesis, The University of Texas at Austin, August 1996

Federal Highway Administration (1996), "Seismic design of bridges: Design example No. 1 – Two span continuous CIP concrete box bridge," Publication No. FHWA-5A-97-006, October 1996.

Federal Highway Administration (1996), "Seismic design of bridges: Design example No. 2 – Two span continuous CIP concrete box bridge," Publication No. FHWA-5A-97-006, October 1996.

Federal Highway Administration (1996), "Seismic design of bridges: Design example No. 3 – Two span continuous CIP concrete box bridge," Publication No. FHWA-5A-97-006, October 1996.

Federal Highway Administration (1996), "Seismic design of bridges: Design example No. 4 – Two span continuous CIP concrete box bridge," Publication No. FHWA-5A-97-006, October 1996.

Federal Highway Administration (1996), "Seismic design of bridges: Design example No. 5 – Two span continuous CIP concrete box bridge," Publication No. FHWA-5A-97-006, October 1996.

Federal Highway Administration (1996), "Seismic design of bridges: Design example No. 6 – Two span continuous CIP concrete box bridge," Publication No. FHWA-5A-97-006, October 1996.

FHWA (1987), Seismic Design and Retrofit Manual for Highway Bridges, Report No. FHWA-IP-87-6, Federal Highway Administration, National Technical Information Service, Springfield, VA.

Foutch, D.A. (1997), "A note on the occurrence and effects of vertical earthquake ground motion," Proceedings of the FHWA/NCEER Workshop on the National Representation of Seismic Ground Motion for New and Existing Highway Facilities, Technical Report NCEER-97-0010.

Gloyd, S., (1997), "Design of ordinary bridges for vertical seismic acceleration" Proceedings of the FHWA/NCEER Workshop on the National Representation of Seismic Ground Motion for New and Existing Highway Facilities, Technical Report NCEER-97-0010.

Naeim, F., Anderson, J.C., (1996), "Design classification of horizontal and vertical earthquake ground motion (1933-1994)," A report to the U.S. Geological Survey (USGS) by John A. Martin & Associates, Inc., August 1996.

Priestley, et al. (1994), "The Northridge earthquake of January 17, 1994 – Damage analysis of selected freeway bridges," Report No. – 94/06, Department of Applied Mechanics and Engineering Sciences, University of California, San Diego.

Saadeghvaziri, M.A. and Foutch, D.A. (1988), "Inelastic response of R/C highway bridges under the combined effect of vertical and horizontal earthquake motions," Structural Research Series No. 540, Department of Civil Engineering, University of Illinois at Urbana-champaign, Urbana, Illinois, June 1988

Saadeghvaziri, M.A. and Foutch, D.A. (1991), "Dynamic behavior of R/C highway bridges under the combined effect of vertical and horizontal earthquake motions," Earthquake Engineering and Structural Dynamics, Vol. 20, 535-549 (1991).

Sadigh, K., C.-Y. Chang, Egan, N.A. Abrahamson, S.J. Chiou and M.S. Power, (1993), " Specification of long-period ground motions: updated attenuation relationships for rock site conditions and adjustment factors for near-fault effects," Proc. ATC-17-1 Seminar on Seismic Isolation, Passive Energy Dissipation and Active Control, March 11-12, San Francisco, California, 59 – 70.

Sadigh, K., Chang, C.-Y., Egan, J.A., Makdisi, F., Youngs, R.R., (1997), "Attenuation relationships for shallow crustal earthquakes based on California strong motion data," Seism. Soc. AM., 68(1), 180-189.

SAP2000, (1997), Integrated finite element analysis and design of structures, Version 6.12, October 1997.

Silva, W.J. (1997), "Characteristics of vertical ground motions for applications to engineering design." Proceedings of the FHWA/NCEER Workshop on the National Representation of Seismic Ground Motion for New and Existing Highway Facilities, Technical Report NCEER-97-0010.

Teng, L., Qu, J. (1995), "The characteristics of earthquake ground motions for seismic design – Task H-9, characterization of vertical ground accelerations," Southern California Earthquake Center, University of Southern California, Los Angeles, California.

Uniform Building Code (1997), Volume 2, Structural Design Provisions.

Yu, C-P. (1996), "Effect of vertical earthquake components on bridge responses," Ph.D. Thesis, The University of Texas at Austin, December 1996.

Yu, C-P., Broekhuizen, D.S., Roesset, J.M., Breen, J.E., Kreger, M.E. (1997), "Effect of vertical ground motion on bridge deck response," The University of Texas of Austin, Austin, Texas.

MULTIDISCIPLINARY CENTER FOR EARTHQUAKE ENGINEERING RESEARCH

A National Center of Excellence in Advanced Technology Applications

University at Buffalo, State University of New York
Red Jacket Quadrangle ▪ Buffalo, New York 14261-0025
Phone: 716/645-3391 ▪ Fax: 716/645-3399
E-mail: mceer@acsu.buffalo.edu ▪ WWW Site: http://mceer.buffalo.edu

University at Buffalo *The State University of New York*

ISSN 1520-295X